B. Nekrasov

HYDRODYNAMICS

For Aeronautical Engineers

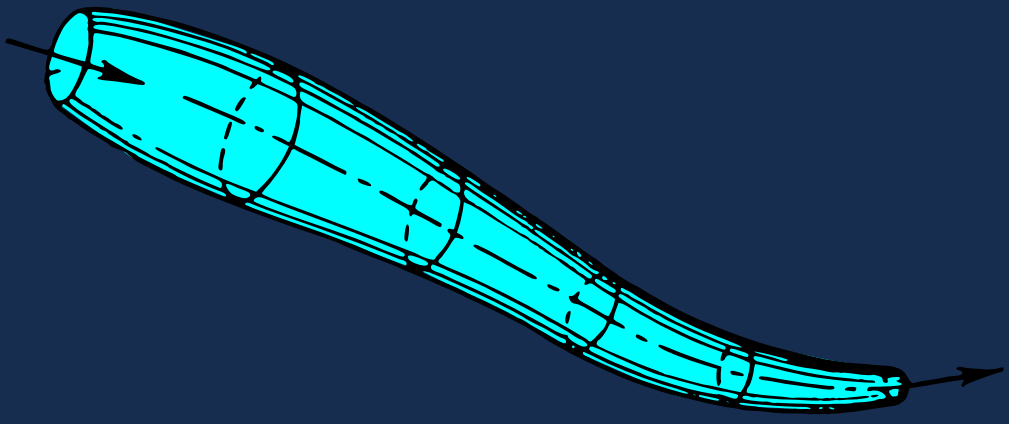

B. NEKRASOV

HYDRAULICS

For Aeronautical Engineers

PEACE PUBLISHERS
Moscow

TRANSLATED FROM THE RUSSIAN
BY V. TALMY

Б. Б. НЕКРАСОВ

ГИДРАВЛИКА

На английском языке

Printed in the Union of Soviet Socialist Republics

Boris Nekrasov is an eminent Soviet expert in hydraulics and its industrial applications. An excellent textbook originally written for aeronautical engineering students, it also presents the main general hydraulic problems as well as fundamentals of the theory of hydraulic machinery employed in aircraft systems.

The practical applications of hydraulic theory, being the author's main concern, the book contains many worked problems for simple hydraulic systems and machinery. One hundred and seventy-eight drawings and diagrams amply illustrate the principles and their practical applications discussed in the book.

CONTENTS

Page

NOTATION AND ABBREVIATIONS 9

CHAPTER I. INTRODUCTION

1. The Subject of Hydraulics 11
2. Historical Background 13
3. Forces Acting on a Fluid. Pressure 17
4. Properties of Liquids 18

CHAPTER II. HYDROSTATICS

5. Hydrostatic Pressure 25
6. The Basic Hydrostatic Equation 27
7. Pressure Head. Vacuum. Pressure Measurement 28
8. Fluid Pressure on a Plane Surface 33
9. Fluid Pressure on Cylindrical and Spherical Surfaces. Buoyancy and Floatation 36

CHAPTER III. RELATIVE REST OF A LIQUID

10. Basic Concepts 42
11. Liquid in a Vessel Moving with Uniform Acceleration in a Straight Line 43
12. Liquid in a Uniformly Rotating Vessel 44

CHAPTER IV. THE BASIC EQUATIONS OF HYDRAULICS

13. Basic Concepts 49
14. Rate of Discharge. Equation of Continuity 51
15. Bernoulli's Equation for a Stream Tube of an Ideal Liquid . . . 52
16. Bernoulli's Equation for Real Flow 57
17. Head Losses (General Considerations) 60
18. Examples of Application of Bernoulli's Equation for Engineering Problems 64

CHAPTER V. FLOW THROUGH PIPES. HYDRODYNAMIC SIMILARITY

19. Flow Through Pipes 69
20. Hydrodynamic Similarity 72
21. Cavitation 77

CHAPTER VI. LAMINAR FLOW

22. Laminar Flow in Circular Pipes 80
23. Entrance Conditions in Laminar Flow. The α Coefficient . . 84
24. Laminar Flow Between Parallel Boundaries 87

CHAPTER VII. TURBULENT FLOW

25. Turbulent Flow in Smooth Pipes 92
26. Turbulent Flow in Rough Pipes 97
27. Turbulent Flow in Noncircular Pipes 101

CHAPTER VIII. LOCAL FEATURES AND MINOR LOSSES

28. General Considerations Concerning Local Features in Pipes . . . 104
29. Abrupt Expansion 105
30. Gradual Expansion 107
31. Pipe Contraction 111
32. Pipe Bends 113
33. Local Disturbances in Laminar Flow 118
34. Local Features in Aircraft Hydraulic Systems 122

CHAPTER IX. FLOW THROUGH ORIFICES, TUBES AND NOZZLES

35. Sharp-Edged Orifice in Thin Wall 124
36. Suppressed Contraction. Submerged Jet 129
37. Flow Through Tubes and Nozzles 132
38. Discharge with Varying Head (Emptying of Vessels) 137
39. Injectors 140

CHAPTER X. RELATIVE MOTION AND UNSTEADY PIPE FLOW

40. Bernoulli's Equation for Relative Motion 149
41. Unsteady Flow Through Pipes 151
42. Water Hammer in Pipes 155

CHAPTER XI. CALCULATION OF PIPELINES

43. Plain Pipeline 162
44. Siphon 166
45. Compound Pipes in Series and in Parallel 167
46. Calculation of Branching and Composite Pipelines 170
47. Pipeline with Pump 172

CHAPTER XII. CENTRIFUGAL PUMPS

48. General Concepts 182
49. The Basic Equation of Centrifugal Pumps 183
50. Characteristics of Ideal Pump. Degree of Reaction 187
51. Impeller with Finite Number of Vanes 190
52. Hydraulic Losses in Pump. Plotting Rated Characteristic Curve 193
53. Pump Efficiency 196
54. Similarity Formulas 197
55. Specific Speed and Its Relation to Impeller Geometry 202
56. Relation Between Specific Speed and Efficiency 205

57. Cavitation Conditions for Centrifugal Pumps (According to S. S. Rudnev) 210
58. Calculation of Volute Casing 214
59. Choice of Pump Type. Special Features of Centrifugal Pumps Used in Aeronautical and Rocket Engineering 216

CHAPTER XIII. DISPLACEMENT PUMPS

60. General Considerations 222
61. Types of Rotary Pumps 224
62. Characteristics of Rotary Displacement Pumps 230

CHAPTER XIV. HYDRAULIC TRANSMISSIONS

63. Translational Hydraulic Actuator 236
64. Follow-up Systems and Boosters 239
65. Rotary Hydraulic Transmissions 248
66. Rotodynamic Transmissions 253

APPENDIX. DIFFERENTIAL EQUATIONS OF IDEAL FLUID FLOW AND THEIR INTEGRATION 257

Index 268

NOTATION AND ABBREVIATIONS

a — acceleration
a — celerity of water-hammer pressure wave
A — parameter characterising injector geometry
A_{eq} — equivalent injector parameter
b_2/d_2 — relative width of pump impeller
C — constant of integration
°C — degrees centigrade
D, d — diameter
D_2/D_1 — relative diameter of pump impeller
e — specific energy
E — energy, work
g — acceleration of gravity
G — weight of a fluid
G — weight rate of discharge
h — capillary rise or depression
h — piezometric head
h — loss of energy or head
h_{con} — loss of head due to contraction
h_{exp} — loss of head due to expansion
h_f — loss of head due to friction
h_{in} — inertia head of liquid moving with acceleration
h_l — local losses
H — total head
H_{av} — available head
H_{in} — inertia head of liquid in accelerated channel
H_{tz} — head generated by idealised centrifugal pump with definite number of vanes
$H_{t\infty}$ — head generated by idealised centrifugal pump with infinite number of vanes
H_m — mean total head
H_{req} — required head
H_t — theoretical or ideal head
j — resultant of body forces
j — acceleration of moving fluid
J_x — moment of inertia about an axis x
k — capillarity
k — roughness size of projections
k — any coefficient
k_{eq} — absolute roughness equivalent to Nikuradse's granular roughness
K — volume or bulk, modulus of elasticity
K — pipe entrance factor
k/r_0 — relative roughness
l — length
l_{ent} — entrance, or transition, length of pipe
l_{eq} — equivalent pipe length
M — mass
M — mass rate of discharge
n — rate of divergence of diffuser
n — speed of rotation
n_s — specific speed
n_x — tangential g-load
n_y — normal g-load
N — power
N_0 — shaft, or brake, horsepower
N_x — tangential acceleration
N_y — normal acceleration
p — pressure
p_{ab} — absolute pressure
p_{atm} — atmospheric pressure
p_b — buoyancy force
p_f — pressure loss due to friction
p_g — gauge pressure
p_l — local loss of pressure
p_t — saturation vapour pressure

p_{vac} — vacuum, or negative, pressure
p_{wh} — water-hammer pressure
P — pressure force
Q — volume rate of discharge
$\dot{Q}$ — delivery, or capacity, of pump
Q_t — theoretical, or ideal, delivery of pump
r — radius
R — surface force
R — radius of curvature
R_h — hydraulic radius, or hydraulic mean depth
Re — Reynolds number
Re_{cr} — critical Reynolds number
Re_t — theoretical, or ideal, Reynolds number
S — area
t — temperature
T — friction, or shear, force
T — torque
u — peripheral velocity at pump impeller
v — velocity
v_{cr} — critical velocity
v_m — mean velocity
v_t — theoretical, or ideal, velocity of efflux
w — relative velocity at pump impeller
W — volume
y — distance
z — number of vanes in pump impeller
z — vertical distance from any datum level, elevation
α (alpha) — diffuser divergence angle
α — dimensionless coefficient accounting for nonuniform velocity distribution
β (beta) — vane angle
β_p — coefficient of compressibility
β_t — coefficient of thermal expansion
γ (gamma) — specific weight
γ_{ef} — effective specific weight
Γ (gamma) — circulation
δ (delta) — specific gravity
δ — pipe bend angle
δ — thickness
δ_e — laminar sublayer thickness
ε (epsilon) — coefficient of contraction of a jet
ζ (dzeta) — loss coefficient
ζ_f — friction loss coefficient
η (eta) — efficiency
η_h — hydraulic efficiency
η_m — mechanical efficiency
η_v — volumetric efficiency
λ (lambda) — friction factor
λ_l — friction factor for laminar flow
λ_t — friction factor for turbulent flow
μ (mu) — coefficient of discharge of orifice
μ — vane number coefficient
μ — dynamic viscosity
ν (nu) — kinematic viscosity
ξ (xi) — form coefficient of orifice
π (pi) — perimeter
ϱ (rho) — density
σ (sigma) — stress
σ — cavitation parameter
τ (tau) — shear stress
φ (phi) — coefficient of velocity of an orifice
ψ (psi) — coefficient taking into account stream contraction by pump impeller vanes or hub
ω (omega) — angular velocity

ABBREVIATIONS

atm — atmosphere = 14.7 lb/sq. in.
cm — centimetre = 0.3937 in.
cst — centistoke
g — gram = 0.03527 oz (avdp)
hr — hour
kg — kg = 1,000 g = 2.205 lb (avdp)
lit — litre = 0.2642 gal
ln — natural (Napierian) logarithm
log — common (Briggs) logarithm
m — metre = 100 cm = 1,000 mm = = 3.281 ft
mm — 0.03937 in.
rpm — revolutions per minute
sec — second
kg-m — kilogram-metre = 0.009 Ltu

CHAPTER I

INTRODUCTION

1. THE SUBJECT OF HYDRAULICS

The branch of mechanics which treats of the equilibrium and motion of liquids and gases and the force interactions between them and bodies through or around which they flow is called *hydromechanics* or *fluid mechanics*. *Hydraulics* is an applied division of fluid mechanics covering a specific range of engineering problems and methods of their solution. It studies the laws of equilibrium and motion of fluids and their applications to the solution of practical problems.

The principal concern of hydraulics is fluid flow constrained by surrounding surfaces, i. e., flow in open and closed channels and conduits, including rivers, canals and flumes, as well as pipes, nozzles and hydraulic machine elements.

Thus, hydraulics is mainly concerned with the internal flow of fluids and it investigates what might be called "internal" problems, as distinct from "external" problems involving the flow of a continuous medium about submerged bodies, as in the case of a solid body moving in water or in the air. These "external" problems are treated in hydrodynamics and aerodynamics in connection with aircraft and ship design.

It should be noted that the term *fluid* as employed in hydromechanics has a broader meaning than generally implied in everyday life and includes all materials capable of an infinite change of shape under the action of the smallest external forces.

The difference between a liquid and a gas is that the former tends to gather in globules if taken in small quantities and makes a free surface in larger volumes. An important property of liquids is that pressure or temperature changes have practically no effect on their volume, i. e., for all practical purposes they can be regarded as incompressible. Gases, on the other hand, contract readily under

pressure and expand infinitely in the absence of pressure, i. e., they are highly compressible.

Despite this difference, however, under certain conditions the laws of motion of liquids and gases are practically identical. One such condition is low velocity of the gas flow as compared with the speed of sound through gas.

The science of hydraulics concerns itself mainly with the motion of liquids. The internal flow of gases is studied only insofar as the velocity of flow is much less than that of sound and, consequently, their compressibility can be disregarded. Such cases are frequently encountered in engineering, as for example, in the flow of air in ventilation systems and in gas mains.

Investigation of the flow of liquids, and even more so gases, is a much more difficult and complicated task than studying the motion of rigid bodies. In rigid-body mechanics one deals with systems of rigidly connected particles; in fluid mechanics the object of investigation is a medium consisting of a multitude of particles in constant relative motion.

To the great Galileo belongs the maxim that it is easier to study the motion of remote celestial bodies than that of a stream running at one's feet. Because of these difficulties, fluid mechanics as a science developed along two different paths.

The first was the purely theoretical path of precise mathematical analysis based on the laws of mechanics. It led to the emergence of theoretical hydromechanics, which for a long time existed as an independent science. Its methods provided an attractive and effective means of scientific research. A theoretical analysis of fluid motion, however, encounters many stumbling blocks and does not always answer the questions arising in real situations.

The urgent requirements of engineering practice, therefore, soon gave rise to a new science of fluid motion, hydraulics, in which researchers took to the second path, that of extensive experimenting and accumulation of factual data for application to engineering problems. At its origin, hydraulics was a purely empirical science. Today, though, whenever necessary it employs the methods of theoretical hydromechanics for the solution of various problems; and, conversely, in theoretical hydromechanics experiments are widely used to verify the validity of its conclusions. Thus, the difference in the methods employed by either science is gradually disappearing, and with it the boundary line between them.

The method of investigating fluid flow in hydraulics today is essentially as follows. The phenomenon under investigation is first simplified and idealised and the laws of theoretical mechanics are applied. The results are then compared with experimental data, the discrepancies are established and the theoretical formulas and solu-

tions adjusted so as to make them suitable for practical application.

Many phenomena are so involved as to practically defy theoretical analysis and are investigated in hydraulics on the sole basis of experimental measurement, the results being expressed in empirical formulas. Thus, hydraulics can be called a semiempirical science.

At the same time it is an applied, engineering, science insofar as it emerged from the demands of life and is widely used in engineering. Hydraulics provides the methods of calculating and designing a wide range of hydraulic structures (dams, canals, weirs and pipelines for transporting fluids), machinery (pumps, turbines, fluid couplings) and other devices used in many branches of engineering, in machine-tool design, foundry practice, the manufacture of plastics, etc. Modern aircraft design, with its fluid drives, fuel and lubricating systems, hydraulic shock absorbers, etc., relies extensively on the science of hydraulics.

2. HISTORICAL BACKGROUND

The emergence of hydraulics as a science followed the discovery of certain laws and the elucidation of a number of problems connected with the equilibrium and motion of fluids.

In the second half of the fifteenth century Leonardo da Vinci studied questions of hydraulic engineering. In his paper *On the Flow of Water and River Structures* he set forth his observations and experience gained in the construction of hydraulic installations in Milan, Florence and other places. In 1612 there appeared Galileo's *Discorso intorno alle cose che stanno su l'acqua* which contained the first systematic study of the fundamentals of hydrostatics. In 1643, Galileo's pupil Torricelli enunciated the law of free flow of liquids through orifices. In 1650 was discovered the law of the pressure distribution in a liquid, known as Pascal's law. The important law of friction in a moving fluid was formulated, in approximate form, by Isaac Newton; to him also goes the credit of introducing the concept of fluid viscosity and of laying the foundations of the theory of hydrodynamic similarity.

These, however, were only isolated laws and problems, and until the mid-eighteenth century there existed no comprehensive science of the behaviour of fluids. The theoretical foundations of fluid mechanics and hydraulics as a science were laid by Daniel Bernoulli and Leonhard Euler in the eighteenth century.

Daniel Bernoulli (1700-1782) belonged to a famous Swiss family from which came eleven celebrated scientists, most of them mathematicians or mechanics. As member of the then new Russian Academy of Sciences he spent much of his life in St. Petersburg. Later

he was elected to honorary membership of the Academy. Between 1728 and 1778 Bernoulli published 47 papers on mathematics, mechanics and other subjects in publications of the Russian Academy. In 1738, in his *Hydrodynamics* Bernoulli formulated the fundamental law of fluid motion giving the relation between pressure, velocity and head of a fluid. The Bernoulli equation is one of the bedrocks of fluid mechanics in general and hydraulics in particular.

The celebrated mathematician, physicist and astronomer Leonhard Euler (1707-1783), also of Swiss parentage, lived in St. Petersburg for many years, where he worked at the Russian Academy. In 1755 he developed the general differential equations of flow for so-called ideal (nonviscous) fluids, integration of which gives the Bernoulli equation as a partial solution. This marked the beginning of the theoretical method of analysis in fluid mechanics.

Euler is also credited with the general equation of work for all rotodynamic hydraulic machines (turbines, centrifugal pumps and fans) and with laying the foundations of the theory of buoyancy.

In his work Euler kept in contact with the great Russian scientist Mikhail Lomonosov and was undoubtedly influenced by him. Lomonosov is known to have studied many physical problems having a direct bearing on the flow of liquids and gases and he showed considerable interest in engineering hydraulics. The works of Bernoulli, Euler and Lomonosov concluded the first period in the development of hydraulics by laying its foundations as a science.

The second period, embracing the latter part of the eighteenth and most of the nineteenth centuries, is characterised chiefly by the accumulation of experimental data on the flow of fluids in open and closed channels and the determination of correction factors for the Bernoulli equation. As to the theoretical research of that time, it was based on the ideal fluid concept and could not meet all practical requirements as it failed to take into account such an important property as viscosity.

The second period of hydraulics is associated with the names of such celebrated experimentalists as Antoine Chezy, Henri Darcy and Jean Poiseuille in France, Julius Weisbach and G. Hagen in Germany and many others. Especially thorough and comprehensive in scope were Weisbach's (1806-1871) experiments, and his empirical formulas were in wide use up till the very latest years. Among the outstanding theoreticians in the sphere of fluid mechanics of the period were Lagrange, Helmholtz and Saint-Venant.

In the next period, commencing at the turn of the century, the theoretical basis of hydraulics was further extended by taking into account the viscosity of fluids; the theory of similarity and other theoretical and practical problems were elaborated. This period

in the development of hydraulics, as of other engineering disciplines, gained impetus from the rapid expansion of the productive forces and technological progress. It is associated with the names of George Stokes (1819-1903), Osborne Reynolds (1842-1912), Nikolai Joukowski (1847-1921), N. Petrov (1836-1920) and others. Stokes laid the foundations of the theory of fluid flow taking into account viscosity and elaborated other theoretical problems.

Reynolds is credited with establishing the criteria of similarity, which made it possible to summarise and systematise the vast amount of experimental data that had been accumulated by then. He was also the first to study turbulent flow, the most complex type of fluid motion.

In Russia, Professor N. P. Petrov's classical experiments proved the validity of Newton's law of friction in a fluid, till then treated as hypothetical. This served as the basis for his theory of machine lubrication, which played an important part in the further investigation of that question.

Of tremendous importance for the development of hydraulics were the works of the great Russian scientist Nikolai Joukowski. In the first period of his versatile and extremely fruitful studies (the nineteen-eighties and nineties), before he took up aerodynamics, Joukowski published several papers on hydraulics which brought him world-wide fame.

His major work in the field is his investigation of so-called water hammer in pipelines, a cause of many breakdowns. Not only did he develop the theory of the complex phenomenon caused by the sudden closure of a valve, turbine gate or faucet, but he also carried out many experiments at the Moscow waterworks which confirmed his theory and ensured its practical application. The treatise was soon translated into many languages and Joukowski's water-hammer theory is today included in all textbooks on hydraulics.

Joukowski laid the foundations of the theory of flow of ground water (the theory of percolation), also in connection with the needs of the Moscow waterworks. He developed the basic equations of ground-water flow and obtained results of practical importance. Joukowski studied problems of liquid flow through orifices, the theory of lubrication, velocity distribution in water mains, the reaction of fluid jets and vibration of fluids, and he established the analogy between wave formation on a liquid surface and pressure jump in air at supersonic speeds.

Joukowski's interest in hydraulics, one of his pupils writes, lasted till the end of his life. Joukowski can be regarded as the founder of the school in hydraulics which combines theoretical and experimental findings and carries research to the stage where it yields practical results.

This combination of the methods of theoretical fluid mechanics and experimental hydraulics and the growing tendency towards the merging of the two formerly isolated disciplines, with their entirely different methods, is one of the characteristic features of modern hydraulics.

In speaking of contemporary hydraulics, the names of Ludwig Prandtl, Theodor von Kármán and Johann Nikuradse should be mentioned first. Prandtl and Kármán, who are famous for their researches in fluid mechanics and aerodynamics, contributed substantially to the theory of turbulent flow, while Nikuradse, who worked in contact with them, carried out many laboratory experiments on flow in pipes, the results of which are widely known.

The construction of huge hydroelectric plants, canals and pipelines and the development of hydraulic machinery confronted Soviet scientists and hydraulic engineers with more and more new problems which had to be studied and solved for practical needs.

An important part in the development of the theory and calculation of hydraulic structures was played by the works of Academician N. N. Pavlovsky, one of the founders of the Soviet school of hydraulics. His numerous works in various spheres of hydraulics, especially on flow in open channels and the theory of seepage, represent an outstanding contribution to science.

Credit for the development of the Soviet school of hydraulics also goes to Academician L. S. Leibenzon and his pupils. Their works deal mainly with the hydraulics of highly viscous fluids, petroleum hydraulics and the theory of percolation (ground-water hydraulics).

Major contributions in other spheres of general hydraulics and its specialised branches have been made by the eminent Soviet scientists—Academicians S. A. Chaplygin, A. N. Kolmogorov and S. A. Khristianovich, Professors A. N. Akhutin, I. I. Agroskin, M. A. Velikanov, L. G. Loitsyansky, M. D. Chertousov, I. A. Charny and others.

Soviet scientists and engineers have achieved marked success in hydraulic engineering. Soviet hydroturbine construction owes much to Professors I. N. Voznesensky, N. N. Kovalyov and I. I. Kukolevsky. The great advances in this branch of Soviet engineering are reflected in the design and manufacture of turbines for the world's biggest hydroelectric stations.

The successful launchings of manned spaceships present another spectacular example of the great achievements of Soviet science. Their orbiting required powerful multistage rockets, in the construction of which hydraulic engineers took part together with scientists and engineers of other fields.

3. FORCES ACTING ON A FLUID. PRESSURE

In hydraulics, a fluid is treated as a continuum, i. e., a continuous medium filling a portion of space completely, without having any empty spaces. Thereby the molecular structure of matter is neglected and even infinitely small fluid particles are assumed to consist of a great number of molecules.

As a fluid will always yield with time to the slightest stress, it cannot be subject to concentrated forces. Any force acting upon a fluid is distributed uniformly throughout the volume (mass) or along the surface. Accordingly, the external forces acting on any given volume of fluid may be body or surface forces.

Body forces are proportional to the mass or, for homogeneous substances, the volume of the fluid. They arise, first of all, from the force of gravity and the forces produced in a fluid at rest inside an accelerated vessel or flowing in a channel which itself is moving with an acceleration. Body forces also appear as the "effective" D'Alembert forces in developing equations of fluid motion.

Surface forces are distributed continuously over the whole surface of a fluid and, in the case of uniform distribution, are proportional to the surface area. These forces are due to the direct action of all the surrounding fluid on a given volume or to the action of other bodies (solid, liquid or gaseous) in contact with the given fluid.

In the most general case, a surface force ΔR acting on a given area ΔS may be directed at an angle to that area and it can be resolved into a normal component ΔP and a tangential component ΔT (Fig. 1). The former is called the *pressure force*, the latter is the *friction, or shear, force*.

Both body and surface forces are usually considered as unit forces, i. e., they are referred to the corresponding units: body force to a unit mass and surface force to a unit area. As body force equals the product of mass times acceleration, a body force acting on a unit mass is numerically equal to the respective acceleration.

By *hydrostatic pressure* (often referred to as simply "pressure") is meant the pressure force exerted on a unit area. If the pressure force is uniform over the area, or if the mean value of the hydrostatic pressure is required, the latter is given by the formula

$$p=\frac{\Delta P}{\Delta S}\ \text{kg/m}^2. \tag{1.1}$$

In the most general case the hydrostatic pressure at a point corresponds to the limiting value of the ratio $\Delta P/\Delta S$ as the elementary area ΔS shrinks to differential value at this point:

$$p=\lim_{\Delta S\to 0}\frac{\Delta P}{\Delta S}. \tag{1.2}$$

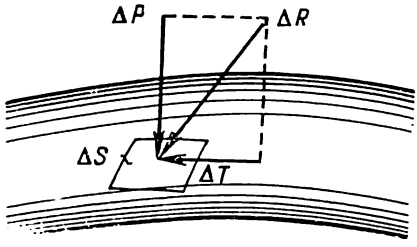

Fig. 1. Components of a surface force

If pressure is measured above absolute zero, it is called *absolute* pressure. If it is measured either above or below atmospheric pressure as a base, it is called *gauge* pressure. Hence, absolute pressure p_{ab} equals atmospheric, or barometric, pressure p_{atm} plus gauge pressure p_g:

$$p_{ab} = p_{atm} + p_g.$$

A unit of pressure commonly used in engineering is the standard atmosphere:

$$1 \text{ atm} = 1 \text{ kg/cm}^2 = 10{,}000 \text{ kg/m}^2 = 14.22 \text{ lb/in}^2.$$

The *shear stress*, or friction force, in a liquid is denoted by the Greek letter τ (tau) and, like pressure, is given by the limit

$$\tau = \lim_{\Delta S \to 0} \frac{\Delta T}{\Delta S}. \tag{1.3}$$

4. PROPERTIES OF LIQUIDS

In this course of hydraulics we shall be concerned mainly with liquids, therefore we shall begin with an examination of their basic physical properties.

We shall accept the following definitions and symbols. The *specific weight* of a liquid is its weight per unit volume:

$$\gamma = \frac{G}{W} \text{ kg/m}^3, \tag{1.4}$$

where G = weight of the liquid;
W = volume of the liquid.

Specific weight, thus, has dimension and its value depends on the units employed. The specific weight of water at 4°C, for example, is

$$\gamma = 1{,}000 \text{ kg/m}^3 = 0.001 \text{ kg/cm}^3.$$

The *density* of a liquid is its mass per unit volume:

$$\varrho = \frac{M}{W} \text{ kg-sec}^2/\text{m}^4. \tag{1.5}$$

where M = mass of the given volume W of the liquid.

Specific weight and density are related as follows (remembering that $G = (gM)$:

$$\varrho = \frac{G}{gW} = \frac{\gamma}{g}. \tag{1.6}$$

For a nonhomogeneous liquid, formulas (1.4) and (1.5) give the average specific weight and density, respectively. To determine the absolute values of γ and ϱ at any point, the volume must be regarded as tending to zero and the limit of the corresponding ratio calculated.

The *specific gravity* δ of a liquid is the ratio of its specific weight to that of water at 4°C:

$$\delta = \frac{\gamma_{liquid}}{\gamma_{water}}. \tag{1.7}$$

We shall discuss briefly the following physical properties of liquids: compressibility, thermal expansion, tensile strength, viscosity and evaporability.

1. *Compressibility* characterises the ability of a fluid to change its volume under pressure. The relative change of volume per unit pressure is given by the *coefficient of compressibility*:

$$\beta_p = -\frac{1}{W}\frac{dW}{dp} \text{ cm}^2/\text{kg}. \tag{1.8}$$

The minus sign is due to the fact that a positive pressure increment results in a negative volume increment, i. e., an increase in pressure causes a decrease in volume.

The reciprocal of the coefficient of compressibility is called the *volume*, or *bulk*, *modulus of elasticity*. Expressing volume in terms of density, we obtain instead of Eq. (1.8)

$$K = \varrho\frac{dp}{d\varrho} \text{ kg/cm}^2.$$

The volume modulus of liquids increases somewhat with temperature and pressure. Thus, for water it rises from $K = 18{,}900$ kg/cm^2, at $t=0$°C and $p=5$ kg/cm^2, to $K=22{,}170$ kg/cm^2, at $t=20$°C and $p=5$ kg/cm^2, the mean value being $K=20{,}000$ kg/cm^2. Consequently, when the pressure is increased by 1 kg/cm^2, the volume of water decreases by only 1/20,000 th. The volume modulus of other liquids is of the same order, and in the overwhelming majority of cases liquids are treated as practically incompressible and their specific weight γ as being independent of pressure.

2. *Thermal expansion* is characterised by the relative change in volume when the temperature increases by 1°C:

$$\beta_t = \frac{1}{W}\frac{dW}{dt}. \tag{1.9}$$

For water β_t increases with pressure and temperature from 14×10^{-6}, at 0°C and 1 kg/cm^2, to 700×10^{-6}, at 100°C and 100 kg/cm^2.

For oil products β_t may be from half again as much to twice that of water.

3. The *tensile strength* of liquids is negligible. Thus, the required stress for water rupture is 0.00036 kg/cm^2, and even this grows smaller with the temperature increasing. If a tensile load is of very short duration the resistance may be greater, but for practical purposes liquids are assumed to be incapable of resisting any direct tensile stress.

Liquid surfaces are subjected to *surface tension*, which tends to collect a liquid volume into a sphere and which accounts for a certain additional pressure in liquids. This pressure, however, is manifest only when the working dimensions are small. In narrow tubes it causes a liquid to rise above (or drop below) the surface level, producing the so-called *capillary* or *meniscus* effect. Capillary rise (or depression) in a glass tube of diameter d is determined by the equation

$$h = \frac{k}{d} \text{ mm}, \tag{1.10}$$

where the value of k, in sq mm, is + 30 for water, — 14 for mercury and + 12 for alcohol.

The three properties of real liquids considered above are of small importance in hydraulics as they are usually manifest to a very small degree. The reverse is true of the following property of liquids, viscosity.

4. *Viscosity* is the property of a fluid to resist the shearing or sliding of its layers. This displays itself in the appearance, under certain conditions, of shearing stresses. Viscosity is the reciprocal of fluidity; viscous liquids, such as glycerine and lubricants, are less fluid, and vice versa.

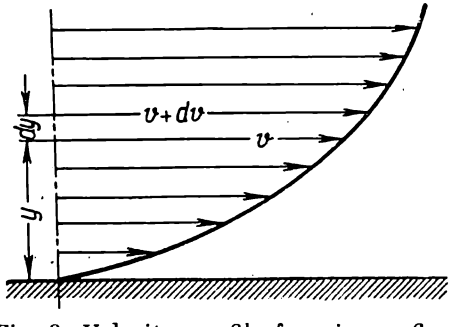

Fig. 2. Velocity profile for viscous flow along a wall

When a viscous liquid flows along a solid boundary, there takes place a change in the velocity across the flow due to viscosity (Fig. 2). The velocity v of the moving layers is the lower the closer they are to the solid boundary; at $y = 0$, $v = 0$. Thus, the different layers are moving with respect to each other and shear, or friction, forces appear.

According to the hypothesis first formulated by Isaac Newton in 1686, and proved experimentally by Prof. N. P. Petrov in 1883, shear strain depends on the fluid and the type of flow; in laminar flow it is directly proportional to the so-called *velocity gradient* at right angles to the flow:

$$\tau = \mu \frac{dv}{dy} \text{ kg/m}^2, \tag{1.11}$$

where μ = *absolute*, or *dynamic*, *viscosity* of the fluid;
dv = velocity increment corresponding to the increment dy (see Fig. 2).

The velocity gradient dv/dy characterises the change of velocity per unit length in the y direction and, consequently, the intensity of shear in the liquid at the given point.

In the case when the shear stress is uniform over an area S, the total shearing strain (the frictional force) acting over that area is

$$T = \mu \frac{dv}{dy} S. \tag{1.12}$$

The dimension of absolute viscosity is obtained by solving Eq. (1.11) with respect to μ:

$$\mu = \frac{\tau}{\frac{dv}{dy}} \text{ kg-sec/m}^2.$$

In the CGS system the unit of viscosity is the *poise*:

$$1 \text{ poise} = 1 \text{ dyne-sec/cm}^2.$$

As 1 kg (force) = 981,000 dynes, and 1 sq m = 10^4 sq cm,

$$1 \text{ poise} = \frac{1}{98.1} \text{ kg-sec/m}^2.$$

Another characteristic of the viscosity of a fluid is its so-called *kinematic viscosity*:

$$\nu = \frac{\mu}{\varrho} \text{ m}^2/\text{sec}. \tag{1.13}$$

The name "kinematic" viscosity was suggested by the absence of a force dimension (kg) in it. The unit of kinematic viscosity is the *stoke*:

$$1 \text{ stoke} = 1 \text{ cm}^2/\text{sec}.$$

The viscosity of liquids depends to a great extent on temperature, decreasing when the latter increases (Fig. 3). In gases the reverse is

true, and viscosity increases with temperature. This is explained by the different nature of viscosity in liquids and gases.

In liquids, the molecules are much more tightly packed than in gases, and viscosity is due to molecular cohesion. The cohesive forces between molecules decrease with the temperature increasing, and viscosity decreases accordingly.

In gases, viscosity is due to the disorderly heat motion of molecules, the intensity of which increases with temperature. Therefore, the viscosity of gases increases with temperature.

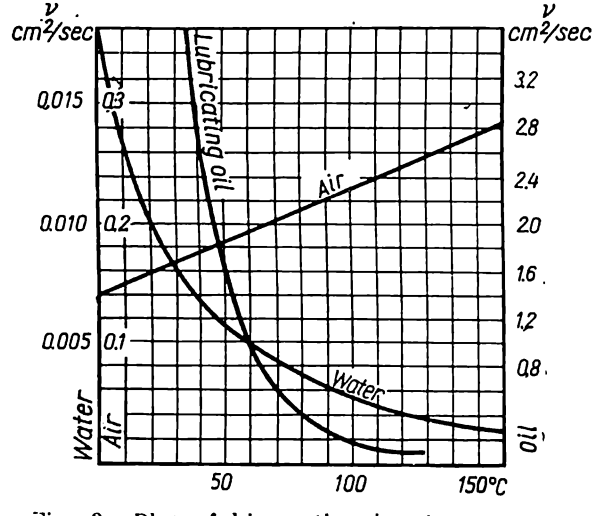

Fig. 3. Plot of kinematic viscosity ν versus temperature

The change in the dynamic viscosity μ of both liquids and gases caused by pressure is so small that it is usually neglected. It is taken into account only when extremely high pressures are involved. Hence, the shear stress in a fluid may also be regarded as being independent of absolute pressure.

It follows from Eq. (1.11) that shear stresses can appear only in a moving fluid, i. e., that the viscosity of a fluid is manifest only when it flows. In a fluid at rest there are no shear stresses.

The above considerations lead to the conclusion that the laws of friction in fluids due to viscosity are of an entirely different nature than the laws of friction of solid bodies.

5. *Evaporability* is characteristic of all liquids. Intensity of evaporation varies for different liquids and depends on specific conditions.

One of the indices characterising evaporation is the boiling temperature of a liquid at normal atmospheric pressure. The higher the boiling temperature, the less the rate of evaporation. In aircraft hydraulic systems one frequently has to deal with cases of evaporation and even boiling of liquids in closed circuits at different temperatures and pressures. Accordingly, a more general characteristic of vaporisation is used: the *saturation vapour pressure* p_t as a function of temperature. The higher the saturation pressure of a liquid at a given temperature, the higher the rate of evaporation.

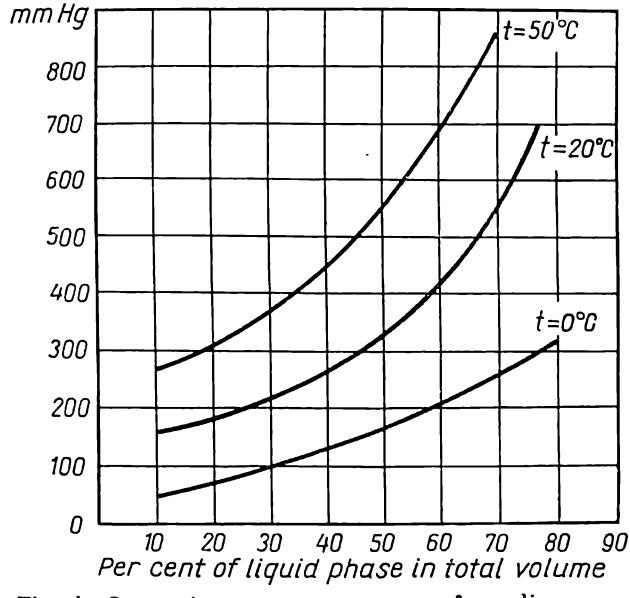

Fig. 4. Saturation vapour pressure of gasoline as a function of phase-temperature ratio

The saturation pressure of different liquids increases with temperature to a different extent.

For simple liquids the relationship $p_t = f(t)$ has a definite expression. For compound liquids, such as gasoline, the saturation pressure p_t depends not only on physico-chemical properties and temperature but also on the relative volumes of the liquid and vapour phases. The vapour pressure increases when the portion occupied by the liquid phase increases. Fig. 4 shows the dependency of the vapour pressure of gasoline on the liquid-to-vapour ratio for three temperature levels.

Table 1 on the next page presents the physical properties of some liquids employed in aircraft and rocket systems.

Table 1

Basic Physical Properties of Some Liquids Employed in Aircraft and Rocket Systems

Liquid	Specific gravity δ	Kinematic viscosity ν at temperature t, centistokes						Vapour pressure p_t, mm Hg			Volume modulus K, kg/cm²	
		+70°C	+50°C	+20°C	0°C	−20°C	−50°C	+60°C	+40°C	+20°C		
Aviation gasoline B95/130	0.750	—	0.54	0.73	0.93	1.26	2.60	—	195	90	13,300	
Kerosene T-1	0.800-0.850	1.2	1.5	2.5	4.0	8.0	25	59	27	11.5	13,000	
Kerosene T-2	0.775	—	—	1.05	2.0	—	5.5	—	100	—	13,000	
Lubricating oil MC-20	0.895	65	155	1,100	10,100	congeals						
Lubricating oil MK-8	0.885	—	8.3	30	—	498	—					
Hydraulic fluid AMG-10	0.850	7.5	10	16	42	130	1,250				13,300	
Nitric acid (98%)	1.510	0.30	0.38	0.58	0.70	0,83	1.72	355	156	60		
Ethyl alcohol	0.790	—	—	1.52	—	—	6.5	352	135	44		
Hydrogen peroxide (80%)	1.34	—	—	0.95	1.42	—	—	61.4	56.7	46.4		
Liquid oxygen	1.15-1.25	t	−175°C	−184°C	−190°C	−200°C	−204°C	t	−140°C	−160°C	−190°C	−200°
		ν cst	0.125	0.170	0.193	0.257	0.297	p_t atm	21	7	0.45	0.11

CHAPTER II

HYDROSTATICS

5. HYDROSTATIC PRESSURE

It was mentioned before that the only stress possible in a fluid at rest is that of compression, or *hydrostatic pressure*. The following two properties of hydrostatic pressure in fluids are important.

1. The hydrostatic pressure at the boundary of any fluid volume is always directed inward and normal to that boundary.

This property arises from the fact that in a fluid at rest no tensile or shear stresses are possible. Hydrostatic pressure can act only normal to a boundary, as otherwise it would necessarily have a tensile or shearing component.

By "boundary" is meant the real or imaginary surfaces of any elementary fluid body taken within a given volume.

2. The hydrostatic pressure at any point in a fluid is the same in all directions, i. e., pressure in a fluid does not depend on the inclination of the surface on which it is acting at a given point.

To prove this statement, imagine inside a fluid at rest an elementary body having the shape of a right-angled tetrahedron with three edges dx, dy and dz parallel to the respective axes of a coordinate system (Fig. 5).

Let there be acting near this elementary volume a unit body force whose components are X, Y and Z, let p_x, p_y and p_z be the respective hydrostatic pressures acting on the faces normal to the x, y and z axes, and let p_n

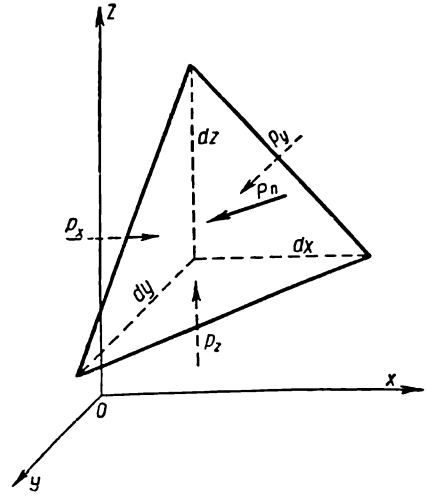

Fig. 5. Notation for studying hydrostatic pressure in a fluid

be the hydrostatic pressure on the inclined face of area dS. All the pressures are, of course, normal to the respective areas.

Now let us develop the equilibrium equation for the elementary volume parallel to the x axis. The sum of the projections of the pressure forces on axis ox is

$$p_x = p_x \frac{1}{2} dydz - p_n dS \cos(\widehat{p_n, x}).$$

The mass of a tetrahedron is equal to its volume times its density, i. e., $\frac{1}{6} dxdydz\varrho$; hence the body force acting on the tetrahedron parallel to the x axis is

$$F_x = \frac{1}{6} dxdydz\varrho X.$$

The equilibrium equation for the tetrahedron takes the form

$$\frac{1}{2} dydzp_x - p_n dS \cos(\widehat{p_n, x}) + \frac{1}{6} dxdydz\varrho X = 0.$$

Dividing through by $\frac{1}{2} dydz$ [which is the projection of the area of the inclined face dS on plane yOz and is therefore equal to $dS \cos(\widehat{p_n, x})$], we have

$$p_x - p_n + \frac{1}{3} dx \varrho X = 0.$$

When the tetrahedron is made to shrink infinitely, the last member of the equation, which contains the term dx, will tend to zero, the pressures p_x and p_n remaining finite.

Hence, in the limit

$$p_x - p_n = 0,$$

or

$$p_x = p_n.$$

Developing similar equations for equilibrium parallel to the y and x axes, we obtain

$$p_y = p_n \text{ and } p_z = p_n,$$

or

$$p_x = p_y = p_z = p_n. \tag{2.1}$$

As the dimensions dx, dy and dz of the tetrahedron were chosen arbitrarily, the inclination of face dS is also arbitrary, and, consequently, when the tetrahedron shrinks to a point the pressure at that point is the same in all directions.

This can also be proved very easily by means of the formulas of strength of materials for compression stresses acting along two and three mutually perpendicular directions.* For this we only have to assume the shearing stress in these formulas equal to zero, and we obtain

$$\sigma_x = \sigma_y = \sigma_z = -p.$$

These two properties of hydrostatic pressure, which were proved for a fluid at rest, also hold good for ideal fluids in motion. In a real moving fluid, however, shearing stresses are developed which were not taken into account in our reasoning. That is why, strictly speaking, hydrostatic pressure does not display these properties in a real fluid.

6. THE BASIC HYDROSTATIC EQUATION

Let us consider the basic case of equilibrium of a fluid when the only body force acting on it is the force of gravity and develop an equation which would enable us to determine the hydrostatic pressure at any point of a given fluid volume. In this case, of course, the free surface of a liquid is a horizontal plane.

Referring to Fig. 6, acting on the free surface of the liquid in the vessel is a pressure p_0. Let us determine the hydrostatic pressure p at an arbitrary point M at a depth h from the surface.

Taking an elementary area dS with point M as its centre, erect a vertical cylindrical fluid element of height h and consider the equilibrium conditions for this element. The pressure of the liquid on the base of the cylinder is external with respect to the latter and is normal to the base, i. e., it is directed upward.

Summing the forces acting vertically on the cylinder, we have

$$p\,dS - p_0\,dS - \gamma h\,dS = 0,$$

where the last term represents the weight of the liquid in the cylinder. The pressure forces acting on the sides of the cylinder do not enter the equation as they are normal to the side surface. Eliminating dS and transposing,

$$p = p_0 + h\gamma. \tag{2.2}$$

This is the *hydrostatic equation* with which it is possible to calculate the pressure at any point of a still liquid. The hydrostatic

---

* These equations have the form:

$$\sigma_n = \sigma_x \cos^2 \varphi + \sigma_y \sin^2 \varphi; \quad \tau = \frac{1}{2}(\sigma_x - \sigma_y) \sin 2\varphi.$$

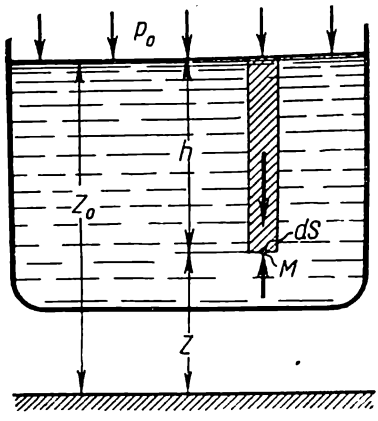

Fig. 6. Notation for developing the basic hydrostatic equation

pressure, it will be observed, is composed of the external pressure p_0 acting on the boundary surface of the liquid and the pressure exerted by the weight of the overlying layers of the liquid.

The value of p_0 is the same for any point of a liquid volume. Therefore, taking into account the second property of hydrostatic pressure, it may be said that a liquid transmits pressure *equally* in all directions (Pascal's law).

It will be also observed from Eq. (2.2) that pressure in a liquid increases with depth according to a linear law and is the same for all points at a given depth.

A surface layer where the pressure is the same at all points is called a *surface of equal pressure*, or *equipotential surface*. In the case considered the equipotential surfaces are horizontal planes, the free surface being one of them.

Let us take at an arbitrary elevation a horizontal datum level from which a vertical coordinate z is to be measured. Denoting the coordinate of point M as z and the coordinate of the free surface of the liquid as z_0, and substituting $z_0 - z$ for h in Eq. (2.2), we obtain

$$z + \frac{p}{\gamma} = z_0 + \frac{p_0}{\gamma}.$$

But M is an arbitrary point, hence, for the stationary fluid element

$$z + \frac{p}{\gamma} = \text{const}. \tag{2.3}$$

The coordinate z is called the *elevation*. The term $\frac{p}{\gamma}$, which is also a linear quantity, is called the *pressure head*, and the sum $z + \frac{p}{\gamma}$ is called the *piezometric head*.

The piezometric head is thus constant for the whole volume of a stationary fluid.

These results can be obtained in more definite form by integrating the differential equilibrium equations for a fluid (see Appendix).

7. PRESSURE HEAD. VACUUM. PRESSURE MEASUREMENT

The pressure head $\frac{p}{\gamma}$ represents the height of a column of a given liquid referred to a given absolute or gauge pressure p. The pressure

head referred to gauge pressure can be measured with a so-called piezometer, which is the simplest device for measuring pressure. A piezometer is a vertical glass tube the upper end of which is open to the atmosphere while the lower end is connected to a small hole in the wall of a liquid container (Fig. 7).

Applying Eq. (2.2) to the liquid in the piezometer, we obtain

$$p_{ab} = p_{atm} + h_p\gamma,$$

where p_{ab} = absolute pressure of the liquid at the level of the attached end of the piezometer;

p_{atm} = atmospheric pressure.

From this, the height of the liquid in the piezometer is

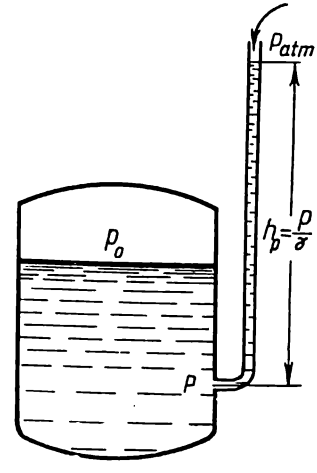

Fig. 7. Piezometer tapped to a tank

$$h_p = \frac{p_{ab} - p_{atm}}{\gamma} = \frac{p_g}{\gamma}, \qquad (2.4)$$

where p_g = gauge pressure at the same level.

Obviously, if the free surface of a still liquid is subjected to atmospheric pressure, the pressure head at any point of the liquid is equal to the depth of that point.

Pressure in fluids is often expressed numerically in terms of head according to Eq. (2.4). One atmosphere, for example, corresponds to:

$$h_1 = \frac{p}{\gamma_{water}} = \frac{10,000}{1,000} = 10 \text{ m of water;}$$

$$h_2 = \frac{p}{\gamma_{mercury}} = \frac{10,000}{13,600} = 0.735 \text{ m of mercury.}$$

If the absolute pressure in a fluid is less than atmospheric, we have a partial or complete *vacuum*. The magnitude of a vacuum is measured as the difference between the atmospheric and absolute pressures:

$$p_{vac} = p_{atm} - p_{ab},$$

or

$$h_{vac} = \frac{p_{atm} - p_{ab}}{\gamma}.$$

Take, for example, a tube with a tightly fitting piston, lower one end of it into a container with a liquid and then draw the piston up (Fig. 8). The liquid will follow the piston and rise together with it to some height h above the free surface, which is subject to atmospheric pressure. For the points immediately under the piston the depth

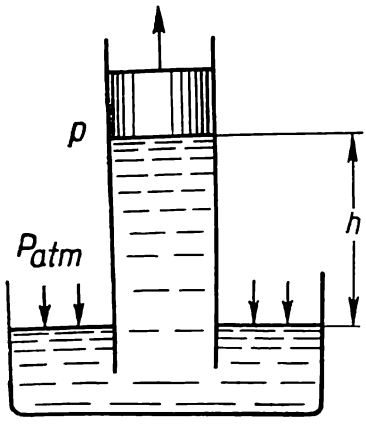

Fig. 8. Liquid drawn into cylinder by a piston

with respect to the free surface is negative. Hence, from Eq. (2.2), the absolute pressure in the liquid below the piston is

$$p = p_{atm} - h\gamma, \qquad (2.5)$$

and the vacuum is

$$p_{vac} = p_{atm} - p = h\gamma,$$

or

$$h_{vac} = \frac{p_{atm} - p}{\gamma} = h.$$

As the piston rises the absolute pressure in the liquid decreases. The lower limit for the absolute pressure is zero; the maximum value of vacuum is numerically equal to atmospheric pressure. Hence, the maximum elevation of the liquid in our example, i. e., the maximum height of suction, can be found from Eq. (2.5), assuming $p = 0$ (or, more precisely, $p = p_t$).

Thus, neglecting the vapour pressure p_t, we have

$$h_{max} = \frac{p_{atm}}{\gamma}.$$

At normal atmospheric pressure (1.033 kg/cm^2) the height h_{max} is 10.33 m for water, 13.8 m for gasoline ($\gamma = 750$ kg/m^3) and 0.76 m for mercury.

The simplest device for measuring vacuum, or negative pressure, is a glass U-tube arranged either with one end open, like the right-hand tube in Fig. 9, or inverted with the free end submerged in a liquid, like the left-hand tube.

In laboratories, besides piezometers, various manometers and mechanical gauges are used to measure the pressure of liquids and gases.

The U-tube manometer (Fig. 10*a*) has the bend of a transparent tube filled with mercury or, if the pressures are small, alcohol, water or tetrabromo-ethane ($\delta = 2.95$). If the pressure of a liquid is measured at a point M and the connecting tube is filled with the same liquid, the elevation of the manometer above M must be taken into account. Thus, the gauge pressure at point M is

$$p_M = h_1\gamma_1 + h_2\gamma_2.$$

A modification of the U-tube manometer in which one limb is widened (Fig. 10*b*) is more convenient as only one level of the work-

ing liquid has to be read. When the diameter of the wider limb is appreciably greater than that of the tube, the level in the former can be regarded as constant. For very small pressures of gas and greater

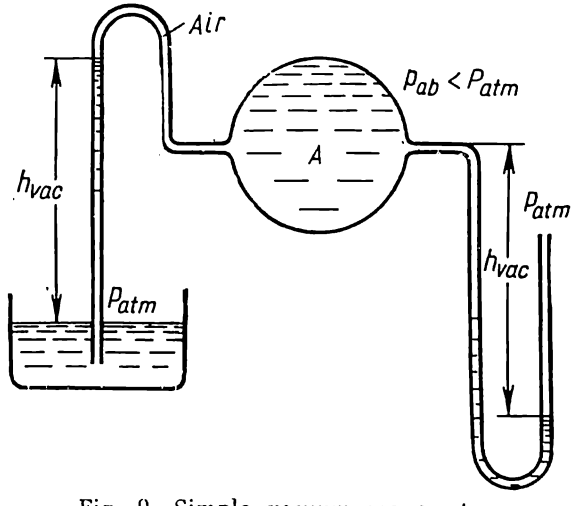

Fig. 9. Simple vacuum manometers

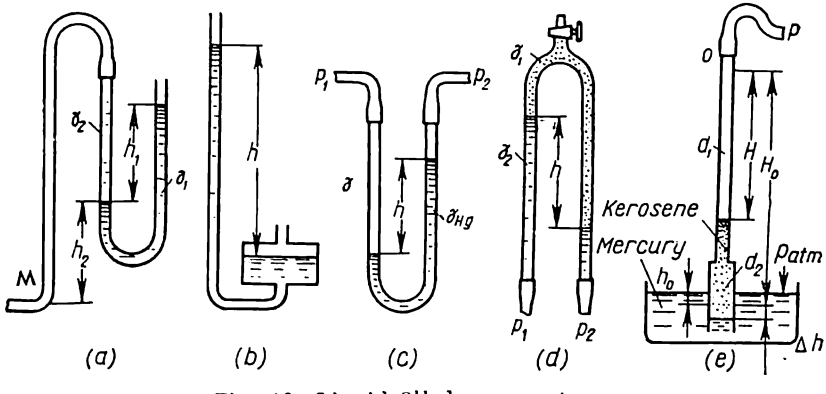

Fig. 10. Liquid-filled manometers

accuracy the manometer tube is inclined to the horizontal. The length of the column of liquid is inversely proportional to the sine of the angle of inclination, the accuracy of reading improving accordingly.

Differences of pressure at two points are measured with differential manometers, the simplest of which is the U-tube (Fig. 10*c*). When such a manometer, with mercury in the bend, is used to meas-

ure the difference between pressures p_1 and p_2 in a liquid of specific weight γ which completely fills the connecting limbs, we have

$$p_1 - p_2 = h(\gamma_{Hg} - \gamma).$$

For measuring small pressure differentials of water an inverted U-tube is used with oil or kerosene filling the upturned bend(Fig. 10*d*). For this case we have

$$p_1 - p_2 = h(\gamma_2 - \gamma_1).$$

The well-type manometer in Fig. 10*e* is designed for measuring air pressures or vacuums from about 0.1 to 0.5 atm. An alcohol or water manometer would require a very high column, making it unwieldy, while a mercury-filled manometer would be inaccurate due to the low column of mercury. This type of manometer is used in high-speed wind tunnel tests.

The well is filled with mercury and the tube with alcohol, kerosene or some other liquid. Kerosene is especially convenient due to its low rate of evaporation. A judicious selection of the diameters of the upper and lower portions of the tube (d_1 and d_2) enables any effective specific weight γ_{ef} to be obtained from the equation

$$p = H\gamma_{ef},$$

where p = measured pressure or vacuum;
H = manometer reading.

The expression for γ_{ef} is obtained from the following equations (see Fig. 10*e*):

$$H_0\gamma_k = h_0\gamma_{Hg},$$

which is the equilibrium equation for the mercury and kerosene columns at $p = p_{atm}$;

$$p + (H_0 - H + \Delta h)\gamma_k = (h_0 + \Delta h)\gamma_{Hg},$$

which is the equilibrium equation at $p > p_{atm}$; and

$$H d_1^2 = \Delta h d_2^2,$$

which is the equation of volumes (the volume of the kerosene moving from the upper tube d_1 to the lower tube d_2 is equal to the volume of the displaced mercury).

Substituting and transposing, we obtain

$$\gamma_{ef} = \frac{d_1^2}{d_2^2}\gamma_{Hg} + \left(1 - \frac{d_1^2}{d_2^2}\right)\gamma_k.$$

At $d_2 = 2d_1$, for example, $\gamma_{ef} = 0.25 \times 13{,}600 + 0.75 \times 800 = 4{,}000$ kg/m^3.

Pressures higher than two or three atmospheres are measured with mechanical gauges of the Bourdon-tube or diaphragm type. Their action is based on the deflection of a hollow tube, diaphragm or bellows caused by the applied pressure. The deflection is transmitted through a suitable mechanism to a needle which indicates the pressure on a dial.

In aircraft systems manometers are used to measure the pressure of fuel supplied to the injectors of a gas turbine engine or to the carburettor of a reciprocating engine, the pressure of oil in the lubricating system, etc.

The most widely used in aircraft systems is the electrical manometer, as well as different types of mechanical gauges. The sensor element of an electrical manometer is a diaphragm which deflects under the applied pressure and actuates the slide of a potentiometer.

8. FLUID PRESSURE ON A PLANE SURFACE

The total pressure on a plane surface inclined at an arbitrary angle α to the horizontal (Fig. 11) can be determined with the help of the hydrostatic equation (2.2). For this calculate the pressure P of the fluid on any portion of the surface of arbitrary outline of area S. The x axis is directed along the line of intersection of the plane with the free surface, and the y axis is perpendicular to that line in the given plane.

The elementary pressure on a differential area dS is

$$dP = p\,dS = (p_0 + h\gamma)\,dS = p_0 dS + h\gamma\,dS,$$

where p_0 = pressure on the free surface;

h = depth of the area dS.

To determine the total pressure P, integrate over the whole area S:

$$P = p_0 \int_S dS + \gamma \int_S h\,dS =$$

$$= p_0 S + \gamma \sin\alpha \int_S y\,dS,$$

where y = distance of the centre of the area dS from the x axis.

The quantity $\int_S y dS$, it will be recalled from the course in mechanics, is the

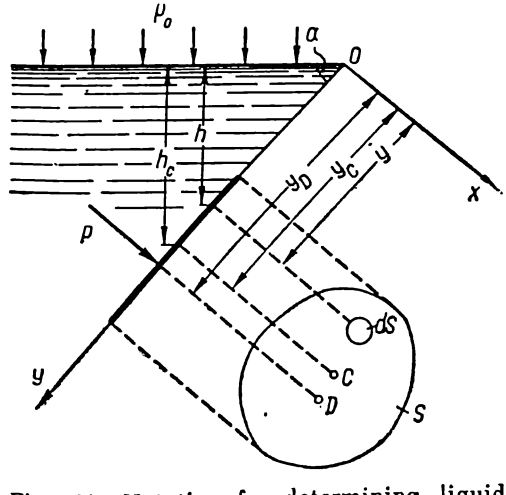

Fig. 11. Notation for determining liquid pressure on a plane surface (side elevation and plan)

moment of the area S about the axis Ox and is equal to the product of the area and the distance y_C of its centre of gravity from that axis. Hence,

$$\int_S y\, dS = y_C S,$$

whence

$$P = p_0 S + \gamma \sin\alpha\, y_C S = p_0 S + \gamma\, h_C S,$$

where h_C = depth of submersion of the centre of gravity; and finally

$$P = (p_0 + \gamma\, h_C)\, S = p_C S, \tag{2.6}$$

i.e., *the total pressure of a liquid on a plane area is equal to the product of the area and the static pressure at its centre of gravity.*

If the pressure p_0 is atmospheric, the gauge pressure of the liquid on a plane surface is

$$P_g = h_C \gamma\, S = p_{Cg} S. \tag{2.6'}$$

The *centre of pressure*, which is the point of application of the resultant force on the area, is found as follows.

As the external pressure p_0 is transmitted equally to all points of the area S, its resultant is applied at the centre of gravity of the area. The location of the point of application of the resultant gauge pressure (point D) is found from the well-known equation of mechanics which states that the moment of a resultant about an axis Ox is equal to the sum of the moments of the component forces about that axis, i.e.,

$$P_g y_D = \int_S y\, dP_g,$$

where y_D = distance of the point of application of force P_g from the x axis.

Expressing P_g and dP_g in terms of y_C and y to determine y_D, we have

$$y_D = \frac{\gamma \sin\alpha \int_S y^2 dS}{\gamma \sin\alpha\, y_C S} = \frac{J_x}{y_C S},$$

where $J_x = \int_S y^2 dS$ = moment of inertia of the area S about the axis Ox.

Taking into account that

$$J_x = J_{x0} + y_C^2 S,$$

where J_{x_0} = moment of inertia of the area S about its own centre

line parallel to Ox, we finally obtain

$$y_D = y_C + \frac{J_{x0}}{y_C S}. \tag{2.7}$$

Thus, the point of application of force P_g is located below the centre of gravity of the area at a distance

$$\Delta y = \frac{J_{x0}}{y_C S}.$$

If p_0 is equal to atmospheric pressure and if it acts on both sides of the surface, point D will be the centre of pressure. If p_0 is greater than atmospheric pressure, the centre of pressure is found according to the laws of mechanics as the point of application of the resultant of forces P_g and $p_0 S$. The greater the latter force as compared with the former the closer, apparently, is the centre of pressure to the centre of gravity of the area S.

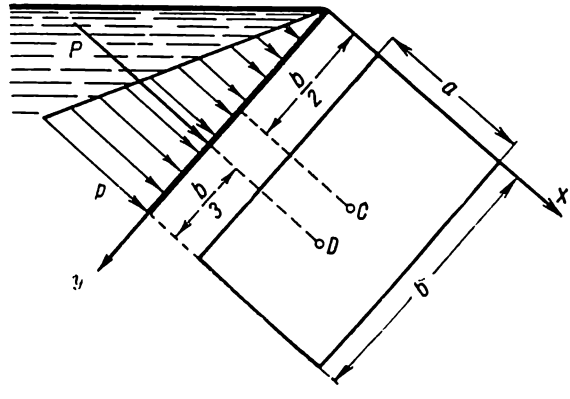

Fig. 12. Pressure distribution on a rectangular wall

To determine the second coordinate x_D of the centre of pressure, the moment equation should be written with respect to the y axis.

In the special case when the surface is a rectangle with one side in the free surface of the liquid the centre of pressure is located very simply. As the pressure diagram for the forces acting on a submerged surface represents a right-angled triangle (Fig. 12) whose centre of gravity is located at 1/3 the altitude b of the triangle, the centre of pressure will also be located at 1/3 b from the lower edge of the rectangle.

In engineering we often have to deal with the pressure of fluids on plane surfaces, e.g., against pistons in various hydraulic machines

and devices (see examples and Chapter XIV). In these cases the pressure p_0 is usually so great that the centre of pressure may be assumed to coincide with the centre of gravity of the area on which it is acting.

9. FLUID PRESSURE ON CYLINDRICAL AND SPHERICAL SURFACES. BUOYANCY AND FLOATATION

Problems involving the pressure of fluids on surfaces of arbitrary shape are rather difficult as they require the determination of three components of the total force and three moments. Fortunately, such cases are not so frequently encountered in practice. Usually we have to deal with cylindrical or spherical surfaces having a vertical plane of symmetry. In this case the pressure can be reduced to a resultant in the plane of symmetry.

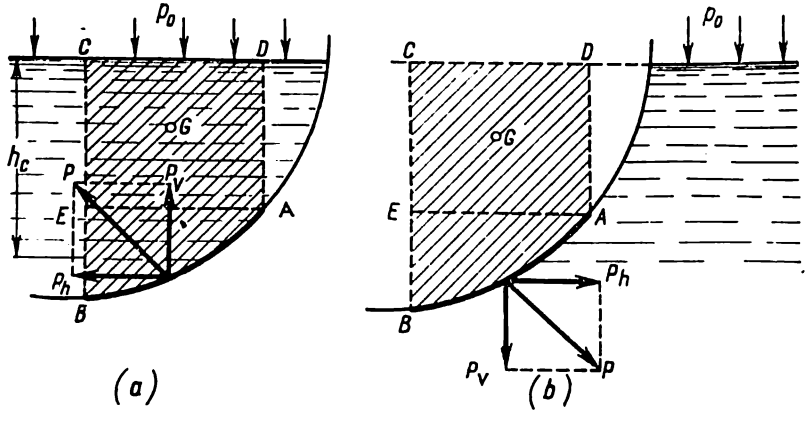

Fig. 13. Liquid pressure on a curved surface

Consider a curved surface AB whose generator is perpendicular to the page (Fig. 13). Two cases are possible: (a) the liquid lies above the surface and (b) the liquid lies below the surface.

Case (a): consider the liquid volume $ABCD$, where AB is the curved surface, BC and AD are vertical surfaces, and CD is the free surface of the liquid. Let us investigate the equilibrium conditions in the vertical and horizontal directions. If the liquid exerts a thrust P on surface AB, the latter can be said to be exerting an equal and oppositely directed force on the liquid. In Fig. 13 this reaction force is shown together with its horizontal and vertical components P_h and P_v.

The condition for the vertical equilibrium of the volume $ABCD$ is

$$P_v = p_0 S_h + G, \tag{2.8}$$

where p_0 = pressure acting on the free surface;
S_h = area of the horizontal projection of AB;
G = weight of the liquid in the volume under consideration.

In writing the condition for horizontal equilibrium account is taken of the fact that the thrust of the liquid on areas EC and AD is balanced and only the pressure on area BE (which is the vertical projection S_v of surface AB) remains:

$$P_h = S_v \gamma h_C + p_0 S_v. \quad (2.9)$$

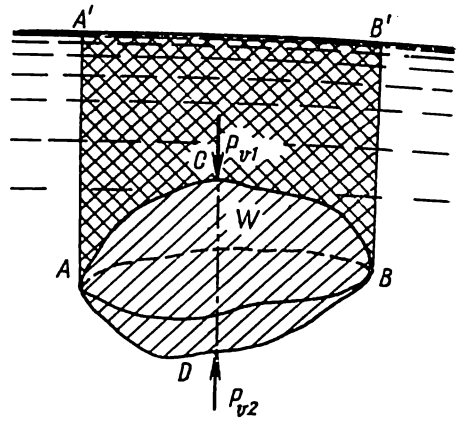

Fig. 14. Notation for proving Archimedes' law

Equations (2.8) and (2.9) give the vertical and horizontal components of the total pressure P, whence

$$P = \sqrt{P_v^2 + P_h^2}. \quad (2.10)$$

Case (b) (Fig. 13*b*): the hydrostatic pressure has the same magnitude at all points of AB, as in case (a), but it is oppositely directed. The forces P_v and P_h are given by the Eqs (2.8) and (2.9) with the signs reversed. As in case (a), G is the weight of the liquid corresponding to the volume $ABCD$ (which, of course, is actually empty).

The centre of pressure of a curved area can be readily located if the magnitude and direction of forces P_v and P_h are known, i. e., if the centre of pressure of the vertical projection of the area and the centre of gravity of the volume $ABCD$ are known. The problem is simplified when the curved surface is circular. In this case the resultant force intersects with the centre line of the surface, which follows from the fact that any elementary pressure dP is normal to the surface, i. e., it is directed along the radius.

This method of determining the pressure on a cylindrical area can be used for spherical surfaces. The resultant passes through the centre of the area in the vertical plane of symmetry.

The method of finding the vertical component of the pressure force on a curved area can also be used to prove the famous Archimedes' law.

Let any body of volume W be immersed in a liquid (Fig. 14). A vertical generator moving around the body describes a curve which divides the body into two parts ACB and ADB. The vertical component P_{v_1} of the gauge pressure acting on the part of the surface above

AB is directed downward and is equal to the weight of the liquid in the volume $AA'B'BCA$. The vertical component P_{v2} of the pressure acting on the lower portion of the body is directed upward and is equal to the weight of the liquid contained in the volume $AA'B'BDA$.

It follows, then, that the vertical resultant of the pressure exerted by the liquid on the body is directed upward and is equal to the weight of the liquid contained in the difference between the two volumes, i. e., in the volume of the body:

$$P_b = P_{v2} - P_{v1} = G_{ACBD} = W\gamma.$$

This is known as Archimedes' law, which states: *A body immersed in a fluid loses as much of its weight as the weight of the fluid displaced by it.* The law, of course, holds good for partially immersed bodies as well. The force P_b is called the *buoyancy force* and its point of application, which is the centre of gravity of the displaced liquid, is called the *centre of buoyancy.*

Depending on the ratio of the weight G of a body and the buoyancy force P_b, three cases are possible: (i) $G > P_b$, and the body sinks; (ii) $G < P_b$, and the body rises; (iii) $G = P_b$, and the body floats.

For the stability of a floating body it is necessary, besides the equality of forces G and P_b, that the total moment be zero. The latter condition is fulfilled when the centre of gravity and the centre of buoyancy lie on the same vertical. The stability of floating bodies, however, will not be discussed in this book.

Example 1. Many aircraft hydraulic systems include a gas-loaded accumulator for energy storage. Stripped of the unessentials, an accumulator consists of a cylinder with a piston on one side of which there is air under pressure p and on the other side the hydraulic fluid, which is injected by pump (Fig. 15).* The energy is stored by the fluid pushing the piston to the left and compressing the air volume W. The stored energy is delivered by the expanding air.

Determine the energy stored in an accumulator with a pressure load $p_2 = 150$ kg/cm² if it can be unloaded to a pressure $p_1 = 75$ kg/cm², which corresponds to an air volume $W_1 = 3$ lit.

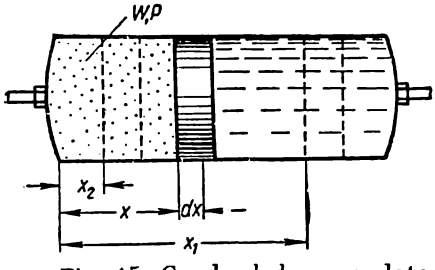

Fig. 15. Gas-loaded accumulator

The following assumptions are made: (i) the compression and expansion of the air is an isothermal process; (ii) the air volume is proportional to the displacement x of the piston; (iii) the piston moves without friction.

Solution. The elementary work done by the accumulator is

$$dE = pS\,dx,$$

* Another type is a spherical accumulator with an elastic diaphragm separating the fluid from the compressed air (see Fig. 18).

where S = area of the piston and, as assumed,

$$p = p_1 \frac{W_1}{W} \text{ and } W = W_1 \frac{x}{x_1}.$$

Hence,

$$dE = p_1 x_1 S \frac{dx}{x} = p_1 W_1 \frac{dx}{x}.$$

The stored energy is determined by integration:

$$E = p_1 W_1 \int_{x_2}^{x_1} \frac{dx}{x} = p_1 W_1 \ln \frac{x_1}{x_2} = p_1 W_1 \ln \frac{p_2}{p_1},$$

whence, substituting the numerical values,

$$E = 75 \times 10^4 \times 3 \times 10^{-3} \times 2.3 \times 0.3 = 1{,}550 \text{ kg-m}.$$

Example 2. In Fig. 16 is shown schematically a hydraulic machine which can operate either as a press or as a jack. When working as a jack, *1* is the load to be lifted; when working as a press, *1* is a rigid support attached to the foundation by vertical columns *8* (shown by broken lines) and body *2* is the pressed object.

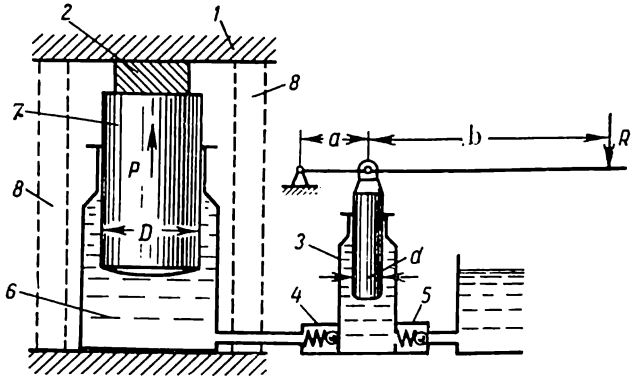

Fig. 16. Hydraulic press (jack)

The hand-driven pump *3*, where *5* is the intake, or suction, valve and *4* is the discharge, or pressure, valve, is used to supply pressure into cylinder *6*, thereby developing an upward thrust P on the lifting ram *7*.

Determine force P if $R = 20$ kg, $a/b = 1/9$ and $D/d = 10$.

Solution.

$$P = R \frac{a+b}{a} \left(\frac{D}{d} \right)^2 = 20 \times 10 \times 100 = 20{,}000 \text{ kg}.$$

Example 3. The hydraulic pressure intensifier in Fig. 17 is used to increase the pressure p_1 supplied by a pump or accumulator. The pressure p_1 is supplied into a cylinder *1* in which moves a hollow ram *2* of weight G and diameter D. The hollow ram slides along a fixed ram *3* of diameter d in which is bored an outlet for the fluid at the increased pressure p_2.

Determine the pressure p_2 if $G = 300$ kg, $D = 125$ mm, $p_1 = 100$ kg/cm^2 and $d = 50$ mm. Neglect friction.

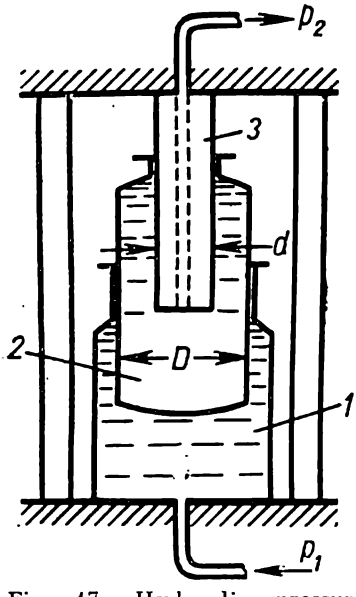

Fig. 17. Hydraulic pressure intensifier

Solution. From the equilibrium conditions for the hollow ram *2* we have

$$\frac{\pi D^2}{4} p_1 = \frac{\pi d^2}{4} p_2 + G,$$

whence

$$p_2 = p_1 \left(\frac{D}{d}\right)^2 - \frac{4G}{\pi d^2} = 100 \left(\frac{125}{50}\right)^2 - \frac{4 \times 300}{\pi 5^2} = 610 \text{ kg/cm}^2.$$

Example 4. A component of aircraft hydraulic systems is an automatic relief valve (Fig. 18) which works in the following manner. When the fluid in the system is idling the pump charges a hydraulic accumulator *4* until a pressure p_{max} is reached at which piston *d* moves down, letting the fluid into space *A* via pipe *a*. The pressure p_{max} drives piston *D* down; the piston rod opens a ball valve connecting the pressure pipe of the pump with the tank. The pump delivers the fluid back into the tank as long as the pressure in the system remains above p_{min}, at which piston *d* moves up and the fluid in space *A* drains into the tank. When this happens spring *2* pushes piston *D* up, the ball valve closes and the pump supplies pressure to the receiver.

Calculate the characteristics of springs *1* and *2* if $p_{max} = 140$ atm, $p_{min} = 80$ atm, $d = 8$ mm, $l = 16$ mm, $D = 10$ mm, $a = 2$ mm and $d_1 = 6$ mm.

Solution. Determine the maximum and minimum loads on spring *1*

$$P_{max} = p_{max} \frac{\pi d^2}{4} = 140 \frac{\pi 0.8^2}{4} = 70.4 \text{ kg};$$

$$P_{min} = p_{min} \frac{\pi d^2}{4} = 80 \frac{\pi 0.8^2}{4} = 40.2 \text{ kg}.$$

The deflection of the spring is

$$h_1 = l - a = 16 - 2 = 14 \text{ mm}.$$

Now calculate the stiffness of spring *1*:

$$\frac{P_{max} - P_{min}}{h_1} = \frac{70.4 - 40.2}{14} = 2.16 \text{ kg/mm}.$$

In order to open the ball valve, the thrust on the piston should be sufficient to overcome the resistance of spring *2*, the friction of the piston packing, the pressure acting on the ball valve and the thrust of spring *3*. Assuming the frictional force to be 0.1 of the pressure force and the thrust of spring $3Q = 30$ kg, we obtain the following equation for determining the maximum stress F_{max} of spring *2*:

$$p_{max} \frac{\pi D^2}{4} 0.9 = F_{max} + p_{max} \frac{\pi d_1^2}{4} + Q,$$

whence

$$F_{max} = 140 \times 0.25\pi (1^2 \times 0.9 - 0.6^2) - 30 = 30 \text{ kg}.$$

But, on the other hand, the thrust of spring *2* should be sufficient to reverse the motion of piston *D* against the friction of the packing of the unloaded pis-

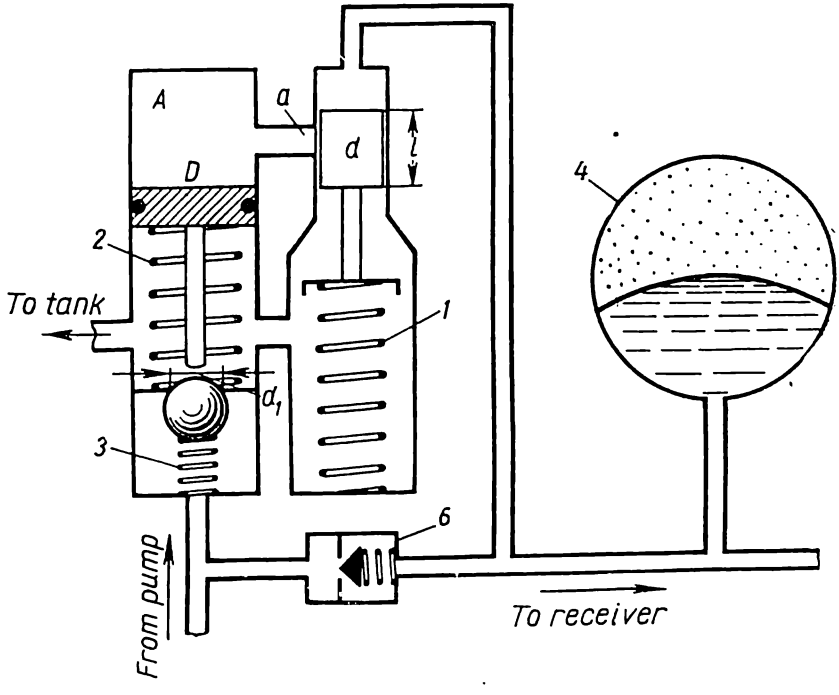

Fig. 18. Automatic relief valve

ton. Assuming the frictional force to be 10 kg, we obtain

$$F_{min} = 10 \text{ kg}.$$

The stiffness of spring *2* required for an upward displacement of the piston $h_2 = 10$ mm is

$$\frac{F_{max} - F_{min}}{h_2} = \frac{30 - 10}{10} = 2 \text{ kg/mm}.$$

CHAPTER III

RELATIVE REST OF A LIQUID

10. BASIC CONCEPTS

In the previous chapter we considered the equilibrium of a liquid subjected to the action of only one body force, gravity. This is the case of a liquid at rest in a vessel that is motionless or is moving uniformly in a straight line with respect to the earth.

If a vessel containing a liquid is in nonuniform or nonrectilinear motion, all the particles of the liquid are subjected, in addition to gravity, to the forces developed by accelerated motion. These forces tend to displace the fluid in its vessel in some way, and if they are uniform in time the fluid occupies a new equilibrium position, i. e., it comes to rest relative to the walls of the vessel. This case of fluid equilibrium is called *relative rest.*

The free surface, as well as the other surfaces of equal pressure (see Sec. 6) of a liquid relatively at rest may differ substantially from the surfaces of equal pressure of a liquid in a motionless vessel, which are horizontal planes. In determining the shape and position of the free surface of a liquid in relative rest conditions, the basic property of any surface of equal pressure must be taken into account, namely, that the resultant body force is always normal to the surface of equal pressure.

If the resultant body force were directed at an angle to the surface of equal pressure its tangential component would displace the liquid particles along that surface. But in relative rest the particles of a liquid are at rest with respect to the walls of the vessel and to each other. Hence, the only possible direction of the resultant body force is normal to the free surface and the other surfaces of equal pressure.

Furthermore, no two surfaces of equal pressure can intersect, as otherwise points on the line of intersection would be simultaneously subjected to two different pressures, which is impossible.

We shall consider two characteristic cases of relative rest of a liquid: (i) the vessel moves with uniform acceleration in a straight line, and (ii) the vessel rotates uniformly about a vertical axis.

11. LIQUID IN A VESSEL MOVING WITH UNIFORM ACCELERATION IN A STRAIGHT LINE

Let a vessel containing a liquid, say an aircraft fuel tank, be moving in a straight line with a uniform acceleration a. The resultant body force acting on the liquid is found as the vector sum of the acceleration force, which is directed opposite the acceleration a, and the force of gravity (Fig. 19).

Denoting the resultant body force referred to unit mass by the symbol j, we have

$$\bar{j} = \bar{a} + \bar{g}.$$

The resultant body forces of all the particles of the liquid volume under consideration are parallel, and the surfaces of equal pressure are perpendicular to the forces. Hence, all the surfaces of equal pressure, including the free surface, are parallel planes. Their angle of inclination to the horizontal is determined from the condition of their perpendicularity to force j.

In order to determine the position of a liquid free surface in a vessel moving with uniform acceleration in a straight line, the foregoing condition must be supplemented by the equation of volumes, i. e., we must know the volume of the liquid in the vessel in terms of the dimensions B and H of the vessel and the initial level h of the liquid.

The equation for determining the pressure at any point of the fluid volume can be developed in the same way as in Sec. 6.

Take at a point M an area dS parallel to the free surface and erect normal to the free surface a cylindrical volume with dS as its face. The condition of equilibrium of this volume is

$$p\,dS = p_0\,dS + j\varrho l\,dS,$$

where the last term is the total body force acting on the liquid volume and l is the distance from point M to the free surface. Cancelling out dS, we obtain

$$p = p_0 + j\varrho l. \qquad (3.1)$$

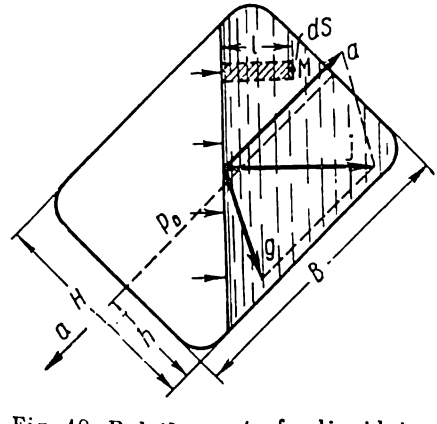

Fig. 19. Relative rest of a liquid in a vessel moving with uniform acceleration in a straight line

In the special case when $a = 0$, $j = g$, and Eq. (3.1) turns into the basic hydrostatic equation (2.2).

In investigating the action of acceleration forces in aviation practice the concept of g-loading is used. The g-load may be tangential (n_x) or normal (n_y). In straight flight the g-load is equal to

$$n_x = \frac{a}{g}.$$

Normal g-loading develops when an airplane flies in a curved path (diving, nosing up, banking) and it is given by the equation

$$n_y = \frac{a+g}{g} = \frac{v^2}{Rg} + 1,$$

where v = speed of flight;

R = radius of curvature.

The example considered above referred to a tangential g-load, but in view of the small dimensions of an aircraft fuel tank compared with the radius R, the reasoning set forth can be applied to normal g-loading, the acceleration a being calculated from the equation

$$a = \frac{v^2}{R}.$$

It should be noted that in airplane flight the normal g-loading is usually much greater than the tangential g-loading (eight to ten times).

When the g-load is great and the amount of fuel in a tank is small, the displacement of the fuel may lay bare the fuel intake pipe and cut out the fuel supply. To prevent this special devices are provided around the intake.

12. LIQUID IN A UNIFORMLY ROTATING VESSEL

Let us first consider an open cylindrical vessel containing a liquid and revolving about its vertical axis with an angular velocity ω. The liquid gradually attains the same angular velocity as the vessel and its free surface becomes a concave surface of revolution (Fig. 20).

Acting on the liquid are two body forces, gravity and a centrifugal force, respectively equal to g and $\omega^2 r$ when referred to unit mass. Due to its second component, the resultant body force j increases with the radius while its inclination to the horizontal decreases. This force is normal to the free surface, owing to which the inclination of the surface increases with the radius.

Let us develop the equation of the curve AOB for a z-r coordinate system with the origin at the centre of the bottom of the vessel. Since the force j is normal to the curve AOB, we find from the drawing that

$$\tan\alpha = \frac{dz}{dr} = \frac{\omega^2 r}{g}.$$

Hence,

$$dz = \frac{\omega^2 r}{g}\,dr,$$

and, integrating,

$$z = \frac{\omega^2 r^2}{2g} + C.$$

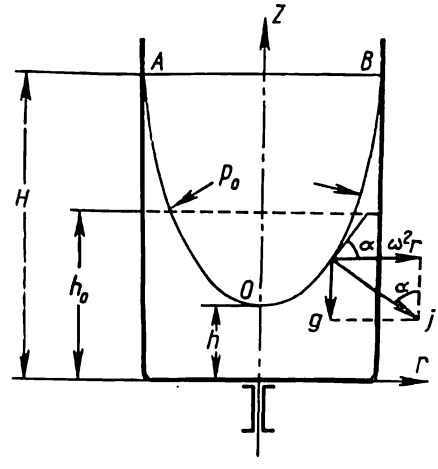

Fig. 20. Rotation of an open vessel about its vertical axis

From the stated conditions it follows that at the intersection of curve AOB with the rotation axis $C = h$, whence we finally have

$$z = h + \frac{\omega^2 r^2}{2g}, \tag{3.2}$$

i. e., curve AOB is a parabola and the free surface is a paraboloid of revolution.

Equation (3.2) can be used to determine the position of the free surface in the vessel, for instance, the maximum rise H of the liquid and the elevation of the summit of the paraboloid at a given velocity of rotation ω. For this, however, the volume equation must be employed in which the volume of liquid at rest is equal to its volume during rotation.

A more common case in practice is when a vessel containing a liquid revolves about a horizontal or arbitrary axis and the angular velocity ω is so great that gravity can be neglected as compared with the centrifugal forces.

The pressure gradient in the liquid can easily be obtained by considering the equilibrium equation for an elementary volume of base area dS and height dr taken along the radius (Fig. 21). The volume is subjected to pressure and centrifugal forces. Let p be the pressure at the centre of area dS, r the distance of dS from the axis of rotation, $p + dp$ the pressure on the second face of the volume, and $r + dr$ the distance of the latter from the axis. The equilibrium equation for the volume in the direction of the radius is

$$p\,dS - (p + dp)\,dS + \rho\omega^2 r\,dr\,dS = 0,$$

or

$$dp = \varrho\omega^2 r\,dr,$$

whence, integrating,

$$p = \varrho\omega^2 \frac{r^2}{2} + C.$$

The constant C is found from the condition that, at $r = r_0$, $p = p_0$, whence

$$C = p_0 - \varrho\omega^2 \frac{r_0^2}{2}.$$

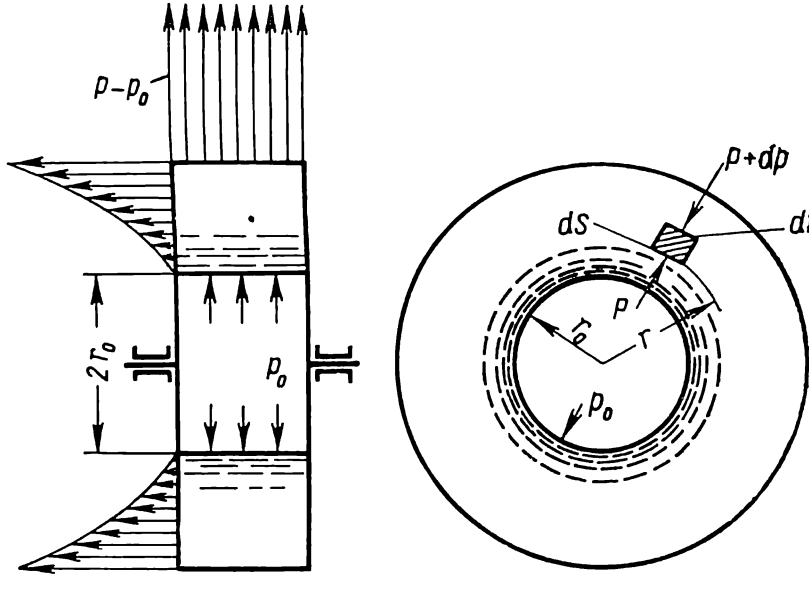

Fig. 21. Rotation of a vessel with liquid about its horizontal axis

Finally, we obtain the relation between p and r in the form

$$p = p_0 + \varrho \frac{\omega^2}{2}(r^2 - r_0^2). \tag{3.3}$$

The surfaces of equal pressure are evidently circular cylinders whose centre lines are on the axis of rotation of the liquid. If the vessel is only partially filled, the free surface, as one of the surfaces of equal pressure, is a cylinder of radius r_0 and the pressure is p_0.

It is frequently necessary to calculate the thrust of a liquid rotating with a vessel exerted on the wall normal to the axis of rotation (or on a ring section of the wall).

For this the thrust on an elementary ring surface of radius r and width dr must be determined from Eq. (3.3):

$$dP = pdS = \left[p_0 + \varrho \frac{\omega^2}{2} (r^2 - r_0^2)\right] 2\pi r dr,$$

integration of this equation gives the solution.

If a liquid is made to rotate very quickly the thrust on the walls may be considerable. This is utilised in certain types of friction clutches in aircraft engines where considerable normal pressures are required for the torque to be transmitted from one shaft to another. The method described here is used to calculate the axial pressure of a liquid on the impellers of centrifugal pumps.

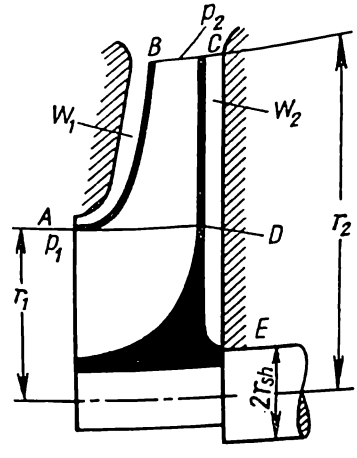

Fig. 22. Notation for determining axial thrust acting on centrifugal pump impeller

The same equations for the examined cases of relative rest can be developed by integrating the differential equations of fluid equilibrium (see Appendix).

Example. Determine the axial thrust acting on the impeller of a centrifugal pump in a Walter liquid-propellant rocket if in the spaces W_1 and W_2 (Fig. 22) between the impeller vanes and the pump casing the liquid rotates with an angular velocity equal to half the velocity of the impeller and the leakage at A is small enough to be neglected.

The discharge pressure $p_2 = 38$ atm, intake pressure $p_1 = 0$, speed of rotation $n = 16{,}500$ rpm; impeller dimensions: $r_2 \approx 50$ mm, $r_1 = 25$ mm, $r_{sh} = 12$ mm; specific weight of fluid $\gamma = 918$ kg/m^3.

Solution. The thrust exerted by the fluid on surfaces AB and CD is balanced. The only unbalanced force is the axial pressure on surface DE, i. e., a ring area bounded by circles of radii r_1 and r_{sh}. The required force is directed to the left and is equal to

$$P = 2\pi \int_{r_{sh}}^{r_1} prdr,$$

where, from Eq. (3.3) and substituting p_2 and r_2 for p_0 and r_0, respectively,

$$p = p_2 - \gamma \frac{\omega_f^2}{2g} (r_2^2 - r^2),$$

where ω_f = angular speed of rotation of the fluid.

Hence,

$$P = 2\pi \int_{r_{sh}}^{r_1} \left[p_2 - \gamma \frac{\omega_f^2}{2g} (r_2^2 - r^2) \right] r dr = \pi \, (r_1^2 - r_{sh}^2) \left[p_2 - \gamma \frac{\omega_f^2}{2g} \left(r_2^2 - \frac{r_1^2 + r_{sh}^2}{2} \right) \right],$$

whence, substituting the numerical values, we obtain

$$P = \pi (2.5^2 - 1.2^2) \left[38 - 0.000918 \left(\frac{\pi 16,500}{2 \times 30} \right)^2 \times \frac{1}{2 \times 981} \times \right.$$
$$\left. \times \left(5^2 - \frac{2.5^2 + 1.2^2}{2} \right) \right] = 460 \text{ kg}.$$

CHAPTER IV

THE BASIC EQUATIONS OF HYDRAULICS

13. FUNDAMENTAL CONCEPTS

We shall commence our study of liquids in motion with an examination of so-called ideal-fluid flow. An ideal fluid is an imaginary fluid whose viscosity is zero. As in real motionless fluids, the only strains possible in a nonviscous fluid are normal compressive strains, i.e., pressure forces.

Pressure forces in a flowing ideal fluid possess the same properties as in a motionless fluid, i. e., on the boundary they are directed along the inward normal; at any point inside the fluid they are the same in all directions.*

Flow may be steady or unsteady.

In *steady flow* the flow characteristics at a fixed position in space do not change with time; pressure and velocity change only with the change of position of a fluid particle. Mathematically this can be expressed as follows:

$$p = f_1(x, y, z); \quad v = f_2(x, y, z),$$

$$\frac{\partial p}{\partial t} = 0; \quad \frac{\partial v_x}{\partial t} = 0; \quad \frac{\partial v_y}{\partial t} = 0; \quad \frac{\partial v_z}{\partial t} = 0,$$

where the velocity subscripts denote the respective projections on a set of cartesian axes.

In the general case of *unsteady flow*, pressure and velocity vary with both position and time, i. e.,

$$p = F_1(x, y, z, t); \quad v = F_2(x, y, z, t).$$

Unsteady flow is observed when a liquid pours under gravity out of a sink in the bottom of a vessel and in the suction and pressure

* The latter is proved in the same way as for a motionless fluid (see Sec. 5): the equations of motion are developed for an elementary tetrahedron, taking into account the D'Alembert inertia forces which, together with the body forces, tend to zero when the tetrahedron is contracted to a point.

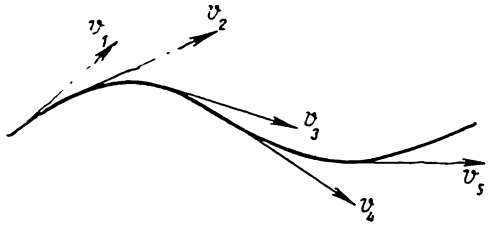

Fig. 23. Streamline

pipes of an ordinary reciprocating piston pump.

Steady flow is observed when a liquid is flowing out of a vessel in which a constant level is maintained or in a looped pipeline through which a liquid is driven by a centrifugal pump with a uniform speed of rotation.

Investigation of steady flow is much simpler than of unsteady flow. In this book we shall consider mainly steady flow, only touching on some special cases of unsteady flow.

In steady flow the fluid particles travel along pathlines which do not change with time.

In unsteady flow different particles passing through a given point in space will be moving along different pathlines. Accordingly, to investigate the flow pattern for every given moment of time the concept of streamline is introduced.

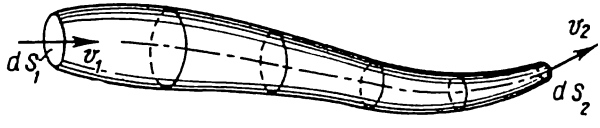

Fig. 24. Stream tube

A *streamline* is a line in a flowing fluid the tangent to which at any point shows the direction of the velocity vector of the fluid particle at that point (Fig. 23). In steady flow, evidently, streamlines and pathlines coincide and do not change with time.

A *stream tube* is a tubular space bounded by a surface consisting of streamlines (Fig. 24). When the cross-section of a stream tube is contracted to zero, a streamline is obtained in the limit.

The velocity vectors at all points of the surface of a stream tube are tangential to the surface. There being no normal components of the velocity, no particle of the liquid can enter or leave the stream tube, except at the ends. Thus, a stream tube can be regarded as surrounded by impenetrable walls and therefore treated as an elementary stream.

At first we shall imagine streams of finite size as being made up of bundles of elementary stream tubes. Due to differences in velocity the stream tubes slip with respect to one another, but there is no mixing.

A *cross-section* of a stream is, generally, a surface passed through the stream normal to the streamlines. We shall usually be considering portions of streams in which the streamlines are parallel and, therefore, the cross-sections are plane.

14. RATE OF DISCHARGE. EQUATION OF CONTINUITY

The *rate of discharge* (commonly shortened to "discharge" or "flow") is defined as the quantity of fluid flowing per unit time across any section of a stream. It may be expressed in units of volume, weight or mass: *volume* rate of discharge Q, *weight* rate of discharge G and *mass* rate of discharge M.

The cross-sectional area of an elementary stream tube is infinitely small throughout its length, therefore the velocity v can be assumed to be uniform at all the points of each section. Hence, the volume rate of discharge through an elementary stream tube is

$$dQ = v dS \text{ m}^3/\text{sec}, \tag{4.1}$$

where dS = area of the cross-section;

the weight rate of discharge is

$$dG = \gamma\, dQ \text{ kg/sec}, \tag{4.2}$$

and the mass rate of discharge is

$$dM = \varrho\, dQ = \varrho\, v dS \text{ kg-sec/m}. \tag{4.3}$$

In a finite stream the velocity will generally vary across a section; the rate of discharge is therefore computed as the sum of the elementary rates of discharge of the stream tubes, i. e.,

$$Q = \int_S v dS. \tag{4.4}$$

Commonly the mean velocity across the section is considered:

$$v_m = \frac{Q}{S}, \tag{4.5}$$

whence

$$Q = v_m S. \tag{4.5'}$$

No fluid crosses the wall of a stream tube. Hence, from the law of conservation of matter the rate of discharge of an incompressible liquid in steady flow must be the same through all sections of an elementary stream tube (Fig. 24), i. e.,

$$dQ = v_1 dS_1 = v_2 dS_2 = \text{const} \quad \text{(along a stream tube)}. \tag{4.6}$$

This is the *equation of continuity* for an elementary stream tube.

Introducing the mean velocity instead of the actual velocity for a finite stream contained in impermeable walls, we obtain:

$$Q = v_{m1}S_1 = v_{m2}S_2 = \text{const (along a stream)}. \qquad (4.7)$$

Equation (4.7) shows that for an incompressible liquid the mean velocity varies inversely as the cross-sectional area of the stream:

$$\frac{v_{m1}}{v_{m2}} = \frac{S_2}{S_1}. \qquad (4.7')$$

The equation of continuity is thus a special case of the law of conservation of matter.

15. BERNOULLI'S EQUATION FOR A STREAM TUBE OF AN IDEAL LIQUID

We shall consider the steady flow of an ideal liquid subjected to a single body force, that of gravity, and develop the basic equation which gives the relation between pressure and velocity.

Consider a stream tube and in it a liquid volume of arbitrary length between sections *1* and *2* (Fig. 25). The area of section *1* is dS_1, the velocity through it is v_1, the pressure is p_1 and the elevation of the centre of gravity of the section above an arbitrary datum level is z_1. The respective quantities for section *2* are dS_2, v_2, p_2 and z_2.

In a differential time interval dt the external forces move the liquid volume to configuration *1'-2'*. To the volume can be applied the theorem of mechanics according to which the work done by external forces on a body is equal to the change in the kinetic energy of the body. In our case these forces are the normal pressure forces on the sides of the stream tube and gravity.

Let us calculate the work done by the pressure forces and gravity and the change in the kinetic energy of the body of fluid in the time dt.

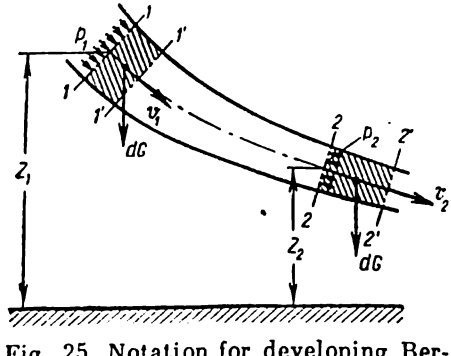

Fig. 25. Notation for developing Bernoulli's equation for a stream tube

The work done by the pressure forces on section *1* is positive, as they are acting in the direction of the displacement, and it is equal to the product of the force $p_1 dS_1$ and the path $v_1 dt$:

$$p_1 dS_1 v_1 dt.$$

The work done by the pressure forces on section *2* is negative

as they are acting against the displacement, and it is equal to

$$-p_2 dS_2 v_2 dt.$$

The pressure forces acting on the side walls of the stream tube do no work as they are normal to the walls and, therefore, normal to the displacement.

Thus, the work done by the pressure forces is

$$p_1 v_1 dS_1 dt - p_2 v_2 dS_2 dt. \tag{4.8}$$

The work done by the gravity force is equal to the change in the potential, or position, energy of the liquid volume. Subtracting the potential energy of volume *1'-2'* from that of volume *1-2*, we obtain, as the potential energy of volume *1'-2* cancels out, the difference between the potential energies of portions *1-1'* and *2-2'* of the stream tube. From the continuity equation (4.6) the volumes and the weights of these portions are equal, i. e.,

$$dG = \gamma v_1 dS_1 dt = \gamma v_2 dS_2 dt. \tag{4.9}$$

Hence, the work done by gravity is found as the product of the change in elevation and the weight dG:

$$(z_1 - z_2)\, dG. \tag{4.10}$$

To determine the change in the kinetic energy of the liquid volume in the time dt, the kinetic energy of volume *1-2* must be subtracted from the kinetic energy of volume *1'-2'*. The energy of the intermediate volume *1'-2* cancels out, leaving the difference between the kinetic energies of the volumes *2-2'* and *1-1'*, the weight of both being dG. Thus, the change in the kinetic energy is equal to

$$(v_2^2 - v_1^2)\frac{dG}{2g}. \tag{4.11}$$

Adding the work done by the pressure forces (4.8) and the work done by gravity (4.10) and equating the sum to the change in kinetic energy (4.11), we obtain

$$p_1 dS_1 v_1 dt - p_2 dS_2 v_2 dt + (z_1 - z_2)\, dG = (v_2^2 - v_1^2)\frac{dG}{2g}.$$

Dividing through by the weight dG, for which we have the two expressions (4.9), and cancelling out, we obtain

$$\frac{p_1}{\gamma} - \frac{p_2}{\gamma} + z_1 - z_2 = \frac{v_2^2}{2g} - \frac{v_1^2}{2g}.$$

Transposing the terms referring to the first section to the left-hand side of the equation and those referring to the second section to the right-hand side, we obtain:

$$z_1 + \frac{p_1}{\gamma} + \frac{v_1^2}{2g} = z_2 + \frac{p_2}{\gamma} + \frac{v_2^2}{2g}. \tag{4.12}$$

This is *Bernoulli's equation for an ideal liquid*. It was developed by Daniel Bernoulli in 1738.

The terms in Eq. (4.12) represent linear quantities; they are called:

z = elevation head, or potential head, or geodetic head;

$\frac{p}{\gamma}$ = pressure head, or static head;

$\frac{v^2}{2g}$ = velocity head.

The sum

$$z + \frac{p}{\gamma} + \frac{v^2}{2g} = H$$

is called the *total head*.

Equation (4.12) is written for two arbitrary cross-sections of a stream tube and it expresses the equality of the total head H at the sections. As the sections were chosen arbitrarily, it follows that the total head is the same at any other section of the same stream tube, i. e.,

$$z + \frac{p}{\gamma} + \frac{v^2}{2g} = H = \text{const (along a stream tube)}.$$

Thus, *the sum of the elevation, pressure and velocity heads of an ideal liquid is constant along a stream tube.*

This is illustrated by the diagram in Fig. 26, which shows the change in the three heads at different points of a stream tube. The line joining the pressure heads is called the *piezometric line* or *hydraulic gradient*; it is the locus of the levels that would appear in piezometric columns mounted along the stream tube.

It follows from Bernoulli's equation and the equation of continuity that the *smaller* the cross-section of a stream tube, i. e., the narrower the stream, the faster the flow and the lower the pressure; conversely, the *wider* the stream the slower the flow and the higher the pressure.

Let us examine the physical, or, to be more precise, the energy, meaning of Bernoulli's equation. The *specific energy* of a liquid is its energy per unit weight:

$$e = \frac{E}{G}.$$

Specific energy is a linear quantity, like the terms in Bernoulli's equation. In fact, the latter express the different types of energy which a liquid possesses, viz.,

z = *potential energy* due to position and gravity; the potential energy of a liquid particle of weight ΔG at an elevation z is ΔGz, whence the specific potential energy per unit weight is $\frac{\Delta Gz}{\Delta G} = z$;

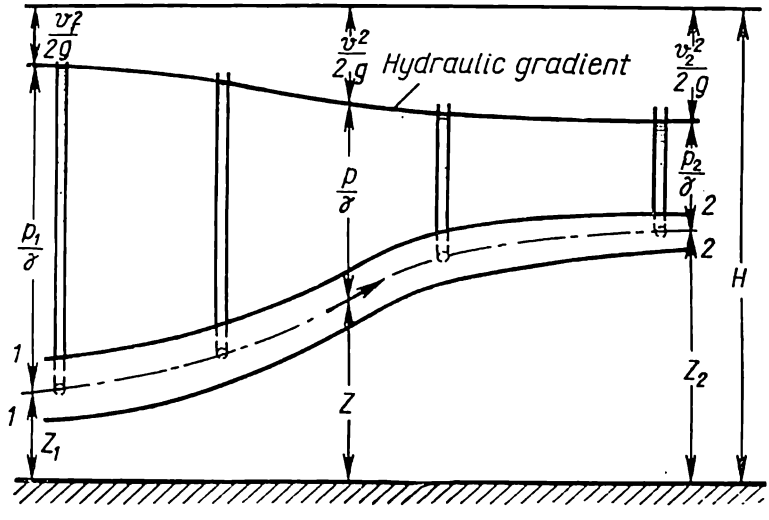

Fig. 26. Variation of elevation, pressure and velocity heads along a stream tube of an ideal liquid

$\frac{p}{\gamma}$ = *pressure energy* due to the pressure existing in a moving liquid; a particle of weight ΔG subjected to a pressure p rises to a height $\frac{p}{\gamma}$, thereby acquiring a potential energy equal to $\Delta G\frac{p}{\gamma}$; divided by ΔG this gives the specific pressure energy $\frac{p}{\gamma}$;

$z + \frac{p}{\gamma}$ = *total potential energy* of a liquid;

$\frac{v^2}{2g}$ = *kinetic*, or velocity, *energy* of a liquid;

the specific kinetic energy of a particle ΔG referred to unit weight is

$$\Delta G\frac{v^2}{2g}: \quad \Delta G = \frac{v^2}{2g};$$

$$H = z + \frac{p}{\gamma} + \frac{v^2}{2g} = \text{total energy of a flowing liquid.}$$

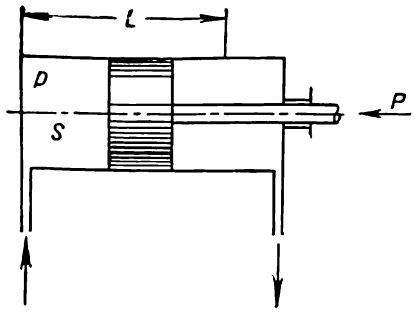

Fig. 27. Cylinder with piston and piston rod

The total energy of an ideal liquid is constant along a streamline. Bernoulli's equation, therefore, expresses the law of conservation of mechanical energy in an ideal liquid.

Thus, in fluids mechanical energy may be present in the three forms of position, pressure and kinetic energy. The first and third are characteristic of both solids and fluids; pressure energy, however, is characteristic of fluids only.

In an ideal liquid one type of energy may change into another, but the total energy, as demonstrated by Bernoulli's equation, is constant.

Energy is easily converted into mechanical work. The simplest device for this is a cylinder with a piston (Fig. 27). Let us show that in the course of this conversion the work done by every unit weight of a liquid is numerically equal to the pressure head.

If the movable piston area is S, the stroke is L, the gauge pressure of the fluid supplied into the left-hand portion of the cylinder is p, and the gauge pressure on the right-hand side is zero, then the total pressure force P, which is equal to the resistance overcome in the displacement of the piston from its extreme left to extreme right position, will be

$$P = pS,$$

and the work done by this force is

$$E = pSL.$$

The weight of the fluid supplied into the cylinder to do the required work is

$$G = SL\gamma.$$

The work done per unit weight is

$$e = \frac{E}{G} = \frac{pSL}{SL\gamma} = \frac{p}{\gamma}.$$

Bernoulli's equation is often written in another form. Multiplying Eq. (4.12) through by γ, we obtain

$$z_1\gamma + p_1 + \gamma\frac{v_1^2}{2g} = z_2\gamma + p_2 + \gamma\frac{v_2^2}{2g}. \qquad (4.13)$$

All the terms now have the dimension of pressure (kg/m^2), and they are called:

$z\gamma$ = weight pressure;

p = static pressure, or pressure intensity, or simply pressure;

$\gamma \frac{v^2}{2g} = \varrho \frac{v^2}{2}$ — dynamic pressure *.

Bernoulli's equation for an ideal stream tube can also be obtained by integrating the differential equations of motion for an ideal fluid (see Appendix).

16. BERNOULLI'S EQUATION FOR REAL FLOW

In going over from a differential stream tube of an ideal liquid to real flow, i. e., a stream of viscous fluid having finite dimensions and constrained by walls, it is necessary to take into account: first, nonuniform velocity distribution across the sections and, second, energy (head) losses, both of which are due to viscosity.

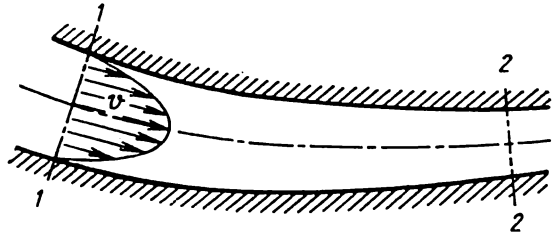

Fig. 28. Velocity distribution in a stream

When a viscous liquid moves along a solid surface, say in a pipe, the flow is retarded due to viscosity and molecular adhesion between the liquid and the walls. The velocity, therefore, is greatest along the centre line of the stream. The closer to the walls the less the speed, down to zero. The result is a velocity profile like the one shown in Fig. 28.

The velocity variations mean that layers of the liquid are slipping relative to one another as a result of which tangential shearing strains, or friction stresses, appear. Furthermore, in a viscous liquid the particles often move erratically in swirls and eddies. This results in loss of energy, therefore the total energy, or total head, of a

* It should be borne in mind that the only real pressure in this equation is the static pressure p. The other two terms, $z\gamma$ and $\varrho \frac{v^2}{2}$, however, can easily be expressed in terms of pressure p, which is why they are also called "pressures".

viscous stream is not constant as in the case of an ideal liquid. It is gradually dissipated in overcoming the resistances and drops along the stream.

Owing to nonuniform velocity distribution the notions of mean velocity v_m across a section (see Sec. 14) and mean specific energy at that section must be introduced.

Before investigating Bernoulli's equation for a real liquid we shall assume that the basic hydrostatic law holds good for the cross-sections considered in the form of Eq. (2.3), i. e., that the piezometric head is constant for a given section:

$$z + \frac{p}{\gamma} = \text{const (across the section)}.$$

Thereby we assume that stream tubes in a moving liquid exert the same transverse pressure on each other as in a motionless liquid. This is actually the case, and it can be proved theoretically for the case of parallel streamlines across a given section, which is the kind of cross-sections we shall consider.

Let us introduce the concept of power of a flow. *Power* is defined as the total energy of a flow transferred through a given section per unit time. As the energy of the fluid particles varies across a section, let us first express the elementary power, i. e., the power of a differential stream tube, in terms of the total specific energy of the fluid at a given point and the differential weight rate of discharge. We have

$$dN = H\gamma\, dQ = (z + \frac{p}{\gamma} + \frac{v^2}{2g})\gamma\, v dS.$$

The power of the whole stream is found by integrating the foregoing expression over the whole of area S:

$$N = \gamma \int_S \left(z + \frac{p}{\gamma} + \frac{v^2}{2g} \right) v dS,$$

or, taking into account the assumption made,

$$N = \gamma \left(z + \frac{p}{\gamma} \right) \int_S v dS + \frac{\gamma}{2g} \int_S v^3 dS.$$

The mean total specific energy of the fluid across the section is found by dividing the total power of the stream by the weight rate of discharge. Using the expression (4.4), we have

$$H_m = \frac{N}{Q\gamma} = z + \frac{p}{\gamma} + \frac{1}{2gQ} \int_S v^3 dS.$$

Multiplying and dividing the last term by v_m^2, we obtain

$$H_m = z + \frac{p}{\gamma} + \frac{\int_S v^3 dS}{v_m^3 S} \frac{v_m^2}{2g} = z + \frac{p}{\gamma} + \alpha \frac{v_m^2}{2g}, \tag{4.14}$$

where α is a dimensionless coefficient introduced to take account of nonuniform velocity distribution and equal to

$$\alpha = \frac{\int_S v^3 dS}{v_m^3 S}. \tag{4.15}$$

Multiplying the numerator and denominator of this expression by $\frac{\varrho}{2}$, we find that the coefficient α represents the ratio of the actual kinetic energy of the stream at a given section to its kinetic energy if the velocity distribution was uniform across the section. For the commonly observed velocity distribution (Fig. 28), α is always greater than unity*, being unity when the velocity profile is a straight line.

Consider two cross-sections of a real stream, denoting the mean total head at those sections by H_{m1} and H_{m2}, respectively. Then,

$$H_{m1} = H_{m2} + \sum h, \tag{4.16}$$

where Σh = total loss of energy (or head) along the stream between the two sections.

Applying Eq. (4.14), the foregoing equation can be rewritten as follows:

$$z_1 + \frac{p_1}{\gamma} + \alpha_1 \frac{v_{m1}^2}{2g} = z_2 + \frac{p_2}{\gamma} + \alpha_2 \frac{v_{m2}^2}{2g} + \sum h. \tag{4.16'}$$

This is *Bernoulli's equation for real flow*. It differs from the equation for a differential stream tube in an ideal liquid by the term representing the loss of energy (head) and the coefficient which takes into account the nonuniform velocity distribution. Furthermore, the equation contains the mean velocities across the respective sections.

Graphically this equation can be represented by a diagram like the one drawn for an ideal fluid, but taking into account the head losses. The latter increase steadily along the flow (Fig. 29).

* This can be proved by expressing the velocity v in Eq. (4.15) as a sum $v = v_m + \Delta v$, dividing the integral into four integrals and analysing the numerical value of each.

Whereas Bernoulli's equation for an ideal fluid stream tube is an expression of the law of conservation of mechanical energy, for real flow it represents an energy-balance equation taking losses into account. The energy dissipated by the flow does not vanish, of course. It changes into another form of energy, heat, which raises the temperature of the liquid.

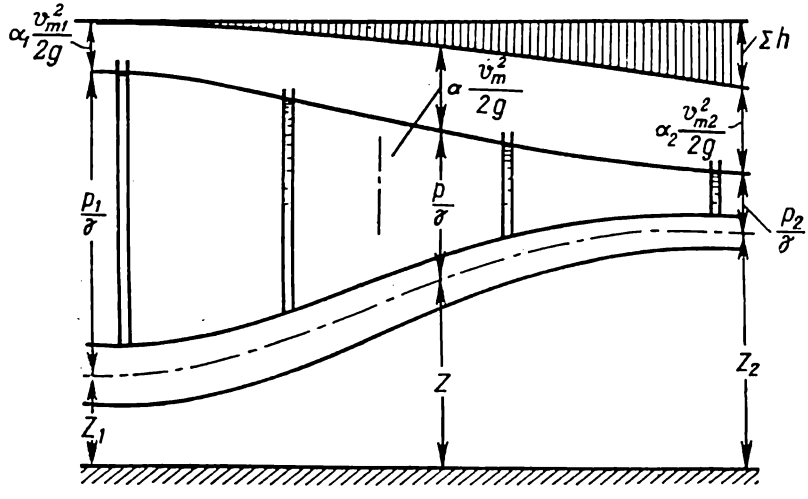

Fig. 29. Diagrammatic representation of Bernoulli's equation for real flow

The drop in the mean value of the total energy between any two points of a stream referred to unit length is called the *energy gradient*. The change in the potential energy of a fluid referred to unit length is called the *hydraulic gradient*. In a pipe of uniform diameter with a constant velocity profile the two gradients are apparently the same.

17. HEAD LOSSES (GENERAL CONSIDERATIONS)

Losses of energy, or head losses as they are commonly called, depend on the shape, size and roughness of a channel, the velocity and viscosity of a fluid; they do not depend on the absolute pressure of the fluid. Viscosity alone, though basically the primary cause of all head losses, hardly ever accounts for any substantial loss of energy. This will be examined in detail further on.

Experiments show that in many cases head losses are approximately proportional to the square of the velocity. Very long ago

this prompted the following general expression for head losses:

$$h = \zeta \frac{v_m^2}{2g}, \tag{4.17}$$

and for pressure losses:

$$p = h\gamma = \zeta \frac{v_m^2}{2g}\gamma.$$

The convenience of this expression is that it contains a dimensionless coefficient of proportionality ζ, called the *loss coefficient*, and the velocity head from Bernoulli's equation. The loss coefficient represents the *ratio of head losses to velocity head.*

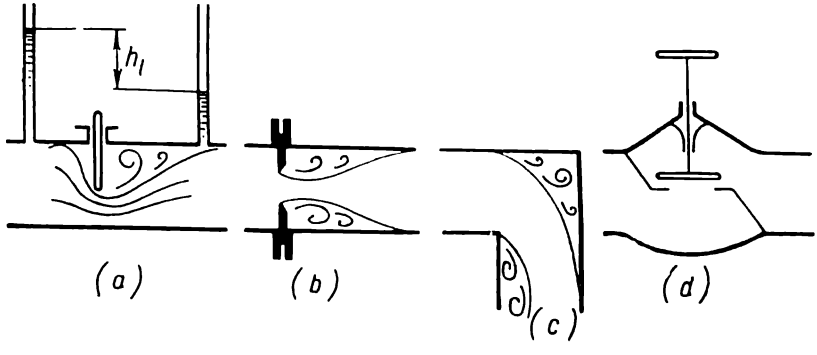

Fig. 30. Local pipe features

Head losses are commonly divided into *local losses* (also *form* or *minor* losses) and *friction* (or *major*) *losses.*

Local losses are caused by local features, or so-called hydraulic resistances, such as change of shape or size of a channel. When a fluid flows through such local features its velocity changes and eddies may appear. Examples of local loss features are shown in Fig. 30: (*a*) gate, (*b*) orifice, (*c*) elbow, (*d*) valve. Local losses are determined from Eq. (4.17):

$$h_l = \zeta_l \frac{v^2}{2g}, \tag{4.17'}$$

or

$$p_l = \zeta_l \frac{v^2}{2g}\gamma,$$

which is known as Weisbach's formula.

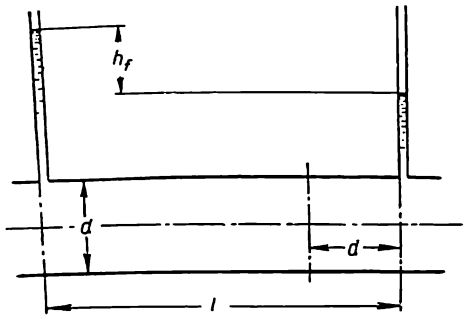

Fig. 31. Loss of head due to friction in a pipe

Here v is the mean velocity across the pipe section for which the local loss was determined.* If the diameter, and hence the velocity of flow, changes along the length of a pipe, it is more convenient to take the highest velocity (i. e., the velocity through the narrowest portion) as the basis for calculation. Every local feature is characterised by a certain loss coefficient ζ_l, which can, in many cases, be regarded as approximately constant for a given type of feature. Local losses will be further considered in Chapter VIII.

Friction, or major, losses are energy losses which develop in straight pipes of uniform cross-section, i. e., with uniform flow, and they increase as the length of the pipe (Fig. 31). These losses are due to the internal friction in a fluid and therefore they appear not only in rough pipes but in smooth pipes as well.

Loss of head due to friction can be expressed according to the general equation of head losses (4.17), i. e.,

$$h_f = \zeta_f \frac{v^2}{2g}. \tag{4.18}$$

A more convenient form, however, is one in which the loss coefficient ζ_f is correlated with the relative length $\frac{l}{d}$ of a pipe.

Consider a portion of circular pipe equal in length to its diameter. denoting the loss coefficient in Eq. (4.18) by the symbol λ. Then for the whole pipe of length l and diameter d (see Fig. 31) the loss coefficient will be $\frac{l}{d}$ times greater, i. e.,

$$\zeta_f = \lambda \frac{l}{d},$$

and instead of Eq. (4.18) we have

$$h_f = \lambda \frac{l}{d} \frac{v^2}{2g}, \tag{4.18'}$$

* Henceforth the subscript m will be used for v only when confusion is possible between mean velocity and local velocity.

or

$$p_f = \lambda \frac{l}{d} \frac{v^2}{2g} \gamma. \tag{4.19}$$

Equation (4.18′) is commonly known as Darcy's formula.

The dimensionless coefficient λ is called the *friction factor*. It represents a coefficient of proportionality between the friction losses, on the one hand, and the product of relative pipe length and velocity head, on the other.

The physical meaning of λ is easily found from a consideration of the condition for uniform flow in a cylindrical pipe of length l and diameter d (see Fig. 31), namely that the sum of the two forces acting on the volume—pressure and friction—be zero. This equation has the form

$$\frac{\pi d^2}{4} p_f - \pi d l \tau_0 = 0,$$

where τ_0 is the shear stress at the pipe wall.

From this, and taking into account Eq. (4.19), we readily obtain

$$\lambda = \frac{4\tau_0}{\gamma \frac{v^2}{2g}}; \tag{4.20}$$

i. e., the friction factor λ is proportional to the ratio of the shear stress at the pipe wall and the dynamic pressure computed according to the mean velocity.

Head losses in closed conduits (pipes) in which a liquid is completely enclosed by solid boundaries (i. e., has no free surface) are due to the specific potential energy $\left(z + \frac{p}{\gamma}\right)$ decreasing along the flow. In this case, if the specific kinetic energy $\frac{v^2}{2g}$ does change at the given rate of discharge, this is due not to energy losses but to a change in the cross-section of the channel, as kinetic energy is a function of velocity only, which in turn depends on the rate of discharge and cross-sectional area:

$$v = \frac{Q}{S}.$$

Consequently, in a pipe of uniform cross-section the velocity and specific kinetic energy of a liquid are constant, irrespective of local disturbances and head losses. Loss of head in this case is determined

as the difference between the level of the liquid in two open piezometer tubes (see Figs 30 and 31).

Computation of head losses for various specific cases is one of the fundamental problems of hydraulics, and the two following chapters will be devoted to this.

18. EXAMPLES OF APPLICATION OF BERNOULLI'S EQUATION TO ENGINEERING PROBLEMS

Bernoulli's equation is an expression of the basic law of steady flow. It can be used in the form developed here to investigate and analyse the work of a number of devices whose design is based on this fundamental law. Let us consider some of them.

1. **The venturi meter** (Fig. 32) is used to measure pipe flow. It consists of a tube with a conical entrance and constricted throat (the nozzle) followed by a gradually diverging portion (the diffuser). In the converging portion the velocity of the flow increases and the pressure decreases. The pressure drop is measured by means of a pair of piezometer tubes or a U-tube differential gauge. The relation between the pressure drop and the rate of discharge is found as follows.

Let the velocity of flow at section *1-1* immediately before the nozzle be v_1, the pressure p_1 and the cross-sectional area S_1; at the throat *2-2* the cross-sectional area is S_2 and the velocity and pressure v_2 and p_2, respectively. The difference between the levels in the piezometer tubes at the respective sections is ΔH.

Assuming a uniform velocity distribution, write Bernoulli's equation and the continuity equation for the two cross-sections:

$$\frac{p_1}{\gamma}+\frac{v_1^2}{2g}=\frac{p_2}{\gamma}+\frac{v_2^2}{2g}+h_l;$$

$$v_1S_1=v_2S_2,$$

where h_l = loss of head between sections *1-1* and *2-2*.

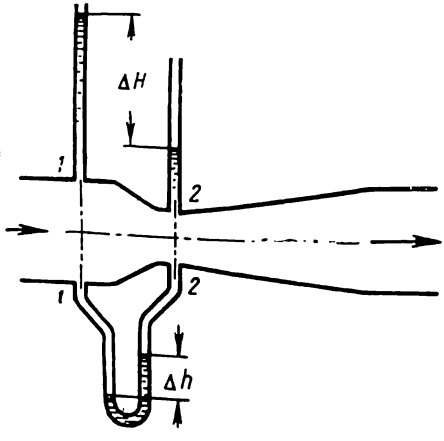

Fig. 32. Venturi flow meter

Taking into account that

$$h_l=\zeta\frac{v_2^2}{2g} \quad \text{and} \quad \frac{p_1-p_2}{\gamma}=\Delta H,$$

we can use these equations to determine one of the velocities, say v_2. We have

$$v_2=\sqrt{\frac{2g\Delta H}{1-\left(\frac{S_2}{S_1}\right)+\zeta}},$$

whence the volume rate of discharge is

$$Q=v_2S_2=S_2\sqrt{\frac{2g\Delta H}{1-\left(\frac{S_2}{S_1}\right)+\zeta}}, \tag{4.21}$$

or

$$Q = C\sqrt{\Delta H} \tag{4.21'}$$

where

$$C = S_2 \sqrt{\frac{2g}{1-\left(\frac{S_2}{S_1}\right)^2 + \zeta}}$$

is a constant for the given meter.

Knowing C and observing the piezometer readings, it is easy to determine the rate of discharge at any moment of time from Eq. (4.21'). The constant C can be computed theoretically, but greater accuracy is obtained by experiment, that is, by calibrating the meter.

The relation between ΔH and Q is that of a parabolic function, and the square of the rate of discharge laid off on the axis of abscissas gives a straight line.

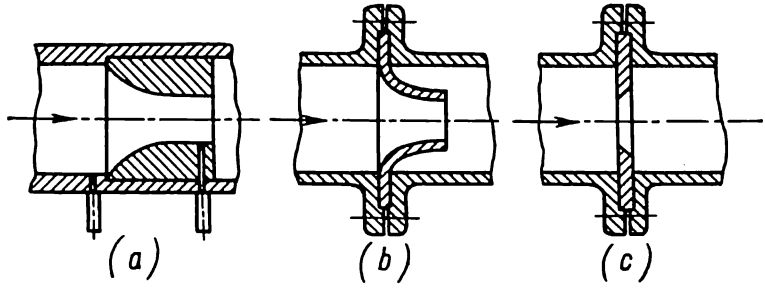

Fig. 33. Flow nozzles and diaphragm

Often a differential mercury gauge is used instead of a pair of piezometer tubes to measure the pressure drop (see Fig. 32). Taking into account that the liquid above the mercury is the same in both limbs and its specific weight is γ, we can write

$$\Delta H = \Delta h \frac{\gamma_{Hg} - \gamma}{\gamma}.$$

Incidentally, a diffuser is not essential for flow measurement, and a flow nozzle alone placed inside a pipe (Fig. 33*a*) or between flanges (Fig. 33*b*) can be used. In this case the convergence of the flow is gradual, as in the case of a venturi meter, but the divergence beyond the nozzle is abrupt and eddies form. The resistance of a flow nozzle is greater than that of a venturi meter with a diffuser.

Another instrument for measuring fluid flow is an orifice meter (Fig. 33*c*). Owing to additional compression experienced by the fluid, the stream is narrowest a bit downstream from the orifice and its diameter is slightly less than the orifice diameter.

Equation (4.21') is valid for these flow meters, with correction coefficients available for standard-type flow meters in relevant handbooks.

2. **Carburettors** (Fig. 34) are used in reciprocating internal-combustion engines to meter, atomise and mix the fuel with air. The stream of air passes through a venturi tube in which a fuel jet is placed. The velocity of the air increases in the venturi and the pressure drops according to Bernoulli's equation. The reduction in pressure at the venturi throat causes fuel to flow through the fuel jet into the air stream.

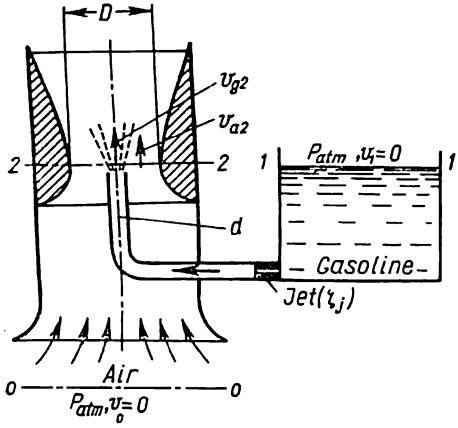

Fig. 34. Carburettor

Let us find the relation between the weight rate of discharge of the fuel (gasoline) G_g and air G_a if the dimensions D and d and the loss coefficients ζ_a of the venturi throat and ζ_j of the jet are known (neglecting the resistance of the gasoline supply pipe).

Writing Bernoulli's equation for the air stream (sections *0-0* and *2-2*) and for the gasoline stream (sections *1-1* and *2-2*), we obtain (at $z_1 = z_2$ and $\alpha = 1$)

$$\frac{p_{atm}}{\gamma_a} = \frac{p_2}{\gamma_a} + \frac{v_{a2}^2}{2g} + \zeta_a \frac{v_{a2}^2}{2g};$$

$$\frac{p_{atm}}{\gamma_g} = \frac{p_2}{\gamma_g} + \frac{v_{g2}^2}{2g} + \zeta_j \frac{v_{g2}^2}{2g},$$

whence

$$\gamma_a \frac{v_{a2}^2}{2g}(1+\zeta_a) = \gamma_g \frac{v_{g2}^2}{2g}(1+\zeta_j).$$

As the weight rates of discharge are

$$G_a = \frac{\pi D^2}{4} v_{a2}\gamma_a \quad \text{and} \quad G_g = \frac{\pi d^2}{4} v_{g2}\gamma_g,$$

we obtain

$$\frac{G_g}{G_a} = \left(\frac{d}{D}\right)^2 \sqrt{\frac{\gamma_g(1+\zeta_a)}{\gamma_a(1+\zeta_j)}}.$$

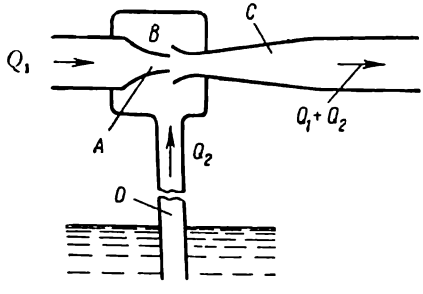

Fig. 35. Air ejector pump

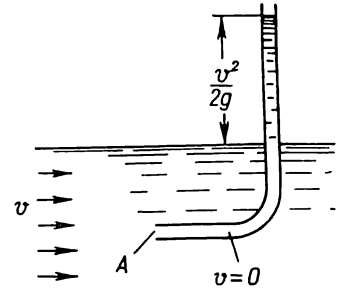

Fig. 36. Pitot tube

3. **An air ejector** (Fig. 35) consists of a nozzle A, in which the stream converges, and a gradually widening diffuser C placed at a distance from the nozzle inside a suction chamber B. The increased velocity of the stream leaving the nozzle causes the pressure in the stream and in the whole of the suction chamber

to drop considerably. In the diffuser the velocity decreases and the pressure increases approximately to atmospheric (if the fluid is ejected into the air). Consequently, the pressure in the suction chamber is also below atmospheric, i. e., a partial vacuum is created.

This vacuum causes the liquid in the bottom reservoir to rise along pipe D to the suction chamber where it is entrained by the stream issuing from the nozzle. Ejectors are used in various machines, notably in liquid-propellant rocket motors.

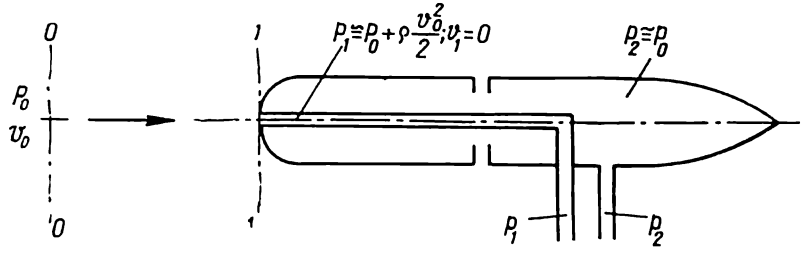

Fig. 37. Pitot tube for measuring aircraft speed

4. A Pitot tube (Fig. 36) is used to measure flow velocity. Let a liquid be flowing in an open channel with a velocity v. If a bent tube is immersed with the opening facing the flow as shown, the liquid will rise in the vertical limb above the free surface to a height equal to the velocity head. This is because the velocity of the liquid particles entering the Pitot tube at point A (the stagnation

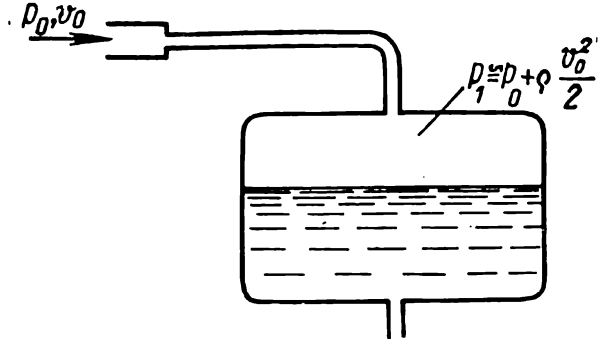

Fig. 38. Tank pressurisation

point) is zero and, consequently, the pressure increases by the value of the velocity head. By observing the height of the liquid in the tube the velocity may be calculated.

The measurement of the velocity of a flying aircraft is based on the same principle. Fig. 37 presents a schematic drawing of a Pitot tube for measuring velocities comparable with the speed of sound.

coloured streak which does not mix with the stream of water and is apparent along the whole length of the pipe. This indicates the stratified nature of the flow with no mixing: laminar flow.

When the velocity of the stream is gradually increased by further opening the faucet, the flow pattern first remains unchanged. Then, at a certain moment, a rapid change takes place. The streak of dye begins to oscillate and then diffuses into the water, eddies and rotational motion of the liquid being quite apparent. This means that turbulent flow has set in (inset of Fig. 39). When the velocity is reduced the flow again becomes laminar.

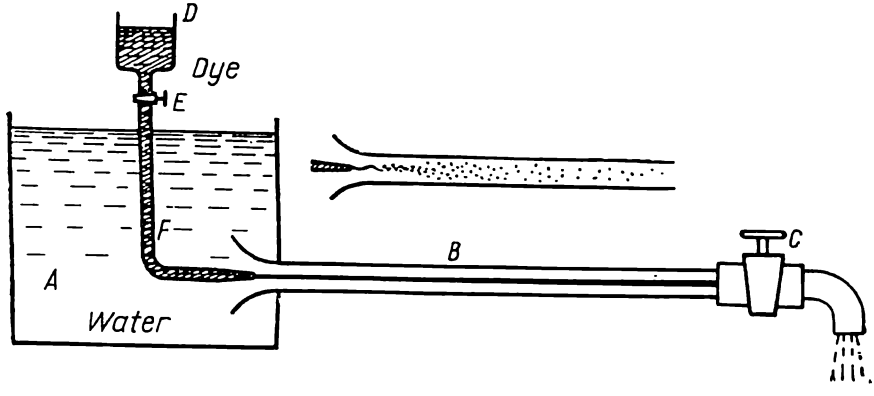

Fig. 39. Setup for demonstrating flow regimes

The change of flow in any given pipe takes place at a certain *critical velocity* v_{cr}. Experiments show that the critical velocity is directly proportional to the kinematic viscosity ν of the fluid and inversely proportional to the pipe diameter d:

$$v_{cr} = k \frac{\nu}{d}.$$

The dimensionless coefficient of proportionality k was found to be the same for all liquids and gases and any pipe diameters.

This means that the change in the flow takes place at a certain ratio between velocity, pipe diameter and viscosity

$$k = \frac{v_{cr} d}{\nu}.$$

This dimensionless number is called the *critical Reynolds number*, in honour of the English scientist Osborne Reynolds who presented

it, and it is denoted:

$$\mathrm{Re}_{cr} = \frac{v_{cr} d}{\nu}. \tag{5.1}$$

Experimental data set the critical Reynolds number at about 2,300.

In addition to the critical Reynolds number corresponding to the change in flow regime, there is also introduced the actual Reynolds number for a specific stream, which is expressed in terms of its actual velocity:

$$\mathrm{Re} = \frac{vd}{\nu}. \tag{5.2}$$

Thus, we have a criterion according to which we can determine whether the flow in a pipe will be laminar or turbulent. As laminar flow takes place at low velocities, it follows that at any value of $\mathrm{Re} < \mathrm{Re}_{cr}$ the flow is laminar. At $\mathrm{Re} > \mathrm{Re}_{cr}$ the flow is usually turbulent.

Knowing the velocity of flow, the pipe diameter and the viscosity of the liquid, it is possible to predict the type of motion. This is very important for hydraulic calculations.

In practice laminar flow occurs when very viscous liquids, such as lubricants and glycerine, flow through pipes.

Turbulent flow usually occurs in water mains and in pipes in which gasoline, kerosene, alcohols and acids are transported. Thus, in aircraft systems both laminar and turbulent flow is encountered: the former in oil and hydraulic transmission systems, the latter in fuel systems.

The change in the type of flow on reaching the critical Reynolds number is explained by the fact that the one type of flow becomes unsteady and the other steady. At $\mathrm{Re} < \mathrm{Re}_{cr}$, laminar flow is steady and any artificially induced turbulence (by shaking the pipe, submerging a vibrating body in the stream, etc.) is dampened by the viscosity of the fluid and laminar flow is restored as the turbulent regime in this case is unsteady. At $\mathrm{Re} > \mathrm{Re}_{cr}$, on the other hand, turbulent flow is steady and laminar flow is unsteady.

Actually, the critical Reynolds number corresponding to the changeover from laminar to turbulent flow is usually somewhat greater than Re_{cr} for the reverse change. In laboratory conditions, when all factors facilitating turbulence are removed, it is possible to sustain laminar flow at Reynolds numbers much higher than the critical. Laminar flow in such cases, however, is so unstable that the slightest jolt is sufficient to change it immediately into turbulent flow. In practice, notably in aircraft pipelines, conditions usually

contribute to turbulence (vibrations of the pipes, local disturbances, irregular discharge, etc.), and, in hydraulics, such sustained laminar flow is rather of theoretical than practical interest.*

The theory of steady laminar flow and turbulence has not yet been developed. Experiments show, however, that in a pipe of given cross-section turbulence is facilitated by such factors as distance from walls, velocity and the velocity gradient dv/dy across a section. The distance from the walls is greatest and the velocity is highest along the centre of the stream, the velocity gradient being zero. At the walls, on the other hand, the velocity gradient is largest, while the velocity and distance y vanish. Consequently, initial turbulence in laminar flow in a straight pipe of uniform cross-section begins somewhere between the centre line and the wall of the pipe, closer to the latter.

20. HYDRODYNAMIC SIMILARITY

The Reynolds number plays a significant part in hydraulics, as well as in aerodynamics, as an important criterion of the *similarity* of fluid flow. When incompressible liquids are considered similarity must be geometric, kinematic and dynamic.

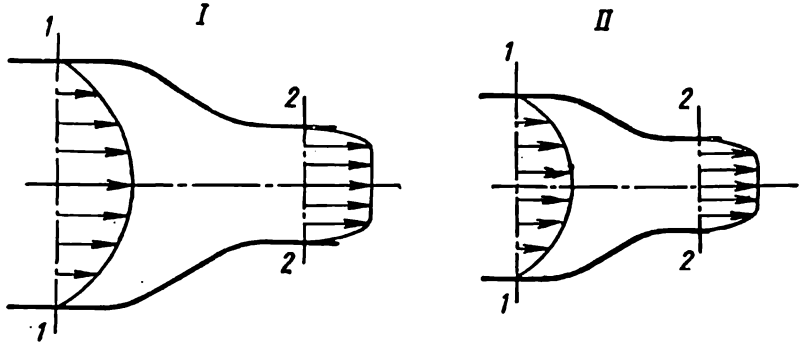

Fig. 40. Similar flows

Geometric similarity, it will be recalled from the course of geometry, means proportionality of corresponding dimensions and equality of corresponding angles. In hydraulics geometric similarity is interpreted to mean similarity of the surfaces constraining fluid flow, i. e., similarity of channels and their relative positions (Fig. 40).

* This consideration is of practical importance in the aerodynamics of airfoils (laminar-flow wings).

Kinematic similarity implies similarity of streamlines and proportionality of corresponding velocities. Obviously, kinematic similarity of flow requires geometric similarity of the channels.

Dynamic similarity implies proportionality of the forces acting on the corresponding elements of kinematically similar streams and equality of the direction angles of those forces.

Fluid flow is usually subjected to a variety of forces, such as pressure, viscosity (friction) and gravity. For complete hydrodynamic similarity, proportionality of all these different forces must be observed.

For example, the proportionality of the pressure forces P and the friction forces F_f acting on the corresponding volumes in streams I and II (Fig. 40) can be written down in the form

$$\left(\frac{P}{F_f}\right)_{\mathrm{I}} = \left(\frac{P}{F_f}\right)_{\mathrm{II}}.$$

In actual investigations it is usually very difficult to achieve complete hydrodynamic similarity. Experimenters commonly deal with partial (incomplete) similarity, in which only the main forces are proportional. For flow under pressure in closed conduits (through pipes, hydraulic machines, etc.) these main forces, as calculations show, are pressure, friction and their resultants. In similar streams the resultant forces are proportional to the product of the dynamic pressure $\frac{\varrho v^2}{2}$ times the characteristic area S.

For a fluid particle of dimension Δl, force is the product of mass times acceleration:

$$\Delta F = k\varrho\,(\Delta l)^3 \frac{dv}{dt} = k\varrho\,(\Delta l)^3 \frac{dv}{ds}\frac{ds}{dt} = k\varrho\,(\Delta l)^3\, v\,\frac{dv}{ds},$$

where k = dimensionless coefficient of proportionality depending on the shape of the particle;

ds = elementary path of the particle.

Now multiply and divide the foregoing expression through by l^2 and v_m^2, thereby introducing quantities characterising the flow as a whole. We have

$$\Delta F = k\frac{\Delta l}{ds}\left(\frac{\Delta l}{l}\right)^2 \frac{v}{v_m}\, d\left(\frac{v}{v_m}\right) \varrho\, v_m^2 l^2.$$

The five dimensionless terms in the expression for ΔF have the same value for geometrically and kinematically similar streams and corresponding particles. Consequently, replacing the equality sign

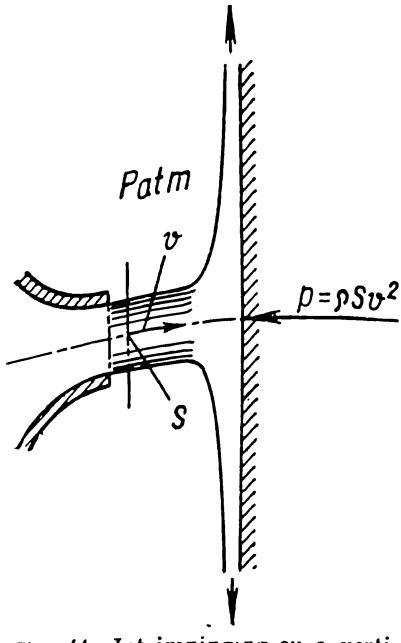

Fig. 41. Jet impinging on a vertical wall

by a proportionality sign, we can write for these streams:

$$\Delta F \sim \varrho v_m^2 l^2,$$

whence, as $l^2 \sim S$ and $\Delta F \sim F$, we finally obtain

$$F \sim \varrho v_m^2 S. \tag{5.3}$$

For similar streams *I* and *II* we have

$$\frac{F_{\mathrm{I}}}{F_{\mathrm{II}}} = \frac{(\varrho v_m^2 S)_{\mathrm{I}}}{(\varrho v_m^2 S)_{\mathrm{II}}},$$

or

$$\left(\frac{F}{\varrho v_m^2 S}\right)_{\mathrm{I}} = \left(\frac{F}{\varrho v_m^2 S}\right)_{\mathrm{II}}.$$

The last relation, which is the same for similar streams, is called the Newton number, denoted Ne.

It should be noted that in similar streams the product $\varrho v_m^2 S$ is also proportional to the thrust which a flow exerts (or is capable of exerting) on obstacles, such as walls, vanes, submerged bodies, etc. Thus, if a jet impinges normally on a flat plate of infinite area (Fig. 41) the direction of flow turns through 90°; from the well-known momentum equation of mechanics the impulse is

$$P = \varrho Q v = \varrho v^2 S. \tag{5.4}$$

This is the dynamic force acting on the plate. If the angle of approach is different or if the obstacle has different shape or dimensions the proportionality factor is not unity.

Let us first consider the simplest case: motion of an ideal liquid in a horizontal plane, that is, motion not affected by viscosity or gravity.

For this case $z_1 = z_2$, and Bernoulli's theorem for cross-sections *1-1* and *2-2* in Fig. 40 takes the form:

$$\frac{p_1}{\gamma} + \frac{v_1^2}{2g} = \frac{p_2}{\gamma} + \frac{v_2^2}{2g},$$

or

$$\frac{p_1 - p_2}{\varrho \frac{v_2^2}{2}} = 1 - \frac{S_1^2}{S_2^2}.$$

For two geometrically similar streams the right-hand sides of the equation have the same value, hence the left-hand members are also equal, i. e., the pressure differences are proportional to the dynamic pressures:

$$\left(\frac{\Delta p}{\rho v^2}\right)_{\mathrm{I}} = \left(\frac{\Delta p}{\rho v^2}\right)_{\mathrm{II}}. \tag{5.5}$$

Thus, for the case of an ideal incompressible fluid moving without the participation of gravity forces, geometric similarity alone ensures complete similarity of flow. The dimensionless quantity representing the ratio of the pressure difference to the dynamic pressure (or of the head pressure difference to the velocity head) is called the *pressure coefficient*, or the *Euler number*, denoted Eu.

Let us examine the conditions that must be satisfied by the geometrically similar streams just considered for hydrodynamic similarity when shear forces are acting and, hence, there is a degradation of energy, i. e., the conditions in which the Euler numbers are the same for the two flows.

Bernoulli's equation now takes the form

$$\frac{p_1}{\gamma} + \alpha_1 \frac{v_1^2}{2g} = \frac{p_2}{\gamma} + \alpha_2 \frac{v_2^2}{2g} + \zeta \frac{v_2^2}{2g},$$

or

$$\frac{2(p_1 - p_2)}{\rho v_2^2} = \mathrm{Eu} = \alpha_2 - \alpha_1 \frac{S_2^2}{S_1^2} + \zeta. \tag{5.6}$$

The latter equation shows that Eu is the same for both streams, hence they are similar if the loss coefficients are equal (the equality of the coefficients α_1 and α_2 for the corresponding cross-sections of the two streams follows from their kinematic similarity). Thus, in similar streams the coefficients ζ must be the same, which means that the head losses in corresponding portions (see Fig. 40) are proportional to the velocity heads, i. e.,

$$\left(\frac{h_{1-2}}{\frac{v_2^2}{2g}}\right)_{\mathrm{I}} = \left(\frac{h_{1-2}}{\frac{v_2^2}{2g}}\right)_{\mathrm{II}}.$$

Let us consider an important case of fluid motion: flow with friction in circular pipes, for which (see Sec. 16)

$$\zeta = \lambda \frac{l}{d}.$$

In geometrically similar streams the ratio $\frac{l}{d}$ is the same, hence the similarity condition in this case is equality of the factor λ for both streams. The latter, from Eq. (4.20), is expressed in terms of the shear stress τ_0 at the wall and the dynamic pressure as follows:

$$\lambda = \frac{4\tau_0}{\varrho \frac{v^2}{2}}.$$

Hence, for the two similar streams *I* and *II* we can write

$$\left(\frac{\tau_0}{\varrho v^2}\right)_{\text{I}} = \left(\frac{\tau_0}{\varrho v^2}\right)_{\text{II}}, \tag{5.7}$$

i. e., the shear stresses are proportional to the dynamic pressure. Taking into account Newton's law of shear, the foregoing proportionality can be replaced by the following:

$$\left[\frac{\mu\left(\frac{dv}{dy}\right)_0}{\varrho v^2}\right]_{\text{I}} = \left[\frac{\mu\left(\frac{dv}{dy}\right)_0}{\varrho v^2}\right]_{\text{II}}.$$

But, as in kinematic similarity we have the proportionality

$$\frac{dv}{dy} \sim \frac{v}{d},$$

then

$$\left(\frac{\mu \frac{v}{d}}{\varrho v^2}\right)_{\text{I}} = \left(\frac{\mu \frac{v}{d}}{\varrho v^2}\right)_{\text{II}}.$$

After the necessary transformations we obtain the condition for the similarity of fluid flow, taking viscosity into account:

$$\left(\frac{\nu}{vd}\right)_{\text{I}} = \left(\frac{\nu}{vd}\right)_{\text{II}}$$

or, going over to the reciprocal quantities,

$$\text{Re}_{\text{I}} = \text{Re}_{\text{II}}. \tag{5.8}$$

This is Reynolds's law of similarity: *For two geometrically similar streams of viscous fluids to be dynamically similar, the Reynolds*

numbers for two corresponding sections of the streams must be identical.

Now we see why the transition from one type of flow to another takes place at a specific Reynolds number. Furthermore, we find the physical meaning of the number for flow through pipes: it is a quantity characterising the ratio of the dynamic pressure to the shear stress. The greater the velocity and the cross-section of a flow and the less the viscosity of a fluid, the larger the Reynolds number. For an ideal fluid Re is infinite since the viscosity is zero.

The problem of similarity is more difficult in cases when the difference in elevation heads cannot be neglected in Bernoulli's equation. In such cases yet another similarity criterion is introduced: the Froude number, which takes into account the effects of gravity on fluid flow. However, for the overwhelming majority of problems of interest to the mechanical engineer this characteristic is not essential and we shall not consider it.

To sum up, in similar streams the corresponding dimensionless coefficients and numbers α, ζ, λ, Eu, Ne, Re, and several others to be introduced later on, are identical. A change in the Reynolds number means a change in the relation between the basic forces acting in a stream in view of which the other factors may also change to some extent. Thus they can all be regarded as functions of Re.

21. CAVITATION

In some cases of fluid motion in closed conduits there takes place a phenomenon which is due to a change in the physical state of a liquid: vapourisation and evolution of gases dissolved in it.

When a liquid flows through a narrowing in a pipe its velocity increases and the pressure intensity decreases. If the absolute pressure drops to the vapour pressure of the liquid for the given temperature, evaporation commences and gases evolve. In short, the liquid simply begins to boil locally. When the stream diverges after the narrowing, the velocity drops, the pressure increases and the boiling stops; the vapour then condenses partially or completely and the gases redissolve.

This local boiling of a flowing liquid is known as *cavitation*.

A simple device enables the phenomenon to be observed visually. Water or some other liquid is brought under pressure to a valve (Fig. 42) through which it flows into a glass tube with a venturi contraction.

When the valve is opened slightly the discharge is small, the velocity of the stream is low, the pressure drop at the throat of the tube is small and the stream is transparent: no cavitation takes place. The wider the valve is opened, the faster the velocity of the stream and the lower the pressure in the narrowing.

At $p_{ab} = p_t$, where p_t is the saturation vapour pressure, a distinct cavitation zone appears, which increases in size as the valve is opened wider.

Cavitation announces itself by characteristic noise and vibrations. Prolonged cavitation has an erosive effect on metal walls. The reason for this is that condensation of the bubbles of vapour takes place very rapidly and the cavities collapse abruptly with high compressive stresses due to local water-hammer effects. The pitting of walls occurs not at the point where the vapour pockets appear but where they collapse.

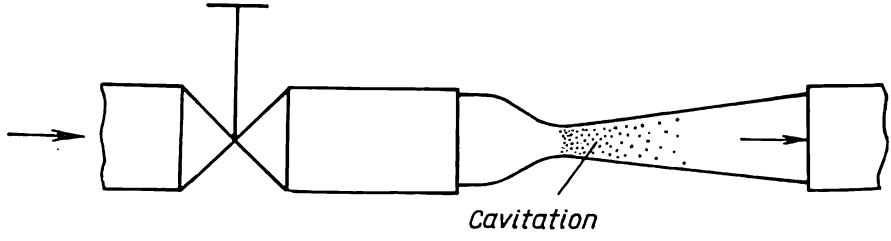

Fig. 42. Venturi tube for demonstrating cavitation

Cavitation thus has an adverse effect on pipelines and hydraulic systems. When cavitation develops the resistance of pipes increases sharply, with a corresponding reduction in discharge.

Cavitation may develop in any local narrowings followed by expansions, such as faucets, valves, gates, orifices and jets.

In some cases cavitation may also develop when a narrowing is not followed by a diverging section and in straight pipes when the elevation head or energy losses increase.

Cavitation may occur in hydraulic machines, such as pumps or turbines, and on the blades of rapidly revolving ship propeller screws. In these cases the result is a sharp decline in the efficiency of a machine and a gradual wearing of its parts.

In aircraft hydraulic systems cavitation may occur because of a reduced barometric pressure with height. In this case the cavitation zone extends over a considerable portion of the low-pressure pipelines (suction pipes) and even along the whole length. When this happens the stream in the pipe divides into a liquid and vapour phase.

In the initial stage the vapour phase appears as minute bubbles spread evenly along the flow (Fig. 43*a*). As vapourisation continues and the amount of vapour increases the bubbles grow larger and drift along the upper surface of the pipe (Fig. 43*b*). Finally the liquid and vapour phases may separate completely into two streams, the former below and the latter above (Fig. 43*c*). In thin pipes vapour locks may form and the two phases move in intermittent columns (Fig. 43*d*).

It is evident that the greater the vapour phase the less the discharge through a pipe. Condensation (partial or complete) of the vapour takes place in the pump of a system, where pressure increases sharply, or in the pressure pipe through which the liquid is pumped to the consumer.

Cavitation phenomena are different in plain (simple) and component (complex) liquids. In a plain liquid the pressure at which cavitation occurs corresponds to the saturation vapour pressure, which depends only on temperature. The phenomena were described above.

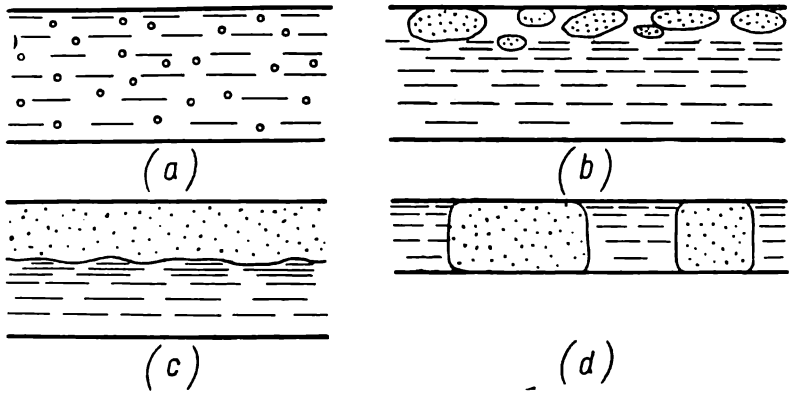

Fig. 43. Vapourisation in low-pressure pipes

A component liquid consists of so-called light and heavy fractions. The lighter fractions have a higher vapour pressure and the start boiling before the heavy ones. Condensation takes place in the reverse order.

Multicomponent liquids containing light fractions are more subject to cavitation and the vapour phase persists longer, but the process is not so pronounced as in plain liquids.

Example. Determine flow conditions of АМГ-10 fluid in a pipe of an aircraft hydraulic system if the pipe diameter $d = 12$ mm, the rate of discharge $Q = 0.25$ l/sec and the temperature is zero centigrade (see Table 1 on p. 24). At what temperature will flow conditions change?

Solution. (i) From Table 1, $\nu = 42$ cst $= 0.42$ cm²/sec.

(ii) The Reynolds number is

$$\mathrm{Re} = \frac{vd}{\nu} = \frac{4Q}{\pi d\nu} = \frac{4 \times 250}{\pi 1.2 \times 0.42} = 632.$$

The flow is *laminar*.

(iii) The viscosity corresponding to the change of the flow regime is

$$\nu_{cr} = \frac{4Q}{\pi d \mathrm{Re}_{cr}} = \frac{4 \times 250}{\pi 1.2 \times 2{,}300} = 0.115 \text{ cm}^2/\text{sec}.$$

(iv) Plotting a graph of the coefficient ν as a function of temperature from the data in Table 1, we find that $t_{cr} = 40°\text{C}$.

CHAPTER VI

LAMINAR FLOW

22. LAMINAR FLOW IN CIRCULAR PIPES

As stated in Sec. 19, laminar flow takes place in stratified layers without any mixing of the fluid; it obeys Newton's friction law (see Sec. 4) and is completely determined by the latter. Therefore the theory of laminar flow is based on Newton's law of viscous shear.

Consider a section of a straight horizontal pipe of diameter $d = 2r_0$ between cross-sections *1-1* and *2-2* at distance l apart (Fig. 44) taken sufficiently far away from the entrance to the pipe. The pressure is p_1 at section *1-1* and p_2 at section *2-2*. In view of the uniformity of the pipe diameter, the velocity and α coefficient are constant along the pipe, and Bernoulli's equation for the two sections takes the form

$$\frac{p_1}{\gamma} = \frac{p_2}{\gamma} + h_f,$$

where h_f = loss of head due to friction.

Hence,

$$h_f = \frac{p_1 - p_2}{\gamma} = \frac{p_f}{\gamma},$$

which is shown by piezometers tapped at the cross-sections.

Now consider a cylindrical control volume of radius r inside the stream, such that it is coaxial with the pipe and its two bases lie in the cross-sections.

The equation of uniform flow for the control volume is given by the equality to zero of the sum of the pressure forces and friction forces acting on the volume. Expressing the shear stress at the boundary of the cylinder by τ, we have

$$(p_1 - p_2)\pi r^2 - 2\pi r l \tau = 0,$$

whence,

$$\tau = \frac{p_f r}{2l}.$$

The equation shows that shear stress across the pipe section varies according to a linear law as a function of the radius. The shear stress profile is shown on the left side of Fig. 44.

Now, introducing Newton's friction law, express the shear stress τ in terms of the dynamic viscosity and velocity gradient [Eq. (1.11)]

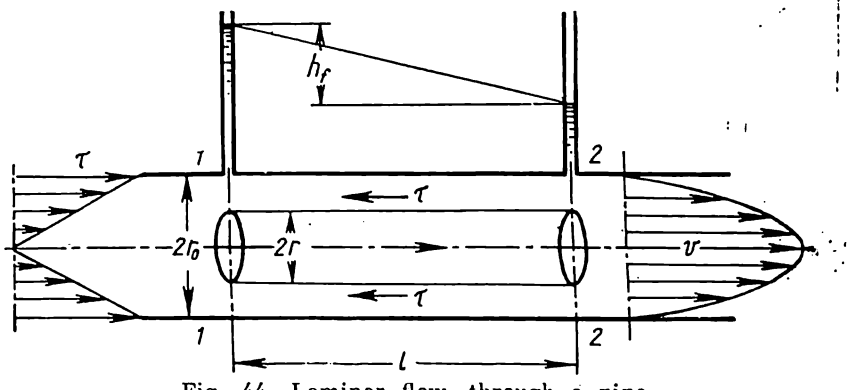

Fig. 44. Laminar flow through a pipe

and substitute for the variable y (the distance from the pipe wall) the radius r:

$$\tau = \mu \frac{dv}{dy} = -\mu \frac{dv}{dr}.$$

The minus sign is due to the fact that r is measured in the opposite direction of y.

Substituting the expression for τ into the previous equation, we obtain

$$\frac{p_f r}{2l} = -\mu \frac{dv}{dr},$$

from which we find the velocity increment dv:

$$dv = -\frac{p_f}{2\mu l} r dr.$$

To the positive radius increment there corresponds a negative velocity increment (i. e., a retardation), which is demonstrated by the velocity profile in Fig. 44.

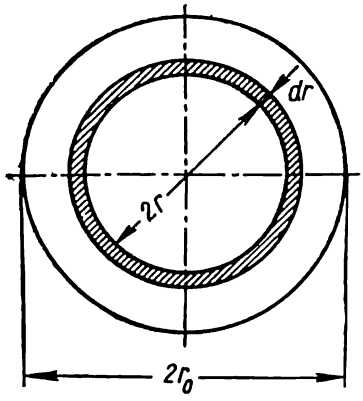

Fig. 45. Elementary ring area

Integrating, we have

$$v = -\frac{p_f}{2\mu l}\frac{r^2}{2} + C.$$

The integration constant C can be found from the boundary conditions where, at $r_0 = r$, $v = 0$, whence

$$C = \frac{p_f}{4\mu l} r_0^2.$$

The velocity at any point on a circle of radius r is

$$v = \frac{p_f}{4\mu l}(r_0^2 - r^2). \qquad (6.1)$$

This is the law of velocity distribution across a circular pipe section when the flow is laminar. The velocity distribution curve is a parabola of the second order. The maximum velocity is at the centre of the cross-section, where $r = 0$, and is equal to

$$v_{max} = \frac{p_f}{4\mu l} r_0^2. \qquad (6.2)$$

The ratio $\frac{p_f}{l}$ in Eq. (6.1), as is apparent from Fig. 44, represents the hydraulic gradient multiplied by γ. This quantity is constant along a straight pipe of uniform diameter.

The law of velocity distribution (6.1) can be used to compute the rate of discharge of a pipe. First express the elementary discharge across a differential area dS:

$$dQ = v\,dS.$$

Here v is a function of the radius determined by Eq. (6.1); the area dS is conveniently taken as a ring of radius r and width dr (Fig. 45). Then,

$$dQ = \frac{p_f}{4\mu l}(r_0^2 - r^2)\,2\pi r\,dr.$$

Integrating over the cross-section, i. e., from $r = 0$ to $r = r_0$, we have

$$Q = \frac{\pi p_f}{2\mu l}\int_{r=0}^{r=r_0}(r_0^2 - r^2)\,r\,dr = \frac{\pi p_f}{8\mu l} r_0^4. \qquad (6.3)$$

The mean velocity at the section is found by dividing the discharge by the area:

$$v_m = \frac{Q}{\pi r_0^2} = \frac{\pi p_f r_0^4}{8\mu l \pi r_0^2} = \frac{p_f}{8\mu l} r_0^2. \tag{6.4}$$

Comparing this expression with Eq. (6.2), we arrive at the conclusion that in laminar flow the mean velocity is just one-half of the maximum velocity:

$$v_m = 1/2\, v_{max}.$$

To obtain the friction law, i. e., to express the loss of head due to friction h_f in terms of rate of discharge and pipe dimensions, determine p_f from Eq. (6.3):

$$p_f = \frac{8\mu l Q}{\pi r_0^4}.$$

Dividing through by γ, we obtain the loss of head:

$$h_f = \frac{p_f}{\gamma} = \frac{8\mu l Q}{\pi r_0^4 \gamma}.$$

Substituting $\nu\varrho$ for μ, and $g\varrho$ for γ, and going over from r_0 to $d = 2r_0$, we finally obtain

$$h_f = \frac{128\nu l Q}{\pi g d^4}. \tag{6.5}$$

The friction law shows that in laminar flow through a circular pipe the loss of head due to friction varies as the rate of discharge and the viscosity and inversely as the fourth power of the diameter. This law, commonly known as the Hagen-Poiseuille equation, is used to calculate pipelines with laminar flow.

In Sec. 17 we agreed to express friction losses in terms of the mean velocity by Eq. (4.18). Let us develop Eq. (6.5) into the form

$$h_f = \lambda \frac{l}{d} \frac{v_m^2}{2g}.$$

For this, in Eq. (6.5) substitute the expression $\frac{\pi d^2}{4} v_m$ for the rate of discharge. After the necessary cancellations, we have

$$h_f = \frac{64\nu l v_m}{2g d^2}.$$

Multiplying and dividing through by v_m and rearranging, we obtain

$$h_f = \frac{64\nu}{v_m d} \frac{l}{d} \frac{v_m^2}{2g} = \frac{64}{\mathrm{Re}} \frac{l}{d} \frac{v_m^2}{2g},$$

or, finally, bringing to the form of Eq. (4.18'),

$$h_f = \lambda_l \frac{l}{d} \frac{v_m^2}{2g}, \tag{6.6}$$

where

$$\lambda_l = \frac{64}{\mathrm{Re}}, \tag{6.7}$$

the subscript at λ denoting that the flow is laminar.

Friction loss in laminar flow, it should be borne in mind, is proportional to the first power of the velocity. The square of the velocity in Eq. (6.6) was obtained artificially, as a result of multiplication and division by v_m, and the coefficient λ_l is inversely proportional to Re, and consequently, to v_m.

The theory of laminar flow through circular pipes set forth here is generally confirmed by experience and the friction law does not require any correction factors, with two exceptions:

1. At the beginning of a pipe, where the parabolic velocity profile has not yet developed. Resistance along the entrance portion of the pipe is greater than further on. This consideration, however, need be taken into account only in short pipelines. It will be analysed in the following section.

2. When considerable heat exchange is taking place, that is when the flowing fluid is heated or cooled. The resistance in this case is usually above the average.

23. ENTRANCE CONDITIONS IN LAMINAR FLOW. THE α COEFFICIENT

In the case of a straight pipe of uniform diameter leading from a reservoir, when the flow is laminar the velocity distribution at the entrance is practically uniform, especially if the entrance is rounded (Fig. 46). Further on viscous forces cause the velocity to change across a section: the layers in the vicinity of the wall are slowed down, but as the rate of discharge is constant for successive sections the velocity in the centre must be accelerated. More and more layers are gradually retarded until finally the parabolic velocity profile characteristic of laminar flow develops.

The section of a pipe from the entrance to the point where the parabolic velocity profile develops is called the *entrance*, or *transition*,

length (denoted l_{ent}). Beyond the entrance length steady laminar flow takes place and the velocity profile is parabolic as long as the pipe is straight and of same diameter. The laminar flow theory set forth here is valid only for steady laminar flow and cannot be applied to entrance conditions.

The entrance length can be determined from the following approximate formula in terms of the pipe diameter and Reynolds number:

$$\frac{l_{ent}}{d} = 0.029\,\mathrm{Re}. \tag{6.8}$$

Substituting $\mathrm{Re}_{cr} = 2{,}300$ into Eq. (6.8), we obtain the maximum entrance length, which is 66.5 diameters.

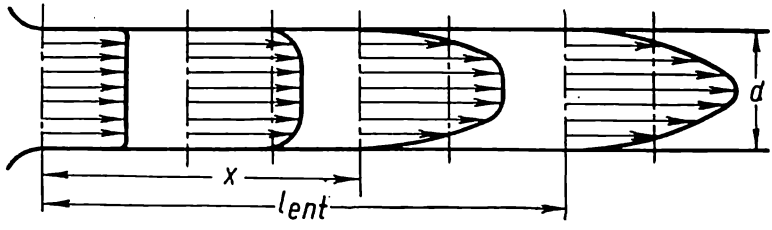

Fig. 46. Development of parabolic velocity profile

As mentioned, resistance to flow in the entrance length is greater than in subsequent sections. The reason is that the value of the derivative *dv/dy* at the pipe wall in the entrance length is larger than in the steady-flow portions of the pipe. As a result, the shear stress, as determined by Newton's law, is greater, the more so the closer the considered section is to the pipe entrance, i. e., the smaller the coordinate x.

Loss of head in a pipe section, when $l \leqslant l_{ent}$, is determined by Eqs (6.5) or (6.6) and (6.7), with a correction factor K greater than unity. The value of K can be found from the graph in Fig. 47, where it is given as a function of the dimensionless parameter $\frac{x}{\mathrm{Re}d}\,10^3$. The greater the parameter the smaller K until, at

$$\frac{x}{\mathrm{Re}\,d} = \frac{l_{ent}}{\mathrm{Re}\,d} = 0.029,$$

i. e., at $x = l_{ent}$, $K = 1.09$. Thus, the resistance of the entrance length of a pipe is 9 per cent higher than the resistance of an equal length with steady laminar flow.

For short pipes the factor K, as is apparent from the diagram, is substantially greater than unity.

When the length l of a pipe is greater than the entrance length l_{ent}, the loss of head comprises the loss in the entrance length and the loss in the steady-flow portion, i. e.,

$$h_f = \left[1.09\lambda_l \frac{l_{ent}}{d} + \lambda_l \frac{(l - l_{ent})}{d}\right] \frac{v^2}{2g}.$$

Taking into account Eqs (6.7) and (6.8) and after the necessary transformations and computations,

$$h_f = \left(0.165 + \frac{64}{\mathrm{Re}} \frac{l}{d}\right) \frac{v^2}{2g}. \tag{6.9}$$

If the relative length of the pipeline $\frac{l}{d}$ is large enough, the number 0.165 inside the parentheses can be neglected. However, when

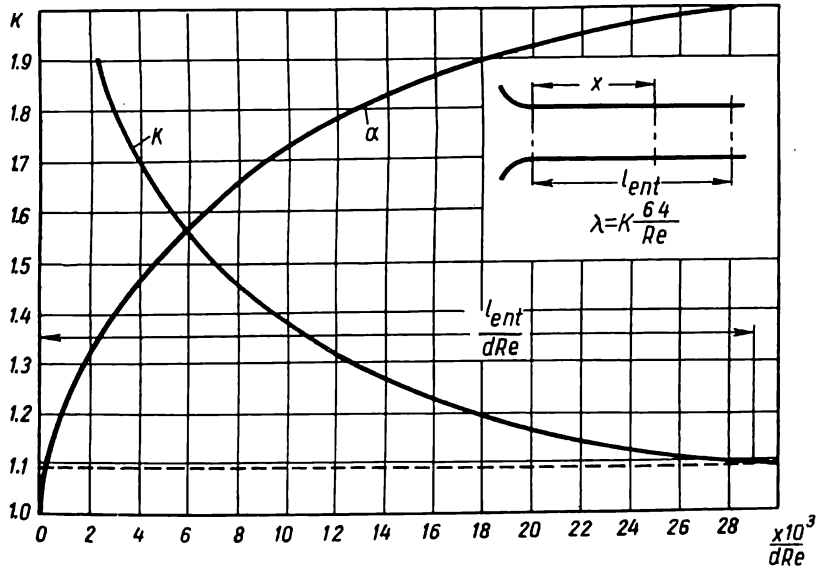

Fig. 47. Plot of coefficients K and α

accurate calculations are necessary for pipelines whose length is commensurable with l_{ent} it must be taken into account.

Knowing the velocity distribution law (6.1) and the relation between mean velocity and loss of head (6.4) it is simple to determine the value of the coefficient α, which takes into account nonuniform velocity distribution when Bernoulli's equation is applied to steady laminar flow in circular pipes.

Take Eq. (4.15) and substitute into it the expressions (6.1) and (6.4) for the velocity and mean velocity, respectively. Then, taking into account that

$$S = \pi r_0^2$$

and

$$dS = 2\pi r dr,$$

and after the necessary cancellations, we obtain

$$\alpha = \frac{1}{v_m^3 S}\int_S v^3 dS = 16\int_0^{r_0}\left(1 - \frac{r^2}{r_0^2}\right)^3 \frac{r dr}{r_0^2}.$$

Substituting the variable

$$1 - \frac{r^2}{r_0^2} = z,$$

we obtain

$$\alpha = -8\int_1^0 z^3 dz = 2\left|z^4\right|_0^1 = 2. \qquad (6.10)$$

Thus, the actual kinetic energy of a stream with laminar flow with parabolic velocity distribution is twice the kinetic energy of an identical stream with uniform velocity distribution.

It can be demonstrated in like manner that the momentum of laminar flow with parabolic velocity distribution is β times greater than the momentum of a similar flow with uniform velocity distribution, the coefficient β being constant:

$$\beta = \frac{4}{3}.$$

For the transition length of a pipe with a rounded entrance the coefficient α increases from 1 to 2 (see Fig. 47).

24. LAMINAR FLOW BETWEEN PARALLEL BOUNDARIES

We shall now consider laminar flow between two parallel flat walls (Fig. 48). Placing the origin of our coordinate system halfway between the two walls, the x axis is pointed in the direction of flow and the y axis is normal to the walls.

Passing two cross-sections normal to the flow the distance between which is l, consider a rectangular volume of thickness $2y$ and unit

width perpendicular to the page (Fig. 48). The condition for uniform motion of the control volume along the x axis is:

$$2yp_f = -\mu \frac{dv}{dy} 2l,$$

where $p_f = p_1 - p_2$ is the difference between the pressure intensities at the two cross-sections. The minus is due to the negative value of the derivative dv/dy.

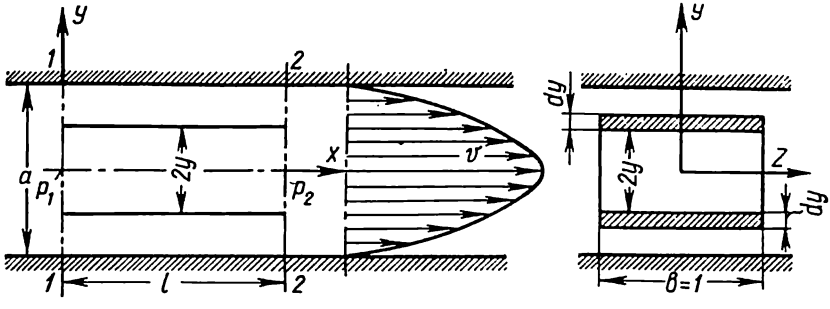

Fig. 48. Laminar flow between parallel flat walls

From the foregoing, determine the velocity increment dv corresponding to the coordinate increment dy:

$$dv = -\frac{p_f}{\mu l} y dy.$$

Integrating,

$$v = -\frac{p_f}{2\mu l} y^2 + C.$$

As, at $y = \frac{a}{2}$, $v = 0$, then $C = \frac{p_f}{2\mu l} \frac{a^2}{4}$, whence finally

$$v = \frac{p_f}{2\mu l} \left(\frac{a^2}{4} - y^2 \right). \tag{6.11}$$

To compute the rate of discharge per unit width, first take two elementary areas of size $1 \times dy$ located symmetrically relative to the z axis and express the elementary discharge:

$$dQ = vdS = \frac{p_f}{2\mu l} \left(\frac{a^2}{4} - y^2 \right) 2dy,$$

whence

$$Q = \frac{p_f}{\mu l}\int_0^{\frac{a}{2}}\left(\frac{a^2}{4} - y^2\right)dy = \frac{p_f a^3}{12\mu l}. \qquad (6.12)$$

From this, expressing the pressure loss in terms of the mean velocity $v_m = \frac{Q}{a}$,

$$p_f = \frac{12\mu l v_m}{a^2}. \qquad (6.13)$$

The relations obtained can be used to investigate flow through a space between two nested cylinders parallel to their centre lines if the space a is small in relation to the cylinder diameters: otherwise the law is more complicated, and we shall not examine it here.

When one of the walls is moving parallel to the other with velocity U, the pressure intensity in the space being constant along its length, the moving wall carries the fluid along. The velocity distribution is linear (Fig. 49) and therefore expressed in the form

$$v = \left(\frac{1}{2} - \frac{y}{a}\right)U. \qquad (6.14)$$

The rate of discharge per unit width of the spacing perpendicular to the page is determined from the mean velocity, which is $\frac{1}{2}U$, i. e.,

$$Q = \frac{U}{2}a. \qquad (6.15)$$

If there is a pressure drop in the fluid filling the spacing, the velocity distribution law across the space is found as the sum (or difference, depending on the direction of motion of the wall) of expressions (6.11) and (6.14):

$$v = \frac{p_f}{2\mu l}\left(\frac{a^2}{4} - y^2\right) \pm \left(\frac{1}{2} - \frac{y}{a}\right)U.$$

The resultant velocity distribution across the space is shown in Fig. 50 when (a) the wall moves in the direction of flow due to the

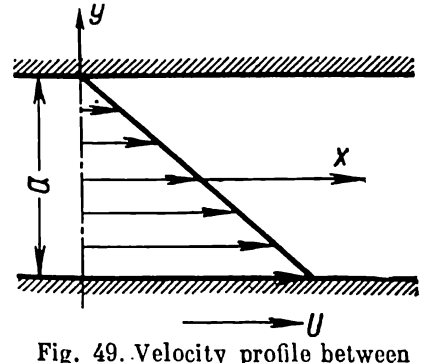

Fig. 49. Velocity profile between moving walls

pressure drop, and (*b*) the wall moves in the opposite direction.

The rate of discharge is determined as the sum of the discharges given by Eqs (6.12) and (6.15):

$$Q = \frac{p_f a^3}{12 \mu l} \pm \frac{U}{2} a.$$

This kind of flow through narrow spaces is found in pumps and other hydraulic machines.

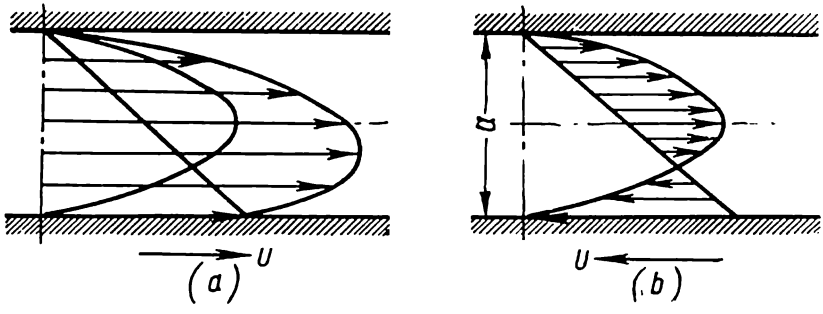

Fig. 50. Velocity profiles between moving walls with pressure drop

Example. Determine whether an aircraft lubricating system with the characteristics given below will function in horizontal flight at an altitude of 16,000 m ($p_{atm}/\gamma_{Hg} = 77.1$ mm Hg) (i. e., determine absolute pressure at pump intake

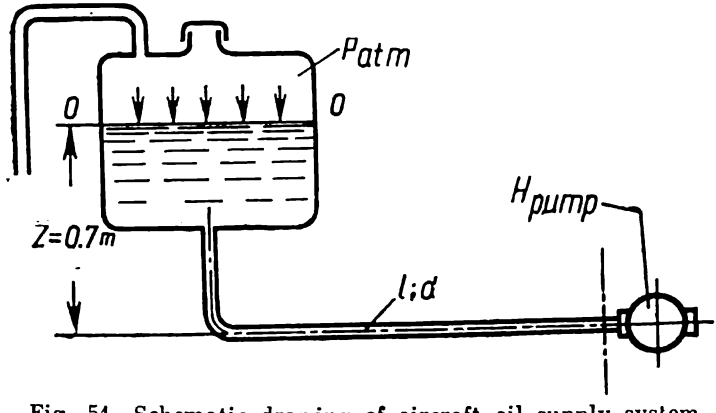

Fig. 51. Schematic drawing of aircraft oil supply system

in mm Hg). The length of the intake pipeline is $l = 2$ m, the diameter d — 18 mm; elevation of the oil surface in the tank above the pump $z = 0.7$ m; the pressure in the oil tank is atmospheric (Fig. 51). The required flow rate to ensure the necessary heat transfer into the oil at maximum performance of the engine is $Q = 16$ lit/min; viscosity of MK-8 oil $\nu = 0.11$ cm²/sec, $\gamma_{oil} = 900$ kg/m³. Neglect local losses.

Solution. (i) Velocity of oil in pipeline:

$$v = \frac{4Q}{\pi d^2} = \frac{4 \times 16 \times 10^3}{\pi 1.8^2 \times 60} = 105 \text{ cm/sec.}$$

(ii) Reynolds number:

$$\mathrm{Re} = \frac{vd}{\nu} = \frac{105 \times 1.8}{0.11} = 1{,}720.$$

(iii) Friction loss in intake pipe:

$$h_f = \lambda_l \frac{l}{d} \frac{v^2}{2g} = \frac{64}{1{,}720} \times \frac{200}{1{,}8} \times \frac{105^2}{2 \times 981} = 23.2 \text{ cm.}$$

(iv) Pressure at pump intake from Bernoulli's equation between sections *0-0* and *1-1*:

$$z + \frac{p_{atm}}{\gamma_{oil}} = \frac{p_1}{\gamma_{oil}} + \alpha \frac{v^2}{2g} + h_f,$$

whence

$$\frac{p_1}{\gamma_{oil}} = z + \frac{p_{atm}}{\gamma_{oil}} - \alpha \frac{v^2}{2g} - h_f = 70 + 7.71 \frac{13.6}{0.9} - \frac{2 \times 105^2}{2 \times 981} - 23.2 = 152 \text{ cm,}$$

or

$$h_{Hg} = 152 \frac{0.9}{13.6} = 10 \text{ cm} = 100 \text{ mm Hg.}$$

CHAPTER VII

TURBULENT FLOW

25. TURBULENT FLOW IN SMOOTH PIPES

It was mentioned in Sec. 19 that turbulent flow is characterised by a mixing of the fluid and fluctuations of velocity and pressure. A sensitive recorder of velocity fluctuations would draw a graph like the one in Fig. 52. The magnitude of the velocity varies erratically about a certain mean value which is constant for a given condition.

The pathlines traced by fluid particles through a fixed point in space are curves of different shape, despite the straightness of the pipe. The streamlines also vary greatly at any given instant (Fig. 53). Thus, strictly speaking, turbulent flow is unsteady as the velocity, pressure intensity and pathlines of the fluid particles change with time.

Nevertheless, turbulent flow can be regarded as steady if the mean velocity and pressure and the total discharge do not change with time. This kind of flow is frequently encountered in engineering practice.

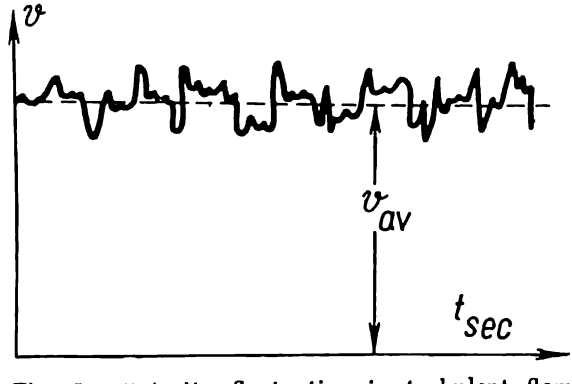

Fig. 52. Velocity fluctuation in turbulent flow

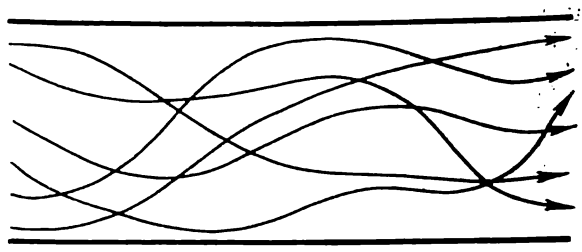

Fig. 53. Streamlines in turbulent flow

As the fluid is not laminar and it mixes continuously, Newton's friction law is not applicable to turbulent flow. Because of mixing of the fluid and continuous transport of momentum across the flow, the intensity of shear at the pipe boundary is much greater than in laminar flow with the same Re and dynamic pressure as computed for the mean velocity and density of the fluid.

The velocity distribution (averaged over a period of time) across a section of turbulent flow differs markedly from velocity distribution in laminar flow.

A comparison of the velocity profiles in the same pipe and with the same discharge (same mean velocity) in conditions of laminar and turbulent flow reveals a pronounced difference (Fig. 54). Velocity distribution in turbulent flow is somewhat more uniform and the increase in velocity at the boundary is steeper than in laminar flow, in which, it will be recalled, the velocity profile is a parabola.

Consequently, the α coefficient, which takes account of nonuniform velocity distribution in Bernoulli's equation (see Sec. 16), is much smaller in turbulent flow. Unlike laminar flow, where α does not depend on Re (see Sec. 23), in turbulent flow α is a function of Re, decreasing with the latter increasing from 1.13 at $Re = Re_{cr}$ to 1.025 at $Re = 3 \times 10^6$. As the graph in Fig. 55 shows, the curve of α as a function of Re approaches unity asymptotically. In most cases of turbulent flow α can be assumed to be unity.

Energy losses in turbulent flow through pipes of uniform cross-section (i. e., head losses due to friction) also differ from the case of laminar flow. In the former friction losses are much greater for the same rate of discharge, viscosity and pipe size.

This increased loss is due to the formation of eddies, mixing and curving of pathlines. Whereas in laminar flow friction losses increase as the first

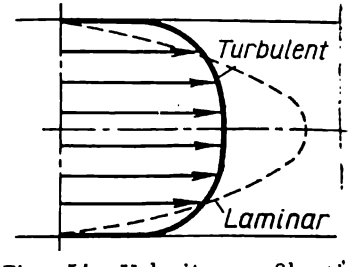

Fig. 54. Velocity profiles in laminar and turbulent flow

power of the velocity (and the discharge), in transition to turbulent flow a jump is observed in the resistance and then a steeper increase of h_f along a curve approaching a parabola of the second power (Fig. 56).

In view of the complexity of turbulent flow and the difficulty of analytical study, the theory of turbulent flow lacks precision. The so-called semiempirical, approximate turbulence theories of Prandtl, von Kármán and others are applied, but we shall not consider them here.

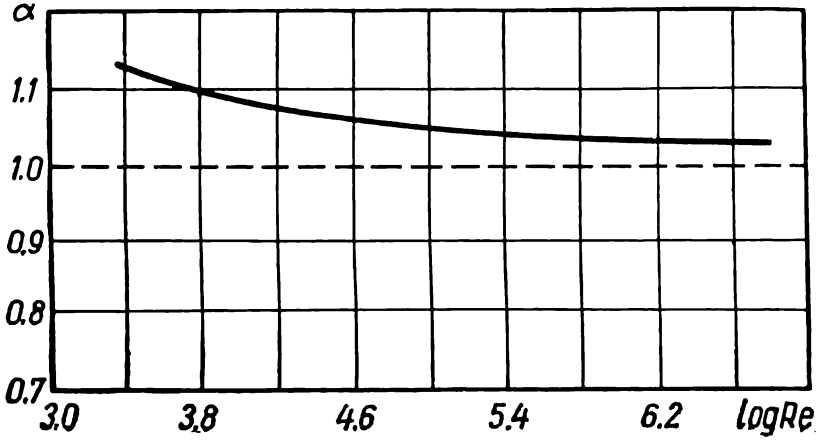

Fig. 55. Plot of α versus Re

In most cases engineering calculations of turbulent flow in pipes are based on purely experimental data systematised on the basis of hydrodynamic similarity.

The fundamental equation for turbulent flow in circular pipes is the experimental formula (4.18), which follows directly from similarity considerations and has the form

$$h_f = \lambda_t \frac{l}{d} \frac{v^2}{2g},$$

or

$$h_f = \lambda_t \frac{l}{d} \times \frac{16\,Q^2}{2\,g\pi^2 d^4},$$

where λ_t = friction factor for turbulent flow.

This basic formula is valid for both turbulent and laminar flow (see Sec. 22), the difference lying in the value of λ.

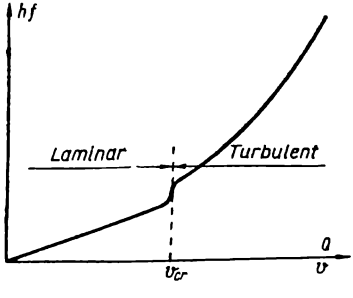

Fig. 56. Plot of friction loss h_f versus v and Q.

As in turbulent flow friction losses vary approximately as the square of the velocity (and the square of the rate of discharge), the friction factor in Eq. (4.18) can, to a first approximation, be assumed constant.

However, it follows from the similarity law (Sec. 20) that λ_t, like λ_l, should be a function of the fundamental criterion of similarity, the Reynolds number, which includes velocity, diameter and kinematic viscosity, i. e.,

$$\lambda_t = f(\mathrm{Re}) = f\left(\frac{vd}{\nu}\right).$$

There are a number of empirical and semiempirical formulas which express this function for turbulent flow through smooth pipes;

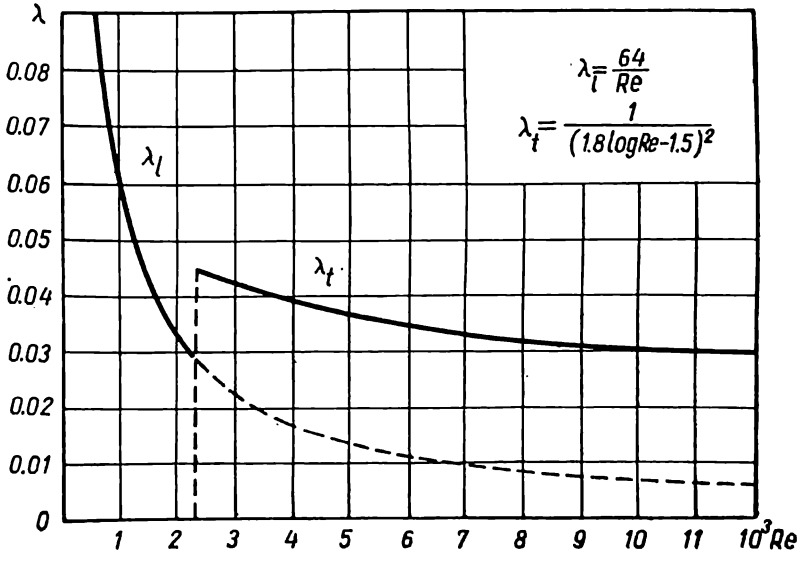

Fig. 57. Plot of friction factors λ_l and λ_t versus Re

one of the most convenient and commonly used is a formula developed by the Russian scientist P. K. Konakov:

$$\lambda_t = \frac{1}{(1.81g\mathrm{Re} - 1.5)^2}, \tag{7.1}$$

which holds good for values ranging from $\mathrm{Re} = \mathrm{Re}_{cr}$ to several millions.

When $2{,}300 < \mathrm{Re} < 10^5$ the old Blasius equation can be used:

$$\lambda_t = \frac{0.3164}{\sqrt[4]{\mathrm{Re}}}. \tag{7.2}$$

It will be observed that with Re increasing λ_t decreases somewhat, though to a much smaller degree than in laminar flow (Fig. 57).

This difference in the change of λ is due to the fact that the effect of viscosity on friction is much less in turbulent than in laminar flow. Whereas in the latter friction losses vary directly as the viscosity (see Sec. 22), in turbulent flow, as is evident from Eqs (4.18) and (7.2), they vary as the 1/4th power of viscosity. This is because of mixing and momentum transport in turbulent flow.

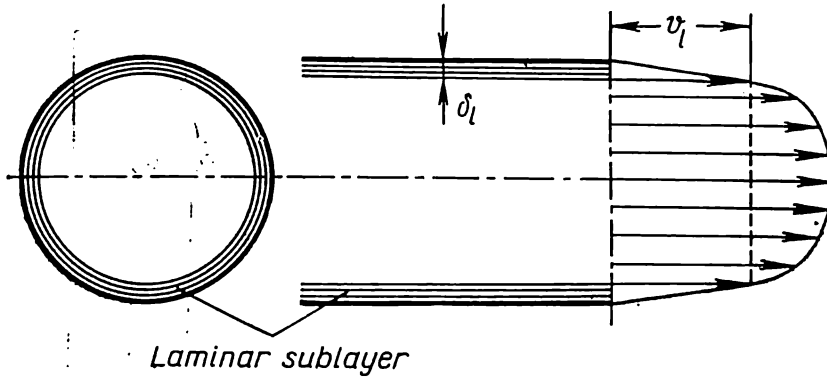

Fig. 58. Laminar sublayer in a pipe

Eqs (7.1) and (7.2) for determining the friction factor λ_t in terms of Re are valid for so-called technically smooth pipes, the roughness of which is small enough so as practically not to affect resistance. To a sufficient degree of accuracy, as technically smooth can be regarded drawn nonferrous (including aluminium alloy) tubing and special seamless high-grade steel pipes. Thus, the pipes used in aircraft fuel systems and hydraulic transmissions can be regarded as smooth and the foregoing equations used in calculating them. Since steel water pipes and cast iron pipes offer greater resistance, they cannot be treated as smooth, and Eqs (7.1) and (7.2) are not valid for them.

The resistance of rough pipes will be examined later on.

It is known from similarity theory, and confirmed by experiments carried out by a number of researchers (Nikuradse, G. G. Gurzhiyenko and others) that in turbulent flow a laminar sublayer usually

forms at the pipe walls (Fig. 58). This is a very thin layer in which the fluid moves much slower and without mixing.

Within the sublayer the velocity increases steeply from zero at the wall to a certain value v_l at the sublayer boundary. The sublayer is very thin; the Reynolds number computed for δ_l, the velocity v_l and the kinematic viscosity ν, was found to be a constant quantity:

$$\frac{v_l \delta_l}{\nu} = \text{const}, \tag{7.3}$$

where δ_l = sublayer thickness.

This quantity is a universal constant, like the critical Reynolds number for flow through pipes. When the velocity of motion and, consequently, the Reynolds number increase, the velocity v_l increases as well and the sublayer thickness δ_l decreases. At large values of Re the laminar sublayer practically disappears.

26. TURBULENT FLOW IN ROUGH PIPES

In smooth pipes friction losses were completely determined by the Reynolds number. In rough pipes, however, the value of λ_t depends also on the roughness of the inside pipe surface. The important point is not so much the absolute roughness size k of the projections as the so-called relative roughness $\frac{k}{r_0}$: for the same absolute roughness may have no effect on the resistance of a large pipe and considerably increase the resistance of a small one. Furthermore, the shape and distribution of the projections may affect the resistance of a pipe. The simplest case of roughness is that in which all the projections are of the same shape and size, known as uniform granular wall roughness.

In the case of uniform granular roughness the friction factor λ_t depends both on Re and on the ratio $\frac{k}{r_0}$:

$$\lambda_t = f\left(\text{Re}; \frac{k}{r_0}\right).$$

The effect of these two parameters on pipe friction is shown on the graph in Fig. 59, which is based on Nikuradse's experiments. Nikuradse investigated the resistance of artificially roughened pipes. He coated several different sizes of pipe with sand grains which had been segregated by sieving so as to obtain different sizes of grain of uniform diameter. In this way he obtained uniform granular roughness.

The pipes were tested in a broad range of relative roughnesses $\left(\frac{k}{r_0} = 1/500 \text{ to } 1/15\right)$ and Reynolds numbers (Re = 500 to 10^6). Fig. 59 contains the results of his experiments in the form of curves on a logarithmic plot relating log (1,000 λ) to log Re for various ratios $\frac{k}{r_0}$.

The inclined straight lines *A* and *B* correspond to the resistance laws for smooth pipes, i. e., Eqs (6.7) and (7.2), which, multiplied

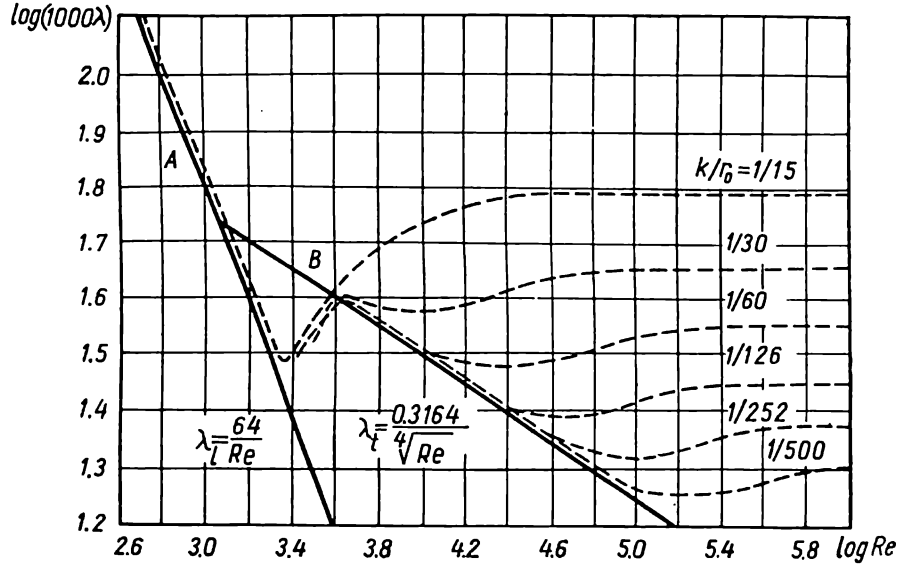

Fig. 59. Plot of log (1000λ) versus log Re for rough pipes (after J. Nikuradse)

by 1,000 and the logarithm taken, give linear equations for the given coordinate system:

$$\log (1{,}000\lambda_l) = \log 64{,}000 - \log \mathrm{Re}$$

and

$$\log (1{,}000\lambda_t) = \log 316.4 - \frac{1}{4} \log \mathrm{Re}.$$

The broken lines are curves plotted for pipes with different relative roughness. The following basic conclusions can be drawn from the graph:

1. In laminar flow roughness does not affect resistance; the broken curves corresponding to various degrees of roughness practically coincide with line *A*.

2. The critical Reynolds number practically does not depend on roughness. The broken curves diverge from line A at about the same value of Re.

3. In turbulent flow when Re and $\frac{k}{r_0}$ are small roughness does not affect resistance; in some places the broken lines coincide with line B. However, with Re increasing the roughness begins to tell and the curves for rough pipes begin to deviate from the straight line of the resistance law for smooth pipes.

4. At high values of Re and $\frac{k}{r_0}$ the friction factor λ_t no longer depends on Re and becomes constant for a given relative roughness. This corresponds to the horizontal portions of the broken lines after their slight rise.

Thus, for each of the curves corresponding to turbulent flow in rough pipes there are observed three distinct regions of the numbers Re and $\frac{k}{r_0}$ in which the behaviour of the friction factor λ_t is markedly different:

(1) Low Re and $\frac{k}{r_0}$: λ_t is independent of the roughness and is controlled solely by the Reynolds number, just as in smooth pipes. Roughness has no maximum values.

(2) The friction factor λ_t depends on both Re and $\frac{k}{r_0}$.

(3) High Re and $\frac{k}{r_0}$: λ_t is independent of Re and is controlled solely by the relative roughness; the resistance law is quadratic, as λ_t being independent of Re makes head losses proportional precisely to the square of the velocity [see Eq. (4.18)]; this is the "rough-law regime".

In order to gain a correct understanding of the resistance of rough pipes, it is necessary to take into account the existence of the laminar sublayer mentioned in Sec. 25.

It was pointed out that with Re increasing the thickness of the sublayer δ_t decreases. For this reason in turbulent flow in a rough pipe with a low Reynolds number the laminar sublayer covers the projections, which are contained within it and do not affect the pipe resistance. As Re increases the thickness of the sublayer decreases and the projections extend partly outside it, thus beginning to affect the resistance. At large values of Re the sublayer practically vanishes and all the projections reach into the turbulent flow. Eddies form in the wake of each projection, which explains the quadratic resistance law in this regime.

where Π = perimeter of a cross-section;

τ_0 = shear stress at the wall, which depends mainly on the dynamic pressure, i. e., on the mean velocity and viscosity (see Secs 17 and 25).

Thus, for a given cross-sectional area and given discharge (and, consequently, given mean velocity) the frictional force is proportional to the perimeter of the cross-section. Hence, to reduce friction and friction losses, the perimeter must be reduced. A circular cross-section has the smallest perimeter for a given area, and that is why it is the best from the point of view of reducing energy (head) losses in a pipe.

In evaluating the effects of section shape on head losses, the so-called hydraulic radius, or hydraulic mean depth, R_h is introduced, defined as the ratio of the area of a cross-section to its perimeter:

$$R_h = \frac{S}{\Pi}. \tag{7.6}$$

(Sometimes the concept of hydraulic diameter $D_h = 4R_h$ is used.)

The hydraulic radius can be computed for any cross-section. Thus, for a circular cross-section

$$R_h = \frac{\pi d^2}{4\pi d} = \frac{d}{4},$$

whence

$$d = 4R_h; \tag{7.7}$$

for an oblong cross-section with sides $a \times b$

$$R_h = \frac{ab}{2(a + b)};$$

for a square with side a

$$R_h = \frac{a}{4}.$$

For a clearance of height a we have from the foregoing (assuming a very small in comparison with b)

$$R_h = \frac{a}{2}$$

Expressing the hydraulic radius in terms o geometric diameter [Eq. (7.7)] and substituting in o the basic equation for head losses

due to friction (4.18), we obtain

$$h_f = \lambda_t \frac{l}{4R_h} \frac{v^2}{2g}. \tag{7.8}$$

As this equation presents a more general expression than the loss law given by Eq. (4.18), it should be valid for both circular and non-circular pipes.

Experience confirms the validity of Eq. (7.8) for pipes of any shape. The friction factor λ is computed from the same equations (7.1) and (7.2), but the Reynolds number is expressed in terms of R_h:

$$\mathrm{Re} = \frac{4R_h v_m}{\nu}. \tag{7.9}$$

Example. Determine the pressure loss due to friction in the cylindrical portion of the cooling conduit of the combustion chamber of a Reintochter liquid-propellant rocket. The coolant (nitric acid) is delivered through the space between coaxial tubes. The diameter of the inner tube $D = 155$ mm, the clearance between the tubes $\delta = 2$ mm and the length of the conduit $l = 500$ mm. The rate of discharge of the coolant $G = 10$ kg/sec, specific weight $\gamma_k = 1{,}510$ kg/m^3.

Assume the temperature of the acid in the section under consideration to be constant $t_m = 80°C$ ($\nu = 0.25$ cst).

Solution. (i) Velocity of flow through clearance:

$$v = \frac{G}{\gamma \pi D \delta} = \frac{10}{1{,}510 \times \pi \times 0.155 \times 0.002} = 6.8 \text{ m/sec}.$$

(ii) Hydraulic radius of conduit:

$$R_h = \frac{\pi[(D+2\delta)^2 - D^2]}{4\pi(D+2\delta+D)} = \frac{\delta}{2} = 1 \text{ mm}.$$

(iii) Reynolds number:

$$\mathrm{Re} = \frac{4R_h v}{\nu} = \frac{4 \times 0.1 \times 680}{0.0025} = 110{,}000.$$

(iv) Pressure loss due to friction:

$$p_f = \lambda_t \frac{l}{4R_h} \frac{v^2}{2g} \gamma = \frac{1}{(1.81g\mathrm{Re} - 1.5)^2} \times \frac{500}{4 \times 1} \times \frac{6.8^2}{2 \times 9.8} \times 1{,}510 \times 10^{-4} = 0.8 \text{ atm}.$$

Pressure losses in conic sections of the cooling system are much greater, but their computation requires integration.

Nikuradse carried out his experiments with artificially, uniformly granular-roughened pipes. For real rough pipes the dependence of λ_t on Re is somewhat different; notably there is no bulge in the curves following their divergence from the smooth-law curve. Fig. 60 presents a chart of some extremely precise experiments carried out by the Soviet scientist G. A. Murin.

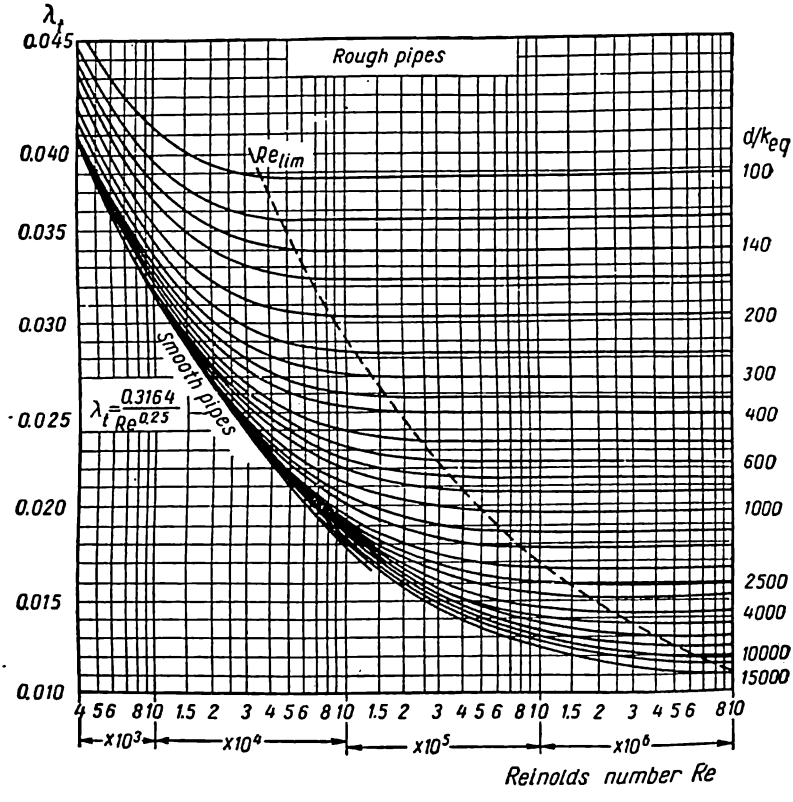

Fig. 60. Plot of friction factor λ_t versus Re for rough pipes

The friction factor λ_t for real rough pipes is given as a function of Re for different values of $\frac{d}{k_{eq}}$, where k_{eq} is the absolute roughness equivalent to Nikuradse's granular roughness. For new steel pipes Murin suggests assuming $k_{eq} = 0.06$ mm, and for used pipes, $k_{eq} = 0.2$ mm.

The following new general formula has been suggested by the Soviet scientist A. D. Altshul for engineering calculatio... the resist-

ance of real rough pipes:

$$\frac{1}{\sqrt{\lambda}} = 1.8 \log \frac{\mathrm{Re}}{\mathrm{Re}\frac{k'}{d} + 7}, \tag{7.4}$$

where d = pipe diameter;

k' = dimension proportional to absolute roughness.

The limiting values of k' for different pipes are presented in Table 2.

Table 2

Pipe material	$10^3\ k'$, mm
Glass tubing	0.0
Drawn tubing, brass, lead, copper	0.0
Seamless steel, high-grade manufacture	0.6-2.0
Steel pipe	3-10
Asphalt-dipped cast iron pipe	10-25
Cast iron pipe	25-50

At low values of $\mathrm{Re}\frac{k'}{d}$ as compared with the number 7, Eq. (7.4) turns into Konakov's Eq. (7.1) for smooth pipes; at large values of $\mathrm{Re}\frac{k'}{d}$ it turns into the equation for the rough-law regime (the quadratic law of resistance):

$$\frac{1}{\sqrt{\lambda}} = 1.8 \log \frac{d}{k}. \tag{7.5}$$

Thus, a comparison of the product $\mathrm{Re}\frac{k'}{d}$ with the number 7 enables a demarcation to be made between the different regimes of turbulent flow through rough pipes.

27. TURBULENT FLOW IN NONCIRCULAR PIPES

The foregoing discourse referred to turbulent flow in circular pipes. The engineer, however, may encounter cases of turbulent flow in noncircular pipes as, for example, in cooling systems. Let us investigate the effect of pipe shape on friction in turbulent flow.

The total friction acting on the boundary surface of a stream of length l can be expressed as follows:

$$T = \Pi l \tau_0,$$

CHAPTER VIII

LOCAL FEATURES AND MINOR LOSSES

28. GENERAL CONSIDERATIONS CONCERNING LOCAL FEATURES IN PIPES

It was mentioned in Sec. 17 that head losses may be of a dual nature: losses due to friction and local, or minor, losses. Friction losses in straight pipes of uniform cross-section were examined for laminar (Chapter VI) and turbulent (Chapter VII) flow. Now we shall examine the so-called minor losses due to local features or disturbances, i. e., to disturbances caused by changes in the size or shape of a conduit which affect the velocity and usually result in eddy formation.

In Sec. 17 there were given several examples of local features and a general formula for expressing minor losses through them (Eq. 4.17′) based on experimental data, viz.,

$$h_l = \zeta \frac{v^2}{2g} = \zeta \frac{16\,Q^2}{2g\pi^2 d^4}.$$

Our task now is to learn to determine the loss coefficients for different types of local features.

The basic local features can be classified as follows:

(i) channel expansion, abrupt and gradual;

(ii) channel contraction, abrupt and gradual;

(iii) channel bend, sharp (elbows) and smooth.

More complicated local disturbances occur as combinations of some or all of the above-mentioned features. Thus, in flowing through a valve (Fig. 30*d*) a liquid passes a bend, a contraction and an expansion to its initial size and eddy currents are set up.

We shall consider the basic local features in the order given in conditions of turbulent flow. It should be noted that the loss coefficient ζ in turbulent flow is determined almost exclusively by the geometry of the local features and changes very little with changes in absolute dimensions, velocity and kinematic viscosity ν, i. e., with changes in the Reynolds number. Therefore, it is commonly

considered to be independent of Re, which means the quadratic resistance law (rough-law flow). Laminar flow through local features will be considered at the end of this chapter.

29. ABRUPT EXPANSION

The values of the local loss coefficient are usually obtained experimentally, and experimental formulas or charts are used.

However, in turbulent flow through an abrupt expansion the loss of head can be determined with sufficient accuracy by purely analytical methods.

An abrupt expansion and the flow pattern therein is shown in Fig. 61. The flow breaks away from the edge of the narrow section and diverges not suddenly, like the pipe, but gradually, with eddies forming in the space between the stream and the pipe. It is this turbulence that causes the dissipation of energy. Experiments show that a continuous exchange of fluid particles between the main stream and the turbulence region takes place.

Consider two cross-sections of the stream: *1-1* through the plane of the expansion and *2-2*, which marks the end of the region of extensive turbulence caused by the expansion. Since the stream between the two cross-sections is gradually diverging, its velocity must be decreasing and its pressure increasing. Therefore the liquid in the second piezometer stands at a level ΔH higher than in the first piezometer. If there were no loss of head the level in the second piezometer would be still higher. The distance by which the second piezometer level falls short of what it might have been is the local loss due to the expansion.

Denoting the pressure, velocity and cross-sectional area at *1-1* by p_1, v_1 and S_1, respectively, and at *2-2* by p_2, v_2 and S_2, write Bernoulli's equation between the sections, assuming the velocity distribution across them to be uniform, i. e., $\alpha_1 = \alpha_2 = 1$. We have:

$$\frac{p_1}{\gamma} + \frac{v_1^2}{2g} = \frac{p_2}{\gamma} + \frac{v_2^2}{2g} + h_{exp}.$$

Now let us apply the theorem of mechanics on the change in momentum to the cylindrical volume between sections *1-1* and *2-2*. For this we must express the impulse of the external forces acting on

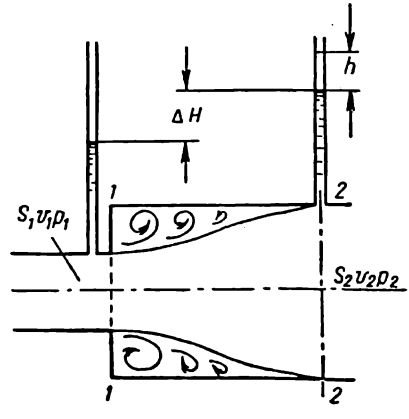

Fig. 61. Abrupt expansion of a pipe

the volume in the direction of the motion, assuming the tangential stress at the surface of the cylinder to be zero. Taking into account that the areas of the cylinder bases are the same and equal to S_2 and assuming that the pressure p_1 at section *1-1* is acting over the whole area S_2, the impulse can be expressed in the form

$$(p_1 - p_2) S_2.$$

The change in momentum corresponding to this impulse is found as the difference between the rate of flow of momenta past the two end sections. With uniform velocity distribution across the sections, this difference is equal to

$$\frac{Q\gamma}{g}(v_2 - v_1).$$

Equating the two quantities,

$$(p_1 - p_2) S_2 = \frac{Q\gamma}{g}(v_2 - v_1).$$

Dividing through by $S_2\gamma$ and taking into account that $Q = S_2 v_2$, and transforming the right-hand side of the equation:

$$\frac{p_1 - p_2}{\gamma} = \frac{v_2}{g}(v_2 - v_1) = \frac{v_2^2}{2g} + \frac{v_2^2}{2g} - \frac{2v_1v_2}{2g} + \frac{v_1^2}{2g} - \frac{v_1^2}{2g}.$$

After rearranging the terms, we obtain:

$$\frac{p_1}{\gamma} + \frac{v_1^2}{2g} = \frac{p_2}{\gamma} + \frac{v_2^2}{2g} + \frac{(v_1 - v_2)^2}{2g}.$$

Comparing this equation with Bernoulli's equation obtained before, we find that the two are completely analogous, whence we draw the conclusion that

$$h_{exp} = \frac{(v_1 - v_2)^2}{2g}, \tag{8.1}$$

i. e., the loss of head (specific energy) due to an abrupt expansion is equal to the velocity head computed for the velocity difference. This formula is commonly known as the Borda-Carnot theorem, in honour of the two French scientists, the former a hydraulicist, the latter a mathematician, who developed it.

Taking into account that, according to the continuity equation,

$$v_1 S_1 = v_2 S_2,$$

the result obtained can also be written down in the following form, corresponding to the general expression for local losses:

$$h_{exp} = \left(1 - \frac{S_1}{S_2}\right)^2 \frac{v_1^2}{2g} = \zeta \frac{v_1^2}{2g}. \qquad (8.1')$$

Consequently, for the case of an abrupt expansion, the loss coefficient is

$$\zeta = \left(1 - \frac{S_1}{S_2}\right)^2. \qquad (8.1'')$$

This theorem is nicely confirmed by experiments in turbulent flow and it is used in calculations.

In the special case when the area S_2 is very large as compared with S_1 and, consequently, the velocity v_2 can be assumed to be zero, the loss due to expansion is

$$h_{exp} = \frac{v_1^2}{2g},$$

i. e., the loss of velocity head and kinetic energy is complete; the loss coefficient is $\zeta = 1$. This is the case of a pipe outlet into a large reservoir.

It should be noted that the loss of head (energy) due to an abrupt enlargement is expended almost exclusively on eddy formation due to separation of the stream from the wall, i. e., on sustaining a continuous rotational motion of the fluid masses and their constant exchange. That is why these losses, which vary as the square of the velocity (discharge), are called eddy losses. Another term occasionally employed is shock losses, as there takes place sudden slowing down and a shock effect as of a fast-flowing liquid suddenly striking a slowly flowing or stationary liquid.

30. GRADUAL EXPANSION

A gradually expanding pipe is commonly called a *diffuser*. In a diffuser the velocity decreases and the pressure increases. The kinetic energy of the particles of the liquid enables them to move against the growing pressure. The degradation of kinetic energy is along the diffuser and from the centre line to the boundary. The energy of layers at the boundary is so small that the increased pressure may stop the flow there or even reverse it. As a result, eddies form and the flow separates from the wall (Fig. 62). The greater the angle of divergence of a diffuser the more pronounced these phenomena and the greater the turbulence loss. Besides, there exist ordinary friction losses like those in pipes of uniform cross-section.

The total loss of head in a diffuser h_{dif} thus comprises two components:

$$h_{dif} = h_f + h_{exp}, \tag{8.2}$$

where h_f = loss of head due to friction;
h_{exp} = loss of head due to expansion (turbulence loss).

The friction loss can be computed approximately in the following manner. Consider a conical diffuser with a divergence angle α; the

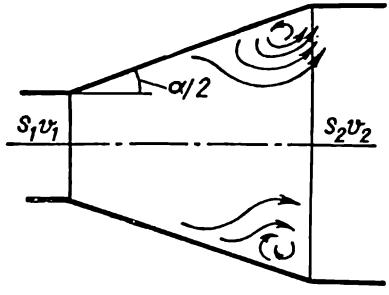

Fig. 62. Eddy formation in a diffuser

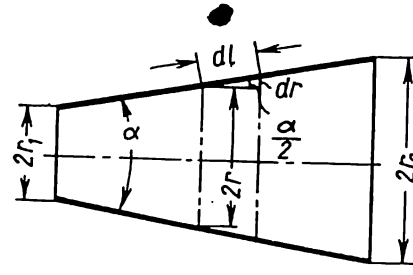

Fig. 63. Diffuser dimensions

radius of the diffuser intake is r_1 and of the outlet base, r_2 (Fig. 63). As the cross-sectional radius and velocity of flow are variable along the diffuser, we should take a differential length dl along the wall and express the differential loss of head due to friction by the basic equation (4.18). We have:

$$dh_f = \lambda_t \frac{dl}{2r} \frac{v^2}{2g},$$

where v = mean velocity across an arbitrary section of radius r.

From the elementary triangle,

$$dl = \frac{dr}{\sin \frac{\alpha}{2}}.$$

From the continuity equation,

$$v = v_1 \left(\frac{r_1}{r}\right)^2,$$

where v_1 = velocity at the diffuser entrance.

Substituting these expressions into the equation for dh_f and integrating from r_1 to r_2, i. e., over the whole of the diffuser, and

assuming the friction factor λ_t constant,

$$dh_f = \lambda_t \frac{dr}{2r \sin \frac{\alpha}{2}} \left(\frac{r_1}{r}\right)^4 \frac{v_1^2}{2g},$$

whence

$$h_f = \frac{\lambda_t}{2 \sin \frac{\alpha}{2}} \frac{v_1^2}{2g} r_1^4 \int_{r_1}^{r_2} \frac{dr}{r^5} = \frac{\lambda_t}{8 \sin \frac{\alpha}{2}} \left[1 - \left(\frac{r_1}{r_2}\right)^4\right] \frac{v_1^2}{2g},$$

and finally

$$h_f = \frac{\lambda_t}{8 \sin \frac{\alpha}{2}} \left(1 - \frac{1}{n^2}\right) \frac{v_1^2}{2g}, \tag{8.3}$$

where $n = \frac{S_2}{S_1} = \left(\frac{r_1}{r_2}\right)^2$ is the so-called rate of divergence of the diffuser.

The second component in Eq. (8.2)—the expansion, or turbulence, loss—is of essentially the same nature in a diffuser as in an abrupt expansion (though its value is smaller) and it is commonly expressed by the same equation (8.1) or (8.1′) with a correction factor k less than unity:

$$h_{exp} = k \frac{(v_1 - v_2)^2}{2g} = k \left(1 - \frac{S_1}{S_2}\right)^2 \frac{v_1^2}{2g} = k \left(1 - \frac{1}{n}\right)^2 \frac{v_1^2}{2g}. \tag{8.4}$$

As the shock produced by a liquid flowing through a diffuser is less than in an abrupt expansion, the factor k is sometimes called the shock reduction factor. The value of k for divergence angles of the order 5-20° can be computed from the following empirical formula developed by the Soviet scientist I. E. Idelchik:

$$k = 3.2 \tan \frac{\alpha}{2} \sqrt[4]{\tan \frac{\alpha}{2}}, \tag{8.5}$$

or according to Fligner's approximate formula

$$k = \sin \alpha. \tag{8.6}$$

Taking Eqs (8.3) and (8.4) into account, the initial equation (8.2) can be rewritten as follows:

$$h_{dif} = \left[\frac{\lambda_t}{8 \sin \frac{\alpha}{2}} \left(1 - \frac{1}{n^2} \right) + k \left(1 - \frac{1}{n} \right)^2 \right] \frac{v_1^2}{2g} = \zeta_{dif} \frac{v_1^2}{2g}, \quad (8.7)$$

and the loss coefficient of a diffuser can be expressed finally by the formula

$$\zeta_{dif} = \frac{\lambda_t}{8 \sin \frac{\alpha}{2}} \left(1 - \frac{1}{n^2} \right) + k \left(1 - \frac{1}{n} \right)^2. \quad (8.8)$$

It will be observed that ζ_{dif} depends on the angle α, the friction factor λ_t and the rate of divergence n.

It is important to establish how ζ_{dif} is dependent on α. With angle α increasing for a given λ_t and n, the first term in Eq. (8.8), which is due to friction, decreases, as the cone is shorter, and the second, which is due to turbulence and separation, increases.

When angle α decreases eddy formation is less, but friction is greater, as for a given rate of divergence n the diffuser is longer and the friction surface increases accordingly.

The function $\zeta_{dif} = f(\alpha)$ is minimum at some optimum value of α (Fig. 64).

The values of the cone angle can be found approximately from Eq. (8.8), replacing $\sin \frac{\alpha}{2}$ by $1/2 \sin \alpha$, as follows: differentiate Eq. (8.8) with respect to α taking into account Eq. (8.6), equate it to zero and solve for α:

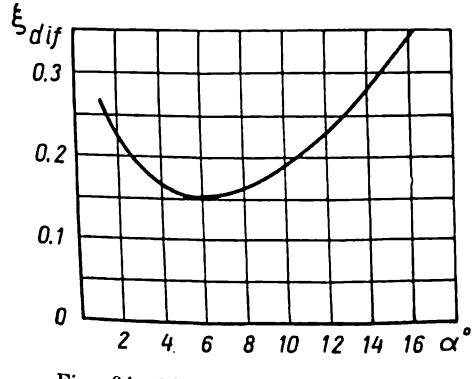

Fig. 64. Plot of ζ_{dif} versus angle α

$$\frac{d\zeta_{dif}}{d\alpha} = -\frac{\lambda_t}{4} \left(1 - \frac{1}{n^2} \right) \frac{\cos\alpha}{\sin^2\alpha} + \cos\alpha \left(1 - \frac{1}{n} \right)^2 = 0,$$

whence

$$\alpha_{opt} = \sin^{-1} \sqrt{\frac{n+1}{n-1} \frac{\lambda_t}{4}}.$$

Substituting into this formula friction factors of the order $\lambda_t = 0.015\text{-}0.025$ and

a rate of divergence of the order $n = 2\text{-}4$, we obtain a mean optimum cone angle of about 6°, which is confirmed by experimental data.

In real solutions, in order to reduce the diffuser length for a given value of n, the cone angle is made somewhat larger, viz., $\alpha = 7\text{-}9°$. The value of α for square diffusers is commonly taken the same.

For rectangular diffusers diverging in one plane (flat diffusers) the optimum divergence angle is greater than for conical or square diffusers, amounting to 10-12°.

If space limitations make it impossible to use divergence angles in the optimum range, at $\alpha > 15\text{-}25°$, specially designed diffusers

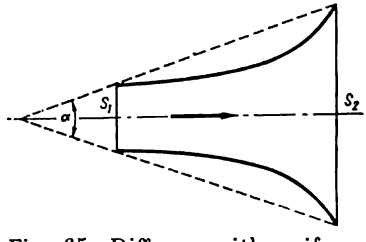

Fig. 65. Diffuser with uniform pressure gradient

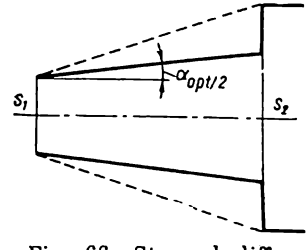

Fig. 66. Stepped diffuser

should be used which ensure a constant pressure gradient along the centre line ($dp/dx = \text{const}$). Such a curved diffuser is shown schematically in Fig. 65.

The reduction in energy loss in such diffusers, as compared with straight cones, is the greater the larger the cone angle α, reaching 40 per cent at α of the order of 40-60°. Furthermore, in a curved diffuser the flow is more stable.

Good results are also obtained by using stepped diffusers, consisting of an ordinary optimum-angle diffuser followed by an abrupt expansion (Fig. 66). The latter does not cause high energy losses as the velocity drops considerably by the time the flow reaches the enlargement. The total resistance of such a diffuser is much less than that of an ordinary diffuser of the same length and rate of divergence.

31. PIPE CONTRACTION

In an *abrupt contraction* (Fig. 67) the loss of energy is always less than in an abrupt expansion with the same area-to-area ratio. The loss components are, first, friction at the entrance to the narrower pipe and, secondly, turbulence losses. The latter are due to the fact that the stream does not flow about the corner but separates and narrows, the annular space around the section of maximum flow contraction being filled with liquid in slow eddy motion.

As the jet expands downstream a loss of energy takes place, which is determined by the abrupt expansion equation. Thus, the total loss of head is

$$h_{con} = \zeta_0 \frac{v_x^2}{2g} + \frac{(v_x - v_2)^2}{2g} = \zeta_{con} \frac{v_2^2}{2g}, \tag{8.9}$$

where ζ_0 = loss coefficient due to friction at the narrow pipe entrance;

v_x = velocity at the section of maximum flow contraction.

The loss coefficient in an abrupt contraction depends on the rate of contraction, i. e., on $n = \frac{S_1}{S_2}$ and can be found from the following semiempirical formula suggested by Idelchik:

$$\zeta_{con} = \frac{1}{2}\left(1 - \frac{S_2}{S_1}\right) = \frac{1}{2}\left(1 - \frac{1}{n}\right). \tag{8.10}$$

It follows from the equation that in the special case when it can be assumed that $\frac{S_2}{S_1} = 0$, e. g., at a pipe entrance in a reservoir of sufficient size, when the entrance corner is not rounded, the loss coefficient is

$$\zeta_{con} = \zeta_{en} = 0.5.$$

A rounding of the corner can considerably reduce the loss of head at the pipe entrance.

In a *gradual contraction* (Fig. 68) velocity increases and pressure drops; the flow is from higher to lower pressure, which eliminates

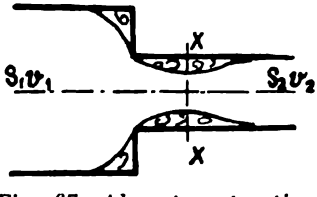

Fig. 67. Abrupt contraction of a pipe

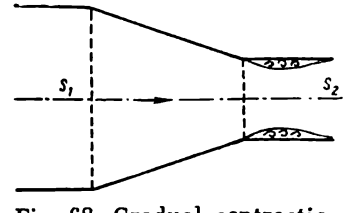

Fig. 68. Gradual contraction of a pipe

the causes of turbulence and separation (as is the case in a diffuser). Losses in a gradual contraction are due to friction only and the resistance of a reducer is always less than that of a similar diffuser.

Friction losses in a reducer can be calculated in the same way as for a diffuser: first express the loss for a differential

section and then integrate:

$$h_f = \frac{\lambda_t}{8 \sin \frac{\alpha}{2}} \left(1 - \frac{1}{n^2}\right) \frac{v_2^2}{2g}, \qquad (8.11)$$

where $n =$ rate of contraction.

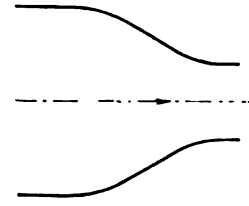

Fig. 69. Nozzle

A slight turbulence, separation of the stream from the wall and contraction of the jet takes place at the reducer outlet. To eliminate this and the resulting losses the cone should be made to merge smoothly into the straight pipe, or a curved reducer can be used instead of a conic frustum to connect the two straight pipes (Fig. 69). In this case the rate of contraction can be increased considerably, with a corresponding shortening of the reducer and reduction of energy losses.

The loss coefficient ζ of such a curved contraction, called a nozzle, varies approximately from 0.03 to 0.1, depending on the rate of contraction, geometry of the curve and the Reynolds number (higher Re corresponds to lower ζ, and vice versa).

32. PIPE BENDS

A sharp bend, or *elbow* (Fig. 70) usually causes considerable energy losses due to flow separation and turbulence, these losses being the greater, the larger the angle δ. The loss coefficient of an elbow of circular cross-section increases sharply with δ (Fig. 71), reaching unity at $\delta = 90°$. Owing to considerable head losses in

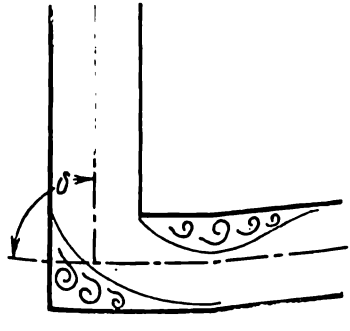

Fig. 70. Elbow

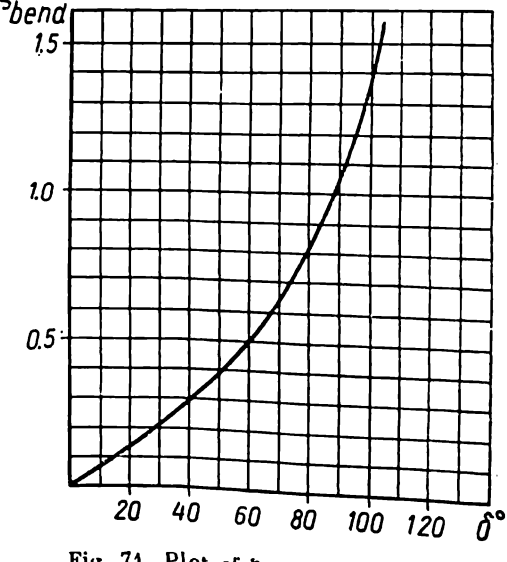

Fig. 71. Plot of ζ_{bend} versus angle δ

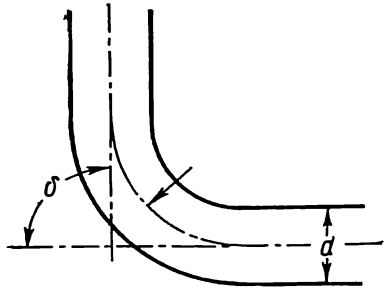

Fig. 72. Smooth bend of a pipe

unrounded elbows they are usually not employed in pipelines.

A *smooth*, or *circular*, *bend* (Fig. 72) tends to reduce turbulence markedly and, consequently the resistance to flow, as compared with a sharp bend. This reduction is the greater the greater the relative radius of curvature $\frac{R}{d}$ of the bend; when it is sufficiently large, turbulence may be eliminated altogether. The loss coefficient in a circular bend depends on the ratio $\frac{R}{d}$, the angle δ and the cross-sectional shape of the pipe.

For smooth bends through $\delta = 90°$ in circular pipes, such that $\frac{R}{d} \geqslant 1$, the following empirical formula can be used:

$$\zeta'_{bend} = 0.051 + 0.19 \frac{d}{R}. \tag{8.12}$$

For $\delta \leqslant 70°$, the loss coefficient is

$$\zeta_{bend} = 0.9 \sin\delta \, \zeta'_{bend}, \tag{8.13}$$

and at $\delta \geqslant 100°$

$$\zeta_{bend} = (0.7 + \frac{\delta}{90} 0.35) \, \zeta'_{bend}. \tag{8.14}$$

It should be remembered that the head loss determined according to the ζ_{bend} coefficients, i. e.,

$$h = \zeta_{bend} \frac{v^2}{2g},$$

is the difference between the total loss in the bend and the loss due to friction in a straight pipe of length equal to the length of the bend; that is, the loss coefficient ζ_{bend} takes into account only the additional resistance caused by the curvature of the pipe. Therefore, in calculating pipelines with bends the length of the bends should be included in the total length of the pipe used to compute the friction losses, to which the bend losses given by the coefficient ζ_{bend} must be added.

The equations (8.12), (8.13) and (8.14) were developed by the author on the basis of charts plotted by Soviet Professor G. N. Abra-

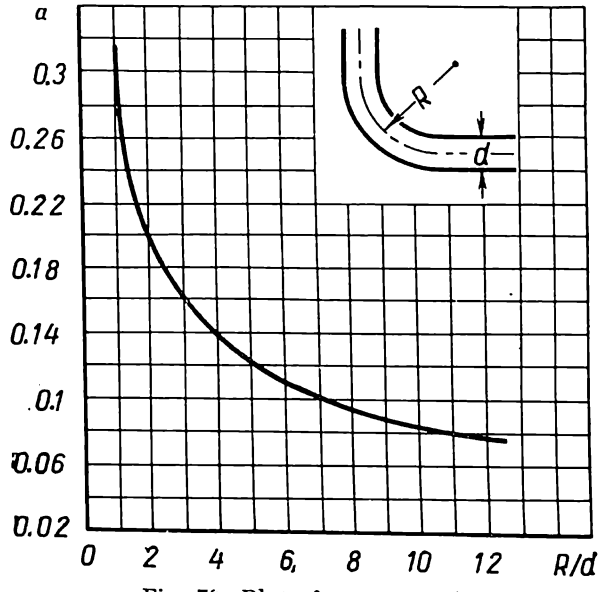

Fig. 73. Plot of a versus R/d

movich, who analysed a number of very reliable experimental investigations of bend losses and proposed the following expression for the loss coefficient of a circular bend:

$$\zeta_{bend} = 0.73\, abc, \tag{8.15}$$

where a = function of the relative radius of curvature given by the plot $a = f_1\left(\frac{R}{d}\right)$ (Fig. 73);

b = function of the bend angle given by the plot $b = f_2(\delta)$ (Fig. 74) (at $\delta = 90°$, $b = 1$);

c = function of the cross-sectional shape of the pipe, which is unity in the case of a circular or square cross-section and is given by the plot $c = f_3\left(\frac{l}{d}\right)$ for oblong cross-sections with sides e and d (side e being parallel to the axis of curvature) (Fig. 75).

From the last chart it will be observed that the function c is minimum when the ratio of the sides of the rectangle $\frac{e}{d} = 2.5$. This is because a twin-eddy "secondary flow" develops in the bend. When a fluid moves along a curved channel centrifugal forces act on all

its particles. As the velocity distribution across a section is not uniform, being greater at the centre and less towards the boundaries, the centrifugal force, which varies as the square of the velocity, is much larger along the middle of the stream than at the boundaries.

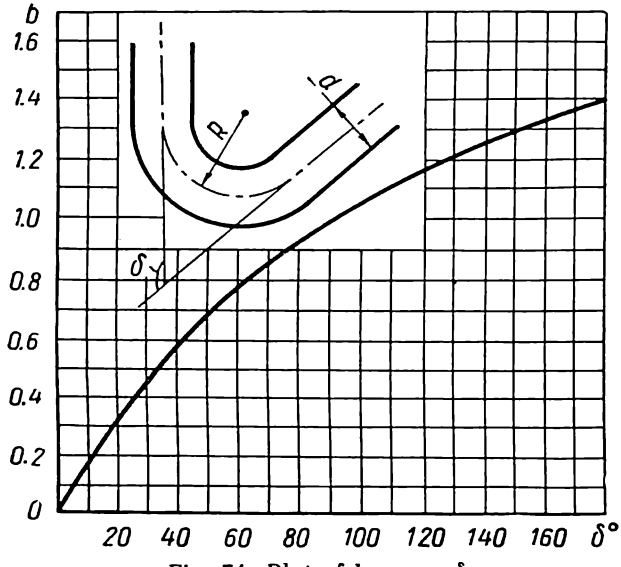

Fig. 74. Plot of b versus δ

As a result, the centrifugal forces develop moments with respect to axes O_1 and O_2 (Fig. 76), which cause the fluid to rotate. Along the centre line of the stream the fluid moves from the inner to the outer wall of the bend, i. e., along the radius of curvature, while along the side walls it moves in the opposite direction, forming a twin-eddy. The circular motion of the fluid plus its translation through the bend divides the flow into two helical streams.

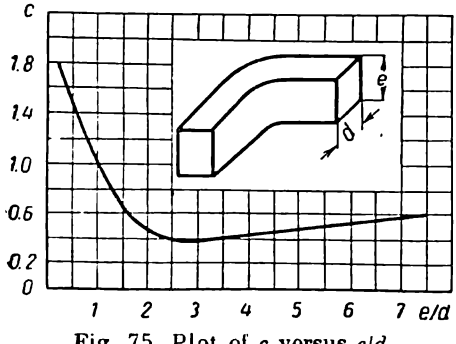

Fig. 75. Plot of c versus e/d

Twin-eddy secondary flow causes a continuous expenditure of energy with a corresponding loss of head, which is proportional to the moment of inertia of the cross-sectional area of the eddy. The minimum moment of inertia is obtained when the eddy is of circular cross-section, which is possible when the ratio of the sides of a rectangular pipe is

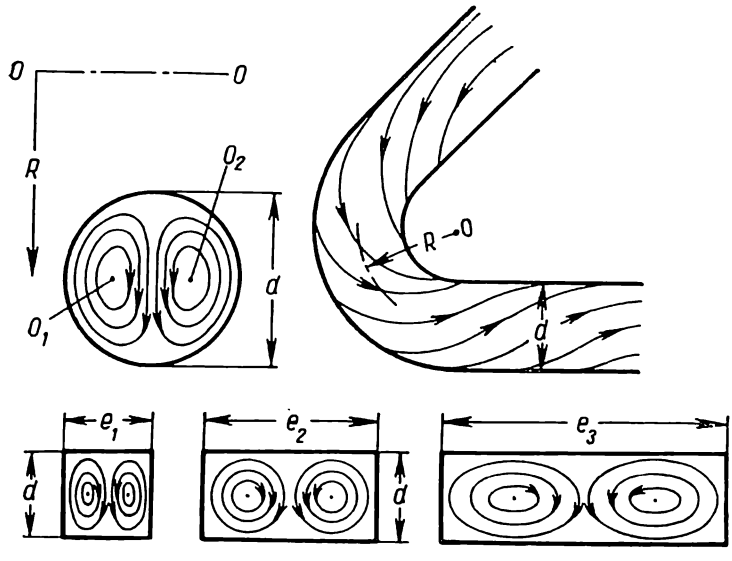

Fig. 76. Flow through a bend

$\frac{l}{d} \approx 2$. Therefore minimum resistance is obtained in a bend in which the ratio of the sides of the rectangle is of the order of two or slightly more. In this case each eddy is of circular cross-section. In all other cases the eddies are flattened in one direction.

Thus, from the point of view of reducing head losses due to friction the best cross-sectional pipe shape is circular, whereas for minimum ζ_{bend} the best is a rectangular section with a side ratio of 2.5, the larger side being parallel to the axis of curvature of the bend. The loss coefficient of such a bend is

$$\zeta = 0.4\,\zeta_{bend},$$

where ζ_{bend} = loss coefficient of a bend in a circular pipe with identical values of $\frac{R}{d}$ and δ.

Thus, an optimum cross-sectional shape used in a bend can reduce the loss coefficient by a factor of 2.5 as compared with a circular cross-section. In some special cases, when losses must be reduced as much as possible, as in the air ducts of some aircraft engines, such special cross-sectional shapes are preferably employed.

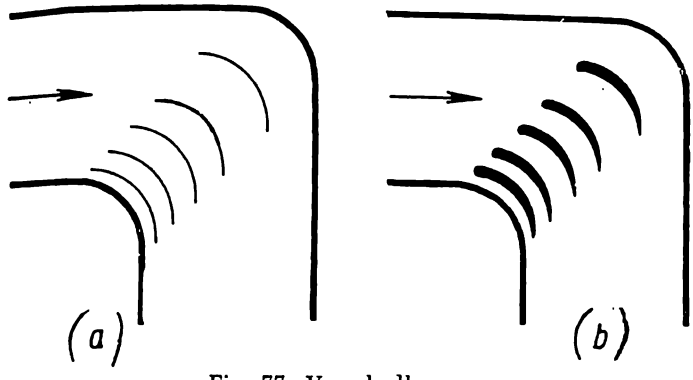

Fig. 77. Vaned elbows

Furthermore, to reduce the resistance of a large-sized elbow (as in wind tunnels) a set of guide vanes is mounted in the bend. In the case of simple nonprofiled vanes of circular bend (Fig. 77*a*) the loss coefficient of the elbow drops to $\zeta = 0.4$; with profiled vanes (Fig. 77*b*) the loss coefficient can be brought down to 0.25.

33. LOCAL DISTURBANCES IN LAMINAR FLOW

All the foregoing in this chapter referred to local disturbances in turbulent flow. In laminar flow local disturbances are usually insignificant as compared with friction and, secondly, the disturbance laws are much more complicated and considerably less studied than in the case of turbulent flow.

In the latter regime of flow local losses can be assumed proportional to the square of the velocity (rate of discharge), the loss coefficients being determined mainly by the local feature causing the disturbance and being practically independent of the Reynolds number. In laminar flow, however, the loss of head h_l at a local feature must be taken as the sum

$$h_l = h_f + h_t, \tag{8.16}$$

where h_f = loss of head due to friction forces (viscosity) in the local feature and proportional to viscosity and the first power of the velocity;

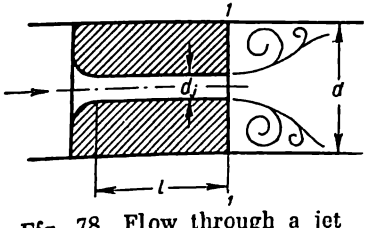

Ffg. 78. Flow through a jet

h_t = loss due to flow separation and turbulence in the local feature or immediately downstream, which is proportional to the square of the velocity.

Thus, for example, in the case of flow through a calibrated jet (Fig. 78) the loss of head upstream

from section *1-1* is due to friction, and downstream, to turbulence.

Taking into account the resistance law for laminar flow, Eqs (6.6) and (6.7) with the correction for entrance length, and also Eq. (4.17), the sum can be rewritten as follows

$$h_l = \frac{A}{\mathrm{Re}} \frac{v^2}{2g} + B \frac{v^2}{2g} \qquad (8.16')$$

where A and B are dimensionless constants depending on the shape of the local feature.

Dividing the expression (8.16) by the velocity head, we obtain the general expression of local loss coefficient in laminar flow:

$$\zeta_l = \frac{A}{\mathrm{Re}} + B. \qquad (8.17)$$

The ratio between the first and second terms in Eqs (8.16) and (8.17) depends on the shape of the local feature and the Reynolds number.

When the local feature is a thin tube substantially longer than it is wide, with a rounded inlet and outlet, as shown in Fig. 79*a*, and small values of Re, the loss of head is determined mainly by friction, and the resistance law is almost linear. In such cases the second term in Eqs (8.16) and (8.17) is zero or very small in comparison with the first one.

If, on the other hand, friction in the local feature is negligible, as in the case of the sharp edge in Fig. 79*b*, the stream breaks away and eddies form, Re is relatively high and the loss of head is approximately proportional to the second power of the velocity (and rate of discharge).

When the Reynolds number varies over a wide range in a local feature, the local disturbance may be described by a linear law (when Re is low), a quadratic law (when Re is high) and an intermediate law for transitional values of Re. A typical plot of ζ as a function of Re in logarithmic coordinates is presented in Fig. 80 for a broad band of Reynolds numbers through four different orifices. The sloped straight lines correspond to a linear resistance law (when ζ varies inversely as Re), the curved portions represent the transient regions, and the horizontals denote a quadratic law, when ζ does not depend on Re. Such graphs for specific local disturbances are usually plotted empirically.

Sometimes the binomial expression of minor losses is replaced by an exponential monomial of the form

$$h_l = kQ^m,$$

where k = dimensional quantity;

m = exponent varying from 1 to 2 depending on shape of local feature and Reynolds number.

When the resistance law is nearly linear for a local feature and given Reynolds number minor losses are frequently expressed in terms of equivalent pipe lengths: to the actual length of a pipe is added a length whose resistance is equal to that of the local features. Thus,

$$l_{rated} = l_{actual} + l_{equivalent}, \tag{8.18}$$

and

$$\sum h = \frac{64}{\mathrm{Re}} \frac{l_{rated}}{d} \frac{v^2}{2g} = \frac{128 \nu l_{rated} Q}{\pi g d^4}. \tag{8.19}$$

The equivalent length (referred to the pipe diameter) is usually determined experimentally for different local features.

The formula for the loss of head in an abrupt expansion developed in Sec. 29 for turbulent flow is not valid for laminar flow. In laminar flow the assumptions made in developing the formula, viz., uniform velocity distribution across sections *1-1* and *2-2*, uniform pressure across the area S_2 at section *1-1*, and absence of shearing stress, are no longer tenable.

Recent laboratory experiments show that the loss coefficient in an abrupt enlargement when the Reynolds number is very low ($\mathrm{Re} < 9$) hardly depends on the area ratio and is determined mainly by Re, the equation being of the form

$$\zeta = \frac{A}{\mathrm{Re}}.$$

This means that no separation takes place and the divergence loss is proportional to the first power of the velocity. At $9 < \mathrm{Re} < 3{,}500$ the loss coefficient depends both on the Reynolds number and on the area ratio. At $\mathrm{Re} > 3{,}500$, the "Borda-Carnot loss" formula [Eq. (8.1)] can be used.

When a liquid flowing through a pipe with a velocity v_1 is discharged into a large reservoir ($v_2 = 0$) all the kinetic energy is dissipated. In steady laminar flow through a circular pipe the kinetic energy is

$$h = \alpha_l \frac{v_1^2}{2g} = \frac{v_1^2}{g}.$$

If the flow is not steady, i. e., if the pipe length $l < l_{ent}$, the coefficient α should be taken from the diagram in Fig. 47.

Example. Determine the loss coeficient of a jet of diameter $d_j = 1$ mm and length $l = 5$ mm installed in a pipe of diameter $d = 6$ mm (see Fig. 78), as a function of Re.

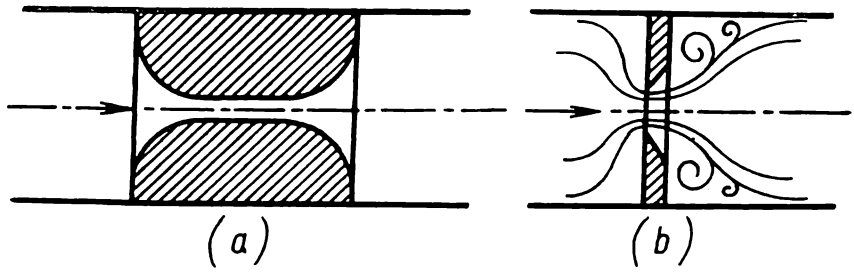

Fig. 79. Two kinds of local features

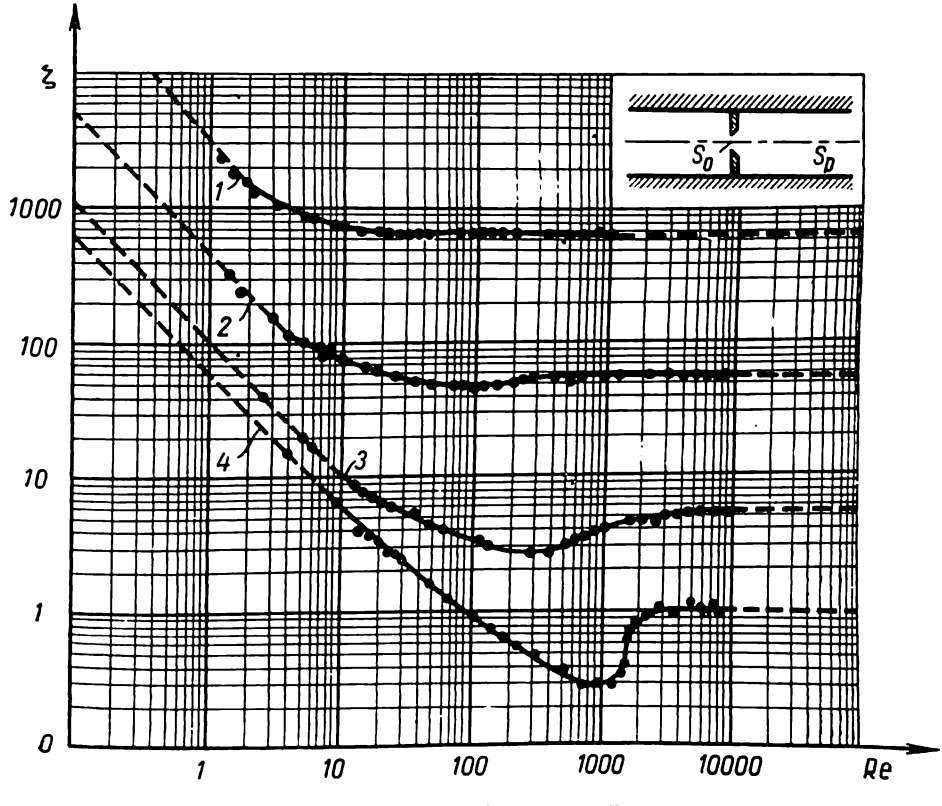

Fig. 80. Plot of ζ versus Re:

1. $\frac{S_0}{S_p}=0.05$; 2. $\frac{S_0}{S_p}=0.16$; 3. $\frac{S_0}{S_p}=0.43$; 4. $\frac{S_0}{S_p}=0.64$

Solution. Regarding the jet as the entrance section of a pipe and assuming that all the kinetic energy is dissipated when the flow diverges, the loss of head in the jet can be represented as the sum (neglecting the loss due to contraction):

$$h_j = h_f + h_{exp} = \left(k \frac{64}{\mathrm{Re}_j} \frac{l}{d} + \alpha\right) \frac{v_j^2}{2g}.$$

Going over from the velocity in the jet v_j to the velocity in the pipe v, the loss coefficient in the jet is:

$$\zeta_j = \frac{2gh_j}{v^2} = \left(k \frac{64}{\mathrm{Re}_j} \frac{l}{d} + \alpha\right) \frac{d^4}{d_j^4}.$$

Assigning several values of Re in the pipe, find the values of Re in the jet from the relationship

$$\mathrm{Re}_j = \frac{v_j d_j}{\nu} = \frac{4Q}{\pi d_j \nu} \qquad \frac{d}{d} = \mathrm{Re} \frac{d}{d_j}.$$

Making use of the graph in Fig. 47 to find the coefficients k and α, the necessary computations give the table:

Table 3

Re	10	100	200	300	400	500
ζ_j	9,500	3,140	2,500	2,200	2,030	1,885

34. LOCAL FEATURES IN AIRCRAFT HYDRAULIC SYSTEMS

Local features in aircraft hydraulic systems and transmissions include filters, taps, valves, bends and other fittings and units of diverse geometrical shapes. Flow through such features may be either laminar or turbulent, depending on the velocity and temperature (viscosity) of the fluid. The Reynolds number varies within a fairly wide range and includes Re_{cr}. Accordingly, the loss coefficient ζ for these features must be regarded as functions of Re.

The logarithmic scale in Fig. 81 presents plots of ζ as a function of Re for some typical local features in aircraft hydraulic systems obtained experimentally by the Soviet engineer N. V. Levkoyeva. The values of Re and ζ were computed according to the velocity of the stream in the pipe and the diameter of the latter.

Note that the dependence of ζ on Re in a felt filter is a linear function up to Re = 5,000. The reason is that in laminar flow through the filter pores friction is very great and practically no turbulence takes place. In the plots for a tap, valve and bend the linear sections

are much shorter; they are followed by considerable transient sections and, finally, a quadratic resistance law ($\zeta = \text{const}$).

The steeper slope of the nonreturn valve curve is accounted for by the fact that with Re increasing the opening of the valve increases (owing to faster flow through it), i. e., the geometric characteristics change.

The Reynolds number is usually much higher in aircraft fuel systems than in hydraulic systems and it can be assumed, without much error, that the local loss coefficients of fuel pipes do not depend on Re.

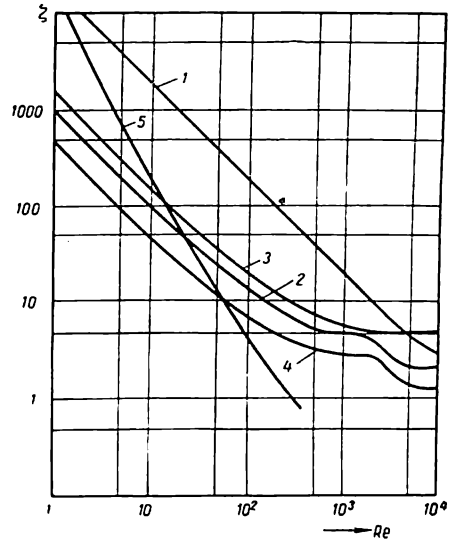

Fig. 81. Plots of ζ versus Re:
1 — felt filter; *2* — tap; *3* — valve; *4* — right-angled elbow; *5* — nonreturn valve

Table 4 presents loss coefficients for some common units and local features of fuel systems. The values of ζ are referred to the velocity head at the intake pipe of the unit or feature.

Table 4

Local feature	ζ
Flexible pipe connection	0.3
Standard 90° elbow (bored body)	1.2-1.3
Tee	3.5
Fuel tap	1-2.5
Nonreturn valve	2.0
Gauze filter	1.5-2.5
Flowmeter sensor with impeller rotating	7.0
with impeller braked	11-12
Pipe entrance (tank outlet)	0.5-1.0
Pipe outlet (tank inlet)	1.0

CHAPTER IX

FLOW THROUGH ORIFICES, TUBES AND NOZZLES

35. SHARP-EDGED ORIFICE IN THIN WALL

In this chapter we shall examine various cases of fluid efflux from reservoirs, tanks or boilers through orifices, tubes and nozzles of different kind into the atmosphere or a vessel filled with a gas or the same fluid. Characteristic of this case of fluid motion is that in the course of efflux the overall potential energy of a liquid (or at least most of it) is converted, with greater or lesser losses, into the kinetic energy of a free jet or a falling liquid.

In aircraft engineering flow through orifices and mouthpieces must be investigated in connection with problems of fuel supply to combustion chambers of gas turbine and liquid-propellant rocket engines, shock-absorber operation and flow through jets in fuel and other aircraft systems. The question of primary interest to us is that of determining the velocity and rate of flow of liquids through orifices and tubes of different shape.

Consider a large tank filled with a liquid under pressure p_0, with a small orifice in the wall at a fairly large depth H_0 from the free surface (Fig. 82). The liquid flows out of the orifice into the atmosphere, the pressure at section *1-1* being p_1.

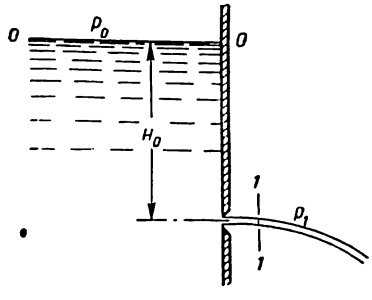

Fig. 82. Efflux from reservoir through small orifice

Let the orifice be shaped as in Fig. 83*a* (a hole with a square shoulder in a thin wall) or as in Fig. 83*b* (a hole with a sharp edge in a thick wall). The conditions of flow through both orifices are identical: the liquid particles approach the aperture from all sides of the adjacent volume, moving with acceleration along converging streamlines as shown in Fig. 83*a*; the jet separates

from the wall at the edge of the orifice and converges into what is called the *vena contracta*. At about one orifice diameter away from the edge the streamlines become parallel. The vena contracta is caused by the necessarily smooth change in the direction of motion of the particles approaching the orifice (including those approaching it at right angles along the tank wall).

In the case of a small orifice as compared with the size of the reservoir and the head H_0, when the free surface and walls do not affect the approach of the liquid to the aperture, the jet contraction is *complete* (suppressed jet contraction will be examined later on).

The degree of contraction is characterised by the coefficient of contraction ε, which is the ratio of the area of the vena contracta to the area of the orifice:

$$\varepsilon = \frac{S_{vc}}{S_0} = \left(\frac{d_{vc}}{d_0}\right)^2. \tag{9.1}$$

Let Bernoulli's equation be written between the free surface of the reservoir (section *0-0* in Fig. 82), where the pressure is p_0 and the velocity can be assumed zero, and section *1-1* where the jet is cylindrical and the pressure is p_1. Assuming the velocity distribution in the jet to be uniform,

$$H_0 + \frac{p_0}{\gamma} = \frac{p_1}{\gamma} + \frac{v^2}{2g} + \zeta\frac{v^2}{2g}$$

where ζ = loss coefficient of the orifice.

Introducing the notation

$$H = H_0 + \frac{p_0 - p_1}{\gamma}$$

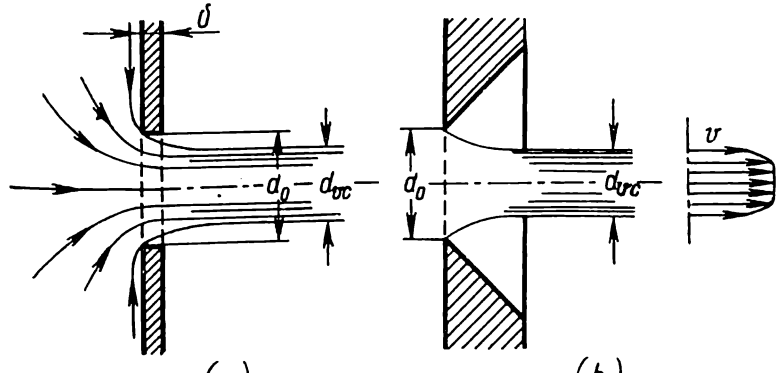

Fig. 83. Circular orifice:
a — in thin wall; *b* — sharp-edged

for the rated head, we obtain

$$H = \frac{v^2}{2g}(1 + \zeta),$$

whence the velocity of efflux is

$$v = \frac{1}{\sqrt{1 + \zeta}} \sqrt{2gH} = \varphi \sqrt{2gH}, \tag{9.2}$$

where

$$\varphi = \frac{1}{\sqrt{1 + \zeta}} \tag{9.3}$$

is the so-called *coefficient of velocity*.

In the case of an ideal liquid $\zeta = 0$, and consequently $\varphi = 1$, whence the theoretical, or ideal, velocity of efflux is

$$v_t = \sqrt{2gH}. \tag{9.4}$$

An investigation of Eq. (9.2) reveals that the coefficient of velocity φ is the ratio of the actual to the theoretical velocity:

$$\varphi = \frac{v}{\sqrt{2gH}} = \frac{v}{v_t}. \tag{9.5}$$

Because of friction, the actual velocity of efflux is always less than the theoretical velocity, and the coefficient of velocity is less than unity.

Velocity distribution, it should be noted, is uniform only in the central portion of a jet; the external layer is retarded by friction (see Fig. 83*b*). Experiments show that the velocity in the central portion of a jet is practically equal to the theoretical velocity $v_t = \sqrt{2gH}$, therefore the velocity coefficient φ refers actually to the mean velocity. When efflux is into the atmosphere, the pressure across the diameter of the jet is atmospheric, which is confirmed by experiments.

Let us compute the rate of discharge through an orifice as the product of the actual velocity and the actual area of the jet. Application of Eqs (9.1) and (9.2) yields:

$$Q = S_{vc} v = \varepsilon S_0 \varphi \sqrt{2gH}. \tag{9.6}$$

The product of the two coefficients

$$\mu = \varepsilon\varphi$$

is called the *coefficient of discharge*.

Thus, Eq. (9.6) can be rewritten

$$\left.\begin{aligned} Q &= \mu S_0 \sqrt{2gH} \\ \text{or} \quad Q &= \mu S_0 \sqrt{2g\frac{p}{\gamma}}, \end{aligned}\right\} \tag{9.6'}$$

where p = rated pressure under which efflux is taking place.

The expression (9.6′) is fundamental as it solves the basic problem of determining the rate of discharge through an orifice and it is valid for all types of efflux. The only difficulty of using it is the accurate determination of the discharge coefficient μ.

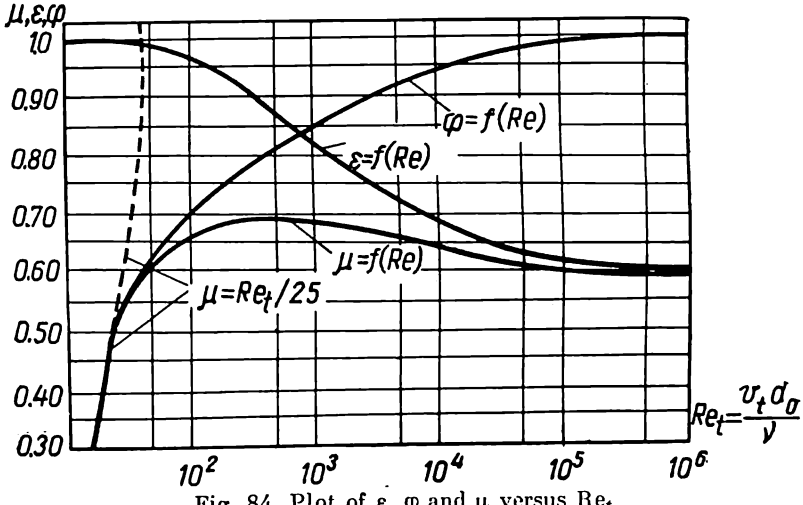

Fig. 84. Plot of ε, φ and μ versus Re_t

It follows from Eq. (9.6′) that

$$\mu = \frac{Q}{S_0\sqrt{2gH}} = \frac{Q}{Q_t},$$

i. e., the coefficient of discharge is the ratio of the actual rate of discharge Q to the theoretical rate of discharge Q_t (discharge without friction or contraction of the jet). The term "theoretical discharge", incidentally, should not be understood absolutely, as $Q_t = S_0\sqrt{2gH}$ is not the rate of discharge of an ideal liquid: an ideal liquid would also display a vena contracta.

Due to contraction of the jet and friction, the actual rate of flow is always less than the theoretical discharge and the coefficient of

discharge is always less than unity. Whether contraction or friction is the governing factor will depend on conditions of efflux.

The coefficients of contraction ε, loss ζ, velocity φ and discharge μ depend, first of all, on the type of orifice or tube and, like all dimensionless hydraulic coefficients, on the Reynolds number, the basic criterion of hydrodynamic similarity.

Fig. 84 presents a diagram in which the coefficients φ, ε and μ for a circular orifice are plotted as functions of the Reynolds number computed for the theoretical velocity:

$$\mathrm{Re}_t = \frac{v_t d_0}{\nu} = \frac{\sqrt{2gH}\, d_0}{\nu}.$$

The graph shows that, with Re_t increasing (i. e., when viscosity ceases to be of importance) φ increases thanks to ζ decreasing, while ε decreases as a result of less velocity retardation at the edge of the orifice and greater permissible radii of curvature at the vena contracta. Both φ and ε asymptotically approach their values corresponding to an ideal liquid, i. e., when $\mathrm{Re}_t \to \infty$, $\varphi \to 1$ and $\varepsilon \to 0.60$.

The coefficient of discharge, which is determined by the product of ε and φ, first increases with Re_t increasing due to φ increasing. On reaching a maximum ($\mu_{max} = 0.69$ at $\mathrm{Re}_t \approx 350$) it falls due to ε rapidly decreasing, and at high values of Re, when $\mu = 0.59$-0.60, it becomes practically constant.

When Re_t is very low ($\mathrm{Re}_t < 25$) the effects of viscosity come into play and the retardation of the velocity of efflux at the orifice edge becomes so great that there is no contraction ($\varepsilon = 1$) and $\varphi = \mu$. The rate of discharge Q in this regime of flow is proportional to the first power of the head, and the coefficient of discharge is proportional to Re_t. For this regime the following theoretical formula, confirmed by experiment, can be used:

$$Q = \frac{\pi d^3 gH}{50\nu} \tag{9.7}$$

to which corresponds

$$\mu = \frac{\mathrm{Re}_t}{25}. \tag{9.8}$$

The efflux coefficients for low-viscous liquids (water, gasoline, kerosene) through circular orifices in thin walls vary insignificantly and in engineering problems the following mean values are commonly taken:

$$\varepsilon = 0.63; \quad \varphi = 0.97; \quad \mu = 0.61; \quad \zeta = 0.065.$$

In the case of flow of low-viscous liquids through a round orifice in a thin wall the jet contraction is considerable and the resistance is small; the coefficient of discharge is much less than unity, mainly due to jet contraction.

36. SUPPRESSED CONTRACTION. SUBMERGED JET

Suppressed contraction occurs when efflux through an orifice is affected by the proximity of the walls of a reservoir. When the orifice is concentric with the centre line of the reservoir (Fig. 85) the walls tend to guide the liquid approaching the orifice, thus preventing full contraction beyond the orifice. The contraction is less than in efflux from a reservoir of infinite size; the coefficient of contraction increases, and as a consequence, the coefficient of discharge increases as well.

A theoretical investigation of the efflux of an ideal fluid from a flat reservoir of finite height and infinite width through a slot in the end wall was carried out by N. E. Joukowski as far back as 1890.

For a low-viscous liquid flowing through a round orifice in the centre of the end wall of a circular cylindrical reservoir the coefficient of contraction can be found in terms of the contraction coefficient for complete contraction from the following empirical formula:

$$\frac{\varepsilon_1}{\varepsilon} = 1 + \frac{0.37}{\varepsilon} n^2, \tag{9.9}$$

where $n = \frac{S_0}{S_1}$ is the ratio of the orifice area to the cross-sectional area of the tank.

When contraction of the jet is suppressed the loss coefficient ζ and the velocity coefficient φ can be regarded as being independent of n (if, of course, n is not too close to unity); for low-viscous fluids the approximate values are

$$\zeta = 0.065 \text{ and } \varphi = 0.97.$$

The discharge coefficient is easily found from the relationship

$$\mu_1 = \varepsilon_1 \varphi_1,$$

and the rate of discharge is given by the formula

$$Q = \mu_1 S_0 \sqrt{2gH}.$$

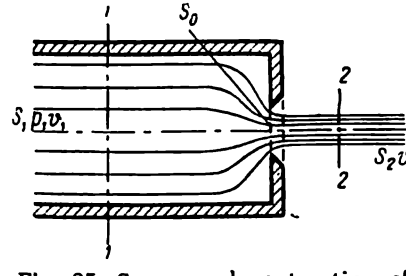

Fig. 85. Suppressed contraction of a jet from a flat reservoir

In applying this equation to the case of suppressed contraction it should be remembered that the rated head is the total head

$$H = \frac{p_1 - p_2}{\gamma} + \frac{v_1^2}{2g}.$$

This means that besides the piezometric head the velocity head in the reservoir must also be taken into consideration. As the velocity head is usually unknown, it is desirable to have a formula expressing the rate of discharge for suppressed contraction not in terms of the total head H but in terms of the piezometric head.

Such a formula is easily obtained from Bernoulli's equation and the continuity equation written between sections *1-1* and *2-2* (see Fig. 85):

$$\frac{p_1}{\gamma} + \frac{v_1^2}{2g} = \frac{p_2}{\gamma} + \frac{v_2^2}{2g} + \zeta \frac{v_2^2}{2g};$$

$$v_1 S_1 = v_2 \varepsilon_1 S_0.$$

From this

$$v_2 = \frac{1}{\sqrt{1 + \zeta - \varepsilon_1^2 n^2}} \sqrt{2g \frac{p_1 - p_2}{\gamma}}$$

and

$$Q = \frac{\varepsilon_1}{\sqrt{1 + \zeta - \varepsilon_1^2 n^2}} S_0 \sqrt{2g \frac{\Delta p}{\gamma}} = \mu_1' S_0 \sqrt{2g \frac{\Delta p}{\gamma}}, \qquad (9.10)$$

where

$$\mu_1' = \frac{\varepsilon_1}{\sqrt{1 + \zeta - \varepsilon_1^2 n^2}}. \qquad (9.11)$$

If an orifice is close to a side wall of a tank the contraction is suppressed over a *part* of the perimeter of the jet as shown in Fig. 86. In this case, too, the contraction and discharge coefficients ε_2 and μ_2 are greater than for unsuppressed contraction.

The coefficient μ_2 can be found from the empirical formula

$$\mu_2 = \mu \left(1 + \xi \frac{\Delta \Pi}{\Pi}\right), \qquad (9.12)$$

where ξ = form coefficient, equal to 0.128 for circular and 0.152 for square orifices;
Π = perimeter of orifice;
$\Delta\Pi$ = fraction of the perimeter adjoining the wall.

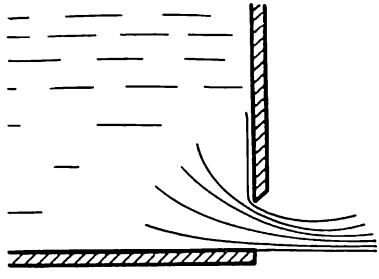

Fig. 86. Suppressed contraction of a jet from an orifice near the bottom of a reservoir

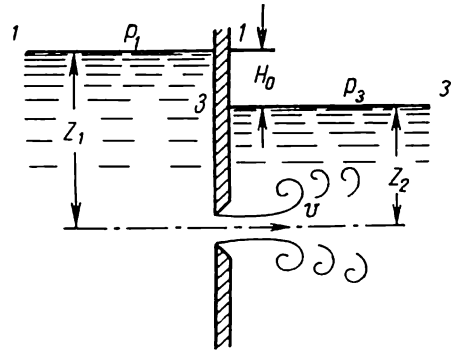

Fig. 87. Submerged jet

Many engineering problems are concerned with discharge of a liquid below the surface of the same liquid in another vessel (Fig. 87). This is known as a *submerged jet.*

The total kinetic energy of the jet is dissipated in eddy formation, as in the case of an abrupt expansion. The Bernoulli equation between sections *1-1* and *3-3* (where the velocities can be assumed zero) takes the form

$$z_1 + \frac{p_1}{\gamma} = z_2 + \frac{p_3}{\gamma} + \sum h = z_2 + \frac{p_3}{\gamma} + \zeta \frac{v^2}{2g} + \frac{v^2}{2g}$$

or

$$H = H_0 + \frac{p_1 - p_3}{\gamma} = (\zeta + 1)\frac{v^2}{2g},$$

where H = rated head;
v = velocity at the vena contracta;
ζ = loss coefficient of the orifice, which is approximately the same as in the case of a free jet.

Hence,

$$v = \frac{1}{\sqrt{1+\zeta}}\sqrt{2gH} = \varphi\sqrt{2gH}$$

and

$$Q = vS_{vc} = \varepsilon\varphi S_0\sqrt{2gH} = \mu S_0\sqrt{2gH}.$$

Thus, the equations are the same as for a free jet, only in the present case the head H is the difference between the piezometric heads on both sides of the wall.

The coefficients of contraction and discharge of a submerged jet can be assumed the same as of a free jet.

37. FLOW THROUGH TUBES AND NOZZLES

A tube is a short unrounded pipe whose length is only several diameters [$l = (2\text{-}6)d$] (Fig. 88*a*). An orifice in a thick wall is actually a tube (Fig. 88*b*).

Two flow regimes are observed in efflux of a liquid through tubes with unrounded edges into a gas. The first regime is shown schematically in Fig. 88*a* and *b*. On entering the tube the jet converges and forms a vena contracta in about the same way, and for the same reason, as in the case of a free jet through an orifice in a thin wall. Then

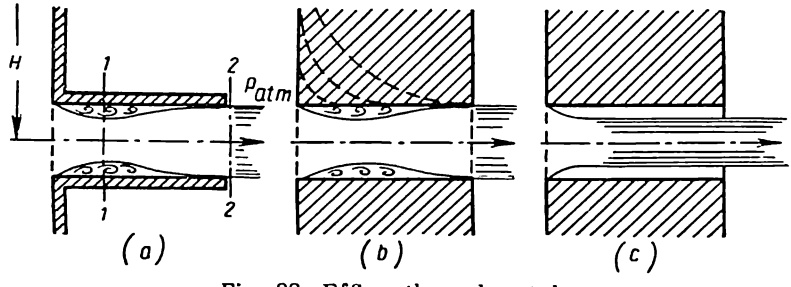

Fig. 88. Efflux through a tube

the jet expands and issues from the tube in a stream of the same diameter as the pipe. Between the vena contracta and tube walls a zone of violently eddying liquid is formed. As the jet has the same diameter as the aperture, $\varepsilon = 1$ and, consequently, $\mu = \varphi$. For low-viscous liquids the mean values of the coefficients are

$$\mu = \varphi = 0.82; \quad \zeta = 0.5.$$

The rate of discharge through a circular tube running full (first regime) is greater than through an orifice in a thin wall; the velocity, on the other hand, is less owing to greater friction.

Consider a jet of liquid issuing under pressure p_0 into a gas having pressure p_2 (say, into the combustion chamber of a liquid-propellant rocket motor). The rated head for unsuppressed contraction is

$$H = \frac{p_0 - p_2}{\gamma}.$$

As the pressure in the jet at the tube outlet is p_2, at the vena contracta inside the tube, where the velocity is greater, the pressure p_1 is lower than p_2. Furthermore, the higher the head under which the jet is issuing, and consequently the greater the rate of discharge, the less the absolute pressure in the vena contracta. The difference

$p_2 - p_1$ varies as the head H. This is demonstrated by Bernoulli's equation written between sections *1-1* and *2-2* (Fig. 88*a*) in the form

$$\frac{p_1}{\gamma} + \frac{v_1^2}{2g} = \frac{p_2}{\gamma} + \frac{v_2^2}{2g} + \frac{(v_1 - v_2)^2}{2g}.$$

The last term is the loss of head due to jet expansion. This is completely analogous to an abrupt expansion, hence the loss of head due to expansion is given by Eq. (8.1). The vena contracta is determined by the same coefficient of contraction as in flow through an orifice. Therefore, from the continuity equation,

$$\frac{v_1}{v_2} = \frac{1}{\varepsilon}.$$

Using this formula to eliminate v_1 from the foregoing Bernoulli equation and writing the velocity v_2 in terms of the velocity coefficient of the tube, $v_2 = \varphi\sqrt{2gH}$, we obtain the pressure drop inside the tube:

$$p_2 - p_1 = \varphi^2 \left[\frac{1}{\varepsilon^2} - 1 - \left(\frac{1}{\varepsilon} - 1\right)^2\right] H\gamma. \tag{9.13}$$

Substitution of the values $\varphi = 0.82$ and $\varepsilon = 0.64$ into this expression yields

$$p_2 - p_1 \approx 0.75\, H\gamma. \tag{9.13'}$$

At some critical head H_{cr} the absolute pressure at section *1-1* in the tube becomes zero and

$$H_{cr} \approx \frac{p_2}{0.75\gamma}. \tag{9.14}$$

But at $H > H_{cr}$ this would mean a negative pressure p_1 which is practically impossible in liquids; it follows then that at $H > H_{cr}$ the first flow regime (tube running full) is impossible. This is confirmed experimentally, and at $H \approx H_{cr}$ the flow regime changes suddenly. The jet springs clear of the walls of the tube and issues from it as shown in Fig. 88*c*.

This regime is identical to efflux through an orifice in a thin-wall and it is characterised by the same jet coefficients. Thus, in a changeover from the first flow regime to the second the velocity increases and the rate of discharge, owing to jet contraction, decreases.

For the case of a jet of water into the atmosphere running clear

$$H_{cr} \approx \frac{p_{atm}}{0.75\gamma} = \frac{10.33}{0.75} \approx 14 \text{ m}.$$

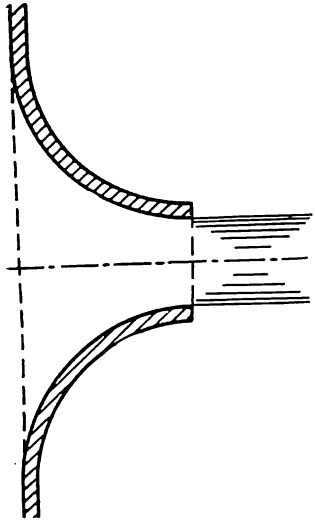

Fig. 89. Bell-mouthed orifice

A submerged jet through a tube cannot run clear and the first regime persists at $H > H_{cr}$. With the head H increasing, however, the discharge coefficient drops and as a result of cavitation inside the tube the loss coefficient increases.

It follows, thus, that circular tubes possess some appreciable shortcomings: in the first regime (running full) resistance is great and the coefficient of discharge is small; in the second regime (running clear) the coefficient of discharge is even less. Furthermore, the flow regime through cylindrical tubes is unstable.

For these reasons cylindrical tubes are not favoured and, in fact, they are almost never specially provided for (with the exception of some liquid-propellant rocket motors). In engineering practice, however, tubes are frequent as bores in thick walls. Their performance can be improved substantially by rounding the inlet edge (broken lines in Fig. 88*b*). The greater the curve the higher the coefficient of discharge and the lower the loss coefficient. In the limit, when the radius of curvature equals the thickness of the wall, the circular tube becomes a bell-mouthed orifice (Fig. 89).

A *bell-mouthed orifice* is a widely used type of mouthpiece with a coefficient of discharge approaching unity, low losses, no vena contracta, a stable flow regime and a firm jet.

The loss coefficient is about the same as for a gradual contraction (Sec. 31):

$$\zeta = 0.03\text{-}0.10,$$

the lower values of ζ corresponding to high Reynolds numbers and vice versa.

Correspondingly,

$$\mu = \varphi = 0.99\text{-}0.96.$$

A *diffuser mouthpiece* (Fig. 90) is a diverging taper pipe affixed to a bell-mouthed orifice. Addition of a tail-pipe leads to lower pressure at the throat of the tube and, consequently, higher velocity and rate of discharge. The discharge of a bell-mouthed orifice can be increased by as much as 2.5 times by the addition of a diverging mouthpiece.

Such mouthpieces are used when the discharge for a given head must be as high as possible through a small orifice. Application, how-

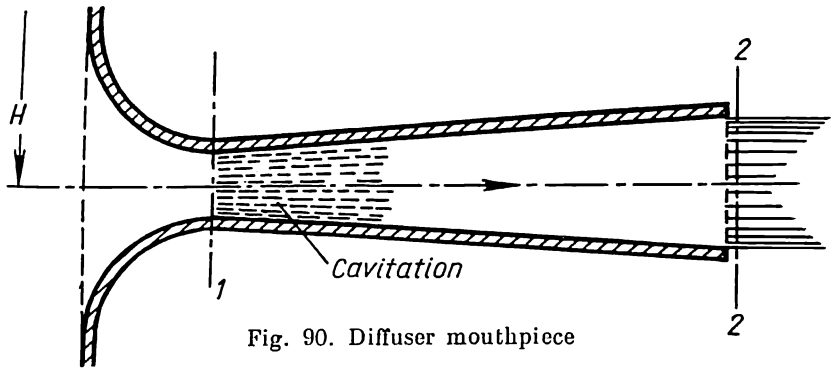

Fig. 90. Diffuser mouthpiece

ever, is limited to low heads ($H = 1$-4 m) as otherwise cavitation develops in the throat, with a resulting increase in resistance and reduction of rate of discharge.

The diagram in Fig. 91 shows how the coefficient of discharge of a diverging mouthpiece is affected by the head increasing due to cavitation at the throat. The discharge coefficient is referred to the cross-sectional area of the throat, i. e.,

$$\mu_1 = \frac{Q}{S_1\sqrt{2gH}}.$$

The curve was obtained in tests with a cone having an optimum angle and rate of divergence ensuring the highest coefficient of discharge.

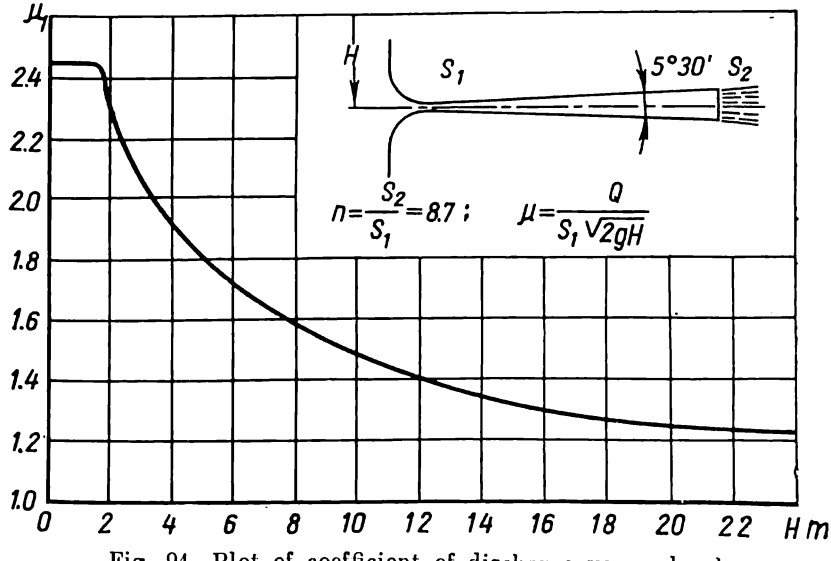

Fig. 91. Plot of coefficient of discharge versus head

Example. In some liquid-propellant rocket motors the fuel components are supplied into the combustion chambers through so-called spray injectors which are simple boreholes. Determine the required number of oxidiser injectors for the motor of a Schmetterling rocket if $G = 1.6$ kg/sec, pressure drop in injector $\Delta p = 6$ kg/cm^2, pressure in the chamber $p_2 = 25$ kg/cm^2, orifice diameter $d_0 = 1.5$ mm, ratio of wall thickness to orifice diameter $\delta/d_0 = 0.5$. The oxidiser is nitric acid, specific weight $\gamma = 1{,}510$ kg/m^3, kinematic viscosity $\nu = 0.02$ cm^2/sec.

How many injectors would be required if $\delta/d_0 = 2.5$?

Solution. (i) Theoretical velocity of efflux:

$$v_t = \sqrt{2g\frac{\Delta p}{\gamma}} = \sqrt{2\times 9.81\,\frac{6\times 10^4}{1{,}510}} = 28 \text{ m/sec.}$$

(ii) Reynolds number:

$$\mathrm{Re}_t = \frac{v_t d_0}{\nu} = \frac{2{,}800\times 0.15}{0.02} = 21{,}000.$$

(iii) The graph in Fig. 84 gives the coefficient of discharge as a function of Re_t: $\mu = 0.62$.

(iv) Total area of all injector mouths:

$$S_0 = \frac{G}{\gamma\mu v_t} = \frac{1.6\times 10^3}{1.51\times 0.62\times 2{,}800} = 0.61 \text{ sq cm.}$$

(v) Number of injectors:

$$z = \frac{4S_0}{\pi d_0^2} = \frac{4\times 0.61}{\pi 0.15^2} = 35.$$

(vi) If the bore ratio were $\delta/d_0 = 2.5$, the efflux would be as from an external cylindrical tube.

To determine the flow regime find Δp_{cr}. Eq. (9.13′) gives

$$\Delta p_{cr} = \frac{25}{0.75} = 33.5 \text{ kg/cm}^2.$$

As $\Delta p_{cr} > \Delta p$, the first flow regime (running full) will obtain and the coefficient of discharge is $\mu = 0.82$. Consequently,

$$z_1 = z\,\frac{\mu}{\mu_1} = 35\,\frac{0.62}{0.82} = 27.$$

38. DISCHARGE WITH VARYING HEAD (EMPTYING OF VESSELS)

Let us investigate efflux of a liquid through an orifice or tube in the bottom of an open vessel with a discharge coefficient μ (Fig. 92). The discharge in this case takes place with a varying, gradually decreasing head, i.e., the flow is, strictly speaking, unsteady.

However, if the head and, consequently, the velocity of discharge are changing slowly, the motion at any given instant can be regarded as steady and Bernoulli's equation can be applied for problem solution.

Let h be the falling elevation of the free surface above the bottom, S the cross-sectional area of the vessel at that elevation and S_0 the area of the orifice. Then, taking a differential time interval dt, the volume equation can be written as follows

$$S\,dh = -Q\,dt, \tag{9.15}$$

or

$$S\,dh = -\mu S_0 \sqrt{2gh}\,dt$$

where dh = fall of free surface in the vessel in time dt.

The minus sign is due to the fact that the positive increment dt corresponds to a negative increment dh.

From this, assuming μ = const, the total time of emptying a vessel of height H can be found in the following way:

$$t = -\frac{1}{\mu S_0 \sqrt{2g}} \int_{h=H}^{h=0} S\,\frac{dh}{\sqrt{h}}. \tag{9.16}$$

The integral can be computed if the law of change of the area S is known as a function of the height h. If the surface area of the vessel is uniform, i. e., S = const,

$$t = \frac{S}{\mu S_0 \sqrt{2g}} \int_0^H \frac{dh}{\sqrt{h}},$$

or

$$t = \frac{2S}{\mu S_0 \sqrt{2g}} \sqrt{H} = \frac{2SH}{\mu S_0 \sqrt{2gH}}. \tag{9.17}$$

The numerator is equal to twice the volume of the vessel, the denominator represents the rate of discharge at the initial moment, i.e., when the

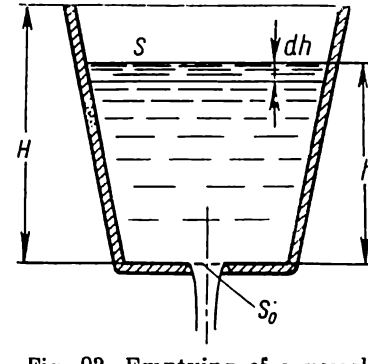

Fig. 92. Emptying of a vessel

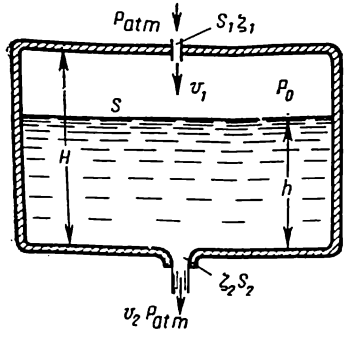

Fig. 93. Emptying of a closed tank

head was H. Consequently, the time of emptying the vessel is twice the time that would have been required if the initial head were maintained.

Equations (9.16) and (9.17) can also be used to determine the time needed to fill a vessel when the head varies from $h = H$ to $h = 0$ as the vessel is filled.

Aeronautical engineers usually have to deal with discharge from closed vessels (tanks) connected with the atmosphere by an orifice or tube of small diameter (Fig.93). In this case liquid efflux causes a vacuum in the tank and atmospheric air flows in through the orifice. As a result, the discharge is retarded, the retardation being the greater the greater the resistance to the penetration of air into the tank.

To determine the time it takes for such a vessel to empty, two Bernoulli equations must be written: one for the flow of air from the motionless atmosphere into the vessel, another for the motion of the liquid from the free surface to its outlet into the atmosphere. Using the notation of Fig. 93,

$$\frac{p_{atm}}{\gamma_{air}} = \frac{p_0}{\gamma_{air}} + (1 + \zeta_1)\frac{v_1^2}{2g};$$

$$h + \frac{p_0}{\gamma_l} = \frac{p_{atm}}{\gamma_l} + (1 + \zeta_2)\frac{v_2^2}{2g}.$$

The compressibility of the air can be neglected and the volume rates of discharge of the air and the liquid can be equated:

$$Q = v_1 S_1 = v_2 S_2.$$

(If the jet contracts, the coefficient ε_1 should be introduced.)

The foregoing equations can now be rewritten as follows:

$$p_{atm} = p_0 + (1 + \zeta_1)\frac{Q^2}{2gS_1^2}\gamma_{air};$$

$$h\gamma_l + p_0 = p_{atm} + (1 + \zeta_2)\frac{Q^2}{2gS_2^2}\gamma_l.$$

Adding these equations and solving for Q yields

$$Q = \sqrt{\frac{2gh\gamma_l}{\frac{1+\zeta_1}{S_1^2}\gamma_{air} + \frac{1+\zeta_2}{S_2^2}\gamma_l}}. \tag{9.18}$$

Substituting Eq. (9.18) into the volume equation (9.15), solving for dt and integrating from $h = H$ to $h = 0$, we obtain

$$t = \frac{2SH}{\sqrt{2gH\gamma_l}} \sqrt{\frac{1+\zeta_1}{S_1^2}\gamma_{air} + \frac{1+\zeta_2}{S_2^2}\gamma_l}. \tag{9.19}$$

This formula is valid for the case of air intake and liquid outflow through pipes, introducing the following expression for the respective loss coefficients:

$$\zeta = \lambda \frac{l}{d} + \sum \zeta_l,$$

where l and d are the length and diameter of the pipe, respectively;
ζ_l = sum of the local loss coefficients in the pipe.

Another example of discharge with varying head is found in the operation of an undercarriage shock-absorber. A hydropneumatic shock-absorber (Fig. 94) contains compressed air at the upper end the pressure of which during flight is p_0. When the airplane wheels touch the ground the hydraulic fluid flows through an orifice of area S_0 and discharge coefficient μ, and the air is compressed to p_1. The height of the air volume is reduced from h_0 to h_1.

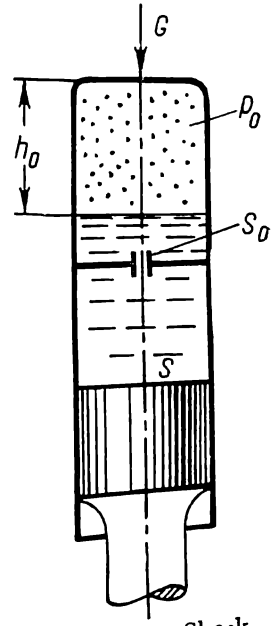

Fig. 94. Shock-absorber

To simplify the actual process of shock-absorption, assume that a uniform force G is suddenly applied to the shock-absorber and that the air compresses according to an isothermic law. Let us find the duration of the shock-absorption process, i.e., the time it takes for the liquid to flow through the orifice until equilibrium is restored.

By analogy with Eq. (9.15),

$$S\,dh = -Q\,dt,$$

where S = piston area;
dh = displacement of cylinder in time dt.

The rate of discharge through the orifice

$$Q = \mu S_0 \sqrt{2g \frac{p_1 - p}{\gamma}},$$

where $p_1 = \frac{G}{S}$ is the constant pressure over the piston;

p = the varying air pressure given by the isothermal equation $p = (p_0 + p_{atm}) \frac{h_0}{h} - p_{atm}$.

Substitution of the expressions for p_1 and p into Eq. (9.15) yields

$$dt = -\frac{S\sqrt{\gamma}}{\mu S_0 \sqrt{2g(p_1 + p_{atm})}} \sqrt{\frac{h}{h - h_1}}\, dh,$$

where

$$h_1 = \frac{p_0 + p_{atm}}{p_1 + p_{atm}} h_0.$$

The required time t is found after integrating from $h = h_0$ to $h = h_1$.

39. INJECTORS

An injector is a specially designed tube or nozzle which atomises the discharged liquid, i.e., the jet into the atmosphere (or a space filled with gas under pressure) is broken up into a fine spray.

The most common type of injector used in gas-turbine aircraft and liquid-propellant rocket engines is the so-called swirl injector for spraying fuel in the combustion chamber.

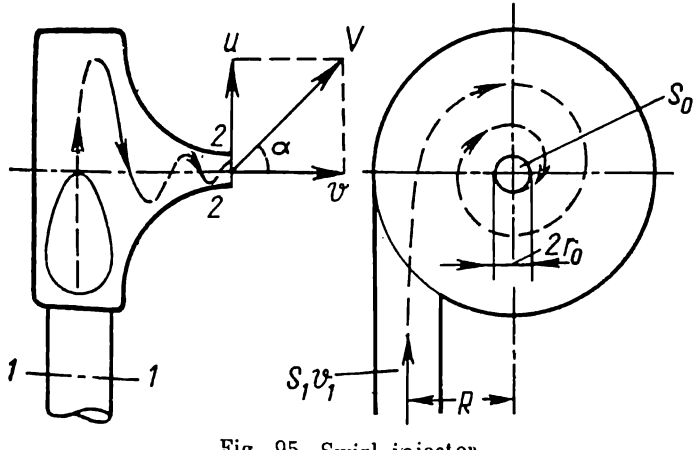

Fig. 95. Swirl injector

In such an injector whirl is imparted to the stream, which is then contracted (Fig. 95). The angular momentum created by the tangential approach of the liquid remains approximately constant during flow through the injector. Consequently, as the stream converges the whirl velocity component increases considerably and large centrifugal forces develop which throw the liquid to the walls, forming a thin film which issues from the injector in a fine spray. Along the centre line of the injector there is formed an air (gas) vortex in which the pressure at the surface is close to atmospheric (if the discharge is into the atmosphere). This vortex is completely analogous to that formed when liquid flows out of a hole in the bottom of a vessel (Fig. 96), though in the injector it is much more intensive.

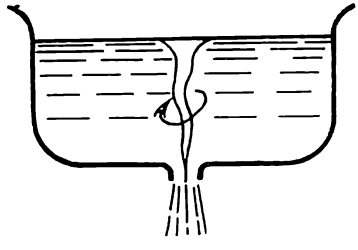

Fig. 96. Free vortex

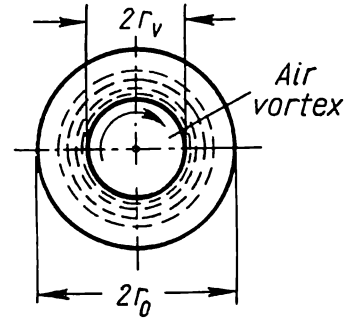

Fig. 97. Cross-section of a vortex in a swirl injector

Thus, the jet issuing from a swirl injector does not fill the whole cross-section of the injector nozzle; it is annular, with an air vortex along the centre (Fig. 97). Therefore, the contraction coefficient ε of a swirl injector is usually much less than unity.

Because of this, and also because the resultant velocity of discharge V is directed at an angle to the cross-section of the injector (Fig. 95), the tangent of which is equal to the ratio of the whirl component u to the axial component v, the coefficient of discharge is always much less than unity, varying within broad limits depending upon the geometry and relative dimensions of the injector.

In order to determine the rate of discharge of an injector according to the basic equation (9.6)

$$Q = \mu S_0 \sqrt{2g \frac{p}{\gamma}},$$

the precise value of the coefficient of discharge μ must be known.

The injector theory developed by Professor G. N. Abramovich enables μ to be determined from the dimensions and geometry of the

injector. We shall consider this theory very briefly for the case of an ideal fluid. The following are the three initial equations:

(i) Bernoulli's equation between sections *1-1* and *2-2* (see Fig. 95):

$$\frac{p_1}{\gamma} + \frac{v_1^2}{2g} = \frac{p_2}{\gamma} + \frac{V^2}{2g}$$

or

$$H = \frac{v^2 + u^2}{2g},$$

where $H = \frac{p_1 - p_2}{\gamma} + \frac{v_1^2}{2g}$ is the rated head;

v and u are the axial and whirl components of the velocity V at the boundary of the air vortex at section *2-2*.

(ii) The equation for the conservation of angular momentum of the fluid with respect to the centre line at the given cross-sections:

$$Q_Q R v_1 = Q_Q u r_v$$

or

$$u = v_1 \frac{R}{r_v},$$

where r_v = radius of the air vortex at section *2-2*.

(iii) The continuity equation between the sections*:

$$v_1 S_1 = \varepsilon S_0 v$$

or

$$v_1 = \frac{\varepsilon S_0 v}{S_1},$$

where

$$\varepsilon = \frac{S_0 - S_v}{S_0} = 1 - \frac{r_v^2}{r_0^2}.$$

From the last expression we have

$$r_v = r_0 \sqrt{1 - \varepsilon},$$

which gives, after substitution into the second equation,

$$u = v_1 \frac{R}{r_0 \sqrt{1 - \varepsilon}}.$$

---

* Assuming a uniform distribution of the axial velocities about the annular cross-section at the injector outlet.

Using the third equation instead of the foregoing one, we obtain

$$u = \frac{\varepsilon S_0 v R}{S_1 r_0 \sqrt{1-\varepsilon}} = A \frac{\varepsilon}{\sqrt{1-\varepsilon}} v,$$

where $A = \frac{S_0 R}{S_1 r_0}$ is a parameter characterising the geometry of the injector.

Substitution of the expression for u into Bernoulli's equation at (i) yields

$$H = \frac{v^2}{2g}\left(1 + A^2 \frac{\varepsilon^2}{1-\varepsilon}\right),$$

whence

$$v = \frac{1}{\sqrt{1 + A^2 \frac{\varepsilon^2}{1-\varepsilon}}} \sqrt{2gH}.$$

Now we can express the rate of discharge as the product of the velocity and the annular area of the stream at the injector outlet, i.e.,

$$Q = \varepsilon S_0 v = \frac{\varepsilon}{\sqrt{1 + A^2 \frac{\varepsilon^2}{1-\varepsilon}}} S_0 \sqrt{2gH}.$$

Thus, the discharge coefficient of the injector is

$$\mu = \frac{\varepsilon}{\sqrt{1 + A^2 \frac{\varepsilon^2}{1-\varepsilon}}} = \frac{1}{\sqrt{\frac{1}{\varepsilon^2} + \frac{A^2}{1-\varepsilon}}}. \qquad (9.20)$$

The coefficient ε, however, is unknown, as we do not know the dimensions of the air vortex (the radius r_v for a given r_0 and A). To determine it some additional condition must be introduced. Such a condition was put forward as a hypothesis by Prof. Abramovich, and later it was confirmed experimentally. He postulated that a steady vortex would be of such size as to ensure a maximum rate of discharge Q for a given head H or, in other words, the flow regime is such that a given discharge is produced by the least possible head.

Let us find the value of ε corresponding to the maximum coefficient of discharge μ. For this differentiate the expression under the radical in Eq. (9.20) with respect to ε and equate the derivative to zero:

$$-\frac{2}{\varepsilon^3} + \frac{A^2}{(1-\varepsilon)^2} = 0,$$

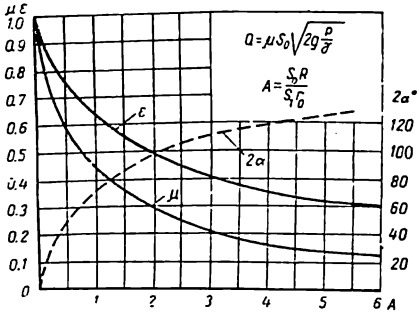

Fig. 98. Plot of ε, μ and α versus A for an injector

whence

$$A = \sqrt{\frac{2}{\varepsilon^3}(1-\varepsilon)}. \qquad (9.21)$$

This formula can be used to plot ε as a function of A. The curve can be used together with Eq. (9.20) to compute values of μ for a series of values of A and to plot a graph of μ as a function of A (Fig. 98).

The diagram shows that with A increasing the coefficient μ decreases. Physically this is explained by the fact that A increasing means a higher whirl velocity u at the injector outlet as compared with the entrance velocity v_1 and, consequently, a more intensive whirl of the fluid. This leads to a vortex of larger diameter and a smaller cross-sectional area of the stream, which means that more and more of the available energy H is dissipated on building up the whirl velocity. At $A = 0$ ($R = 0$), $\mu = 1$, i.e., there is no whirl and the injector works as an ordinary nozzle.

The foregoing equations can be used to determine the angle of divergence of the spray or flame of the injector (see Fig. 98). With A increasing angle α increases and the discharge coefficient drops. Therefore in injector design A must be so chosen as to ensure a sufficiently wide angle α (up to 60°) without reducing μ too much.

The injector theory set forth here is developed for the case of an ideal fluid. The effect of viscosity on injector performance is manifest in that the angular momentum is not uniform, diminishing towards the outlet.

Accordingly, the whirl velocity component at the outlet is usually smaller, and the discharge greater than in the case of an ideal fluid. At first glance this might seem paradoxical.

The effects of viscosity can be taken into account by introducing an equivalent parameter A_{eq}, which is determined from the formula

$$A_{eq} = \frac{A}{1 + \frac{\lambda_i}{2}\left(\frac{\pi R^2}{S_1} - A\right)},$$

where λ_i = friction factor of the injector, which can be taken from Table 5, depending on the Reynolds number computed for the diameter and velocity at the injector inlet.

Table 5

Re_1	1.5×10^3	3×10^3	5×10^3	1×10^4	2×10^4	5.10^4
λ_i	0.22	0.11	0.077	0.055	0.04	0.03

The equivalent injector parameter A_{eq} thus computed is used to determine the discharge coefficient μ and the angle α taking into account viscosity according to Abramovich's diagram in Fig. 98, where A_{eq} now stands for A. Since as a rule $A_{eq} < A$, the coefficient μ taking into account viscosity is somewhat greater, and the angle α is smaller, than in the case of an ideal fluid.

In many liquid-propellant rocket injectors whirl is imparted to the fluid by means of a two- or three-step helix built into the nozzle (Fig. 99).

The injector theory is valid in this case, the factor A being computed according to the formula

$$A = \frac{S_0 r_m \cos\varphi}{S_n n r_0}, \qquad (9.22)$$

where r_m = mean radius of helical groove;
S_n = area of flow cross-section normal to groove;
n = number of coils;
φ = helix angle.

In modern gas-turbine engines there are more commonly used adjustable swirl injectors in which the coefficient of discharge (or the area of the outlet) varies automatically with the changing fuel pressure. Such nozzles enable the range of fuel supply to be increased for a given pressure range while maintaining the required quality of spraying.

Widely employed are twin-nozzle and two-stage injectors and injectors with by-pass arrangement. Common to them all is a valve device which opens (or closes) an auxiliary conduit when the pressure rises, thereby increasing the coefficient of discharge or the outlet area.

The twin-nozzle injector (Fig. 100) actually comprises two

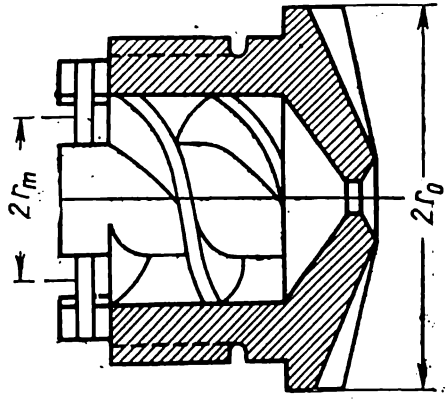

Fig. 99. Injector with helical nozzle

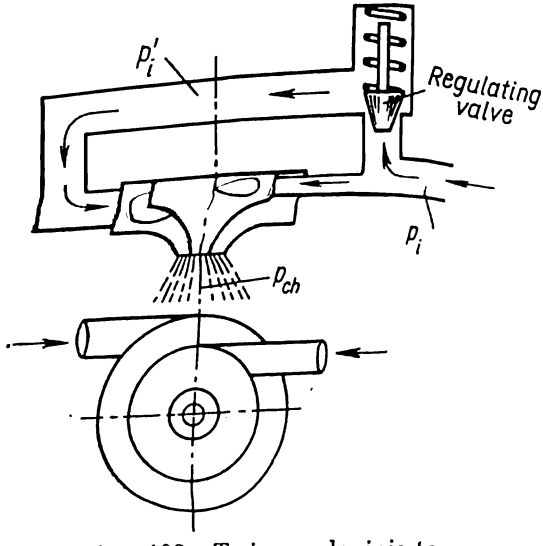

Fig. 100. Twin-nozzle injector

injectors, one inside the other. At low pressures the valve is closed and the inner injector operates; when the pressure rises the valve opens and the second injector becomes operative. The supply of fuel increases sharply.

The two-stage injector (Fig. 101) has one nozzle and one swirl chamber with two inlet pipes. At low pressures the fuel is supplied through one pipe, at high pressures, through both. As a result, the parameter A decreases and the coefficient μ increases.

The by-pass injector (Fig. 102) is provided with a valve-controlled drain. The lower the pressure the wider opens the valve; at peak pressure the valve is closed completely. Thus, at low pressure the intake velocity is higher, which is equivalent to a smaller inlet area, and this means an increase in the equivalent parameter A_{eq} and a reduction of μ. This is just what is needed to widen the discharge range.

These adjustable injectors can be calculated on the basis of Abramovich's theory, with due consideration of specific features (see examples).

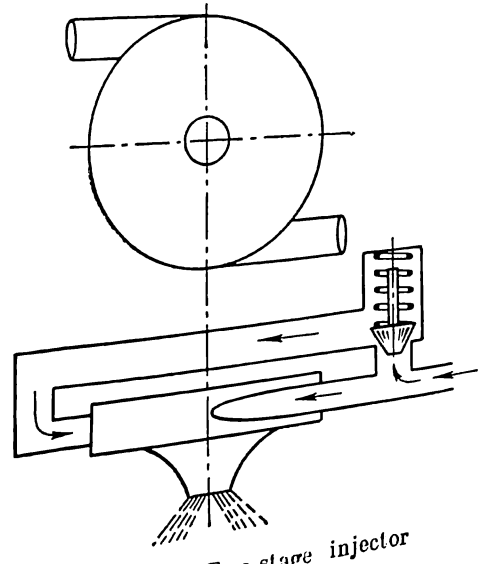

Fig. 101. Two-stage injector

Example 1. Plot the flow characteristics of a twin-nozzle injector (Fig. 100) showing the relationship between the rate of discharge and the pressure drop in the injector, if the second nozzle (the second channel) becomes operative at a pressure drop equal to Δp_0. The geometry of both channels (dimensions and parameters A_1 and A_2) and the flow characteristics of the regulating valve are given. Solve the problem in general form.

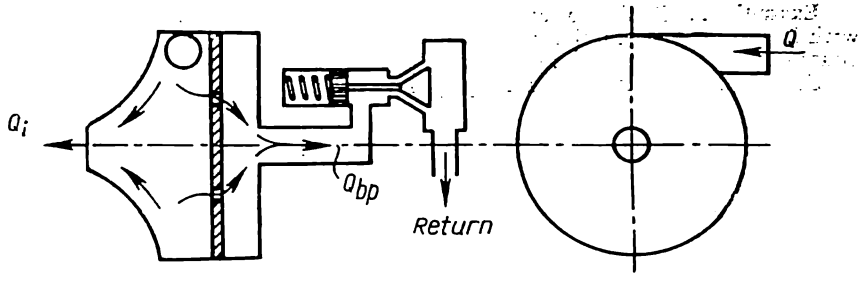

Fig. 102. By-pass injector

Solution. (i) According to the given values of A_1 and A_2 determine μ_1 and μ_2 from the graph in Fig. 98.

(ii) Applying the equations

$$Q_1 = \mu_1 S_1 \sqrt{2g \frac{\Delta p}{\gamma}} \quad \text{and} \quad Q_2 = \mu_2 S_2 \sqrt{2g \frac{\Delta p}{\gamma}},$$

plot the characteristics of the first and second conduits of the injector (Fig. 103).

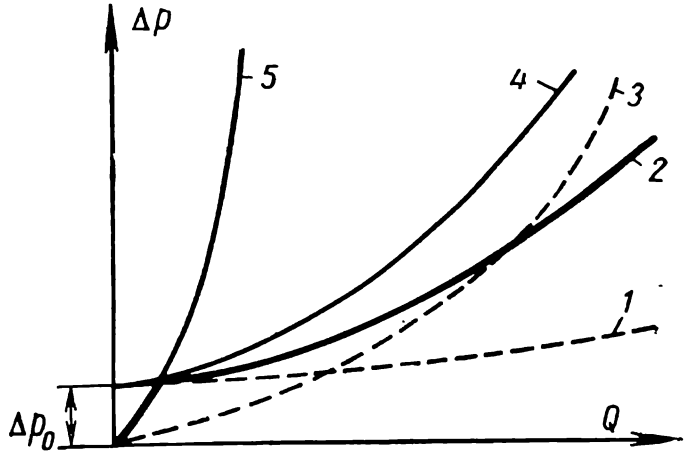

Fig. 103. Characteristic curves of twin-nozzle injector:
1 — valve; *2* — injector; *3* — second conduit; *4* — valve + second conduit; *5* — first conduit

(iii) Sum the characteristics of the control valve and the second conduit. In performing this operation remember that the pressure drop Δp in the second conduit is expended in the injector proper and in the valve. Therefore the ordinates of Δp must be summed for the given rates of discharge.

(iv) To obtain the total flow characteristic of the injector, sum the characteristics of the first and second conduits and the valve, and the rates of discharge (Fig. 103).

Example 2. Find the expression for the parameter A_1 of a swirl injector with by-pass if the total input of fuel is $Q = Q_i + Q_{bp}$, where Q_i is the discharge through the injector nozzle and Q_{bp} is the by-pass discharge (see Fig. 102).

Solution. (i) Introduce a by-pass coefficient k_{bp}:

$$k_{bp} = 1 + \frac{Q_{bp}}{Q_i} = \frac{Q}{Q_i}.$$

(ii) The supply of fuel through the input pipes is

$$Q = k_{bp} Q_i = v_1 S_1.$$

(iii) The quantity of fuel passing through the injector nozzle is

$$Q_i = \varepsilon S_0 v.$$

Consequently,

$$v_1 S_1 = k_{bp} \varepsilon S_0 v,$$

whence

$$v_1 = \frac{k_{bp} \varepsilon S_0 v}{S_1}.$$

(iv) Substituting the expression for v_1 into the angular momentum equation, and then into Bernoulli's equation, determine the velocity v in the same way as before:

$$v = \frac{1}{\sqrt{1 + k_{bp}^2 A^2 \dfrac{\varepsilon^2}{1-\varepsilon}}} \sqrt{2gH}.$$

(v) The fuel supply through the injector is

$$Q_i = \varepsilon S_0 v = \frac{S_0}{\sqrt{\dfrac{1}{\varepsilon^2} + k_{bp}^2 A^2 \dfrac{1}{1-\varepsilon}}} \sqrt{2gH}.$$

(vi) Comparing this equation with the expression (9.20), we find that

$$A_1 = k_{bp} A.$$

CHAPTER X

RELATIVE MOTION AND UNSTEADY PIPE FLOW

40. BERNOULLI'S EQUATION FOR RELATIVE MOTION

Bernoulli's equation in the form (4.16) is valid for all cases of steady flow when gravity is the only body force acting on a liquid. In aircraft and other machines, however, one frequently encounters cases of a flowing liquid being also subjected to the inertial forces of transport motion when the channel through which it is flowing is itself moving with acceleration. If the inertia force is uniform in time, the flow may be steady with respect to the channel walls and the energy equation can be developed taking into account the work done by the inertia force. This is Bernoulli's equation for relative motion, which is commonly written in the form:

$$z_1 + \frac{p_1}{\gamma} + \alpha_1 \frac{v_1^2}{2g} = z_2 + \frac{p_2}{\gamma} + \alpha_2 \frac{v_2^2}{2g} + \sum h + \Delta H_{in}, \qquad (10.1)$$

where ΔH_{in} is the so-called inertia head, which represents the difference between the specific potential energies at the second and first cross-sections due to the action of the inertia force or, alternately, the work done by the inertia force referred to unit weight and with the sign reversed.*

Let us see how the inertia head is calculated for two main cases of steady relative flow corresponding to the two cases of relative rest discussed in Sections 11 and 12.

1. Channel Moving with Uniform Acceleration in a Straight Line. When a channel or pipe with a flowing liquid moves in a straight line with a uniform acceleration a (Fig. 104), all the liquid particles are subject to a constant, uniform inertia force of transport motion. This force may either facilitate or resist the flow.

* The sign is reversed because the term has been transposed to the right side of the equation, whereas in developing Bernoulli's equation in Sec. 15 we wrote the work done by external forces on the left side.

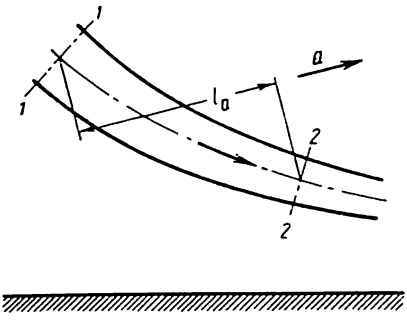

Fig. 104. Flow through pipe moving with acceleration

Referred to unit mass, the inertia force is equal to the corresponding acceleration a and acts in the opposite direction; the inertia force acting on each kilogram of liquid is

$$\frac{1}{g} a.$$

The work done by this force in moving the liquid from the first section to the second does not (as in the case of work done by gravity) depend on the geometry of the path and is determined solely by the difference between the coordinates taken in the direction of the acceleration a. Consequently,

$$\Delta H_{in} = \frac{a}{g} l_a, \tag{10.12}$$

where l_a = projection of the investigated portion of the channel on the direction of the acceleration.

The following rule, arising from the physical aspects of the phenomenon, is useful to make sure of the sign of ΔH_{in} in the right side of the Bernoulli equation.

If the acceleration is directed from the first section to the second and the inertia force is in the opposite direction, the force impedes the flow and the inertia head is positive. The pressure at the second section is lower than at the first and the effect of the inertia head is analogous to the hydraulic losses Σh, which are always included in the right-hand side of the Bernoulli equation with a "plus" sign.

If the acceleration is directed from the second section to the first, the inertia force facilitates the flow and the inertia head must be written with a "minus" sign. In this case the inertia head increases the pressure at the second section, i. e., its action opposes the hydraulic losses.

2. Rotation of a Channel About a Vertical Axis. Let a channel or pipe through which a liquid is flowing be rotating round a vertical axis with a uniform angular velocity ω (Fig. 105). Acting on the liquid will be the inertia force of rotation, which is a function of the radius. To compute the work done by the force or the change in the potential energy due to it integration must be carried out.

The inertia force acting on a unit weight is

$$\frac{\omega^2}{g} r.$$

The work done by the force in a displacement dr along the radius is

$$\frac{\omega^2}{g} r dr.$$

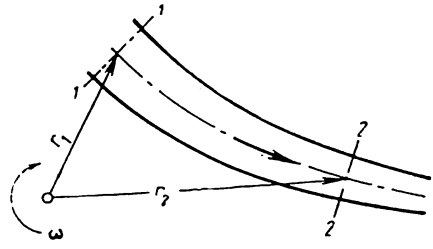

Fig. 105. Flow through a rotating pipe

The work done in a displacement from a radius r_1 to a radius r_2 (along any curve) is found by integrating the foregoing expression over the interval r_1 to r_2. Integration gives the value of the inertia head, only the sign must be reversed (as pointed out before, in developing Bernoulli's equation the term is transposed from the left to the right side of the equation).

Finally we have

$$\Delta H_{in} = -\frac{\omega^2}{g} \int_{r_1}^{r_2} r dr = \frac{\omega^2}{2g} (r_1^2 - r_2^2). \tag{10.3}$$

The sign of the inertia head computed with this formula corresponds to the sign rule explained before.

The Bernoulli equation for these cases of relative motion of an ideal liquid can also be obtained by integrating the differential equations of motion (see Appendix).

41. UNSTEADY FLOW THROUGH PIPES

The general case of unsteady flow is fairly complicated, so we shall restrict ourselves to the main special cases which are found in aeronautical engineering: unsteady flow in a pipe of uniform cross-section and in compound pipes in series.

Take a pipe of length l and diameter d arbitrarily located in space (Fig. 106) and denote by z_1 and z_2 the respective elevation heads of the initial (*1-1*) and terminal (*2-2*) cross-sections. Let a liquid be flowing through the pipe with an acceleration

$$j = \frac{dv}{dt},$$

which, in the general case, may vary with time.

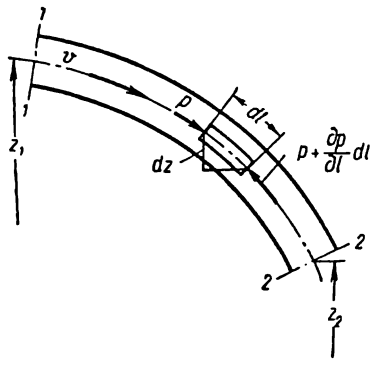

Fig. 106. Unsteady flow through a pipe

The velocity v and the acceleration j, evidently, are the same at all cross-sections of the pipe at a given instant.

We neglect friction losses at first and assume the velocity distribution across the sections to be uniform.

Take a differential cylindrical control volume of length dl and cross-section dS (Fig. 106) and develop its equation of motion.

Projection of the pressure force and the gravity force on the tangent to the centre line of the pipe yields

$$p\,dS - \left(p + \frac{\partial p}{\partial l}\,dl\right) dS + \gamma\,dS\,dl\cos\alpha = \frac{\gamma}{g}\,dS\,dl\,\frac{dv}{dt},$$

or

$$-\frac{\partial p}{\partial l}\,dl + \gamma\cos\alpha\,dl = \frac{\gamma}{g}\,\frac{dv}{dt}\,dl.$$

As

$$\cos\alpha = -\frac{\partial z}{\partial l},$$

then

$$-\frac{\partial p}{\partial l}\,dl - \gamma\,\frac{\partial z}{\partial l}\,dl = \frac{\gamma}{g}\,j\,dl$$

(remembering also that p is a function not only of l but of t as well).

Integrating along the pipe for a specific moment of time, we have

$$\frac{p_1 - p_2}{\gamma} + z_1 - z_2 = \frac{j}{g}\,l,$$

or

$$z_1 + \frac{p_1}{\gamma} = z_2 + \frac{p_2}{\gamma} + h_{in}, \qquad (10.4)$$

where

$$h_{in} = \frac{j}{g}\,l.$$

The equation resembles Bernoulli's equation for relative motion. The term h_{in} is also called the inertia head, not to be confused with

ΔH_{in}, however, as their physical meanings are quite different. The quantity h_{in}, as is evident from Eq. (10.4), represents the difference between the specific energies of the liquid at sections *1-1* and *2-2* at a given time due to the acceleration (or retardation) of the flow in the pipe. The difference is positive when there is acceleration, i. e., the specific energy decreases along the stream; in the case of retardation it is negative, which means that the specific energy is increasing from the first section to the second.

By analogy with the Bernoulli equation, any energy losses (minor or friction) must be written down in the right-hand side of Eq. (10.4):

$$z_1 + \frac{p_1}{\gamma} = z_2 + \frac{p_2}{\gamma} + \sum h + h_{in}. \qquad (10.5)$$

Remember that this equation is valid only for pipes of uniform cross-section. If a pipeline consists of a series of pipes of different cross-sectional areas, S_1, S_2, etc., then, obviously, the inertia head along the whole of the pipeline must be found as the sum of the inertia heads of each portion. The respective accelerations in this case are found from the following equations, which are obtained by differentiating the continuity equations with respect to time:

$$\frac{dQ}{dt} = S_1 j_1 = S_2 j_2 = S_3 j_3 = \ldots \text{ etc.}$$

Furthermore, it follows from the energy considerations cited before that in this case the velocity heads must be considered at the initial and end sections of the pipe.

The equation of unsteady flow between sections *1-1* and *n-n* takes the form

$$z_1 + \frac{p_1}{\gamma} + \alpha_1 \frac{v_1^2}{2g} = z_2 + \frac{p_2}{\gamma} + \alpha_2 \frac{v_2^2}{2g} + \sum h + \sum h_{in}. \qquad (10.6)$$

This equation is used in computing the starting and transient regimes of aircraft hydraulic systems, notably fuel supply systems for liquid-propellant rocket motors.

The following example will illustrate this equation. Let the piston in Fig. 107 be moving to the left with a positive acceleration j. Applying Eq. (10.6) between sections *0-0* and *1-1*, and then between sections *2-2* and *3-3*; and constructing the hydraulic gradient for the moment of time under consideration, we have

$$z_0 = \frac{p_1}{\gamma} + \frac{v^2}{2g} + \lambda \frac{l}{d} \frac{v^2}{2g} + \frac{j}{g} l$$

and

$$\frac{p_2}{\gamma} = z_3 + \lambda \frac{l}{d} \frac{v^2}{2g} + \frac{j}{g} l.$$

Thus, in the first case the inertia head, which is added to the head loss, causes a still greater pressure drop at the piston than in the case of uniform motion. A vacuum forms at section *1-1* and the liquid may even separate from the piston. In the second case, addition of the heads h_f and h_{in} causes a pressure increase at the piston.

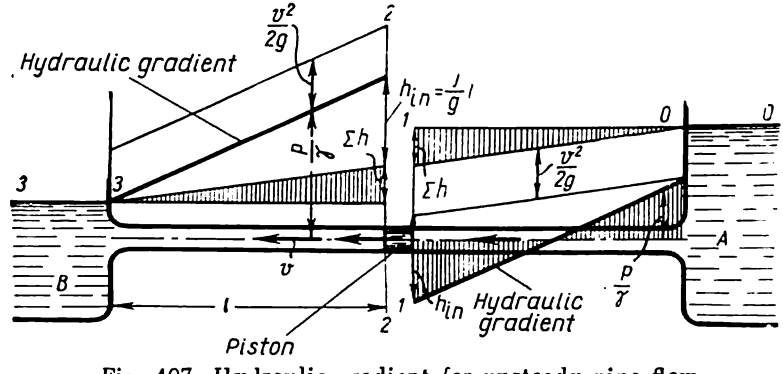

Fig. 107. Hydraulic gradient for unsteady pipe flow

When the acceleration j is negative, i. e., the flow is retarded, the inertia head is negative in both cases and, consequently, it compensates, to a greater or lesser extent, for the loss of head, reducing the vacuum on the one side and increasing the pressure on the other.

Example. Determine the absolute pressure at the intake of the pump of the aircraft lubricating system in the example to Chapter VI (see Fig. 51), if the aircraft dives with a negative g-load of $n_g = -1$ (inertia force is directed upwards).

Solution. The unit inertia force is (see Sec. 11)

$$a = (n_g - 1)\, g = -2g,$$

and the inertia head

$$\Delta H_{in} = -\frac{a}{g} z = +2z.$$

From Bernoulli's equation for relative motion,

$$\frac{p_1}{\gamma_{oil}} = z + \frac{p_{atm}}{\gamma_{oil}} - \alpha \frac{v^2}{2g} - h_f - \Delta H_{in} = 152 - 140 = 12 \text{ cm},$$

or

$$h_1 = 12 \frac{0.9}{13.6} 10 = 8 \text{ mm Hg}.$$

The pressure at the pump intake is too low, which means that steps must be taken to improve the performance of the lubricating system at high altitudes.

42. WATER HAMMER IN PIPES

Water hammer is the name given to a sudden change of pressure that develops inside pipes when a valve is closed rapidly.

The theoretical and experimental investigation of water-hammer phenomena were first carried out by N. E. Joukowski. The explanations set forth here are based on the basic conclusions of his fundamental work, *Water Hammer*, published in 1899.

Water hammer is a very rapid process in which elastic deformations of both liquid and pipe take place.

Consider a liquid flowing through a pipe with a velocity v_0, and let a valve be closed instantaneously (Fig. 108*a*). The velocity of the liquid particles next to the valve becomes zero and their kinetic energy turns into work done in deforming the pipe walls and the fluid. As a result, the pipe walls suffer an expansion and the fluid a compression corresponding to the pressure increase Δp_{wh}.* Other particles collide with the halted particles and also lose their velocity. The result is that the section *n-n* travels to the right with a velocity a; the transient region in which the pressure changes by Δp_{wh} is called the shock, or pressure, wave.

When the shock wave reaches the reservoir, the liquid in the pipe is at rest and in compression and the pipe walls are in tension; the pressure increase Δp_{wh} extends throughout the whole pipe (Fig. 108*b*).

This state, however, is unstable. Due to the pressure difference Δp_{wh}, the liquid particles start to flow towards the reservoir, the motion beginning at the cross-section adjoining the reservoir. The section *n-n* travels back to the valve with the velocity a, leaving in its wake the unloaded pressure p_0 (Fig. 108 *c*).

The liquid and the walls are assumed to be absolutely elastic, therefore they revert to their initial state corresponding to the pressure p_0. The work done in the deformation all turns back into kinetic energy and the liquid obtains its initial velocity v_0, but in the opposite direction.

Now the liquid tends to move away from the valve (Fig. 108*d*) and a negative shock wave — Δp_{wh} develops which travels from the valve to the reservoir with the velocity a, leaving in its wake the pipe walls contracted and the liquid expanded, due to the reduced pressure $-\Delta p_{wh}$ (Fig. 108*e*). The kinetic energy of the liquid once again turns into the work done in deformation, but with the opposite sign.

---

* In this case liquid compressibility cannot be neglected, as is customary in solving hydraulics problems, because the low compressibility of liquids is the very cause for the development of the high water-hammer pressure Δp_{wh}.

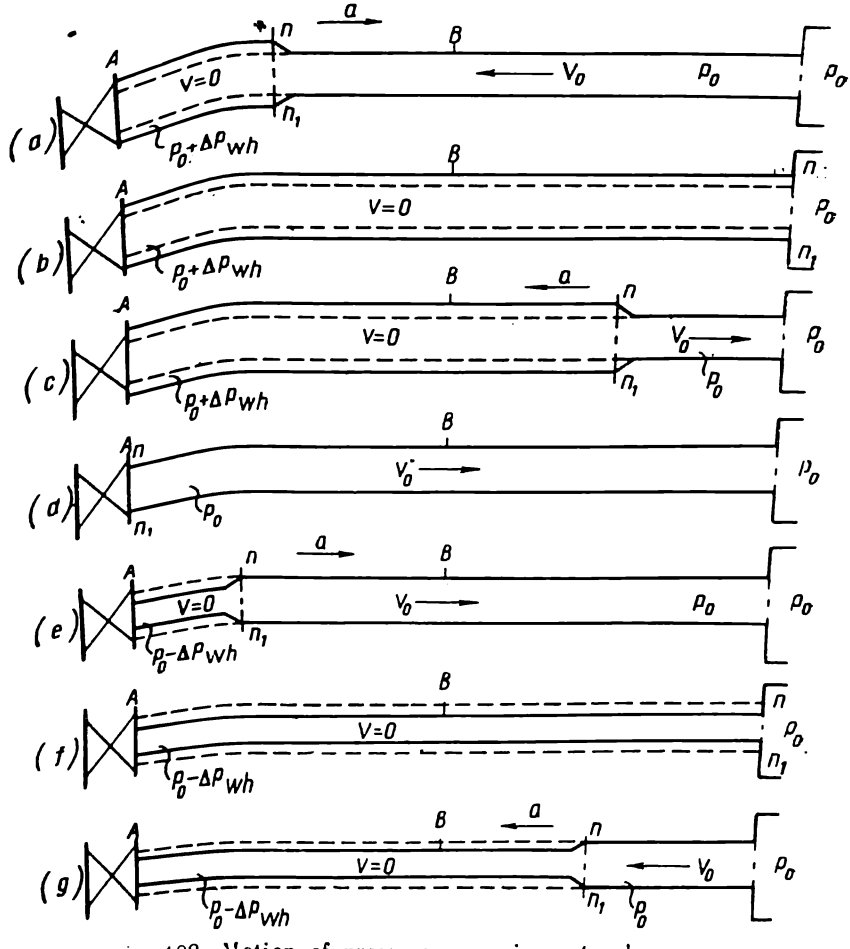

Fig. 108. Motion of pressure wave in water hammer

The state of the pipe when the negative shock wave reaches the reservoir is shown in Fig. 108*f*. As in Fig. 108*b*, the state is unstable, and Fig. 108*g* shows the levelling out of the pressure in the pipe and in the reservoir and the accompanying development of the velocity v_0.

It is evident that as soon as the shock wave $-\Delta p_{wh}$ is reflected from the reservoir and reaches the valve the same conditions that were produced by the closure of the valve reappear and the cycle is repeated.

Joukowski in his experiments registered 12 complete cycles, with Δp_{wh} gradually degrading due to friction and dissipation of energy in the reservoir.

The history of a water hammer is illustrated diagrammatically in Fig. 109.

The upper diagram shows the change in the pressure Δp_{wh} that would be recorded by an indicator installed at the valve at A (the closure is assumed to be instantaneous).

The shock wave reaches B, in the middle of the pipe, after a time interval $\frac{l}{2a}$, and the pressure remains during the time $\frac{l}{a}$ it takes the shock wave to run from B to the reservoir and back; the pressure at B then reverts to p_0 (i. e., $\Delta p_{wh} = 0$) and remains such till the negative shock wave comes from the valve after a time interval $\frac{l}{a}$.

The value of the water-hammer pressure Δp_{wh} is found from a force equation in which the kinetic energy of the liquid turns into the work done in the deformation of the pipe walls and the liquid. The kinetic energy of a liquid in a pipe of radius R is

$$\frac{Mv_0^2}{2} = \frac{1}{2} \pi R^2 l \varrho v_0^2.$$

The work done in the deformation constitutes half the product of the force by the extension. Expressing the work done in expanding the pipe walls as the work done by the pressure forces in a displacement ΔR (Fig. 110), we obtain

$$\frac{1}{2} \Delta p_{wh} 2\pi R l \Delta R.$$

From Hooke's law,

$$\frac{\Delta R}{R} E = \sigma, \tag{10.7}$$

where σ = normal stress in the pipe wall, which is related to the pressure Δp_{wh} and the wall thickness δ by the well-known equation

$$\sigma = \frac{\Delta p_{wh} R}{\delta}. \tag{10.8}$$

Taking the expression for ΔR from Eq. (10.7) and the expression for σ from (10.8) we obtain the following expression for the work done in the deformation of the pipe walls:

$$\frac{\Delta p_{wh}^2 \pi R^3 l}{\delta E}.$$

The work done in compressing a volume W of liquid can be represented as the work done by the pressure forces in the displacement Δl (Fig. 110):

$$\frac{1}{2} S \Delta p_{wh} \Delta l = \frac{1}{2} \Delta p_{wh} \Delta W.$$

By analogy with Hooke's law for linear extension, the relative reduction of the liquid volume $\frac{\Delta W}{W}$ is connected with the pressure by the relationship

$$\frac{\Delta W}{W} K = \Delta p_{wh},$$

where K volume modulus of the liquid (see Sec. 4.)

If W is the volume of liquid in a pipe, the expression for the work done in the compression of the liquid is

$$\frac{1}{2} \times \frac{\Delta p_{wh}^2 \pi R^2 l}{K}.$$

The equation of the acting forces takes the form

$$\frac{1}{2} \pi R^2 l \varrho v_0^2 = \frac{\pi R^3 l \Delta p_{wh}^2}{\delta E} + \frac{\pi R^2 l \Delta p_{wh}^2}{2K}.$$

Solving with respect to Δp_{wh} gives Joukowski's formula:

$$\Delta p_{wh} = \varrho v_0 \frac{1}{\sqrt{\frac{\varrho}{K} + \frac{2\varrho R}{\delta E}}}. \tag{10.9}$$

The quantity

$$\frac{1}{\sqrt{\frac{\varrho}{K} + \frac{2\varrho R}{\delta E}}}$$

has the dimension of velocity. Its physical meaning can be interpreted by assuming the pipe to have absolutely rigid walls, i. e., $E = \infty$. Then the last expression turns into $\sqrt{\frac{K}{\varrho}}$, which is the velocity with which sound propagates ("sonic" or "acoustic" velocity) in a homogeneous elastic medium of density ϱ and volume modulus K.

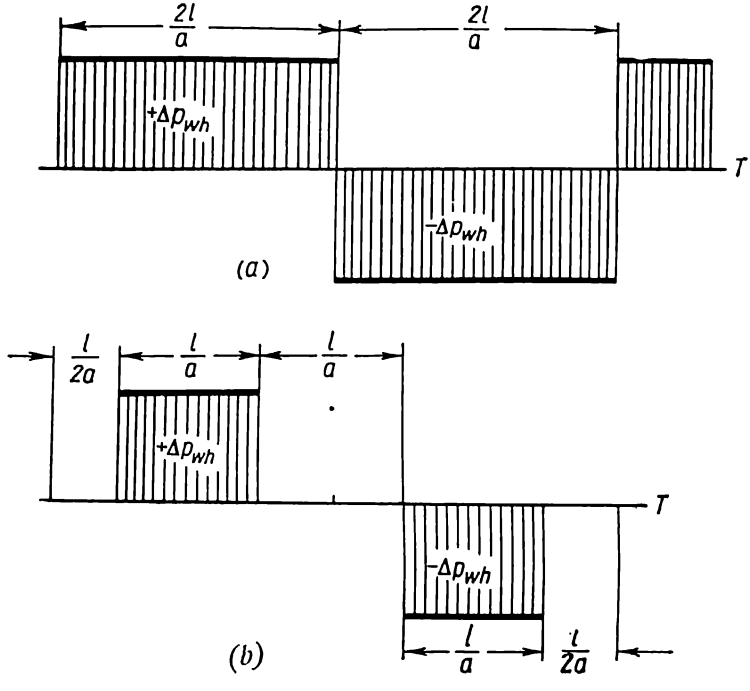

Fig. 109. Pressure history at a valve and at the middle of pipe

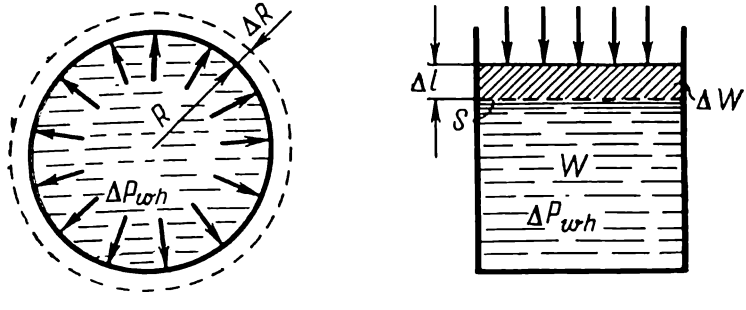

Fig. 110. Expansion of pipe and compression of liquid

Acoustic velocity in water is 1,435 m/sec, in gasoline, 1,116 m/sec, and in oil, 1,400 m/sec.

If, as is the case here, $E \neq \infty$, the quantity $\dfrac{1}{\sqrt{\dfrac{\varrho}{K}+\dfrac{2\varrho R}{\delta E}}}=a$ represents acoustic velocity in a liquid filling a pipe with elastic walls.

It follows from the very nature of acoustic vibrations that the velocity of sound is the speed with which rarefactions or compressions of infinitely small amplitude propagate through a medium. When the density change is relatively small Hooke's law is valid, and it was used in developing Eq. (10.9). We come, thus, to the conclusion that the quantity a is the velocity of the shock wave examined in Fig. 108. Consequently, Joukowski's formula can be written in the form

$$\Delta p_{wh} = \varrho v_0 a. \tag{10.10}$$

This formula is valid for "instantaneous" closure of a valve, i. e., when the time of closure

$$T_c < T_0 = \frac{2l}{a}.$$

At $T_c > T_0$ water hammer is "incomplete" as the shock wave makes its round trip from the reservoir before the valve is completely closed. The pressure rise $\Delta p'_{wh}$ is smaller, and it is commonly assumed that

$$\Delta p'_{wh} = \frac{T_0}{T_c}\,\Delta p_{wh}.$$

Equation (10.10) and the expression for T_0 yield instead of the foregoing

$$\Delta p'_{wh} = \frac{2\varrho l v_0}{T_c}. \tag{10.11}$$

Thus, unlike Δp_{wh}, the quantity $\Delta p'_{wh}$ depends on the length of the pipe and does not depend on the velocity a.

It is evident from all that has been said that water-hammer effects can be reduced by increasing the closure time T_c. If this is not feasible for some reason or other, air chambers or surge tanks are installed in pipelines. They absorb the water-hammer shock, which is equivalent to increasing the time of valve closure.

Example. A receiver in an aircraft hydraulic system is cut out by means of an electromagnetic valve. The time of complete closure is $T_c = 0.02$ sec.

Determine the pressure increase at the valve at the moment of cut-out under the following conditions (Fig. 111):

Length of pipe from valve to accumulator which absorbs shock wave $l = 4$ m; pipe diameter $d = 12$ mm; thickness of pipe wall $\delta = 1$ mm; material, steel ($E = 2.2 \times 10^6$ kg/cm^2); volume modulus of АМГ-10 fluid $K = 13{,}300$ kg/cm^2, density $\varrho = 90$ kg sec^2/m^4; pipe flow velocity $v_0 = 4.5$ m/sec.

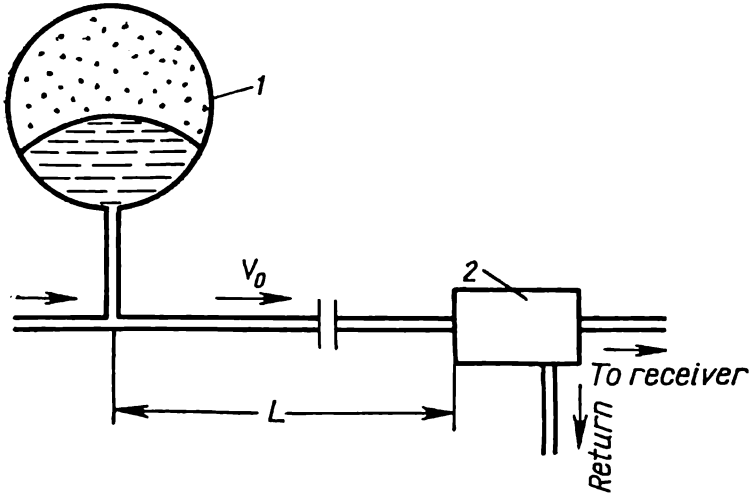

Fig. 111:
1 — gas-loaded accumulator; *2* — electromagnetic valve

Solution. Determine the speed of propagation of a shock wave through pipe filled with АМГ-10 fluid:

$$\frac{1}{a} = \sqrt{\frac{\varrho}{K} + \frac{2R\varrho}{\delta E}} = \sqrt{\frac{90}{13{,}300 \times 10^4} + \frac{2 \times 0.006 \times 90}{0.001 \times 2.2 \times 10^{10}}} = \frac{1}{1{,}170} \text{ sec/m},$$

or

$$a = 1{,}170 \text{ m/sec}.$$

Total water-hammer pressure if the closure were instantaneous would be

$$\Delta p_{wh} = \varrho v_0 a = 90 \times 4.5 \times 1{,}170 = 473{,}000 \text{ kg/m}^2 = 47.3 \text{ kg/cm}^2.$$

In this case, however, water hammer is less pronounced because the return trip of the shock wave takes

$$T_0 = \frac{2l}{a} = \frac{2 \times 4}{1{,}170} = 0.0068 \text{ sec},$$

i. e., less than the time of the complete closure T_c. The pressure increase at the valve is only

$$\Delta p'_{wh} = \Delta p_{wh} \frac{T_0}{T_c} = 47.3 \frac{0.0068}{0.02} = 16.2 \text{ kg/cm}^2.$$

CHAPTER XI

CALCULATION OF PIPELINES

43. PLAIN PIPELINE

We shall call a plain pipeline one of uniform diameter without branchings. The liquid flows along a pipe because its potential energy is higher at the initial point than at the terminal. This drop, or difference, in potential energy level can be produced by various means: difference in elevation, pumping or gas pressure.

In aeronautical engineering liquid flow in pipes is most commonly induced by pumps. In some liquid-propellant rocket systems and devices gas-pressure supply is employed. Liquid flow between different elevations, i. e., due to difference of elevation head, is employed only in ground conditions.

The principles of calculating pipelines set forth in this section (as well as in Secs 45 and 46) are equally applicable to all three methods of liquid supply, i. e., they do not depend on the method of producing the energy drop. The characteristic features of pumped flow are discussed in Sec. 47.

Let there be a plain pipeline of arbitrary geometry (Fig. 112) of total length l and diameter d with a number of local features in it. Suppose that at the initial section *1-1* the elevation head is z_1 and the pressure is p_1, and at the end section *2-2* the respective quantities are z_2 and p_2. Thanks to the uniformity of diameter (with the exception of the local features) the velocity v is uniform along the pipeline. Writing Bernoulli's equation between sections *1-1* and *2-2*, assuming $\alpha_1 = \alpha_2$ and cancelling out the velocity heads, we have,

$$z_1 + \frac{p_1}{\gamma} = z_2 + \frac{p_2}{\gamma} + \sum h,$$

or

$$\frac{p_1 - p_2}{\gamma} = z_2 - z_1 + \sum h.$$

We shall call the pressure-head difference in the left-hand side of the equation the *required head* H_{req}; if the required head has been given in advance we shall call it the *available head* H_{av}. As is evident from the equation, this head comprises the geometrical elevation to which the liquid rises in its flow through the pipeline and the sum of all the head losses in the pipe. The latter can be represented in general form as an exponential function of the discharge. Then,

$$H_{req} = \Delta z + kQ^m, \tag{11.1}$$

where the values of the coefficient k and the exponent m vary depending on the flow regime.

For laminar flow, substituting the equivalent lengths for the local disturbances according to Eqs (6.5) and (8.19),

$$k = \frac{128\nu (l + l_{eq})}{\pi g d^4} \text{ and } m = 1. \tag{11.2}$$

For turbulent flow, according to Eqs (4.17) and (4.18) and expressing the velocity in terms of discharge,

$$k = \left(\sum \zeta + \lambda_t \frac{l}{d}\right) \frac{16}{2g\pi^2 d^4} \text{ and } m = 2. \tag{11.3}$$

Equation (11.1), supplemented by the expressions (11.2) and (11.3), is the basic formula for calculating plain pipelines. It is also the pipeline characteristic equation.

A *pipeline characteristic* is a diagram on which the required head is plotted as a function of the rate of discharge of the pipeline. The larger the required discharge, the higher the required head. In lam-

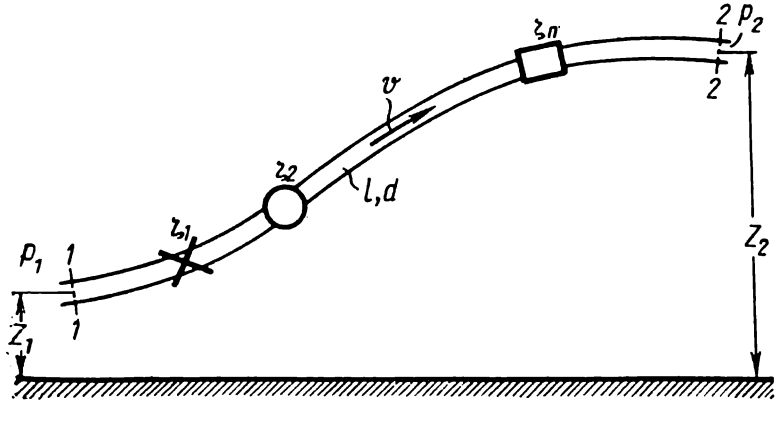

Fig. 112. Schematic representation of plain pipeline

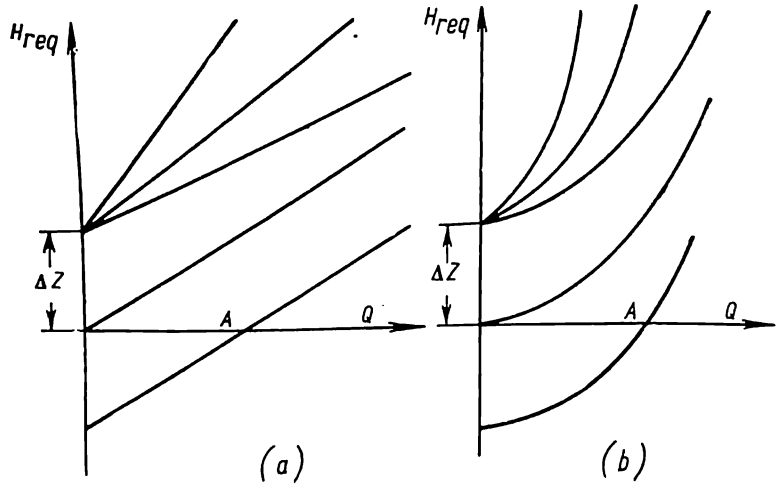

Fig. 113. Pipeline characteristics

inar flow the pipeline characteristic represents a straight (or nearly straight) line, in turbulent flow it is a parabola with an exponent of two (at λ_t = const) or about two (if the dependence of λ_t on Re is taken into account). The value of Δz is positive when the flow is from a lower to a higher elevation and negative when it is from a higher to a lower elevation.

Pipeline characteristics are presented in Fig. 113 for the cases of (*a*) laminar and (*b*) turbulent flow. The slope of the curves depends on the coefficient k, increasing with the length of the pipeline increasing and the diameter decreasing and also with the minor losses increasing in the pipe. Besides, in laminar flow the slope of the curve varies as the viscosity of the liquid.

The intersection of the curve with the axis of abscissas (point A) gives the discharge for flow under gravity, i. e., only due to the elevation head difference Δz. The required head in this case is zero as the pressure at both ends of the pipeline is atmospheric (taking the free surface in the higher reservoir as the beginning of the pipeline) (Fig. 114). If such a gravity pipeline empties into the atmosphere the velocity head must be added to the head losses in equation (11.1).

Let us examine some sample solutions of plain pipelines.

Problem 1. *Given*: discharge Q, fluid properties (γ and ν), pipeline dimensions, material and surface finish (roughness). To determine the required pressure H_{req}.

Solution. First determine the velocity of flow v from the rate of discharge and pipe diameter d; from v, d and ν determine Re and the flow regime; evaluate the minor losses ($\frac{l_{eq}}{d}$ or ζ in laminar flow and ζ in turbulent flow) by the

appropriate formulas or experimentally; determine λ according to Re and the roughness; finally, solve the basic equation (11.1) with respect to H_{req}.

In laminar flow there is no need to compute λ, and k can be determined directly from Eq. (11.2).

Problem 2. *Given*: available head H_{av}, fluid properties, pipeline dimensions and roughness. To determine the rate of discharge Q.

The solutions for laminar and turbulent flow differ markedly. The flow regime must therefore be assumed depending on the type (viscosity) of the liquid.*

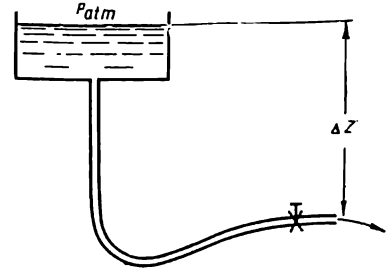

Fig. 114. Schematic representation of gravity pipeline

(a) For laminar flow, substituting the equivalent length for the minor losses, the solution is simple: from Eq. (11.1) and taking into account the expression (11.2), determine the discharge Q, substituting H_{av} for H_{req}.

(b) For turbulent flow the problem has to be solved by trial and error or graphically.

In the first case we have one equation (11.1) with two unknown quantities Q and λ_t. To solve the problem a value is assigned to λ_t according to the roughness of the pipe. As λ_t varies within fairly narrow limits (0.015 to 0.04), the error will not be very great, all the more so that in solving for Q λ_t comes under the radical.

Solution of Eq. (11.1), taking into account (11.3), with respect to Q gives the rate of discharge to a first approximation. The obtained value of Q is used to determine v and Re to a first approximation, and from Re a closer value of λ_t. This new value of λ_t is substituted into the basic equation, which is solved again for Q. The second approximation of the discharge will vary more or less from the first approximation. If the discrepancy is great, the procedure should be repeated until it is small enough. Usually two or three approximations are sufficient for the necessary accuracy.

For a graphical solution of the problem, the pipeline characteristic is plotted, taking into account the variability of λ_t, viz., a number of values are assigned to Q, and v, Re, λ_t and, finally, H_{req} are computed from Eq. (11.1). By plotting H_{req} against Q, and knowing the ordinate $H_{req}=H_{av}$, the corresponding abscissa Q can be found.

Problem 3. *Given*: rate of discharge Q, available head H_{av}, fluid properties and all pipeline dimensions except diameter. To determine the diameter.

First a flow regime is assigned according to the fluid properties (ν).**

---

* The flow regime can be determined by comparing H_{av} with its critical value H_{cr}. Eqs (11.1) and (11.2) give

$$H_{cr}=\Delta z+\frac{128\nu l Q_{cr}}{\pi g d^4}=\Delta z+\frac{32\nu l v_{cr}}{g d^2}\frac{\nu d}{\nu d}=\Delta z+\frac{32\nu^2 l}{g d^3}\,\mathrm{Re}_{cr}.$$

** The flow regime can be determined by comparing H_{av} with H_{cr}, which, for a given Q, is

$$H_{cr}=\Delta z+\frac{128\nu l Q}{\pi g d^4}\,\frac{2\pi^4\nu^4 Q^3}{2\pi^4\nu^4 Q^3}=\Delta z+\frac{\pi^3\nu^5 l\,\mathrm{Re}_{cr}^4}{2gQ^3}.$$

For laminar flow the solution is simple. On the basis of (11.1), and taking into account (11.2),

$$d = \sqrt[4]{\frac{128\nu (l + l_{eq})\, Q}{\pi g (H - \Delta z)}}. \qquad (11.4)$$

Having found d, choose the nearest larger commercial diameter and, using the same equation, recalculate the value of the head for a given Q, or vice versa.

In turbulent flow, Eq. (11.1), taking into account (11.3), is best solved with respect to d in the following manner. Assign a number of standard values of d for a given Q and compute the corresponding values of H_{req}. Then plot a graph of H_{req} against d, and from the given H_{av} find the value of d on the curve. Finally, choose the nearest larger commercial pipe diameter and solve again for H_{req}.

44. SIPHON

A *siphon* is a plain gravity pipeline some portion of which lies higher than the feeding reservoir (Fig. 115). Flow is caused by the elevation head H, the liquid first rising to a height H_1 above the free surface with atmospheric pressure and then flowing down the height H_2.

Characteristic of a siphon is that the pressure in the whole of the ascending section and part of the descending section is less than atmospheric.

For a liquid to start flowing through a siphon the latter must first be filled completely. If the siphon is a small hose it can be filled by immersing into a reservoir or evacuating the air from the lower end. If the siphon is a stationary metal pipeline it must be provided with a valve at the summit to evacuate the air. The air can be evacuated by a displacement pump (see further on) or an air ejector (Sec. 18).

Write Bernoulli's equation between sections *0-0* and *2-2* (Fig. 115), where the velocities are assumed to be zero and the pressure is atmospheric. This gives

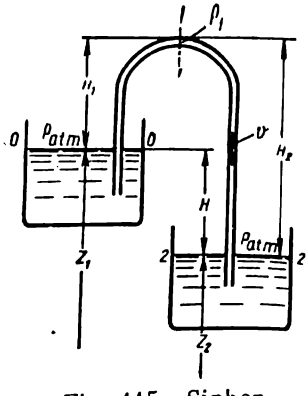

Fig. 115. Siphon

$$z_1 = z_2 + \sum h,$$

or

$$\Delta z = kQ^m = H.$$

Thus, the rate of discharge through a siphon is determined by the difference of the elevations H and the resistance of the pipeline and does not depend on the height of the summit H_1. This, however, is true only within certain limits. With H_1 increasing, the absolute pressure p_1 at the summit (section *1-1*) drops. When it becomes

equal to the vapour pressure cavitation begins and the discharge decreases. Vapour collects at the bend, forming so-called vapour locks, and the flow stops.

Accordingly, in designing siphons precautions must be taken to prevent the pressure p_1 at the summit from falling too low. If the rate of discharge and all the dimensions of the siphon are known, the absolute pressure p_1 can be found from Bernoulli's equation taken between sections *0-0* and *1-1*:

$$\frac{p_{atm}}{\gamma} = H_1 + \frac{p_1}{\gamma} + \alpha \frac{v^2}{2g} + \sum h_{0\text{-}1}.$$

If the minimum permissible pressure p_1 and the rate of discharge are known, the maximum elevation H_1 can be computed from the equation.

45. COMPOUND PIPES IN SERIES AND IN PARALLEL

Consider several pipes of different length and diameter and with different local features joined in series (Fig. 116).

It is evident that the rate of discharge through all portions of the compound pipes is the same and the total loss of head between points

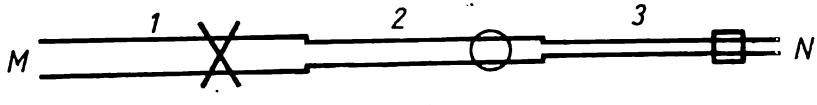

Fig. 116. Compound pipes in series

M and N is the sum of the head losses in each of them. Thus, the basic equations are:

$$\left.\begin{aligned} Q_1 = Q_2' = Q_3 = Q; \\ \sum h_{M\text{-}N} = \sum h_1 + \sum h_2 + \sum h_3. \end{aligned}\right\} \qquad (11.5)$$

These equations define the rule for plotting the characteristics of a compound series of pipes.

Suppose that we are given (or have plotted ourselves) the characteristics of the three pipes in Fig. 117. To plot the curve for the series from M to N, we must, in accordance with Eq. (11.5), compound the head losses for equal rates of discharge, i. e., sum the ordinates of all three curves at equal abscissas.

In the most general case the velocities at the beginning M and end N of the pipeline are different and the expression for the required head for the whole pipeline M-N must contain, unlike Eq. (11.1),

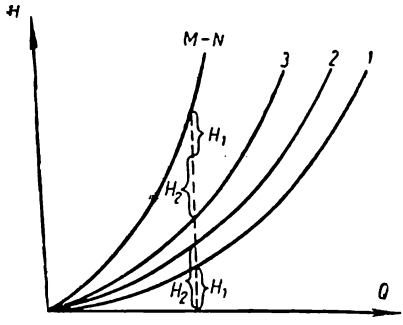

Fig. 117. Characteristics of compound pipes in series

the difference between the velocity heads at the end and the beginning, i. e.,

$$H_{req} = z_M - z_N + \frac{\alpha_N v_N^2 - \alpha_M v_M^2}{2g} + \sum h_{M-N} = \Delta z + CQ^2 + kQ^m, \quad (11.6)$$

where $C = \frac{1}{2g}\left(\frac{\alpha_N}{S_N^2} - \frac{\alpha_M}{S_M^2}\right)$.

Now consider several pipes *joined in parallel* between points M and N (Fig. 118). For simplicity's sake we shall assume them to be all in the horizontal plane.

Notation: pressure at M and $N = p_M$ and p_N respectively; rate of discharge through main (i. e., before and after the loop) $= Q$; rates of discharge through the parallel pipes $= Q_1$, Q_2 and Q_3 respectively; total head losses in the parallel pipes $= \Sigma h_1$, Σh_2 and Σh_3 respectively.

First write down the obvious equation:

$$Q = Q_1 + Q_2 + Q_3. \quad (11.7)$$

Now express the loss of head in each pipe in terms of the pressure at M and N:

$$\sum h_1 = \frac{p_M - p_N}{\gamma};$$

$$\sum h_2 = \frac{p_M - p_N}{\gamma};$$

$$\sum h_3 = \frac{p_M - p_N}{\gamma}.$$

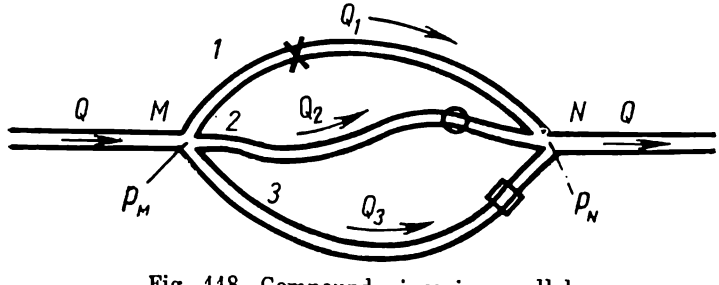

Fig. 118. Compound pipes in parallel

From this we draw the important conclusion that

$$\sum h_1 = \sum h_2 = \sum h_3, \tag{11.8}$$

i. e., the head losses in parallel pipes are equal.

These losses can be expressed in terms of the respective rates of discharge in general form as follows:

$$\sum h_1 = k_1 Q_1^m;$$
$$\sum h_2 = k_2 Q_2^m;$$
$$\sum h_3 = k_3 Q_3^m,$$

where the coefficients k and the exponents m are found, depending on the flow regime, from Eq. (11.2) or (11.3).

Consequently, besides Eq. (11.7), we have from Eq. (11.8) two more equations:

$$k_1 Q_1^m = k_2 Q_2^m; \tag{11.9}$$

$$k_2 Q_2^m = k_3 Q_3^m. \tag{11.10}$$

Equations (11.7), (11.9), (11.10) can be employed to solve such a typical problem as determination of the rates of discharge Q_1, Q_2, Q_3 in parallel pipes if the rate of discharge Q of the main and the pipe dimensions are known.

Applying Eq. (11.7) and the rule (11.8) we can develop as many equations as there are parallel pipes between two points M and N.

In calculating aircraft fuel systems a common problem is: Given total discharge and the lengths of parallel pipes, to determine the diameters necessary to ensure a specified rate of discharge through each of them. The solution of such a problem is presented in an example at the end of the chapter.

The following important rule follows from the relationships in (11.7) and (11.8): in order to plot the characteristics of compound pipes in parallel it is necessary to sum the abscissas (rates of discharge) of the respective curves at equal ordinates (heads). An example of such a construction is presented in Fig. 119.

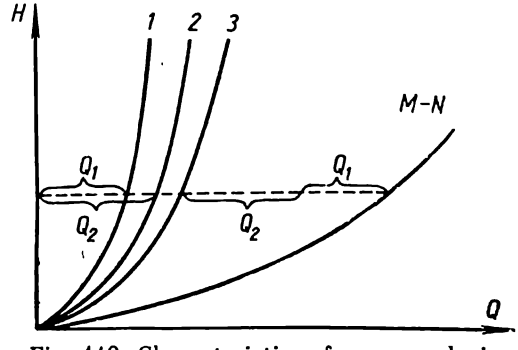

Fig. 119. Characteristics of compound pipes in parallel

Obviously, the relationships and rules for compound pipes in parallel hold good for the case of pipes *1*, *2*, *3*, etc. (see Fig. 118), not converging at one point *N* but delivering the liquid at different points with equal pressures and with equal elevation heads at the end sections. If the latter condition is not observed, the pipes cannot be regarded as parallel and should be considered under the heading of the branching pipe problem in the following section.

46. CALCULATION OF BRANCHING AND COMPOSITE PIPELINES

We shall call a branching pipeline one in which several pipes have a common cross-section where the flows diverge or converge. Such pipelines are common in aircraft fuel systems (main and refuelling), hydraulic transmissions and ground fuel supply systems at aerodromes.

Let a main branch at *M-M* (Fig. 120) into three pipes of different size and with different local features and let the elevation heads z_1, z_2, z_3 at the end sections and the pressures p_1, p_2, p_3 also be different. We shall investigate the relation between the pressure p_M at section *M-M* and the rates of discharge Q_1, Q_2, Q_3 through the respective pipes when the direction of flow is as indicated by the arrows in the drawing.*

As in the case of parallel pipes,

$$Q = Q_1 + Q_2 + Q_3.$$

Bernoulli's equation between section *M-M* and the end section of, say, the first pipe yields (neglecting the difference in velocity head)

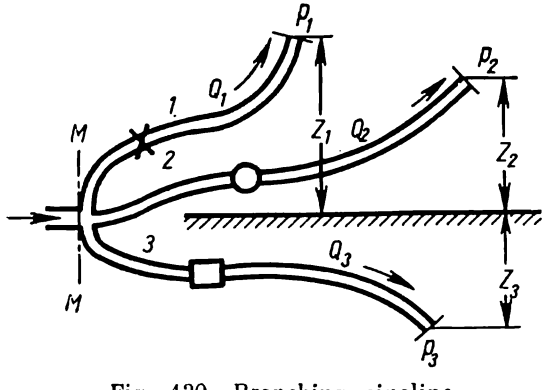

Fig. 120. Branching pipeline

$$\frac{p_M}{\gamma} = z_1 + \frac{p_1}{\gamma} + \sum h_1.$$

Denoting the sum of the first two members in the right-hand side of the equation by z_1' and expressing the last, as before, in terms of the discharge, we obtain

$$\frac{p_M}{\gamma} = z_1' + k_1 Q_1^m.$$

* In aircraft systems reversal of the flow is prevented by nonreturn valves.

Similarly, for the other two pipes

$$\frac{p_M}{\gamma} = z_2' + k_2 Q_2^m;$$

$$\frac{p_M}{\gamma} = z_3' + k_3 Q_3^m.$$

We thus have four equations with four unknown quantities: Q_1, Q_2, Q_3, and p_M. A graphical solution is more convenient. For this, construct a curve for each pipe by plotting $\frac{p_M}{\gamma}$ as a function of Q according to the above equations and then compound them in the same way as in the case of parallel pipes, i. e., sum the abscissas Q for equal ordinates $H = \frac{p_M}{\gamma}$ (Fig. 121). The resulting stepped curve characterises the whole of the branching pipeline and makes it possible to determine the rates of discharge from the pressure p_M and vice versa.

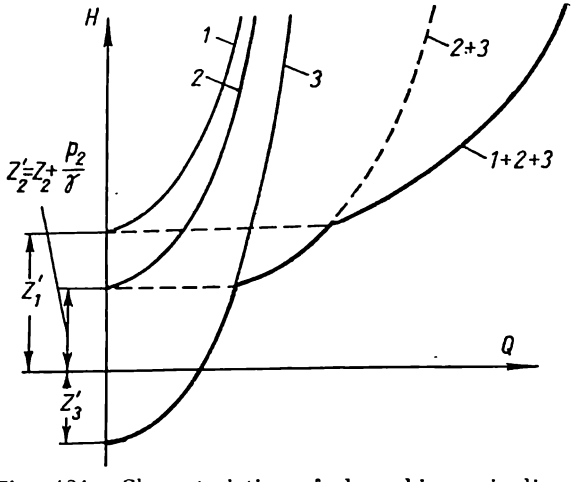

Fig. 121. Characteristics of branching pipeline

If the flow is reversed, i. e., from the several sections *1*, *2*, *3* to the section *M-M* (see Fig. 120), the signs of the head losses are reversed and, consequently, the curves are plotted downwards.

A composite pipeline is one which consists of compound pipes in series and branching or parallel pipes. Composite pipelines, both with gravity flow and with pumps, are usually calculated by the graphoanalytical method, i. e., by using characteristic curves.

To calculate and plot the characteristics of a composite pipeline it is broken down into a number of plain pipelines, the calculations and curve constructions for which are carried out as described before. The characteristics of the parallel or branching pipes are compounded as described in Sec. 45, then the characteristics of the parallel or branching pipes are added to the characteristics of the series according to the equations (11.5).

In this way it is possible to plot the characteristics of any composite pipeline for both turbulent and laminar flow.

Examples on the plotting of composite pipeline characteristics are given at the end of the chapter.

47. PIPELINE WITH PUMP

The foregoing discourse dealt essentially with isolated sections of plain and compound pipelines, not with complete systems of liquid supply (with the exception of the simplest gravity flow system). It was mentioned, furthermore, that in aeronautical engineering forced flow by means of pumps is the main method of liquid supply. Let us investigate the operation of a pipeline with a pump and the principles for calculating such pipelines.

A pipeline with pump may be open, if the liquid is pumped from one place to another, or closed (looped) if a constant volume of liquid is recycled.

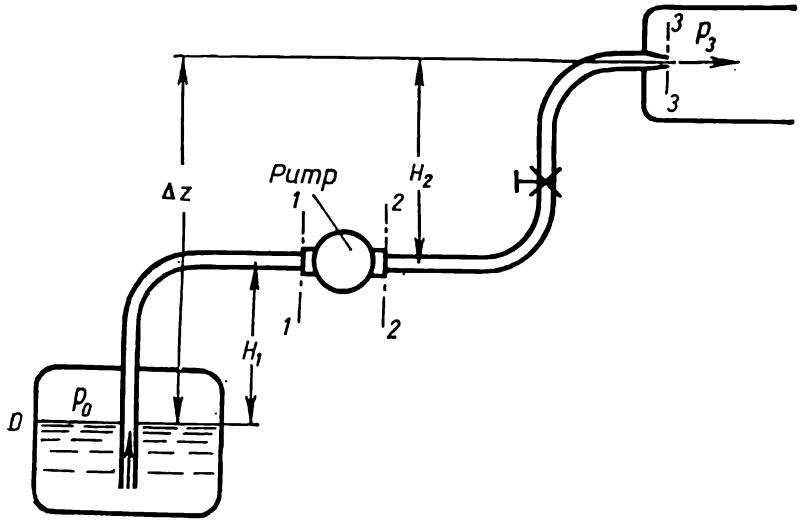

Fig. 122. Schematic representation of pipeline with pump

We shall first consider an open pipeline (Fig. 122) in which the liquid is driven by pump from, say, a reservoir where the pressure is p_0 to the combustion chamber of an engine where the pressure is p_3 or to another reservoir.

The elevation of the pump shaft above the lower level H_1 is the geodetic suction head, the pipe along which the liquid flows to the pump being the suction, or intake, pipe or line. The elevation of the end section of the pipeline, or the upper level of the liquid (H_2), is the geodetic delivered head and the pipe through which the liquid travels from the pump is called the pressure, or discharge, or outlet pipe or line.

Bernoulli's equation for the motion of the liquid in the suction line, i. e., between sections *0-0* and *1-1*, yields

$$\frac{p_0}{\gamma} = H_1 + \frac{p_1}{\gamma} + \alpha \frac{v_1^2}{2g} + \sum h_{0\text{-}1}. \qquad (11.11)$$

This equation shows that the pump develops suction (lifts the liquid to the height H_1), imparts kinetic energy to the liquid and overcomes hydraulic resistances by expending the pressure p_0. As this pressure is usually very limited, it should be expended in such a way as to continuously maintain some pressure reserve p_1 at the pump intake, which is essential for the pump to work without cavitation. It stands to reason that suction lines should therefore be calculated with special care.

Equation (11.11) is the basic formula for this.

The following solutions may be required to calculate a suction pipeline.

1. Given dimensions and rate of discharge. To determine absolute pressure at pump intake.

The solution of the problem is a verification estimate for the suction line. The absolute pressure p_1 as found from Eq. (11.11) is compared with the minimum permissible pressure for the case under consideration.

2. Given minimum permissible absolute pressure p_{1min} at pump intake. To determine one of the following permissible limiting quantities:

$$H_{1max},\ Q_{max},\ d_{min},\ \text{or}\ p_{0min}.$$

Determination of the last quantity is of special importance in aircraft hydraulic systems, in which $p_0 = p_{atm} + \Delta p$. Here Δp is the pressure above atmospheric pressure produced by supercharging or the pressure of an inert gas. The minimum permissible atmospheric pressure $p_{atm\ min}$ is determined from p_{0min}, then the maximum permissible altitude of flight for an aircraft equipped with such a system is determined from a standard atmosphere table.

An increase in the pressure p_0 increases the pressure in the whole of the suction line, which makes for greater altitude range of the system. On the other hand, high pressure in the supply tank means stronger walls and, consequently, greater weight of the tank. Therefore greater altitude range of aircraft hydraulic systems is usually attained by installing an additional pump at the beginning of the suction line to produce a higher pressure in the latter, thereby preventing cavitation at the intake of the main pump.

Bernoulli's equation for a liquid in the pressure pipe between sections *2-2* and *3-3* yields

$$\frac{p_2}{\gamma} + \alpha \frac{v_2^2}{2g} = H_2 + \frac{p_3}{\gamma} + \alpha \frac{v_3^2}{2g} + \sum h_{2\text{-}3}. \qquad (11.12)$$

If the pressure pipe discharges into a reservoir there is no velocity head in the right-hand side of the equation, but the loss of head due to enlargement must be taken into account.

The left-hand side of Eq. (11.12) represents the specific energy of the liquid at the pump outlet.

The specific energy at the intake can be found from Eq. (11.11):

$$\frac{p_1}{\gamma} + \alpha \frac{v_1^2}{2g} = \frac{p_0}{\gamma} - H_1 - \sum h_{0\text{-}1}.$$

Let us find the increase in the specific energy of the liquid in the pump, i. e., determine the energy obtained by every kilogram of the liquid in passing through the pump. This energy is imparted by the pump, and it is called the pumping head, denoted H_{pump}. To determine H_{pump}, subtract the last equation from Eq. (11.12):

$$H_{pump} = \left(\frac{p_2}{\gamma} + \alpha_2 \frac{v_2^2}{2g}\right) - \left(\frac{p_1}{\gamma} + \alpha_1 \frac{v_1^2}{2g}\right) = H_1 + H_2 + \frac{p_3 - p_0}{\gamma} +$$

$$+ \alpha_3 \frac{v_3^2}{2g} + \Sigma h_{0\text{-}1} + \Sigma h_{2\text{-}3},$$

or

$$H_{pump} = \Delta z + \frac{p_3 - p_0}{\gamma} + CQ^2 + kQ^m, \qquad (11.13)$$

where Δz = total geodetic elevation of liquid (see Fig. 122);

$$CQ^2 = \alpha_3 \frac{v_3^2}{2g};$$

kQ^m = total hydraulic losses in suction and pressure pipings.

If we add to the actual change in elevation Δz the pressure head difference $\frac{p_3 - p_0}{\gamma}$ we consider an equivalent added lift

$$\Delta z' = \Delta z + \frac{p_3 - p_0}{\gamma},$$

and Eq. (11.13) can be rewritten

$$H_{pump} = \Delta z + CQ^2 + kQ^m.$$

Compare the expression (11.13) with the required head formula in (11.6). It is evident that

$$H_{pump} = H_{req}. \tag{11.14}$$

This equality can be extended to all cases of steady operation of a pump in a pipeline and formulated as a rule: In the case of steady flow in a pipeline the head developed by the pump is equal to the required head. This is the only condition of steady pump performance. Usually it is maintained automatically.

Equation (11.14) is the basis for a method of calculating pipelines with pumps which consists in plotting two curves to the same scale on one diagram—the characteristic curve of the pipeline $H_{req} = f_1(Q)$ and the characteristic curve of the pump $H_{pump} = f_2(Q)$—and finding their point of intersection (Fig. 123).

Pump characteristics will be discussed in greater detail later on in a special chapter. Still, running ahead somewhat, the following definition must be given: the characteristic of a pump is defined as the dependence of the pumping head on the delivery (rate of discharge) at a constant speed of rotation.

The intersection of the pipeline characteristic and the pump characteristic locates the point of equality between the required head and the pumping head, i. e., Eq. (11.14). This is known as the operating point. The pumping regime is always maintained, as far as possible, so as to correspond to that point.

To obtain another operating point the opening of the control valve (i. e., the pipeline characteristic), or the pump's rpm must be changed. This will be discussed in detail later on.

It should be remembered, however, that this analytical method of determining the operating point is applicable only when the rotation speed of the pump drive does not depend on the power input, i. e., the load on the pump shaft. This is possible when a pump is driven by an alternating-current electric motor or an aircraft engine whose power is many times greater than the power of the pump.

If a pump is driven by a special internal-combustion engine or turbine, the power of which depends

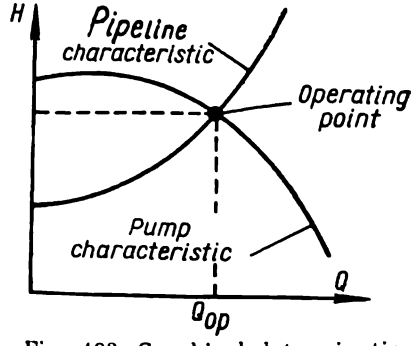

Fig. 123. Graphical determination of operating point

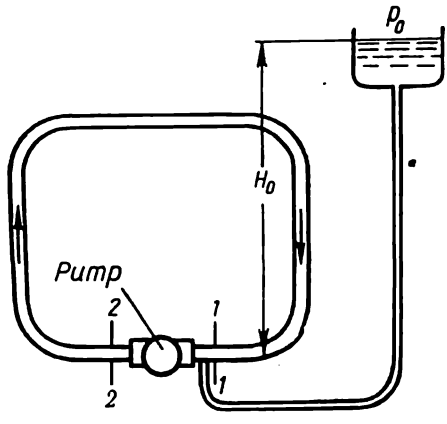

Fig. 124. Looping pipeline

on the pump shaft load, the calculation must necessarily be different. The curves of required and available power must be plotted against the number of revolutions per minute and their point of intersection will then give the operating speed and power.

For a looping pipeline (Fig. 124) the geodetic elevation of the liquid is zero ($\Delta z = 0$), and, consequently, at $v_1 = v_2$,

$$H_{req} = \Sigma h = \frac{p_2 - p_1}{\gamma} = H_{pump},$$

i. e., the same equation is valid for the required head and the pumping head.

A looping pipeline must always be provided with a so-called expansion or compensation tank, usually tapped at the pump intake where pressure is lowest. Without such a tank the absolute pressure inside the pipeline would be unsteady and would also vary with temperature and due to leakage.

With an expansion tank tapped to the pipeline as shown in Fig. 124 the pressure at the pump intake becomes steady and equal to

$$p_1 = p_0 + H_0\gamma.$$

When p_1 is known, the pressure at any cross-section of the loop can be calculated. If the pressure p_0 in the tank changes, the pressure at any point in the system will change by the same value, i. e., Pascal's law of the transmission of pressure in a still liquid (see Sec. 6) is valid. The tank can also be tapped to the loop as shown in Fig. 149.

Example 1. Determine the required head at the outlet of a booster pump in an aircraft fuel system to supply T-1 fuel at a rate of $G = 1{,}200$ kg/hr from the service tank to the engine fuel pump if the length of the duralumin piping is $l = 5$ m, diameter $d = 15$ mm, required pressure at fuel-pump intake $p_2 = 1.3$ kg/cm², kinematic viscosity of kerosene $\nu = 0.045$ cm²/sec, specific weight $\gamma_k = 820$ kg/m³. Local disturbances in piping are shown in Fig. 125. Neglect elevation of liquid in tank.

Solution. (i) Velocity of flow in pipeline:

$$v = \frac{4G}{3{,}600\pi d^2\gamma_k} = \frac{4\times 1{,}200\times 10^3}{3{,}600\times 3.14\times 1.5^2\times 0.82} = 240 \text{ cm/sec}$$

(ii) Reynolds number:

$$\mathrm{Re} = \frac{vd}{\nu} = \frac{240\times 1.5}{0.045} = 8{,}000.$$

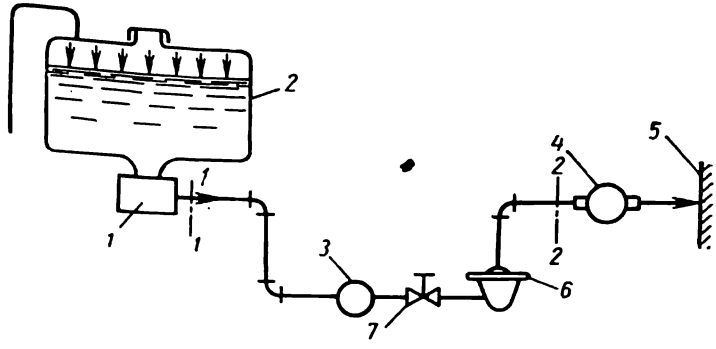

Fig. 125:
1— booster pump; *2* — service tank; *3* — flow meter sensor; *4* — fuel pump; *5* — engine; *6* — filter; *7* — stop cock

(iii) From Konakov's formula, the friction factor $\lambda_t = 0.0328$.

(iv) From Table 2 in Chapter IX, the loss coefficients of the filter, stop cock, flow meter sensor and elbows are

$$\zeta_{filter}=2;\quad \zeta_{cock}=1.5;\quad \zeta_{sensor}=7;\quad \zeta_{elbow}=1.2.$$

(v) Pressure drop in pipeline from booster pump to fuel pump:

$$\Sigma p_f=\gamma_k\left(\lambda_t\frac{l}{d}+3\zeta_{elbow}+\zeta_{sensor}+\zeta_{cock}+\zeta_{filter}\right)\frac{v^2}{2g}=$$

$$=820\left(0.0328\frac{500}{1.5}+3\times1.2+7+1.5+2\right)\frac{2.4^2}{2\times9.81}=6{,}000\ \text{kg/m}^2=0.6\ \text{kg/cm}^2.$$

(vi) Hence the required pressure at the booster pump outlet is

$$p_1=p_2+\Sigma p_f=1.3+0.6=1.9\ \text{kg/cm}^2.$$

Example 2. Referring to Fig. 126, fuel T-1 is delivered from two under-wing tanks to the service tank by higher pressure in the former: $\Delta p = p_{uw} - p_{st} = 0.2$ kg/cm².

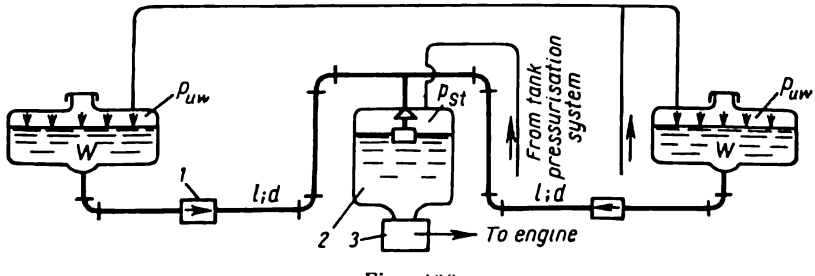

Fig. 126:
1 — nonreturn valve; *2* — service tank; *3* — booster pump

Determine the diameter d of the piping if the two under-wing tanks are to be emptied simultaneously and the total rate of discharge of the fuel is $G = 1{,}500$ kg/hr. The volume of each under-wing tank $W = 450$ lit. The piping

is of duralumin, $l = 7$ m. Kinematic viscosity of kerosene $\nu = 0.045$ cm²/sec, specific weight $\gamma_k = 830$ kg/m³. Neglect height of liquid columns in under-wing tanks.

Solution. (i) Time of engine operation until under-wing tanks are emptied:

$$T = \frac{2W\gamma_k}{G} = \frac{2 \times 450 \times 0.83}{1{,}500} = 0.5 \text{ hr.}$$

(ii) Rate of discharge from each tank.

$$Q = \frac{W}{T} = \frac{450}{0.5} = 900 \text{ lit/hr} = 0.25 \text{ lit/sec.}$$

(iii) Assign several pipe diameters: $d = 12$; 14; 16; and 18 mm.

(iv) Table 2 gives loss coefficients at pipe entrance $\zeta_{entrance}$, nonreturn valve ζ_{valve}, elbow ζ_{elbow}, tee ζ_{tee}, and pipe outlet ζ_{outlet}. After determining Re compute the friction factor λ_t according to Konakov for each value of d.

(v) Determine the required head H_{req} for each value of d from the formula

$$H_{req} = \left(\zeta_{entrance} + \zeta_{valve} + \zeta_{elbow} + \zeta_{tee} + \zeta_{outlet} + \lambda_t \frac{l}{d}\right) \frac{16Q^2}{2g\pi^2 d^4}$$

and plot curve $H_{req} = f(d)$ (Fig. 127).

(vi) Dividing Δp by γ_k, determine available head and from diagram find required diameter, which is $d = 15.7$ mm.

Hence, the commercial pipe diameter to ensure the required flow rate for simultaneous delivery of fuel from under-wing tanks is $d = 16$ mm.

If the pipelines were of different length, their diameters would also have to be different for the given set of conditions and the curves $H_{req} = f(d)$ would have to be constructed for each pipeline.

Example 3. When an airplane is refuelled under pressure all the tanks must be filled simultaneously. A block diagram of the refuelling system is shown in Fig. 128.

Let all the tanks lie in a horizontal plane at an elevation h_t over the refueller pump. The elevation of the fuel main AB above the pump is h_A. The characteristic of the refuelling pump, the length l_{sl} and diameter d_{sl} of the filling sleeve, the length of all pipelines and the volumes of the tanks are given.

Neglecting the height of the liquid columns in the tanks and the gauge pressure in them, solve the following commonly occurring engineering problems:

(I) Determine the refuelling time T if the diameters of the piping are given.

(II) Determine the required pipe diameters d_m, d_1, d_2, d_3 to ensure the simultaneous filling of all the tanks in time T.

(I) The solution is graphoanalytical.

(i) Plot characteristic curve of filling sleeve from pump to the filling connection A.

(ii) Plot characteristic curve for fuel main from A to B.

(iii) Sum both curves according to the rule of compound pipes in series (Fig. 129).

(iv) Plot characteristics for piping from the cross at B to respective tanks.

(v) Sum characteristics in (iv) according to the rule for compound pipes in parallel.

(vi) Summation of the net characteristic of the four parallel pipes and the pipe characteristic from the pump to B gives the characteristic curve of the whole composite pipe system.

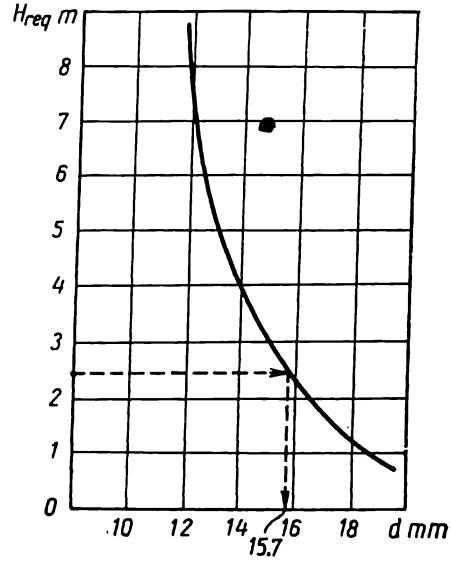

Fig. 127

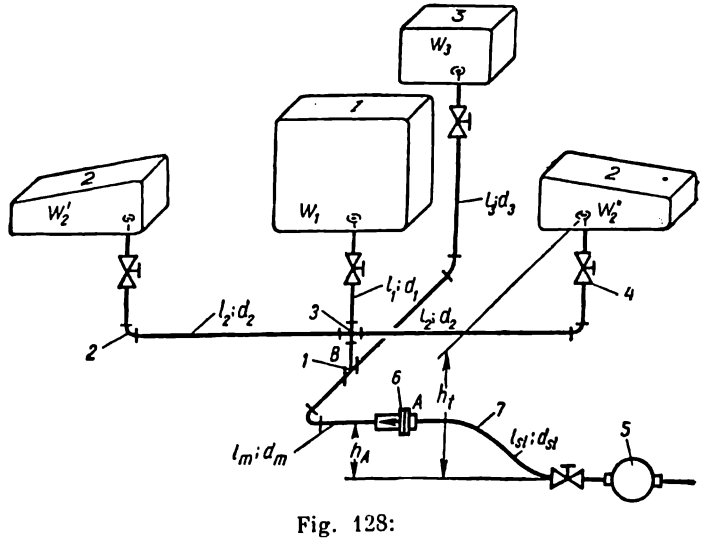

Fig. 128:
1 — tee; *2* — elbow; *3* — cross-pipe; *4* — stop cock; *5* — refueller pump; *6* — nonreturn valve; *7* — filling sleeve

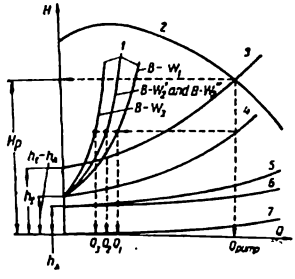

Fig. 129:

1 — characteristic curves of pipes to tanks; *2* — characteristic curves of pump; *3* — characteristic curve of whole pipe; *4* — summarised characteristic of pipes to tanks; *5* — H_A-B+H_{sleeve}; *6* — $H_{sleeve}=f(Q)$; *7* — $H_{A-B}=f(Q)$.

(vii) The intersection of the pipeline characteristic with the refuelling pump characteristic gives the pumping head H_{pump} and the rate of discharge of the pump Q_{pump}.

(viii) The rate of discharge into each tank is determined as shown in Fig. 129.

(ix) The refuelling time T (when all tanks are filled simultaneously) is

$$T=\frac{\Sigma W}{Q_{pump}}=\frac{W_1}{Q_1}=\frac{W_2'+W_2''}{Q_2}=\frac{W_3}{Q_3}.$$

(II) The solution is graphoanalytical.

(i) Determine the rate of discharge Q_{pump} of the refuelling pump necessary to fill all tanks in time T by dividing the total tank volume by T.

(ii) Locate the operating point on the pump characteristic according to Q_{pump}, i. e., the pumping head H_{pump}. The pipe diameters must be so selected as to ensure a rate of discharge equal to Q_{pump} when the head is H_{pump}.

(iii) Determine the rate of discharge through each pipe by dividing the volume of each tank by the time T.

(iv) Determine the loss of head H_{sl} in the filling sleeve, taking into account the minor losses in the nonreturn valve of the filling connection.

(v) Plot the loss of head as a function of the diameter of the fuel main between A and B: $H_{A-B}=f(d)$. For this assign several diameter values and for each d determine: the Reynolds number Re, the friction factor λ_t, and the loss of head H_{A-B}, including the difference between the elevation heads of the fuel main and the refueller pump h_A and losses in the sleeve H_{sl}.

(vi) Plot the head losses as a function of diameter for each pipe to the respective tanks.

The construction is the same as that of the curve $H_{A-B}=f(d)$, but the origin of the coordinate axes is taken at point H_{pump}, the positive direction of the diameter axis being to the left and of the head axis, downwards (Fig. 130). Add to the head losses the head $h_{tank}-h_A$.

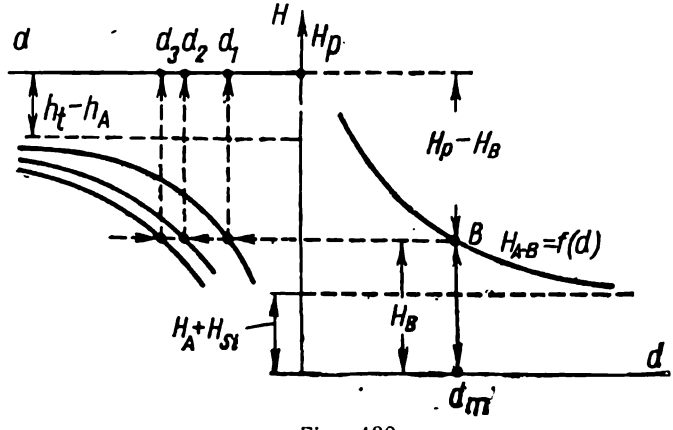

Fig. 130

This rather unusual directing of the coordinate axes and the curves $H_i = \varphi(d_i)$ for the respective pipings simplifies the determination of the required diameters.

Assign a diameter d_m of the fuel main and, from the diagram, determine the diameters d_1, d_2, d_3 as shown by arrows in Fig. 130. The diagram can be used to determine several diameters from which the most economical can be chosen.

Point B on curve $H_{A\text{-}B} = f(d)$ shows the loss of head H_B between the pump and the cross. The remaining head $H_{pump} - H_B$ is used to overcome the resistances to the flow through the pipes to the tanks and the elevation $h_{tank} - h_A$.

This method of problem solution can be employed when the pipes to the respective tanks branch at different points; in this case three curves have to be plotted instead of a single curve $H_{A\text{-}B} = f(d)$.

CHAPTER XII

CENTRIFUGAL PUMPS

48. GENERAL CONCEPTS

A pump is a machine which imparts head to a fluid.

From the physical aspect, the work of a pump consists in transforming the mechanical energy of a motor (drive) into fluid energy, i. e., in imparting power to a flow of fluid passing through it. The energy imparted to the fluid in the pump enables the former to overcome hydraulic resistances and rise to a geodetic elevation.

The energy imparted to each kilogram of fluid in a pump, i. e., the specific energy increase, is linear in dimension and, as mentioned before, represents the pumping head. It was stated in Sec. 47 that the pumping head

$$H_{pump} = \left(\frac{p_2}{\gamma} + \alpha_2 \frac{v_2^2}{2g}\right) - \left(\frac{p_1}{\gamma} + \alpha_1 \frac{v_1^2}{2g}\right),$$

or

$$H_{pump} = \frac{p_2 - p_1}{\gamma} + \frac{\alpha_2 v_2^2 - \alpha_1 v_1^2}{2g}.$$

Thus, in the general case the pumping head is the sum of the increase in pressure head (static head) and the increase in specific kinetic energy (dynamic head).

The second term, however, is usually much smaller than the first and if the intake and outlet pipes have the same diameter ($d_1 = d_2$, whence $v_1 = v_2$) and $\alpha_1 = \alpha_2$, it is zero and

$$H_{pump} = \frac{p_2 - p_1}{\gamma} = \frac{p_{pump}}{\gamma}. \tag{12.1}$$

The rate of discharge of a pump is also called its delivery or capacity, denoted Q.

The *power* of a pump is defined as the energy imparted by the pump to the fluid flow per second:

$$N = \frac{Q\gamma H_{pump}}{75} \text{ h.p.} \tag{12.2}$$

Like any other driven machine, a pump consumes more power than it gives off. The ratio of the actual power developed by the pump (the "water horsepower") to the power supplied by the pump (the "shaft horsepower") gives the *efficiency* of the pump:

$$\eta = \frac{N}{N_0}. \tag{12.3}$$

Hence, the shaft horsepower

$$N_0 = \frac{Q\gamma H_{pump}}{75\eta}, \tag{12.4}$$

and, taking into account Eq. (12.1),

$$N = \frac{Qp_{pump}}{75\eta}. \tag{12.4'}$$

This is the formula used in choosing pump drives.

Total, or overall, pump efficiency takes into account three types of energy losses: hydraulic losses due to fluid friction and turbulence, volume losses due to leakage through internal passages, and mechanical losses due to mechanical friction in bearings, packings, etc.

Pumps used in aeronautical engineering seem to vary enormously in design and principle of action. Nevertheless, they can all be divided into two main types:

1. Rotodynamic pumps, to which belong radial-flow centrifugal, mixed-flow and axial-flow or propeller pumps;
2. Displacement pumps, which include reciprocating and rotary pumps.

This chapter is devoted to centrifugal pumps, which are finding growing application in aeronautical and rocket engineering.

49. THE BASIC EQUATION FOR CENTRIFUGAL PUMPS

A centrifugal pump operates in the following manner. The principal working unit is a vaned rotor, called an impeller (Fig. 131), which is made to revolve at high speed. It accelerates the incoming fluid, increasing both the pressure and absolute velocity of the latter, driving it to the outlet of a spiral casing (the volute). By virtue of

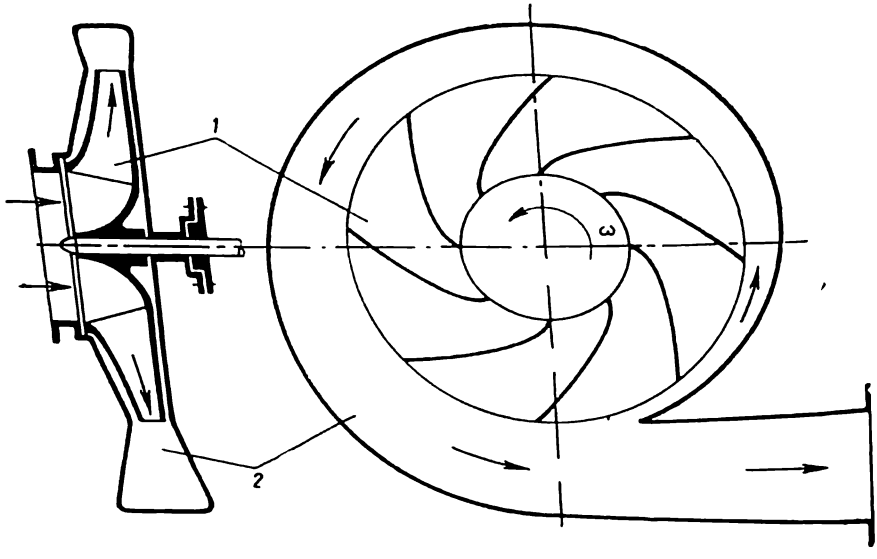

Fig. 131. Centrifugal pump:
1 — impeller; *2* — volute casing

force interaction between the vanes and the fluid, the mechanical energy of the drive is transformed into the energy of flow.

The volute casing guides the fluid to the pump outlet; in the volute the kinetic energy of the fluid is partly converted into pressure energy.

The impeller of a centrifugal pump (Fig. 132) consists of two disk-like walls, sometimes called "shrouds", one of which is mounted on the shaft. The other shroud, coupled to the former by the vanes, has a hole in the centre, called the "eye". The vanes are curved, cylindrical or have more complex surfaces. The fluid enters the impeller along the axis of rotation through the eye, flows radially outward between the vanes, and is discharged around the entire circumference into the casing.

The motion of the fluid through the passages between the vanes can be regarded as consisting of two motions: motion of transport (rotation of the impeller) and motion relative to the impeller. Hence, the absolute velocity vector v of the fluid can be found as the vector sum of the peripheral velocity u and the relative velocity w. Taking a fluid particle sliding along a vane, one can construct a velocity parallelogram for the entrance of the particle to, and discharge from, the vane, assuming the relative velocity w to be tangent to the vane and the peripheral velocity u tangent to the corresponding

circle. A similar velocity parallelogram can be constructed for any point on the vane. The subscript 1 refers to the entrance section, and subscript 2 to the exit section of the vane.

The angle between the vectors of the peripheral and absolute velocities is α, and the angle between the tangent to the vane and the tangent to the circumference of the impeller drawn in the opposite direction of the rotation is β, with the corresponding subscripts. In the general case the angle α changes with the pump performance, i.e., with the speed of rotation n of the impeller (the velocity u) and the discharge Q (the velocity w). Angle β determines the inclination of a vane at every point and, consequently, does not depend on pump performance.

In order to develop the basic equation of centrifugal pump theory, we shall accept the following two assumptions:

1. The impeller consists of an infinite number of uniform vanes of zero thickness ($z = \infty$, $\delta = 0$). This means that we assume such flow in the passages between the vanes in which the geometry of all the stream tubes in the relative motion is identical and corresponds exactly to the vane geometry, and that the velocities depend only on the radius and are the same on a circle of given radius. This is possible in the case when each differential stream tube is guided by its vane. Such flow is shown schematically for one vane passage in Fig. 132.

2. The pump efficiency is unity ($\eta = 1$), i. e., there are no energy losses in the pump and shaft horsepower is converted completely into water horsepower. This is possible in the case of an ideal fluid, no leakage in the pump and no mechanical friction in packings and bearings.

Thus, to facilitate our theoretical investigation of a centrifugal pump we have substantially idealised its performance. We shall

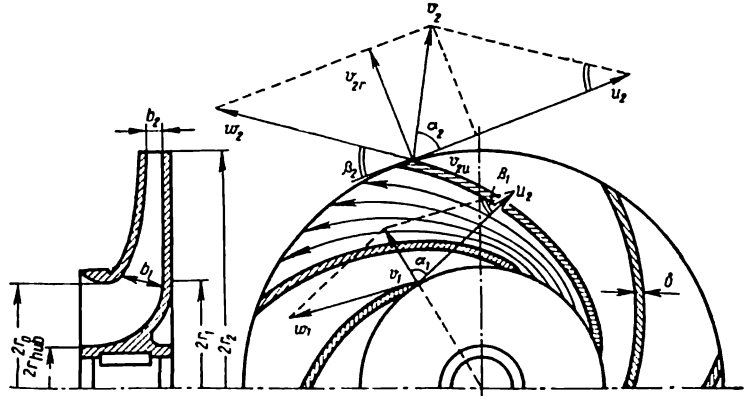

Fig. 132. Flow pattern through centrifugal pump impeller

call such a centrifugal pump, in which $z = \infty$ and $\eta = 1$, an ideal pump. After considering the theory of the idealised pump we shall, naturally, proceed to deal with real pumps.

Let us develop two equations: the power equation and the equation of moments. The former means that the power supplied to the impeller shaft is equal to the energy imparted every second to the fluid in the pump, viz.,

$$T\omega = Q\gamma H_{t\infty}, \tag{12.5}$$

where T = torque on impeller shaft;
ω = angular velocity of impeller;
$H_{t\infty}$ = head developed by theoretical idealised pump or increase of specific energy of fluid in pump (the subscripts "t" and "∞" corresponding to the two assumptions made before).

The meaning of the second equation is as follows: The torque acting on the pump shaft is equal to the increase in the angular momentum of the fluid in the impeller per second. Denoting by r_1 the radius of the cylindrical surface on which the entrance edges of the vanes are located, and by r_2 the peripheral radius of the impeller, we have

$$T = \frac{Q\gamma}{g}(v_2 r_2 \cos\alpha_2 - v_1 r_1 \cos\alpha_1). \tag{12.6}$$

From Eqs (12.5) and (12.6) the head delivered by an idealised pump is

$$H_{t\infty} = \frac{\omega}{g}(v_2 r_2 \cos\alpha_2 - v_1 r_1 \cos\alpha_1). \tag{12.7}$$

This is the basic equation not only for centrifugal pumps but for all rotodynamic machines, such as fans, compressors and turbines. In the case of turbines the angular momentum of the fluid flowing through the rotor decreases, i. e., energy is dissipated, and the signs of the terms in the parentheses should be reversed. Equation (12.7) was developed by Euler and bears his name.

Attention should be paid to the fact that the head delivered by an idealised centrifugal pump in terms of column of pumped liquid does not depend on the type of liquid (i. e., on its specific weight).

As a rule, a liquid entering the impeller has no whirl component.* In the vane passages it moves in radial direction. This means that the vector v_1 is pointed along the radius and the angle $\alpha_1 = 90°$.

* In some machines prerotation is produced by a special vane or worm wheel mounted before the impeller (see further on).

Consequently, the second term in Eq. (12.7) vanishes and the equation takes the form

$$H_{t\infty} = \frac{\omega}{g} v_2 r_2 \cos \alpha_2 \frac{u_2 v_{2u}}{g}, \tag{12.8}$$

where $u_2 = \omega r_2$ = peripheral velocity at vane exit;
v_{2u} = projection of absolute exit velocity on direction of peripheral velocity, i. e., the tangential component of velocity v_2.

Equation (12.8) shows that for a centrifugal pump to deliver a high head the peripheral velocity must be great and, secondly, the vector v_{2u} must be large enough, i. e., sufficient whirl should be imparted to the fluid. The former is achieved by increasing the speed of rotation and impeller diameter, the latter is attained by providing a sufficient number of vanes of suitable size and shape.

50. CHARACTERISTICS OF IDEAL PUMP. DEGREE OF REACTION

Equation (12.8) is inconvenient for calculations as it does not contain the rate of discharge Q. Therefore let us rewrite it to express the head $H_{t\infty}$ as a function of the discharge Q and impeller radius.

From the velocity triangle for the impeller exit (Fig. 133),

$$v_{2u} = u_2 - v_{2r} \cot \beta_2, \tag{12.9}$$

where v_{2r} = projection of absolute exit velocity on radius, i. e., the radial component of vector v_2.

The rate of discharge through the impeller can be expressed in terms of the radial component v_{2r} and impeller radius as follows:

$$Q = 2\pi r_2 b_2 v_{2r}, \tag{12.10}$$

where b_2 = width of vane slot at exit (see Fig. 132).

Hence

$$v_{2r} = \frac{Q}{2\pi r_2 b_2}.$$

Substitution of this expression into Eq. (12.9) yields

$$v_{2u} = u_2 - \frac{Q}{2\pi r_2 b_2} \cot \beta_2. \tag{12.11}$$

Substituting the obtained expression (12.11) for the tangential velocity component

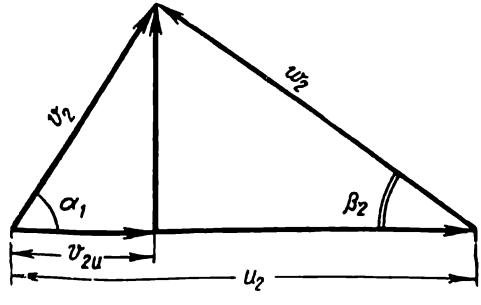

Fig. 133. Velocity triangle at impeller exit

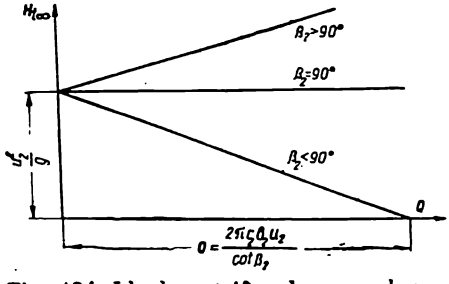

Fig. 134. Ideal centrifugal pump characteristics

v_{2u} in Eq. (12.8), we obtain another form of the basic ideal pump equation:

$$H_{t\infty}=\frac{u_2}{g}\left(u_2-\frac{Q\cot\beta_2}{2\pi r_2 b_2}\right). \quad (12.12)$$

This equation can be used to plot the theoretical characteristics of an idealised centrifugal pump, i. e., a curve of the head generated by the pump as a function of the discharge for a constant speed of rotation. It is evident from Eq. (12.12) that the characteristic curve of such a pump is a straight line the inclination of which depends on the value of the vane angle β_2. The following three cases are possible.

1. Angle $\beta_2 < 90°$. In this case cot β_2 is positive and the head $H_{t\infty}$ decreases with the discharge increasing.

2. Angle $\beta_2 = 90°$, cot $\beta_2 = 0$, and $H_{t\infty}$ does not depend on the discharge and is equal to $\frac{u_2^2}{g}$.

3. Angle $\beta_2 > 90°$, cot β_2 is negative and the head $H_{t\infty}$ increases with the discharge.

These three theoretical pump characteristics are shown in Fig. 134. The corresponding vane shapes and velocity parallelograms for the same values of u_2 and v_{2r} are presented in Fig. 135*a*, *b*, *c*.

It thus follows that the optimum head is produced by a forward-curved vane, when $\beta_2 > 90°$ and the head is highest. In practice, however, the efficiency of such a pump is low, and the performance of backward-curved vanes at $\beta_2 < 90°$ is found to be preferable. Backward-curved vanes are in fact more commonly used, the vane angle usually being about 30°. Radial vanes ($\beta_2 = 90°$) are also employed, but the result is lower efficiency and the considerations to be guided by are usually those of size, strength, etc.

In order to understand why pump efficiency falls with the angle β_2 increasing we must examine the components of the head $H_{t\infty}$ and the way in which the relation between them changes with β_2.

The head $H_{t\infty}$, or what is the same thing, the total increase in the specific energy of a fluid in an impeller, comprises the increase in the specific energy of pressure and the specific kinetic energy, i. e.,

$$H_{t\infty}=\frac{p_2-p_1}{\gamma}+\frac{v_2^2-v_1^2}{2g} \quad (12.13)$$

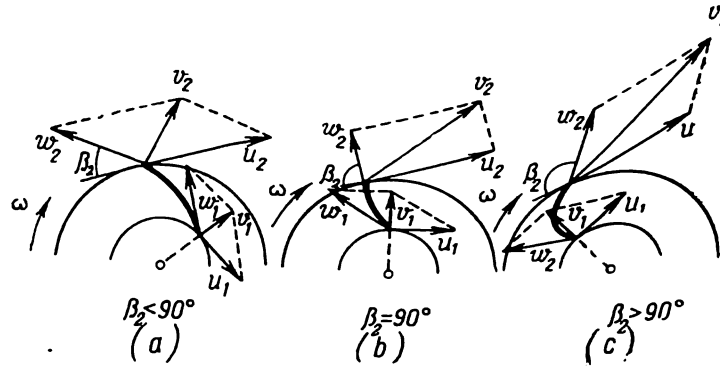

Fig. 135. Vane designs and velocity parallelograms

or, introducing another notation,

$$H_{t\infty} = H_p + H_v. \tag{12.13'}$$

Expressing the velocities v_1 and v_2 in terms of their radial and tangential components, we have

$$v_2^2 - v_1^2 = v_{2u}^2 + v_{2r}^2 - v_{1u}^2 - v_{1r}^2.$$

Assuming the intake and exit areas of the impeller to be approximately equal, we can consider that $v_{1r} = v_{2r}$. Furthermore, as pointed out before, there is usually no prerotation of the fluid at the impeller intake, and $v_{1u} = 0$. Consequently, instead of the foregoing we have

$$v_2^2 - v_1^2 \approx v_{2u}^2.$$

Taking this expression into account, we can now find from Eq. (12.13) the so-called degree of reaction of the pump, which is the ratio of the head imparted to the fluid by the pressure increase to the total head:

$$\frac{H_p}{H_{t\infty}} = 1 - \frac{v_{2u}^2}{2gH_{t\infty}}.$$

Using Eq. (12.8), the latter expression can be rewritten as follows

$$\frac{H_p}{H_{t\infty}} = 1 - \frac{v_{2u}}{2u_2}, \tag{12.14}$$

whence finally, after substituting for v_{2u} from Eq. (12.9),

$$\frac{H_p}{H_{t\infty}} = \frac{1}{2}\left(1 + \frac{v_{2r}}{u_2 \tan \beta_2}\right). \tag{12.15}$$

It will be observed from this expression that the greater v_{2r}/u_2 and the smaller angle β_2, the greater the portion of the head $H_{t\infty}$ that is produced by the pressure increase, i. e., the higher the degree of reaction of the pump. With angle β_2 increasing the portion of the head $H_{t\infty}$ representing the increase in the kinetic energy becomes greater. The kinetic energy, in turn, is associated with higher exit velocity of the fluid from the impeller, which results in considerable energy losses and lower pump efficiency. That is why it is not expedient to use vanes with large values of β_2, i. e., forward-bent vanes.

It follows from Eq. (12.15) that for radial vanes ($\beta_2 = 90°$) the degree of reaction is 1/2, and at $\beta_2 < 90°$ it is more than 1/2 but less than unity.

The way in which the velocity parallelograms change and the increase in the absolute exit velocity v_2 with angle β_2 increasing are illustrated in Fig. 135.

51. IMPELLER WITH FINITE NUMBER OF VANES

So far we have been investigating the performance of an idealised centrifugal pump with an infinite number of vanes and unity efficiency. The physical meaning of these assumptions was examined in Sec. 49.

In going over to real pumps we shall begin with eliminating the first assumption, retaining the second for the time being.

Thus, a pump with a finite number of vanes. Real pumps usually have from six to twelve vanes. The relative flow through the vane passages is not so laminar as assumed before and the velocity distribution is not uniform. On the leading surface of the vane, denoted by a "plus" sign in Fig. 136*a*, the pressure is higher and the velocity lower, and the velocity distribution in the passage is approximately as shown.

The velocity distribution can be regarded as the resultant of two flows: one with uniform velocity distribution, as was the case when

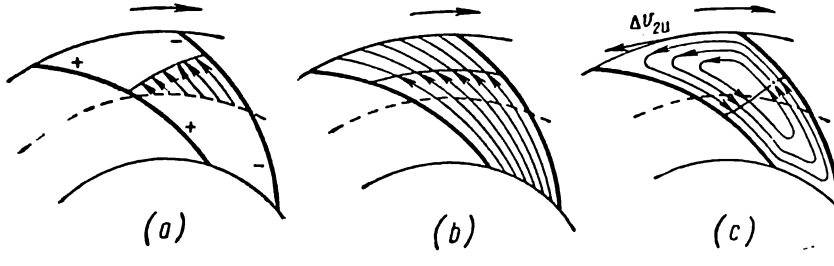

Fig. 136. Flow pattern through vane passage

$z = \infty$ (Fig. 136*b*), and a rotational flow inside the passage in the opposite direction of the rotation of the impeller (Fig. 136*c*). In pure form the rotational flow is present when the discharge through the impeller is zero ($Q = 0$).

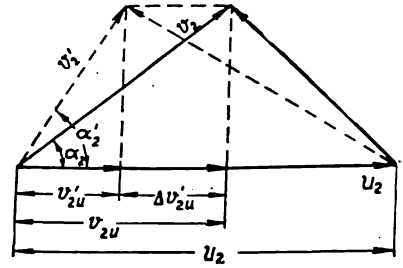

Fig. 137. Change of velocity triangle in going over to finite number of vanes

In view of the nonuniformity of the distribution of the relative and absolute velocities in the vane passages when the number of vanes is finite, the mean velocity for a circle of given radius is introduced. Our interest is the mean value of the tangential component of the absolute exit velocity v_{2u}', which determines the head developed by the pump. This component is smaller for a finite number of vanes than for an infinite number because the less the number of vanes the less the whirl imparted to the fluid by the impeller. In the absence of vanes ($z = 0$) the whirl is zero, i. e., $v_{2u}' = 0$, and the fluid (in the ideal case) issues from the impeller in a radial direction.

A reduction of the velocity v_{2u} in passing over to a finite number of vanes is also accounted for by the prerotation mentioned before. This relative motion gives rise to an additional absolute velocity Δv_{2u} at the outer periphery of the impeller (see Fig. 136*c*), which is directed opposite to v_{2u} and, hence, is subtracted from the latter.

Owing to this the velocity triangle at the impeller exit changes. In Fig. 137, the solid lines give the velocity vectors when the number of vanes is infinite and the broken lines are the velocity vectors for a finite number. The construction was made for identical values of u_2 and v_{2r}, i. e., for identical rotational speeds and rates of discharge. The primed values are for the case of a finite number of vanes.

A reduction of the tangential component v_{2u} in transition to a finite number of vanes results in a drop in the pumping head. The head that would have been generated by a pump if there were no head losses inside the pump is called the theoretical, or ideal, head, denoted H_{tz}. From Eq. (12.8), we have

$$H_{tz} = \frac{u_2 v_{2u}'}{g}. \tag{12.16}$$

We shall call the ratio of H_{tz} to $H_{t\infty}$ the vane-number coefficient:

$$\mu = \frac{H_{tz}}{H_{t\infty}} = \frac{v_{2u}'}{v_{2u}}, \tag{12.17}$$

whence the head in question is

$$H_{tz} = \mu H_{t\infty} = \mu \frac{u_2 v_{2u}}{g}. \tag{12.18}$$

The problem now is to determine the numerical value of μ. Obviously, the coefficient depends first and foremost on the number of vanes z, though it is also affected by the length of the vanes, which depends on the ratio $\frac{r_1}{r_2}$ and on the angle of inclination of the vanes β_2.

Theoretical investigations reveal that μ does not depend on the operating conditions of a pump, i. e., on Q, H_{pump} or n. It is wholly determined by impeller geometry and is constant for a given impeller.

Without going into the theory of the effect of the number of vanes on the head, here is the conclusion of this theory as represented by a formula for μ:

$$\mu = \frac{1}{1 + \dfrac{2\psi}{z\left[1 - \left(\dfrac{r_1}{r_2}\right)^2\right]}}, \tag{12.19}$$

where

$$\psi = (0.55 \text{ to } 0.65) + 0.6 \sin \beta_2.$$

Here, for example, is the value of μ for $\beta_2 = 30°$ and $\frac{r_1}{r_2} = 0.5$ (Table 6).

Table 6

z	4	6	8	10	12	16	24
μ	0.624	0.714	0.768	0.806	0.834	0.870	0.908

Thus, at $z \to \infty$, $\mu \to 1$.

As the ratio between H_{tz} and $H_{t\infty}$ is constant for a given pump, the theoretical characteristic curve for a finite number of vanes, like the characteristic curve of an idealised pump with a uniform speed of rotation (n = const), is a straight line. At $\beta_2 = 90°$, it is parallel to the characteristic curve of an idealised pump, and at $\beta_2 < 90°$ it intersects the latter on the axis of abscissas, as $H_{tz} = 0$ and $H_{t\infty} = 0$ at the same discharge

$$Q = \frac{2\pi r_2 b_2 u_2}{\cot \beta_2}.$$

This follows from Eqs (12.12) and (12.18).

52. HYDRAULIC LOSSES IN PUMP. PLOTTING RATED CHARACTERISTIC CURVE

As stated earlier, H_{tz} is the head that would have been developed by a pump if there were no head losses inside it. The actual head H_{pump} (see Sec. 48) is less than the theoretical head by the total losses inside the pump:

$$H_{pump} = H_{tz} - \Sigma h_{pump}, \tag{12.20}$$

where Σh_{pump} = total head loss in pump (at intake, in impeller and volute).

The ratio of the actual head to the theoretical head for a finite number of vanes is called the hydraulic efficiency, denoted η_h. Thus,

$$\eta_h = \frac{H_{pump}}{H_{tz}} = \frac{H_{tz} - \Sigma h_{pump}}{H_{tz}}. \tag{12.21}$$

Hydraulic efficiency is always higher than total efficiency as it takes into account only head losses inside the pump.

It follows from Eqs (12.18) and (12.21) that

$$H_{pump} = \eta_h H_{tz} = \eta_h \mu H_{t\infty}, \tag{12.21'}$$

where $H_{t\infty}$ is given by Eqs (12.7) and (12.12).

The hydraulic losses inside the pump Σh_{pump} are conveniently treated as the sum of the following two components.

1. *Ordinary hydraulic losses*, i. e., losses due to friction and partly to eddy formation inside the pump. As turbulent flow is the common regime in a centrifugal pump, this type of head losses increases approximately as the square of the discharge and can be expressed by the equation

$$h_1 = k_1 Q^2, \tag{12.22}$$

where k_1 is a constant depending on the hydraulic efficiency and the dimensions of the pump.

2. *Shock losses* at impeller and volute entrances. If the relative velocity w_1 of the fluid at the entrance to a vane passage is tangent to the vane, the fluid is entering the impeller smoothly, without shock or eddy formation. Shock losses in this case are nil. But this is possible only at some definite rated or normal discharge Q_0 and corresponding radial entrance velocity $(v_{1r})_0$ (Fig. 138).

If the actual discharge Q is more or less than the rated discharge Q_0 and the radial entrance velocity v_{1r} is more or less than $(v_{1r})_0$, the relative velocity w makes an angle γ with the tangent to the vane and the fluid flows past the vane at some positive or negative angle of approach. The effect is that of the fluid impinging on the

vane, with eddies forming on the opposite side. Thus, energy is degraded in the impact and eddy formation. The velocity parallelograms for the same peripheral velocities corresponding to these nonrated operating conditions are shown by broken lines in Fig. 138. One of the parallelograms corresponds to the inequality $Q > Q_0$, the other, to — $Q < Q_0$.

Shock losses can be assumed to vary as the square of the difference between the actual discharge and the discharge when they are zero, i. e.,

$$h_2 = k_2 (Q - Q_0)^2. \tag{12.23}$$

Shock losses at the volute entrance are of the same nature as at the impeller intake, the minimum being at about the same rate of discharge Q_0, and are included in the quantity h_2.

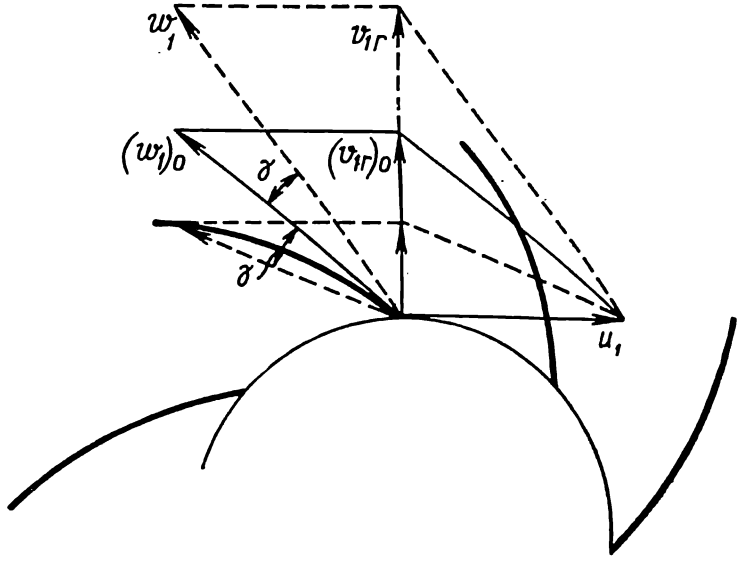

Fig. 138. Velocity parallelograms at impeller entrance

The total loss of head inside the pump is the sum of the two losses considered, i. e.,

$$\Sigma h_{pump} = h_1 + h_2. \tag{12.24}$$

The characteristic curves of a pump at uniform rotational speed (n = const) are plotted as follows.

First draw for H as a function of Q at n = const the theoretical characteristic curves for $z = \infty$ and for a finite number of vanes z. These are inclined straight lines (Fig. 139). Below the Q axis

plot the curves for the change in the two components h_1 and h_2 of the head losses in the pump. Summing the ordinates of the two curves gives the curve Σh_{pump} as a function of the discharge. Now, in accordance with Eq. (12.20), subtract Σh_{pump} from H_{tz}, which gives the curve $H_{pump} = f(Q)$, i. e., the actual characteristic of the pump for a constant rpm.

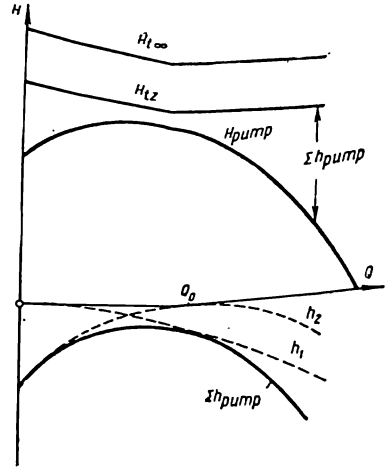

Fig. 139. Plotting rated characteristics

The curve $H_{pump} = f(Q)$ in Fig.139 is typical of a centrifugal pump. The maximum value of the head H_{pump} is commonly obtained neither at zero discharge nor at $Q = Q_0$, but at some intermediate value of Q.

Plotting the characteristic curves by the method described is not very accurate in view of the difficulty of determining the coefficients k_1 and k_2 in Eqs (12.22) and (12.23). Therefore the characteristics are commonly plotted by direct experiment, i. e., in testing a pump.

For this a throttling device (some type of valve) is installed at the outlet pipe of a pump operating at a constant rotational speed. The degree of opening of the valve is gradually changed during a test. For example, at first the valve is wide open. Then the pump is gradually throttled down and the discharge and head are measured. When the valve is completely open, the discharge is maximum and the head is minimum, being equal to the loss of head in the pipeline (point C in Fig. 140). As the valve is throttled, the discharge falls and the head rises to a maximum (point B). As the discharge is further reduced the head also drops somewhat, till at $Q = 0$ (point A), when the valve is closed completely, the head reaches a value higher than the average but below the maximum.

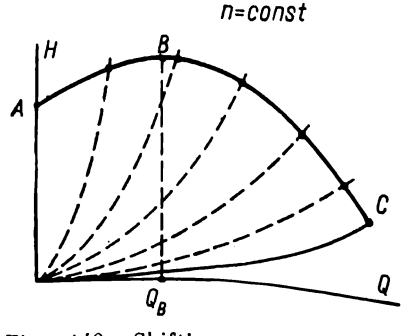

Fig. 140. Shifting of operating point in throttling

This is the so-called shutoff head. It will be observed that even complete closure of the valve does not present any danger to the

pump or pipeline as no further increase in head develops if the number of rpm does not change. For this reason centrifugal pumps, unlike displacement pumps, do not have to be fitted with relief valves.

53. PUMP EFFICIENCY

The energy losses in a pump taken into account in rating the overall efficiency η are:

1. **Hydraulic losses,** examined in the previous section and determined by the hydraulic efficiency [Eq. (12.21)]:

$$\eta_h = \frac{H_{tz} - \Sigma h_{pump}}{H_{tz}} = \frac{H_{pump}}{H_{tz}}.$$

2. **Volumetric losses,** due to leakage through clearance spaces between the impeller and the casing. The impeller drives fluid from the suction pipe to the discharge pipe, but because of the pressure drop it produces some of the fluid leaks back (Fig. 141).

In Sec. 48 we denoted as Q the actual discharge of a pump at the outlet. It follows, then, that the discharge through the impeller is equal to

$$Q' = Q + q, \tag{12.25}$$

where q = internal leakage.

Volumetric energy losses are evaluated by the so-called *volumetric effciency*

$$\eta_v = \frac{Q}{Q+q} = \frac{Q}{Q'}. \tag{12.26}$$

The values of volumetric losses and efficiency will be discussed in Sec. 56.

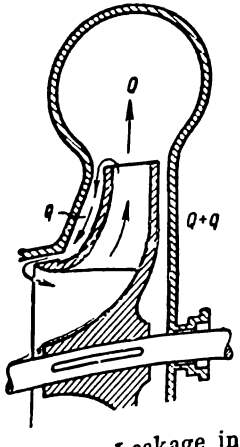

Fig. 141. Leakage in centrifugal pump

3. **Mechanical losses,** which include energy degradation due to friction in packings and bearings as well as surface friction of the fluid on the impeller. Denoting loss of power due to friction by N_m and total shaft horsepower by N_0, the mechanical efficiency of a pump is

$$\eta_m = \frac{N_0 - N_m}{N_0} \tag{12.27}$$

(for method of computing N_m see Sec. 56).

The numerator of this expression represents the so-called internal or hydraulic horsepower and can be expressed by the formula

$$N_h = N_0 - N_m = \frac{1}{75}(Q+q)\gamma H_{tz}. \tag{12.28}$$

Now let us write the expression of the overall efficiency of a pump as a ratio of the water horsepower to the shaft horsepower:

$$\eta = \frac{Q\gamma H_{pump}}{75N_0},$$

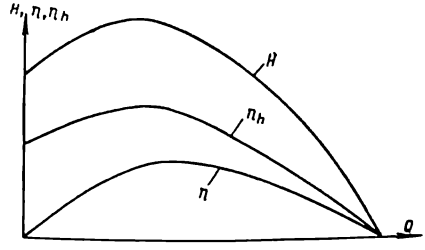

Fig. 142. Plot of H, η and η_h versus rate of discharge

and multiply the numerator of this expression by N_h and the denominator by the same quantity, only as expressed by Eq. (12.28). We have

$$\eta = \frac{Q\gamma H_{pump}}{75N_0} \frac{75N_h}{(Q+q)\gamma H_{tz}},$$

and after cancelling out and rearranging,

$$\eta = \frac{H_{pump}}{H_{tz}} \frac{Q}{Q+q} \frac{N_h}{N_0} = \eta_h \eta_v \eta_m, \qquad (12.29)$$

i. e., *the overall efficiency of a pump is equal to the product of its hydraulic, volumetric and mechanical efficiencies.*

Overall efficiency of centrifugal pumps usually ranges from 0.7 to 0.85; small pumps for auxiliary duty may have lower efficiency values.

Fig. 142 presents a diagram showing the change in overall and hydraulic efficiency and the characteristic curve of a pump operating at constant rpm.

54. SIMILARITY FORMULAS

Let us investigate similar operating conditions of homologous centrifugal pumps. As mentioned before in Sec. 20, hydrodynamic similarity is provided by geometric, kinematic and dynamic similarity. As applied to centrifugal pumps, kinematic similarity means similarity of the velocity triangles constructed for any corresponding points of the impellers. Dynamic similarity is ensured by equality of the Reynolds numbers of the flows through the pumps in question.

When operating conditions of centrifugal pumps are similar a proportionality between heads generated and lost, and between actual delivery and leakage, is observed. It can therefore be assumed that homologous pumps have the same hydraulic and volumetric

efficiencies.* The mechanical efficiencies of homologous pumps will generally vary, but the total efficiency can nonetheless be assumed equal without much error.

Let us consider similar operating conditions of two homologous centrifugal pumps. The values referring to the first pump are denoted by the additional subscript I, and to the second, by the subscript II (Fig. 143).

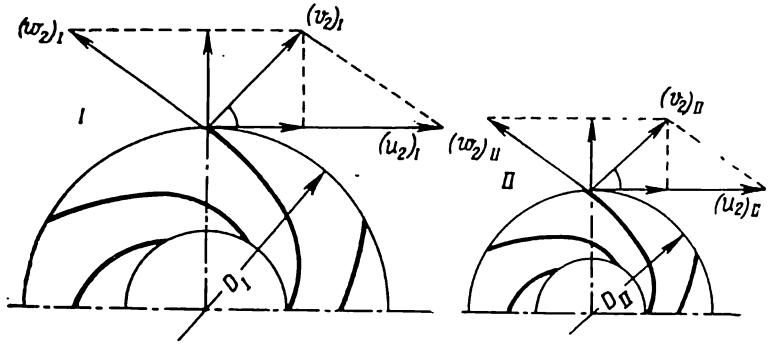

Fig. 143. Similarity of centrifugal pumps

Taking into account that the peripheral velocities of the impellers are proportional to the number of rpm times the respective impeller diameters D, the condition for kinematic similarity at the impeller exit can be written down as follows:

$$\frac{(u_2)_I}{(u_2)_{II}} = \frac{(v_2)_I}{(v_2)_{II}} = \frac{(v_{2u})_I}{(v_{2u})_{II}} = \frac{(v_{2r})_I}{(v_{2r})_{II}} = \frac{(w_2)_I}{(w_2)_{II}} = \frac{(nD)_I}{(nD)_{II}}. \qquad (12.30)$$

Since, from Eq. (12.10),

$$Q = \pi D v_{2r} b_2,$$

and from geometric similarity

$$\frac{D_I}{D_{II}} = \frac{(b_2)_I}{(b_2)_{II}},$$

we can write, from Eq. (12.30),

$$\frac{Q_I}{Q_{II}} = \frac{(nD^3)_I}{(nD^3)_{II}}. \qquad (12.31)$$

* In practice the efficiencies η_h and η_v are not identical in different pumps because of different relative roughness of the inner surfaces, which affect η_h (the so-called scale effect), and to disproportions in the relative spacing dimensions in pumps of different size, which determine leakage.

This means that the rate of discharge of homologous pumps under similar operating conditions is proportional to the rpm and the cube of the diameters.

From Eq. (12.8), the theoretical heads for an infinite number of vanes are proportional to the product of the peripheral and tangential velocities, while the vane-number coefficient μ is the same for homologous impellers. Consequently,

$$\frac{(H_{tz})_{\mathrm{I}}}{(H_{tz})_{\mathrm{II}}} = \frac{(u_2 v_{2u})_{\mathrm{I}}}{(u_2 v_{2u})_{\mathrm{II}}},$$

whence, taking into account (12.30),

$$\frac{(H_{tz})_{\mathrm{I}}}{(H_{tz})_{\mathrm{II}}} = \frac{(n^2 D^2)_{\mathrm{I}}}{(n^2 D^2)_{\mathrm{II}}}. \tag{12.32}$$

The actual head generated by the pump is

$$H_{pump} = \eta_h H_{tz} = H.$$

(We shall henceforth denote the delivered head by the symbol H without a subscript.)

But, as $(\eta_h)_{\mathrm{I}} = (\eta_h)_{\mathrm{II}}$, instead of Eq. (12.32) we can write

$$\frac{H_{\mathrm{I}}}{H_{\mathrm{II}}} = \frac{(n^2 D^2)_{\mathrm{I}}}{(n^2 D^2)_{\mathrm{II}}}, \tag{12.32'}$$

i. e., the actual heads developed by homologous pumps under similar operating conditions are proportional to the square of the product of the rpm times the impeller diameter.

From the expression for the water horsepower of a pump, Eq. (12.2), and the developed equations (12.31) and (12.32'), we can write the relationship between the power generated by homologous pumps under similar operating conditions:

$$\frac{N_{\mathrm{I}}}{N_{\mathrm{II}}} = \frac{(QH\gamma)_{\mathrm{I}}}{(QH\gamma)_{\mathrm{II}}} = \frac{n_{\mathrm{I}}^3 D_{\mathrm{I}}^5 \gamma_{\mathrm{I}}}{n_{\mathrm{II}}^3 D_{\mathrm{II}}^5 \gamma_{\mathrm{II}}}. \tag{12.33}$$

If we wish to consider similar operating conditions of the same pump at different rotational speeds n_1 and n_2, the Eqs (12.31), (12.32') and (12.33) become simpler, as D and γ are the same all

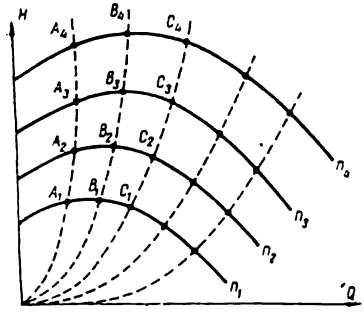

Fig. 144. Pump characteristics for different rotative speeds

through, and take the form

$$\frac{Q_1}{Q_2} = \frac{n_1}{n_2}; \tag{12.34}$$

$$\frac{H_1}{H_2} = \left(\frac{n_1}{n_2}\right)^2; \tag{12.35}$$

$$\frac{N_1}{N_2} = \left(\frac{n_1}{n_2}\right)^3, \tag{12.36}$$

(the subscripts 1 and 2 denoting the different rpm values).

Equations (12.34) and (12.35) are used to compute pump characteristics for different rotative speeds. If the relationship between H and Q at $n_1 = \text{const}$ is given, a similar curve for $n_2 = \text{const}$ can be obtained by computing the abscissas of the points of the former curve (the rates of discharge) proportionally to the rpm ratio, and the ordinates (the heads), proportionally to the square of that ratio (Fig. 144).

Thus it is possible to calculate and plot the characteristics of a pump for any desired rotative speed and to draw a series of characteristic curves for the same pump at different values of n (Fig. 144).

The points A_1, A_2, A_3, A_4 on these curves joined by the coordinate relationships given in (12.34) and (12.35) represent similar operating conditions. The other rows of points (B_1, B_2, B_3, B_4), (C_1, C_2, C_3, C_4), etc., give a second, third, etc., row of similar operating conditions.

It is easy to develop the equations of the curves joining the points of similar operating conditions. According to Eqs (12.34) and (12.35), for any row of points we can write

$$\frac{H_1}{Q_1^2} = \frac{H_2}{Q_2^2} = \frac{H_3}{Q_3^2} = \text{const}_1.$$

Hence, for a row of similar operating conditions we have

$$H = \text{const}_1 Q^2.$$

For another row

$$H = \text{const}_2 Q^2.$$

Consequently, the points representing similar operating conditions in an H-Q coordinate system are located on parabolas of the second power through the point of origin,* shown in dashed lines in Fig. 144.

* It should be noted that the Reynolds number Re changes somewhat along a parabola of similar operating conditions. Experiments show, however, that

On the basis of the afore-mentioned considerations concerning the hydraulic and volumetric efficiency of pumps under similar operating conditions, the parabolas for similar operating conditions are seen to be curves of constant values of η_h and η_v. It can also be assumed, with a fair degree of accuracy, that the overall efficiency is constant along a parabola of similar operating conditions.

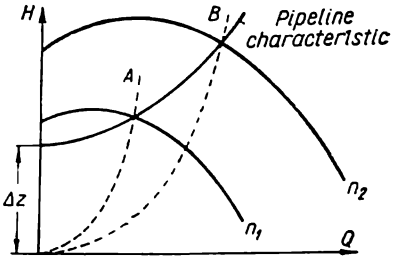

Fig. 145. Operating points when similarity is violated

In connection with similar operating conditions of centrifugal pumps the following question arises: How long are operating conditions similar when the running speed changes, and when does the similarity end?

Pump operating conditions are determined by the point of intersection of the characteristic curves of the pump and the pipeline. Hence, for a constant pipeline characteristic (uniform throttle conditions) a change in pump rpm shifts the operating point along the pipeline characteristic. If the latter is a parabola of the second power through the origin of the coordinate system it will coincide with one of the similarity parabolas, which means that similarity holds through the rpm changes. Thus, a looping pipeline with turbulent flow has a characteristic curve very like a parabola of the second power through the origin of the coordinate system. It can be assumed, therefore, that in this case the change in the running speed of a pump will not affect the similarity of operating conditions.

In the case of a fluid pumped from a lower reservoir to a higher one, when the elevation difference $\Delta z \neq 0$, the pipe characteristic will be of the type shown in Fig. 145. A change in pump speed from n_1 to n_2 will shift the operating point from A to B. But points A and B belong to different similarity parabolas, hence the similarity is violated.

It follows from the foregoing that there are two ways of regulating a centrifugal pump: by throttling, as mentioned in Sec. 52, and by changing the running speed. In the case of throttling the pipeline characteristic changes and the operating point moves along the uniform pump curve (see Fig. 140); when the rpm is changed the pump characteristic varies and the operating point moves along the uniform pipe curve (see Fig. 144).

---

flow regimes in centrifugal pumps approach the rough-law regime, when the value of Re has no perceptible effect (see Sec. 26). Of decisive importance in this case is kinematic similarity.

The second method is more expedient since in changing the rotational speed the efficiency of the pump can be maintained more or less uniform (if the pipeline curve is through the origin of the coordinate axes). On the other hand, running speed adjustment usually involves auxiliary equipment, and throttling is simpler. In throttling the efficiency of the pump varies along the curve shown in Fig. 142 and, consequently, when delivery is reduced considerably pump efficiency falls accordingly.

55. SPECIFIC SPEED AND ITS RELATION TO IMPELLER GEOMETRY

The similarity formulas obtained in the foregoing section can be used to develop a useful practical factor for calculating and designing centrifugal pumps which is commonly known as *specific speed*.

From Eq. (12.31)

$$\frac{D_I^2}{D_{II}^2} = \left(\frac{Q_I}{Q_{II}}\right)^{2/3}\left(\frac{n_I}{n_{II}}\right)^{-2/3}.$$

Substitution into Eq. (12.32) yields

$$\frac{H_I}{H_{II}} = \left(\frac{Q_I}{Q_{II}}\right)^{2/3}\left(\frac{n_I}{n_{II}}\right)^{4/3}.$$

Rearranging and raising to the power of 3/4, we obtain

$$\frac{n_I\sqrt{Q_I}}{H_I^{3/4}} = \frac{n_{II}\sqrt{Q_{II}}}{H_{II}^{3/4}} = \text{const.} \qquad (12.37)$$

This expression is valid not only for two homologous pumps I and II but for any number of homologous pumps operating under similar conditions.

Suppose that among these homologous pumps we have a standard pump with a head delivery $H_s = 1$ m, and a water horsepower $N_s = 1$ h.p. at $\gamma = 1{,}000$ kg/m^3.

Using the power equation (12.2) it is easy to determine the capacity of the standard pump:

$$Q_s = \frac{75N_s}{H_s\gamma} = \frac{75 \times 1}{1 \times 1{,}000} = 0.075 \text{ m}^3/\text{sec} = 75 \text{ lit/sec}.$$

Now let us relate the parameters Q_s, H_s, n_s of the standard pump to the corresponding parameters Q, H, n of any other homologous pump under similar operating conditions using Eq. (12.37):

$$\frac{n_s\sqrt{Q_s}}{H_s^{3/4}} = \frac{n\sqrt{Q}}{H^{3/4}}.$$

Substituting the values of Q_s and H_s, we can determine the rotational speed of the standard pump:

$$n_s = \frac{1}{\sqrt{0.075}} \frac{n\sqrt{Q}}{H^{3/4}} = 3.65 \frac{n\sqrt{Q}}{H^{3/4}}.$$

The expression

$$n_s = 3.65 \frac{n\sqrt{Q}}{H^{3/4}} \tag{12.38}$$

is the specific speed.

The physical meaning of the quantity n_s is apparent from the foregoing reasoning: it is the rpm of a standard pump homologous with a given pump and generating, under similar operating conditions, a head $H_s = 1$ m at a rate of discharge of $Q_s = 0.075$ m³/sec. The hydraulic and volumetric efficiencies of the two pumps are, naturally, the same.

The water horsepower of the standard pump is 1 h. p., provided that $\gamma = 1{,}000$ kg/m³. Pump capacity is less when the liquid is lighter and more when it is heavier. Therefore for general considerations capacity should not be introduced in defining n_s.

It is not difficult now to determine the impeller diameter of a standard pump. From Eq. (12.32)

$$\frac{H_s}{H} = \frac{n_s^2 D_s^2}{n^2 D^2},$$

whence

$$D_s = \frac{nD}{n_s\sqrt{H}}. \tag{12.39}$$

In using Eqs (12.38) and (12.39) the metric units of measure are metres for H, m³/sec for Q and revolutions per minute for n.

Under certain conditions the specific speed n_s characterises the ability of a pump to develop head and ensure a certain delivery. The higher the specific speed the less the head (for a given Q and n) and the greater the capacity (for a given H and n).

Specific speed depends on impeller design. Pumps with low specific speed have impellers with small relative width $\left(\frac{b_2}{D_2}\right)$ but a high value of $\frac{D_1}{D_2}$, i. e., long vanes, which is necessary to obtain a higher head. Flow through such an impeller is in a plane perpendicular to the axis of rotation.

With n_s increasing the ratio $\frac{D_2}{D_1}$ (as well as $\frac{D_2}{D_0}$) decreases, i. e., the vanes are shorter and the relative width of the impeller $\frac{b_2}{D_2}$ is greater. Furthermore, the flow through the impeller departs from the plane of rotation and becomes increasingly three-dimensional. In the limit, at maximum values of n_s, the flow is along the axis of rotation and the impeller is of the axial-flow type.

The vane angle β_2 decreases from about 35° to 15° with n_s increasing from 40 to 200.

Centrifugal and other rotodynamic pumps may be classified according to the specific speed as follows:

(1) low-speed radial-flow: $n_s \leqslant 80$, $\frac{D_2}{D_1}=2.2\text{-}3.5$;

(2) normal-speed radial-flow: $n_s=80\text{-}150$, $\frac{D_2}{D_1}=2.2\text{-}1.8$;

(3) high-speed radial-flow: $n_s=150\text{-}300$, $\frac{D_2}{D_1}=1.8\text{-}1.3$;

(4) mixed-flow: $n_s=300\text{-}600$, $\frac{D_2}{D_1}=1.3\text{-}1.1$;

(5) axial-flow, or propeller: $n_s=600\text{-}1{,}200$, $\frac{D_2}{D_1}=1$.

The impeller shapes corresponding to these five types are presented schematically in Fig. 146.

The first three belong to the true centrifugal pump, the mixed- and axial-flow designs actually representing other pump types. Obviously, no sharp boundaries can be drawn between the different types of pumps, and the centrifugal impeller turns gradually, through a mixed-flow impeller, into a true propeller as n_s increases.

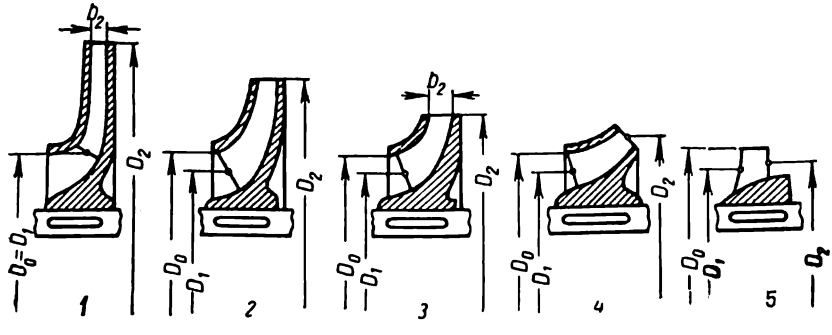

Fig. 146. Types of rotodynamic pump impellers

56. RELATION BETWEEN SPECIFIC SPEED AND EFFICIENCY

Different impeller designs and different specific speeds must evidently affect pump efficiency. The degree of these effects, however, is different for hydraulic, volumetric and mechanical efficiency.

Hydraulic efficiency, experiments show, hardly changes with n_s and is much more dependent on the roughness of the flow passages and pump size. Volumetric and mechanical efficiency, on the other hand, is substantially affected when n_s approaches its lower limit.

With the specific speed decreasing the relative loss of power due to impeller friction increases markedly, with a resulting reduction in the mechanical efficiency of a pump. Internal flow through spaces also increases, relative leakage rises and volumetric efficiency falls.

Thus, the overall efficiency of a centrifugal pump with a low specific speed is relatively lower, decreasing as n_s decreases. This sets a lower limit for n_s imposed by efficiency considerations. These, of course, will depend on the application and working conditions of the pump.

The formulas for relative energy losses in pumps and corresponding efficiencies as functions of specific speed developed below can be used to determine the minimum permissible specific speed and also to facilitate efficiency estimates for different values of n_s.

We shall first investigate relative leakage through pump clearances and determine volumetric efficiency.

Flow through clearance spaces (leakage) can be expressed according to the common flow equation:

$$q = \mu S \sqrt{2gH_{cl}},$$

where μ = coefficient of discharge for flow through clearance space. For common clearances $\mu = 0.4\text{-}0.5$, for special labyrinth clearances $\mu = 0.3$;

H_{cl} = head of flow through clearance;

S = clearance space area. For open (unshrouded) impellers

$$S = \pi D_{cl} \delta,$$

where D_{cl} = diameter of clearance space;

δ = clearance, assumed proportional to D_{cl}: $\delta = \frac{D_{cl}}{m}$.

The value of H_{cl} can be found as the difference between the pressure head developed by the impeller (i. e., the head H_p for a finite number of vanes, with hydraulic losses taken into account) minus the pressure drop in the clearance space between impeller and casing due to fluid rotation. As one of the wearing surfaces is at rest and the other is moving, it is commonly assumed that the fluid is rotating at half the speed of the impeller.

Using Eq. (3.3) for the pressure in the fluid at relative rest and taking into account the foregoing considerations, we have

$$H_{cl} = \mu \eta_h H_p - \frac{\omega^2}{32g} (D_2^2 - D_{cl}^2).$$

The head H_{cl} can be assumed approximately proportional to the delivered head and expressed in the form

$$H_{cl} = k_{cl} H,$$

where $k_{cl} = 0.6\text{-}0.85$.

The clearance space diameter is approximately equal to the eye diameter D_0 which, as will be shown in the following sections, must be made equal to

$$D_1 = k_0 \sqrt[3]{\frac{Q}{n}},$$

where $k_0 = 4.2\text{-}4.5$.

Substituting these values into the leakage equation, determine the ratio of the leakage to the normal discharge as a function of the specific speed. We have

$$\frac{q}{Q} = \frac{\mu \pi D_{cl}^2 \sqrt{2gk_{cl}H}}{mQ} = \frac{\mu \pi k_0^2 \sqrt{2gk_{cl}}}{m} \frac{H^{1/2}}{Q^{1/3} n^{2/3}}.$$

Taking into account the expression for specific speed (12.38), we obtain

$$\frac{q}{Q} = A_1 \frac{1}{\left(\frac{n\sqrt{Q}}{H^{3/4}}\right)^{2/3}} = A_1 \frac{3.65^{2/3}}{n_s^{2/3}} = \frac{A}{n_s^{2/3}},$$

where $A = \frac{\pi \mu k_0^2 \sqrt{2gk_{cl}} 3.65^{2/3}}{m}$.

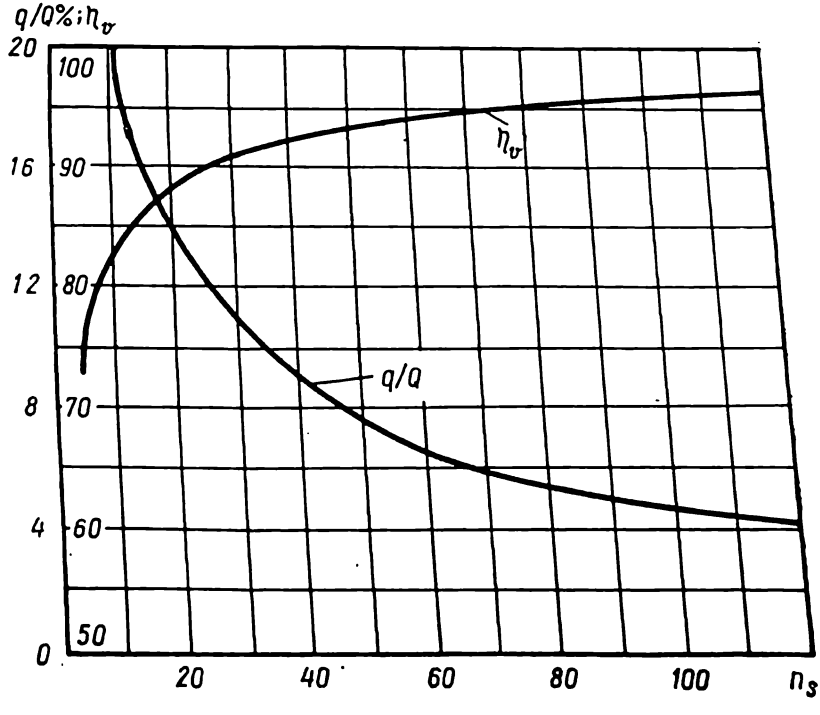

Fig. 147. Plot of q/Q and η_v versus n_s

At $m = 300$, $\mu = 0.5$, $k_{cl} = 0.8$ and $k_0 = 4.5$, the constant $A \approx 1$. For this value of A there is plotted on the diagram in Fig.147 the dependence of the relative leakage $\frac{q}{Q}$ in an open impeller as a function of the specific speed. The curve illustrates graphically how the importance of leakage grows with the specific speed decreasing. For a closed impeller A is twice as much.

The volumetric efficiency of a pump can be expressed in terms of the specific speed by the formula

$$\eta_v = \frac{Q}{Q+q} = \frac{1}{1+\frac{q}{Q}} = \frac{1}{1+\frac{A}{n_s^{2/3}}}. \qquad (12.40)$$

The volumetric efficiency curve is also given in Fig. 147.

Friction between impeller shroud and fluid usually occurs when the flow is turbulent, and the shearing stress τ can therefore be assumed proportional to the product of the specific weight of the fluid times the velocity head, just as in turbulent pipe flow. In this case, however, the velocity head must be expressed in terms of the peripheral speed of the impeller, which is proportional to the radius. Thus,

$$\tau = c_f \gamma \frac{u^2}{2g},$$

where c_f = dimensionless proportionality coefficient called the friction coefficient.

The loss of power due to friction between the impeller shroud and the fluid can be computed by integrating the expression for the differential friction moment multiplied by the angular velocity of rotation of the impeller:

$$N_f' = k\omega \int_0^{D/2} \tau r dS,$$

where dS = differential area equal to $2\pi r dr$;
r = running radius;
k = coefficient taking into account the proportion of the total shroud area exposed to friction; usually $1 < k < 2$.

Substituting the previous expression for τ and taking into account that $u = \omega r$, and assuming that to a first approximation the coefficient of friction c_f in turbulent flow is constant for the whole shroud surface, the integration can be carried out in the form

$$N_f' = C_1 \gamma \omega^3 \int_0^{D/2} r^4 dr = C_2 \gamma \omega^3 D^5,$$

or

$$N_f' = C \gamma u_2^3 D^2$$

where C = constant including all numerical coefficients as well as k, c_f and other constants.

Investigations show that for approximate calculations for highly finished surfaces it can be assumed that $C = 1.2 \times 10^{-6}$ in the MKS system of units; N_f in this case is expressed in horsepower.

Determine the ratio of the friction horsepower to the hydraulic horsepower of the pump (see Sec. 53):

$$\frac{N_f'}{N_h} = \frac{C\gamma u_2^3 D^2}{Q\gamma H} 75\eta_v\eta_h.$$

Now express the impeller diameter D in terms of the peripheral velocity u_2 and the speed of rotation n, and the peripheral velocity in terms of head from the expressions

$$u_2 = \frac{\pi D n}{60} \text{ and } H = k_1 \frac{u_2^2}{2g},$$

whence

$$D = \frac{60u_2}{\pi n} = \frac{60}{\pi n}\sqrt{\frac{1}{k_1} 2gH}.$$

Substituting into the basic equation, we obtain

$$\frac{N_f'}{N_h} = 75\left(\frac{60}{\pi}\right)^2 C\left(\frac{2g}{k_1}\right)^{5/2}\eta_h\eta_v \frac{H^{3/2}}{Qn^2},$$

or, introducing the specific speed n_s and using the foregoing expression for η_v in terms of n_s,

$$\frac{N_f'}{N_h} = \frac{B}{n_s^2}\frac{1}{1+\frac{A}{n_s^{2/3}}}, \tag{12.41}$$

where $B = 3.65^2 \times 75C\left(\frac{60}{\pi}\right)^2\left(\frac{2g}{k_1}\right)^{5/2}\eta_h$.

At $k_1=1.2$, $\eta_h=0.8$ and $C=1.2\times10^{-6}B=377$.

The curve of $\frac{N_f'}{N_h}$ as a function of n_s for the determined values of B and for $A \approx 1$ is presented in Fig. 148, which shows graphically how the relative horsepower loss due to friction between the fluid and the impeller shrouds increases when the specific speed decreases.

To go over from $\frac{N_f'}{N_h}$ to the mechanical efficiency we regard the latter as a product

$$\eta_m = \eta_m'\eta_m'',$$

where η_m' = efficiency taking into account power loss due to friction between impeller shroud and fluid, whence

$$\eta_m' = \frac{N_h}{N_h + N_f'} = \frac{1}{1+\frac{N_f'}{N_h}}; \tag{12.42}$$

η''_m = efficiency taking into account friction in packings and bearings and equal to

$$\eta''_m = \frac{N_0 - N''_f}{N_0} = \frac{N_h + N'_f}{N_0}.$$

In the latter expression N''_f is the loss of power due to friction in the packings and bearings and N_0 is the total shaft power of the pump:

$$N_0 = N_h + N'_f + N''_f.$$

Using the dependence of $\frac{N'_f}{N_0}$ on the specific speed presented above, it is possible to plot η'_m as a function of n_s for the given values of the constants A and B. The factor η''_m can be assumed to be independent of n_s and equal to about 0.95.

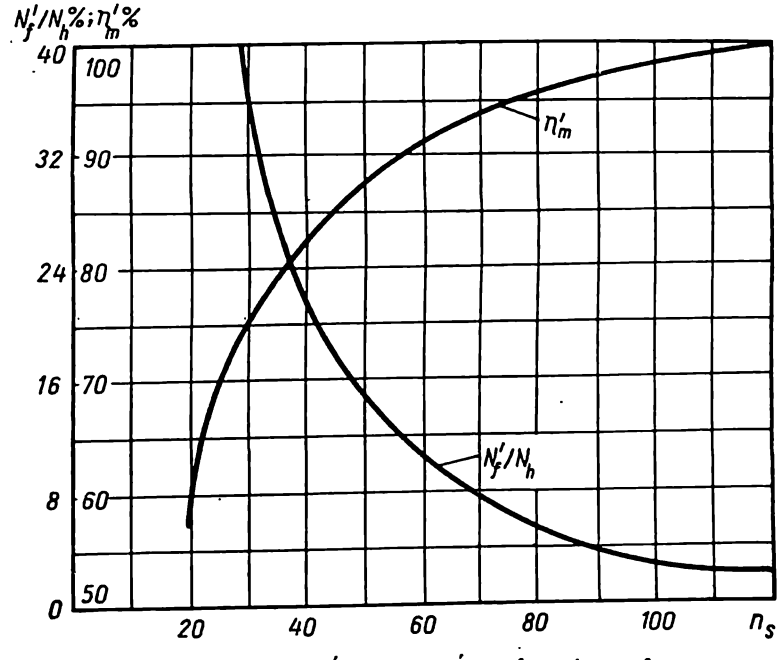

Fig. 148. Plot of N'_f/N_h and η'_m as functions of n_s

The curve showing the drop in η'_m with n_s decreasing is presented in the diagram in Fig. 148.

It should be borne in mind that by judicious design of the passages leading from the clearance between the impeller and casing wearing surfaces to the volute (of the order of 3 per cent of the impeller diameter on each side) a part of the energy dissipated in friction can be restored by utilising the kinetic energy of the fluid carried along by the impeller shroud. The actual mechanical efficiency may therefore be slightly higher than the rated value.

In using the plotted curves of $\frac{q}{Q}$, $\frac{N_f'}{N_h}$, η_v and η_m as a function of n_s, their approximate nature should be borne in mind. To obtain more accurate values of these quantities the values of the constants A and B must be computed each time for the specific data.

It is practically impossible to offer an analytical expression for the total hydraulic losses inside a pump, and consequently for η_h, as this quantity depends on a number of factors the effects of which are poorly known. For high-head (low-speed) impellers the hydraulic efficiency may vary from 0.7 to 0.9, the lower limit referring to small values of n_s and small impeller diameters of the order D = 100-200 mm, and the upper limit corresponding to n_s = 90-120 and D = 500-600 mm.

57. CAVITATION CONDITIONS FOR CENTRIFUGAL PUMPS (ACCORDING TO S.S. RUDNEV)

Any pump, whether centrifugal or of other design, can operate normally only if the absolute pressure in the suction pipe is not too low. Otherwise cavitation develops at the intake, or rather at the entrance of the liquid to the vane passages, where the absolute pressure is lowest (see Sec. 21).

Cavitation results in intermittent stream, due to the evolution of vapour and dissolved gases; a characteristic noise produced by hydraulic shocks in the condensation of vapour bubbles appears; and the delivery, head and efficiency of the pump fall. The intensity of these phenomena increases with the absolute pressure at the impeller eye decreasing, which is demonstrated graphically by the so-called cavitation characteristic curves of a centrifugal pump. The curves are plotted for the head, capacity and efficiency of the pump as a function of the absolute pressure of the liquid at intake. They are usually obtained in special tests in which the speed of rotation and the discharge (by throttling) are maintained constant;

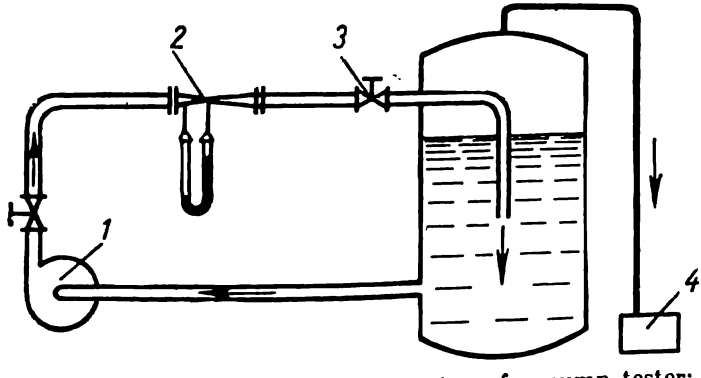

Fig. 149. Diagrammatic representation of a pump tester:
1 — tested pump; *2* — flow meter; *3* — throttle; *4* — vacuum pump

in the course of a test the absolute pressure at the impeller intake is gradually reduced (for instance, by evacuating air from the reservoir).* The setup for experimentally determining the cavitation characteristics of a pump is presented schematically in Fig. 149. The head, capacity and efficiency of the pump are at first constant (Fig. 150); when the pressure drops sufficiently, the characteristic noise appears and the respective values begin to fall rapidly as a result of cavitation at the intake.

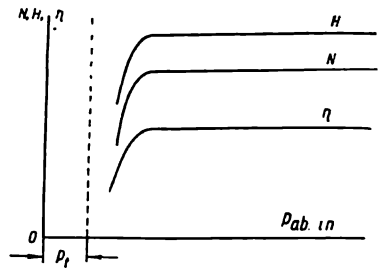

Fig. 150. Cavitation characteristics of pump

The higher the speed of rotation and discharge the higher the velocity of the liquid and the lower the absolute pressure at intake, which facilitates cavitation. Thus, cavitation imposes limitations on the rate of discharge and speed of rotation of a pump.

In the following, liquid flow at impeller intake is investigated, impeller eye diameter is determined from cavitation conditions and a cavitation criterion is developed by the method of Soviet scientist S.S. Rudnev.

Let the velocity of a liquid at the intake of a pump be v_{in}, and the absolute pressure p_{in}; then the specific energy of the liquid at the intake will be

$$H_{in}=\frac{p_{in}}{\gamma}+\frac{v_{in}^2}{2g}.$$

When the liquid approaches the impeller vanes the pressure drops further in proportion to the velocity head as computed according to the relative entrance velocity; there is no cavitation as long as the absolute pressure of the liquid is greater than the saturation vapour pressure for the given temperature.

Thus, the condition under which no cavitation occurs can be expressed by the following inequality:

$$H_{in}=\frac{p_{in}}{\gamma}+\frac{v_{in}^2}{2g}\geqslant h_t+\frac{v_1^2}{2g}+\lambda\frac{w_1^2}{2g},$$

where v_1 = absolute velocity of approach of liquid to vane, approximately equal to the intake velocity v_0 at the impeller eye;
w_1 = relative velocity at the same place;
h_t = saturation vapour pressure divided by γ, i. e.,

$$h_t=\frac{p_t}{\gamma};$$

* Cavitation characteristics may also be obtained for a constant throttle position, i.e., for a reduced delivery due to cavitation.

λ = factor depending on vane geometry and flow conditions;

$\lambda \frac{w_1^2}{2g}$ = pressure drop as liquid reaches vane.

The foregoing inequality can also be written down as follows:

$$H_{in} - h_t \geqslant \frac{v_1^2}{2g} + \lambda \frac{w_1^2}{2g}.$$

The left-hand side of the inequality represents the actual specific energy of the fluid at the pump intake, which in the limit may become equal to the right-hand side. The equation will then correspond to the beginning of cavitation, which is why we shall call the difference $H_{in} - h_t$ critical when it is equal to the right-hand side:

$$(H_{in} - h_t)_{cr} = \frac{v_1^2}{2g} + \lambda \frac{w_1^2}{2g}.$$

Since, as a rule, $w_1^2 = v_1^2 + u_1^2$,

$$(H_{in} - h_t)_{cr} = (1 + \lambda) \frac{v_1^2}{2g} + \lambda \frac{u_1^2}{2g}.$$

Thus, $(H_{in} - h_t)_{cr}$ should be kept as low as possible, for the smaller this critical value the less liable is cavitation to develop. It will be observed from the foregoing that $(H_{in} - h_t)_{cr}$ depends on the velocities v_1 and u_1 which, in turn, depend, for given Q and n, on the diameter D_1, approximately equal to D_0 (see Fig. 132). The problem, then, is of choosing an impeller eye diameter to ensure the lowest possible value of $(H_{in} - h_t)_{cr}$. For this, express the velocities v_1 and u_1 in terms of D_1 and investigate for the minimum. We have

$$(H_{in} - h_t)_{cr} = \frac{1}{2g} \left[(1 + \lambda) \frac{16Q^2}{\pi^2 D_1^4} + \lambda \frac{\pi^2 D_1^2 n^2}{60^2} \right].$$

Differentiating with respect to D_1 and equating the derivative to zero, we obtain

$$\frac{d}{dD_1} (H_{in} - h_t)_{cr} = -4 (1 + \lambda) \frac{16Q^2}{\pi^2 D_1^5} + 2\lambda \frac{\pi^2}{60^2} D_1 n^2 = 0,$$

whence

$$D_{opt} = \sqrt[3]{\frac{4 \times 60}{\pi^2} \sqrt{2}} \sqrt[6]{\frac{1 + \lambda}{\lambda}} \sqrt[3]{\frac{Q}{n}} = 3.25 \sqrt[6]{\frac{1 + \lambda}{\lambda}} \sqrt[3]{\frac{Q}{n}}.$$

And finally we obtain the following expression for the optimum diameter:

$$D_{opt} = k_0 \sqrt[3]{\frac{Q}{n}} \qquad (12.43)$$

where the factor k_0 may vary from 4.3 to 4.5, depending on λ.

For actual solutions, in view of the possibility of overloading, the upper limit should be taken.

From the expression for the optimum diameter, determine the minimum value of $(H_{in} - h_t)_{cr}$:

$$[(H_{in} - h_t)_{cr}]_{min} = \frac{D_{opt}^2}{2g} \left[(1 + \lambda) \frac{16Q^2}{\pi^2 D_{opt}^6} + \lambda \frac{\pi^2}{60^2} n^2 \right],$$

or, after substituting, rearranging and solving,

$$[(H_{in}-h_t)_{cr}]_{min}=\frac{1}{20}\sqrt[3]{\frac{\pi^2}{15}}\sqrt[3]{\lambda^2(1+\lambda)}\,\frac{Q^{2/3}n^{4/3}}{2g}=s\,\frac{(Qn^2)^{2/3}}{2g},$$

where s = factor determined by λ; at $\lambda = 0.25$, $s \approx 0.02$.

Pump tests indicate that this value of s can be used in calculating impellers of conventional geometry. For impellers of special design, for example with increased width b_1, the value of s is reduced to 0.012-0.013.

If the impeller eye diameter D_1 is optimal no-cavitation conditions will be given by the inequality:

$$H_{in}-h_t \geqslant s\,\frac{(Qn^2)^{2/3}}{2g}. \qquad (12.44)$$

The factor s thus offers a criterion of cavitation in a pump which can be used to verify computations and to determine the maximum permissible rpm of a pump for a given Q and H_{in} or the minimum permissible absolute pressure at intake.

The latter, it follows from the previously accepted notation and the foregoing inequality, is determined from the condition

$$(p_{in})_{min}=\gamma\left(H_{in}-\frac{v_{in}^2}{2g}\right)\geqslant\left[s\,\frac{(Qn^2)^{2/3}}{2g}+h_t-\frac{v_{in}^2}{2g}\right]\gamma.$$

The velocity head in the parantheses is often neglected, as this increases the reliability of a pump as far as cavitation is concerned; the difference $p_{in} - p_t$ is called the cavitation pressure allowance.

Often another quantity, called the cavitation parameter, is used

$$\sigma=\frac{(H_{in}-h_t)_{cr}}{H},$$

where H = head delivered by the pump.

The cavitation parameter is readily associated with the specific speed. From the foregoing,

$$\sigma=\frac{(H_{in}-h_t)_{cr}}{H}=\frac{s}{2g\times 3.65^{4/3}}\,\frac{(3.65n\sqrt{Q})^{4/3}}{H}=\frac{n_s^{4/3}}{C},$$

where, at $s = 0.02$,

$$C=\frac{2g3.65^{4/3}}{s}\approx 5\,500.$$

In aircraft and liquid-propellant rocket systems the following measures are taken to prevent cavitation in pumps:

(a) Gas pressure is increased in the tank from which the liquid is pumped. As this calls for heavier tanks the pressure is usually not more than about three atmospheres.

(b) A booster pump is installed at the beginning of the suction pipeline. This is possible only when power can be supplied to drive the pump (say, electricity).

(c) An axial or helical wheel is mounted immediately before the impeller on the same shaft to increase pressure and impart whirl to the flow. The latter results in a reduction of the relative velocity w_1 and improves operating conditions of the impeller. The auxiliary runner can completely prevent cavitation from developing at the impeller, but as its speed of rotation n and rate of discharge Q are the same as those of the impeller, cavitation can develop on the auxiliary runner itself. The best device, therefore, would be one in which the rotational speed of the auxiliary runner is less than that of the impeller.

58. CALCULATION OF VOLUTE CASING

The volute casing of a centrifugal pump is designed to contain the fluid discharged by the impeller and guide it to the pressure pipeline.

Volute calculation and design are based on the assumption that the peripheral velocity component in the volute varies inversely as the radius (the law of velocity distribution across a vortex section or the law of conservation of angular momentum), i. e.,

$$v_u = \frac{\Gamma}{2\pi r},$$

where Γ = so-called circulation along a closed curve enveloping the impeller, which is constant for a given volute and given operating conditions.

With the radius increasing the velocity v_u decreases and the pressure increases correspondingly. Consequently, a degeneration of the kinetic energy of the fluid into pressure energy takes place in the volute. The process continues in the diffuser beyond the volute (Fig. 151).

The circulation Γ can easily be found from the head H generated by the pump and η_h. For, since from Eq. (12.16)

$$H_{tz} = \frac{u_2 v'_{2u}}{g} = \frac{\omega}{g} r_2 v'_{2u},$$

then, on the basis of the foregoing,

$$\Gamma = 2\pi r_2 v'_{2u} = 2\pi \frac{g H_{tz}}{\omega} = 2\pi \frac{gH}{\omega \eta_h}.$$

The rate of discharge through any cross-section of the volute can be assumed to increase in proportion with the angle of inclina-

tion of the cross-section α, counting from the initial (and final) section of the volute, i. e.,

$$Q_\alpha = \frac{\alpha^\circ}{360} Q,$$

where Q = delivery of pump into pipeline.

For a differential discharge through an area of size $b \times dr$ taken in an arbitrary section of the volute at radius r (see Fig. 151)

$$dQ_\alpha = bv_u dr = \frac{\Gamma}{2\pi r} b dr,$$

whence,

$$Q_\alpha = \frac{\alpha^\circ}{360} Q = \frac{\Gamma}{2\pi} \int_{r=r_3}^{r=R} \frac{b}{r} dr,$$

where $r_3 = (1.03\text{-}1.05)r_2$ is the radius of a cylindrical surface enveloping the impeller to which the volute cross-sections are tangent.

For the simplest case of a volute of rectangular cross-section of uniform width (b = const), we obtain from the foregoing

$$\frac{\alpha^\circ}{360} = \frac{\Gamma}{2\pi Q} b \ln \frac{R}{r_3} = \frac{gbH}{\omega \eta_h Q} \ln \frac{R}{r_3}.$$

By assigning a number of values of α from zero to 360°, we obtain a series of values of R, from r_3 to R_{max}, i. e., the geometry of the

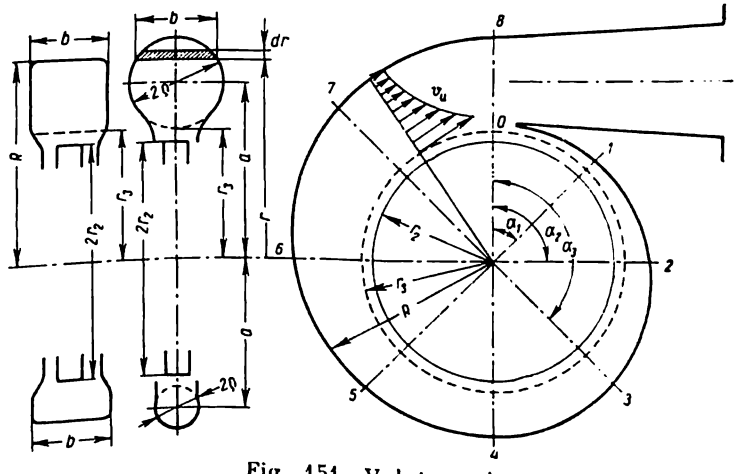

Fig. 151. Volute casing

volute. For a volute of circular cross-section of variable radius ϱ we have

$$b = 2\sqrt{\varrho^2 - (r-a)^2},$$

where a is the distance from the centre of the section to the impeller centre line and, consequently,

$$Q_a = \frac{\Gamma}{\pi} \int_{a-\rho}^{a+\rho} \frac{\sqrt{\varrho^2 - (r-a)^2}}{r}\, dr = \Gamma\,(a - \sqrt{a^2 - \varrho^2}).$$

Substituting in this equation $\frac{\alpha^\circ}{360}\, Q$ for Q_a and $r_3 + \varrho$ for a, and solving for ϱ, we obtain

$$\varrho = \frac{\alpha^\circ}{360k} + \sqrt{\frac{2}{k}\,\frac{\alpha^\circ}{360}\, r_3}, \tag{12.45}$$

where

$$k = \frac{\Gamma}{Q} = \frac{2\pi g H}{\omega \eta_h Q}.$$

The formula obtained makes it possible to calculate the dimensions and shape of a volute casing of circular cross-section. Calculation of a casing of arbitrary cross-section will involve integration.

59. SELECTION OF PUMP TYPE. SPECIAL FEATURES OF CENTRIFUGAL PUMPS USED IN AERONAUTICAL AND ROCKET ENGINEERING

As a rule, the basic criteria governing the selection of pump design are Q, H and n. These quantities enable the specific speed n_s to be computed, suggesting the type of rotodynamic pump to be preferred for given conditions. The procedure in calculating centrifugal pump design is outlined in the example in this section.

If the calculations give a very high specific speed (more than 1,200), it means that two or more pumps joined in parallel should be used.

If, on the other hand, the specific speed turns out to be too low (see Sec. 56) and the speed of rotation cannot be increased, a multistage pump must be used with z impellers mounted on a common shaft. The head developed by each impeller in this case is less by a factor of z, and the specific speed greater by a factor of $z^{3/4}$, than in a single-stage pump.

If such a design is undesirable displacement pumps are used. In this case, however, such fluid properties as viscosity and chemical activity must be taken into account.

In aircraft with gas-turbine engines centrifugal pumps are used mainly as booster pumps in fuel systems. They are usually installed inside the fuel tanks or close to them and are meant to increase the pressure in the whole of the suction pipeline, thereby improving operating conditions for the main fuel pump and minimising the possibility of cavitation.

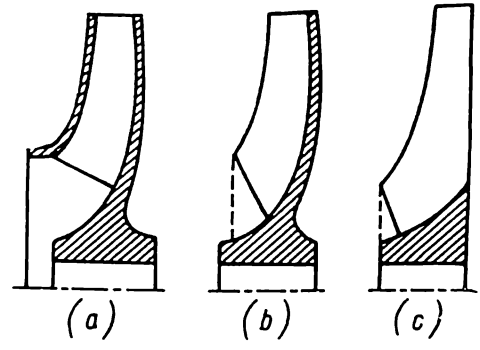

Fig. 152. Pump runners:
a — shrouded; b — unshrouded; c — propeller

Booster pumps are commonly made with open, or unshrouded, impellers consisting of a single disk with vanes mounted on one side (Fig. 152*b*).*

When a booster pump is placed inside a tank a propeller is commonly mounted at the impeller eye (on the same shaft) in order to improve its operating conditions and separate vapour and gas from the liquid. The shaft propeller must be designed for a much higher delivery than the centrifugal pump as some of the liquid delivered by it is hurled away.

Booster fuel pumps usually operate at 6,000 to 10,000 rpm and develop a pressure of 0.6 to 1.2 atm. Their specific speed varies from 100 to 200, that is, they belong to the class of normal- or even high-speed centrifugal pumps.

A recent tendency is to employ centrifugal pumps as the main fuel pumps of gas-turbine engines. The reason is that very high discharge is required and less viscous and more volatile fuels are being used. Centrifugal pumps, furthermore, can operate at very high rotation speeds (several tens of thousands rpm).

In such conditions centrifugal pumps of much smaller size and weight than other types of pumps can ensure the required fuel delivery at sufficiently high pressures. These considerations are also important in selecting pumps for liquid-propellant rocket motors.

In rocket motors centrifugal pumps are widely employed to deliver fuel and oxidiser from the tanks to the combustion chamber. They must generate head high enough to overcome the resistance of pipelines and the pressure in the combustion chamber and to

* The special features of such impellers are analysed further on.

ensure the required pressure difference in the injectors. The required head is several hundreds of metres and the pressure tens of atmospheres.

Displacement pumps are commonly used for such high pressures but if a large discharge is also required (as is the case in rocket motors) and there is a possibility of providing a very high-speed drive (e. g., a gas turbine), centrifugal pumps are to be preferred.

With a high impeller rotation speed and appropriate design centrifugal pumps can deliver liquids at high pressure. It follows from Sec. 55 that the appropriate design is the so-called low-speed centrifugal pump with a minimum specific speed.

The designation "low-speed", it should be remembered, refers to the specific speed and is in no way associated with the actual working speed of rotation, which may be very high.

Thus, the principal feature of centrifugal pumps used in liquid-propellant rocket motors is low specific speed, with all its consequences (see Sections 55 and 56).

In view of this the impellers of rocket-motor pumps are usually of the true radial type in which the flow is normal to the axis of rotation. Characteristic of such impellers is large relative diameter $\frac{D_2}{D_1}$ and small relative width $\frac{b_2}{D^2}$. As mentioned in Sec. 56, lower specific speed means greater relative energy degradation as a result of leakage inside the pump (volumetric losses) and friction between impeller shroud and liquid, i. e., lower η_v and η'_m and, consequently, lower overall pump efficiency. That is why the efficiency factor of pumps for rocket motors is usually low.

Impellers may be "closed", or "shrouded", with two disk-like surfaces or walls enclosing the vanes on both sides (Fig. 152*a*), "semi-open", or "unshrouded", with one disk to which the vanes are attached (Fig. 152*b*) and, finally, propeller-type with no shrouds and the vanes mounted on the hub (Fig. 152*c*). In the first two designs backward-curved vanes are used ($\beta_2 < 90°$), in the third design the vanes are radially mounted for considerations of strength. Energy losses due to disk friction are much lower in pumps with unshrouded and, all the more so, propeller runners than with closed impellers, but volumetric losses are higher.

The method of calculating the relative friction horsepower described in Sec. 56, can be used for unshrouded impellers with an appropriate coefficient k in the formula for N'_f. As to volumetric losses, their determination constitutes a special problem.

Another feature of centrifugal pumps used in liquid-propellant rocket motors is that they usually operate at conditions approaching cavitation owing to their high speeds of rotation. Accordingly, the cavitation estimates set forth before are of special importance.

Example. Calculate to a first approximation the impeller dimensions of a centrifugal pump for a V-2 liquid-propellant rocket motor and determine the required pressure at the pump intake to prevent cavitation. Given:
pumped fluid: 75-per cent ethyl alcohol, $\gamma = 864$ kg/cm^3, $h_t = 44$ mm Hg;
weight rate of discharge of pump: $G = 56$ kg/sec;
pressure developed by pump: $p_{pump} = 20.7$ atm;
rotation speed of impeller: $n = 3{,}800$ rpm.

Solution. (i) Determine volume rate of discharge Q, delivered head H and specific speed n_s:

$$Q = \frac{G}{\gamma} = \frac{56}{864} = 0.065 \text{ m}^3/\text{sec}; \quad H = \frac{p_{pump}}{\gamma} = \frac{20.7 \times 10^4}{864} = 240 \text{ m};$$

$$n_s = 3.65 \frac{n\sqrt{Q}}{H^{3/4}} = 3.65 \frac{3{,}800\sqrt{0.065}}{240^{3/4}} \approx 60.$$

(ii) From specific speed and statistical data (see Secs 55 and 56):

$$\frac{D_2}{D_1} = 2.5; \quad \beta_2 = 30°; \quad \eta_v = 0.88; \quad \eta_m' = 0.92; \quad \eta_m'' = 0.97;$$

$\eta_h = 0.85$ (all approximately).

Hence,

$$\eta = 0.88 \times 0.92 \times 0.97 \times 0.85 = 0.67.$$

(iii) Shaft horsepower:

$$N_0 = \frac{Q\gamma H}{75\eta} = \frac{0.065 \times 240 \times 864}{75 \times 0.67} = 268 \text{ h. p.}$$

(iv) Discharge of liquid through impeller:

$$Q' = \frac{Q}{\eta_v} = \frac{0.065}{0.88} = 0.074 \text{ m}^3/\text{sec}.$$

(v) Optimum impeller eye diameter according to Eq. (12.43):

$$D_{opt} = k_0 \sqrt[3]{\frac{Q'}{n}} = 4.5 \sqrt[3]{\frac{0.074}{3{,}800}} = 0.120.$$

This is the so-called reduced diameter, which disregards stream contraction by the impeller hub. Taking the latter into account, the equality of areas gives a higher value for D_0, viz.,

$$D_0 = \sqrt{D_{opt}^2 + d_{hub}^2},$$

where $d_{hub} = (1.15\text{-}1.25)\, d_{sh}$ is the hub diameter;
d_{sh} = shaft diameter determined from strength considerations.
Without going into strength calculations, let us assume that $D_0 \approx 140$ mm. The diameter D_1 is equal to or slightly less than D_0 owing to the inclination of the entrance edge of the vanes.

(vi) Assuming the radial velocity ratio $\frac{v_{2r}}{v_{1r}} = 1$ and $v_0 \approx v_{1r}$,

$$v_{2r} = v_0 = \frac{4Q'}{\pi D_{opt}^2} = \frac{4 \times 0.074}{\pi 0.12^2} = 6.5 \text{ m/sec}.$$

(vii) Assuming initially $z = 7$, the vane number coefficient is found from Eq. (12.19):

$$\frac{1}{\mu}=1+\frac{2\,(0.6+0.6\times 0.5)}{7\,(1-0.16)}=1.3,$$

whence $\mu = 0.77$.

(viii) From Eq. (12.21′) the theoretical head at $z = \infty$

$$H_{t\infty}=\frac{H}{\mu\eta_h}=\frac{240}{0.77\times 0.85}=367 \text{ m}.$$

(ix) Substituting v_{2r} for the ratio $Q/2\pi r_2 b_2$ in Eq. (12.12) and solving it as a quadratic equation,

$$u_2=\frac{v_{2r}}{2\tan\beta_2}+\sqrt{\frac{v_{2r}^2}{4\tan^2\beta_2}+gH_{t\infty}}=\frac{6.5}{2\times 0.578}+$$
$$+\sqrt{\frac{6.5^2}{4\times 0.578^2}+9.81\times 367}=65.5 \text{ m/sec},$$

whence

$$D_2=\frac{60u_2}{\pi n}=\frac{60\times 65.5}{\pi 3{,}800}=0.33 \text{ m}.$$

(x) Impeller width at exit, taking into account stream contraction by the vanes $\psi_2 = 0.95$:

$$b_2=\frac{Q'}{\pi D_2 v_{2r}\psi_2}=\frac{0.074}{\pi 0.33\times 6.5\times 0.95}=0.012 \text{ m}=12 \text{ mm}.$$

(xi) Impeller width at intake (at $\psi_1 = 0.85$):

$$b_1=\frac{Q'}{\pi D_1 v_{1r}\psi_1}=\frac{0.074}{\pi 0.14\times 6.5\times 0.85}=0.03 \text{ m}=30 \text{ mm}.$$

(xii) Vane angle at intake for shockless approach of liquid:

$$\beta_1=\tan^{-1}\frac{v_{1r}}{u_1}=\tan^{-1}\frac{6.5\times 330}{65.5\times 140}=\tan^{-1}0.23=13°.$$

The computed angle β_1 is usually increased by 3 to 5° to allow for cavitation in case of excessive discharge.

(xiii) Verification of impeller dimensions by repeating calculations in the same order on the basis of finally chosen values for β_2 and z and verified values of the coefficients η, μ, ψ, ψ_2. The latter two are computed from the formulas

$$\psi_1=1-\frac{z\delta}{\pi D_1 \sin\beta_1},$$

and

$$\psi_2=1-\frac{z\delta}{\pi D_2 \sin\beta_2},$$

where δ = vane thickness.

(xiv) Radius ϱ of terminal cross-section of volute case according to Eq. (12.45) at $\alpha = 360°$ (assuming $r_3 = 1.05\ r_2 = 173$ mm):

$$\varrho_{360} = \frac{1}{k} + \sqrt{\frac{2}{k} r_3 = \frac{\omega \eta_h Q}{2\pi g H}} + \sqrt{\frac{2\omega\eta_h Q}{2\pi g H}} r_3 =$$

$$= \frac{398 \times 0.85 \times 0.065}{2\pi \times 9.81 \times 240} + \sqrt{\frac{398 \times 0.85 \times 0.065}{\pi 9.81 \times 240} 0.173} = 0.023 \text{ m}.$$

(xv) Required head at impeller eye from Eq. (12.44):

$$H_{in} = h_t + s \frac{(Qn^2)^{2/3}}{2g} = 0.044 \frac{13{,}600}{864} + 0.02 \frac{(0.065 \times 3{,}8^2 \times 10^6)^{2/3}}{19.6} = 10.5 \text{ m}$$

or, neglecting velocity head,

$$p_{in} = 10.5 \times 864 \times 10^{-4} = 0.91 \text{ kg/cm}^2.$$

CHAPTER XIII

DISPLACEMENT PUMPS

60. GENERAL CONSIDERATIONS

The method of transforming the mechanical energy of a prime mover into the energy of fluid flow in positive displacement pumps is basically different from energy conversion in rotodynamic pumps. In a displacement pump the hydraulic fluid is delivered in intermittent "characteristic volumes" or portions by suitably designed pumping elements. The pumping elements, whatever their design, serve to effectively seal off the intake, suction, side of the pump from the outlet, pressure, side in order to prevent leakage and backflow of the hydraulic fluid. Thus, the delivery of a displacement pump generally fluctuates more or less and the mean delivery over a certain period of time is commonly considered.

The principle of positive-displacement pump operation enables the following expression to be written for the theoretical, or ideal, mean delivery per second:

$$Q_t = \frac{wzn}{60} = \frac{Wn}{60} \text{ m}^3/\text{sec}, \tag{13.1}$$

where w = displacement (i. e., characteristic volume delivered per revolution of pump shaft) of each pumping element;
z = number of pumping elements (i. e., number of characteristic volumes delivered per revolution);
W = pump displacement (i. e., theoretical delivery per revolution). By theoretical delivery is understood the delivery of an incompressible fluid by a pump operating without leakage or cavitation (see. Sec. 57).

According to the manner in which the hydraulic fluid is pumped, positive-displacement pumps are subdivided into reciprocating and rotary pumps.

A reciprocating pump is a positive-displacement machine which delifers pressure by linear reciprocating motion of the pumping

elements. The motion of the pumping elements is most commonly effected by means of a crankshaft mechanism, though camshaft, eccentric and other drives are frequently employed. Classified with reciprocating pumps are also plunger, diaphragm and other pumps having a similar process of fluid ejection.

All reciprocating pumps are provided with intake and outlet valves to regulate fluid flow through the working chamber. The valves usually operate automatically, the degree of opening being governed solely by the force developed by the working fluid.

Reciprocating pumps are capable of developing very high pressures, running into tens and hundreds of atmospheres, but they operate at a rotative speed of the prime mover of no more than 250 to 500 rpm. That is why a reciprocating pump is always much bigger than a centrifugal pump of equal capacity. Powerful mechanically driven reciprocating pumps are employed in the oil and chemical industries for pumping viscous fluids and at thermal electric stations for feeding steam boilers. Small hand-operated pumps are used in a wide range of applications. In water supply systems and other fields reciprocating pumps are being replaced by centrifugal and rotary pumps.

A *rotary pump* is a positive-displacement pump which delivers pressure by a pure rotation or a combined rotation and oscillation of the pumping elements. Any rotary pump consists basically of a stationary housing in which is nested a power-driven rotor carrying one or more pumping elements. A variety of rotor and pumping-element designs have been developed, some of which will be described further on.

The principle of rotary pump operation is as follows: the hydraulic fluid entering the inlet port is trapped by the pumping elements which carry it around to the outlet port, where it is expelled under pressure into the delivery pipeline.

Rotary pumps need no intake or outlet valves, a feature which makes them reversible, i. e., they can work either as pumps or as motors (see Chapter XIV). Furthermore, they do not require a crankshaft mechanism, which enables them to be operated at very high rotative speeds, up to 5,000 rpm and more.

The theoretical delivery of a rotary pump is also determined by Eq. (13.1). The number of pumping elements and consequently of characteristic volumes delivered per revolution, however, is greater than in reciprocating pumps (z = 4-12 and more, as compared with z = 1-3 in reciprocating pumps). Besides, in rotary pumps delivery of characteristic volumes overlaps, i. e., the hydraulic fluid is drawn in at the intake port before an adjacent volume has been expelled at the outlet port (see Sec. 61). This accounts for greater uniformity of delivery than in reciprocating pumps.

These advantages of rotary pumps have gained them numerous applications in many fields, including aviation. In aircraft systems rotary pumps are used in engine fuel and lubricating systems and in hydraulic power transmissions (see Chapter XIV).

61. TYPES OF ROTARY PUMPS

Rotary pumps are classified into three main types:

Gear pumps, which may be of the spur-gear or screw type. Spur-gear pumps deliver the hydraulic fluid at right angles to the rotation axis of the pumping elements; the screw pump delivers the fluid along the rotation axis.

Vane pumps, in which the hydraulic fluid is trapped in spaces between the pump housing, rotor and vanes.

Piston pumps, radial or axial, in which the fluid is trapped in cylinder bores in the rotor.

Let us see how the different types of rotary pumps operate and develop the equations for calculating their theoretical mean delivery, and later the actual delivery.

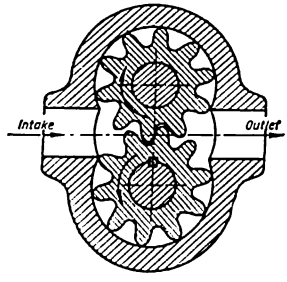

Fig. 153. Gear pump

Gear pumps (Fig. 153) are most commonly constructed with a pair of identical spur gears with involute teeth revolving in a closely fitted housing. The oil coming in at the intake port fills the spaces between the teeth and is carried around the periphery of the revolving gears to the discharge side. The teeth are meshing between the two gears and thus prevent the return of oil from the discharge to the suction. However, as the spaces between the teeth are larger than the teeth, some oil is carried back to the low-pressure side.

The characteristic volume, therefore, is not the volume of a space but the volume of a tooth w_{tooth}. The number of such volumes delivered per revolution equals the number of teeth of the two gears ($2z$). Hence the theoretical displacement of a gear pump is

$$Q_t = \frac{2z w_{tooth} n}{60} \text{ m}^3/\text{sec}. \tag{13.2}$$

Calculation of w_{tooth} requires determination of tooth area and an approximate formula is more conveniently used. It is developed assuming delivery of a continuous fluid lamina of thickness $2h = 2m$ and width b with a velocity equal to the rotative speed u of the gear at pitch circle:

$$Q_t = uS = \frac{2\pi Rn}{60} 2hb = \frac{1}{15} \pi Rnbm \text{ m}^3/\text{sec}, \tag{13.3}$$

where $S = 2hb$ = cross-sectional area of fluid lamina;
h = addendum, equal to module m;
R = pitch circle radius.

A screw pump operates on the same principle but its kinematics is three-dimensional. Despite such substantial advantages as completely uniform delivery and high-speed operation screw pumps have not yet found wide application in aeronautical engineering.

Vane pumps most commonly used in aircraft hydraulic systems have four vanes and the flow is two-dimensional (Fig. 154). The rotor represents a hollow cylinder with radial slots in which the vanes

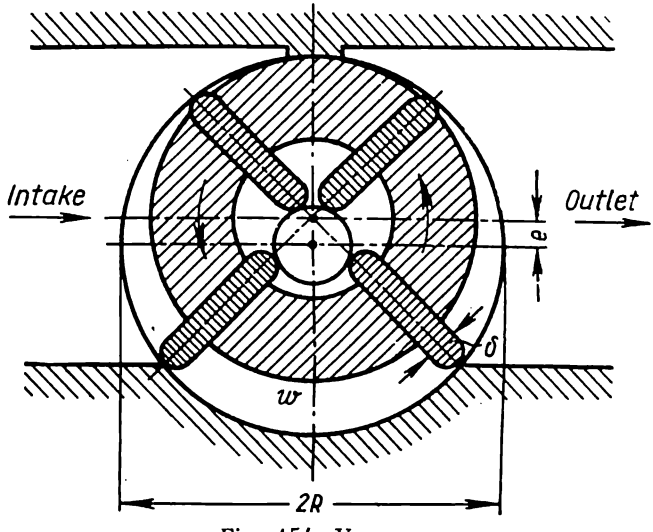

Fig. 154. Vane pump

slide. The rotor is placed eccentrically in relation to the cylindrical housing thanks to which the vanes slide back and forth as it revolves. Centrifugal force keeps the vane tips in contact with the track ring. The inner tips slide around a so-called floating axle without bearings.

When the rotor turns the fluid is drawn in on one side as the spaces formed between the housing, vanes and rotor increase to the characteristic volume w, and is forced out on the pressure side as they decrease.

Introducing the notation:

R = track-ring radius;

e = eccentricity (distance between track-ring and rotor centre lines);

z = number of vanes;

b = vane width;

δ = vane thickness,

the characteristic volumes may be expressed approximately by the formula

$$w = 2eb\left[\frac{2\pi(R-e)}{z} - \delta\right],$$

and the theoretical mean displacement per second, from Eq. (13.1), is

$$Q_t = \frac{wzn}{60} = 2eb[2\pi(R-e) - z\delta]\frac{n}{60}\ \text{m}^3/\text{sec}. \qquad (13.4)$$

Rotary piston pumps may have either two-dimensional or three-dimensional flow characteristics. To the former belong radial-piston pumps in which an eccentric rotor, called the cylinder-barrel or block, carries a number of cylinders in which pistons oscillate when the rotor turns (Fig. 155). The piston tips (sometimes made with rollers) slide along a track ring in the housing.

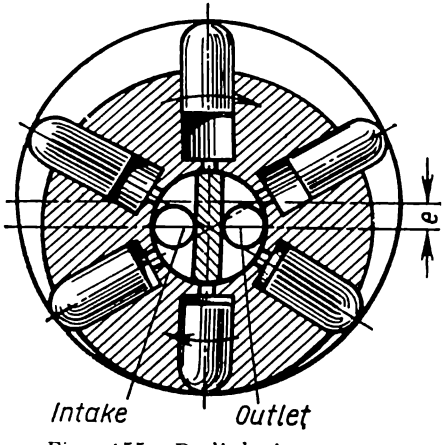

Fig. 155. Radial-piston pump

The rotation of the cylinder block periodically connects the cylinders through small bores in their bottoms with the suction and discharge ports in the centre separated by a dividing wall. The pistons draw in the oil as they pass around the intake side and expell it at the outlet side. The characteristic volume of a piston pump is the volume travelled through by each piston in one stroke:

$$w = \frac{\pi d^2}{4}2e,$$

where d = piston diameter;

e = eccentricity.

The theoretical mean displacement for z pistons is

$$Q_t = \frac{\pi d^2 ezn}{120}\ \text{m}^3/\text{sec}. \qquad (13.5)$$

Three-dimensional flow is characteristic of axial-piston pumps with swashplate or tilted cylinder barrel. A swashplate pump is presented schematically in Fig. 156. The cylinder barrel carries several cylinders parallel to the axis of rotation. The pistons *2* are spring loaded to keep them pressed to the swashplate *3* along which they slide. The oscillation of the pistons produces alternating suction and com-

pression in the cylinders. In the valve plate *4* there are two curved ports *5*, one for intake, the other for outlet. When the cylinder barrel turns the passages *6* move along the ports *5* periodically connecting the cylinders with the suction and discharge sides of the pump. When the passages are stopped by plugs *7* the oil is trapped in the respective cylinders, the volume being maximum in the upper position. The swashplate is hinged so that the tilt can be changed.

The theoretical mean displacement of a swashplate pump per second is

$$Q_t = \frac{\pi d^2}{4} lz \frac{n}{60} = \frac{\pi d^2}{4} D \tan\gamma z \frac{n}{60}, \qquad (13.6)$$

where D = diameter of cylinder circle;
d = piston diameter;
z = number of pistons;
l = piston stroke;
γ = swashplate angle.

In some swashplate pumps the cylinders are inclined at an angle φ to the rotor shaft (Fig. 157). In such a pump additionally acting on the pistons is a component of the centrifugal force created by the rotation, which allows for smaller spring loading of the pistons.

The piston stroke l can be determined from geometric considerations, assuming the piston to touch the swashplate on the former's centre line (Fig. 158). The law of sines yields

$$\frac{l_1}{\sin\gamma} = \frac{D_0}{2\sin(90° - \gamma + \varphi)}$$

and

$$\frac{l_2}{\sin\gamma} = \frac{D_0}{2\sin(90° - \gamma - \varphi)},$$

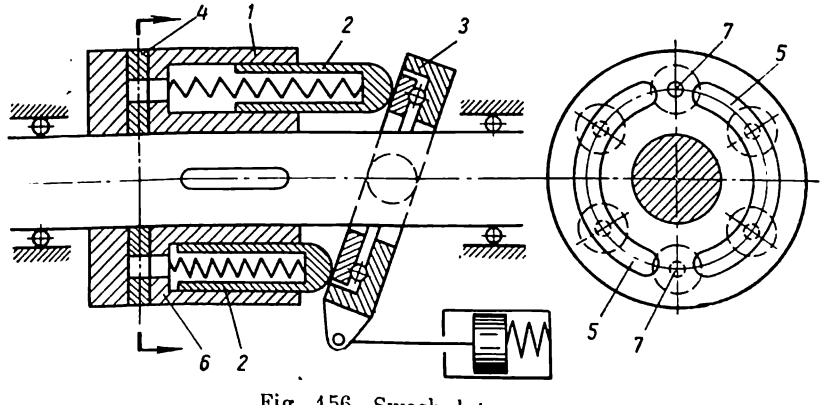

Fig. 156. Swashplate pump

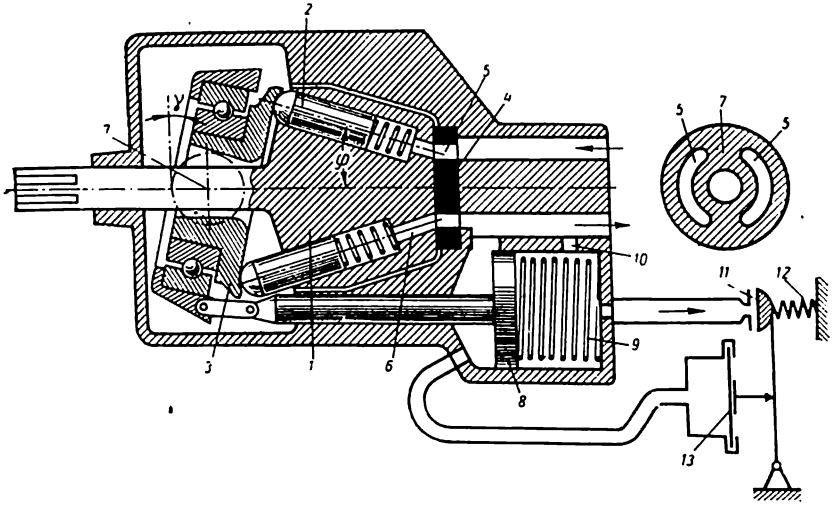

Fig. 157. Variable-displacement swashplate pump:
1 — cylinder barrel; *2* — pistons; *3* — swashplate; *4* — valve plate; *5* — ports; *6* — oil passages; *7* — plugs; *8* — piston; *9* — spring; *10* — jet; *11* — valve; *12* — spring; *13* — membrane

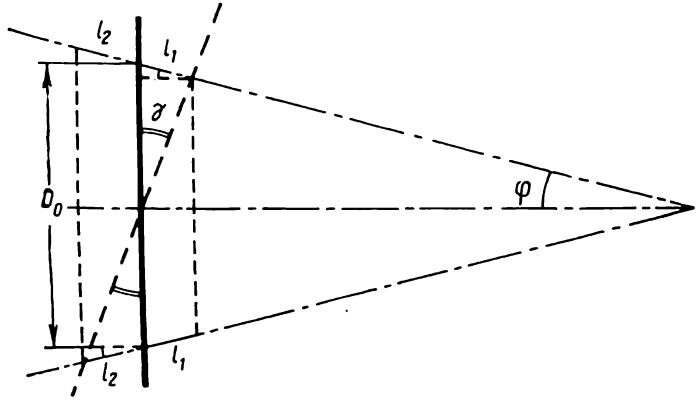

Fig. 158. Diagram for determining pump delivery

where D_0 = diameter of circle traced by piston head on swashplate at $\gamma = 0$.

Hence the piston stroke is

$$l = l_1 + l_2 = \frac{D_0}{2} \sin\gamma \left[\frac{1}{\cos(\varphi - \gamma)} + \frac{1}{\cos(\varphi + \gamma)} \right].$$

The theoretical mean displacement per second is given by the expression

$$Q_t = \frac{\pi d^2}{4} l \frac{zn}{60} = \frac{1}{480} \pi d^2 D_0 zn \sin\gamma \left[\frac{1}{\cos(\varphi - \gamma)} + \frac{1}{\cos(\varphi + \gamma)} \right]. \quad (13.7)$$

At $\varphi = 0$ this expression turns into the foregoing Eq. (13.6).

A diagrammatic sketch of an axial-piston pump with tilted cylinder barrel is presented in Fig. 159. The rotation is transmitted from the drive shaft to the cylinder barrel through a universal joint, which makes it possible to vary the angle between the primary shaft and the cylinder barrel. The cylinder barrel revolves against a swivel port plate with two semicircular ports for suction and discharge. The pistons are actuated by connecting rods carried in a socket ring mounted on the drive shaft.

The nonuniform discharge of positive-displacement pumps was mentioned before. An investigation of their kinematics shows that the relative stroke speed of a piston, as in the case of an ordinary reciprocating mechanism, can be approximately assumed proportional to the sine of the rotation angle α of the cylinder barrel. Delivery by each piston varies according to the sine law as a function of angle α and the time t. The total delivery by all pistons can be found by compounding the ordinates of the sine curves (Fig. 160).

The greater the number of pumping elements (pistons or vanes) the less the nonuniformity of delivery. An interesting feature is that delivery is much more uniform by an uneven number of pumping elements.

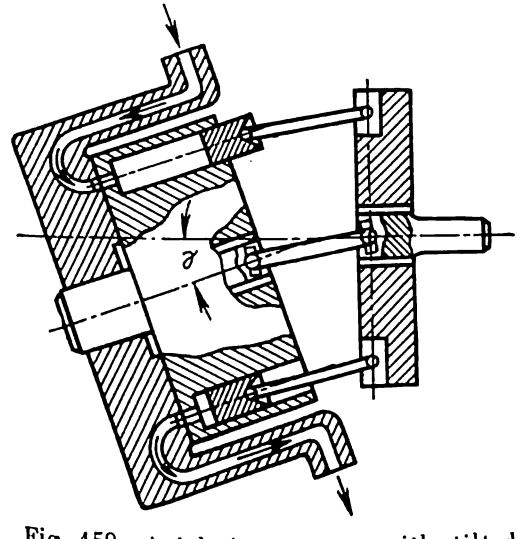

Fig. 159. Axial-piston pump with tilted cylinder barrel

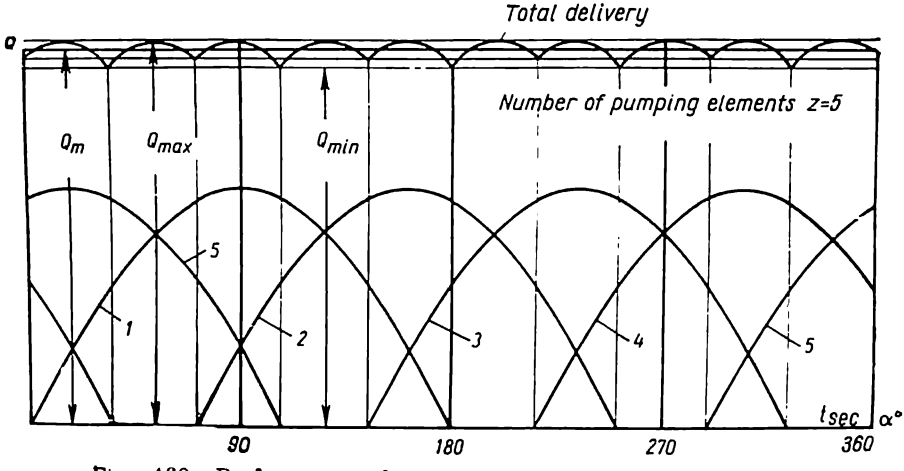

Fig. 160. Performance characteristics of a five-piston pump

Accordingly, piston pumps are usually made with five, seven or nine cylinders.

The degree of nonuniformity of delivery for an uneven number of pumping elements can be estimated according to the approximate formula developed by Soviet scientist N. S. Acherkan:

$$\sigma = \frac{Q_{max} - Q_{min}}{Q_m} 100 = \frac{125}{z^2} \text{ per cent.}$$

Vane and piston pumps can be designed to provide for varying displacement during operation without changing the rotative speed, merely by adjusting the eccentricity of the rotor of a vane or radial-piston pump or the swashplate or cylinder-barrel angle of an axial-piston pump.

62. CHARACTERISTICS OF ROTARY DISPLACEMENT PUMPS

In Secs 47 and 50 we defined the characteristic of a pump as the dependence of the head or pressure developed by the pump on its delivery (rate of discharge) for a constant rotative speed.

From Eq. (13.1), which holds for all rotary displacement pumps, it follows that the theoretical delivery does not depend on pressure. Therefore, the theoretical characteristic curve of such a pump in a coordinate system of p (or H) as a function of Q at n = const is represented by a straight line parallel to the ordinate axis into infinity. The theoretical characteristics of a displacement pump for two different rpm are shown in Fig. 161 by the dashed lines. They indi-

cate that, theoretically, any displacement pump is capable of developing any pressure, irrespective of the rotative speed or discharge. Because of leakage, however, the actual picture differs from the theoretical one. Any real pump has clearances of some size or other between moving and stationary parts, e.g., rotor, pumping elements, housing. The pressure produced by the pump forces some quantity of the fluid through the clearances in the opposite direction of the delivery, i.e., from the high-pressure to the low-pressure side. Leakage per second is denoted by the symbol q, the same as for centrifugal pumps.

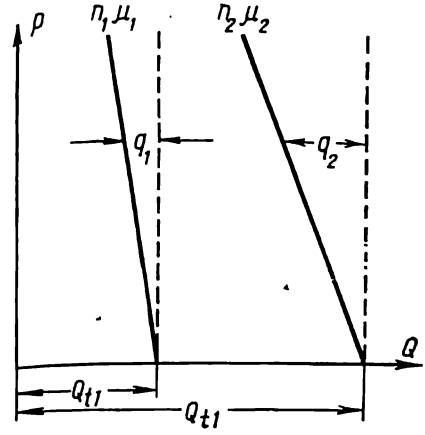

Fig. 161. Characteristics of a rotary pump for n_1, μ_1 and n_2, μ_2

In view of the very small clearances in rotary pumps, the flow regime through them is laminar. Therefore q varies as the pressure generated by the pump and inversely as the absolute viscosity of the fluid, though not in the first power but, as experiments show, in some power m less than unity. For gear pumps it may be assumed that $m = {}^1/_2$. There are no reliable data for other pumps, but presumably it is of the same order.

Thus, we have

$$q = A \frac{p_{pump}}{\mu^m}, \tag{13.8}$$

where A = constant depending on pump design and clearance spaces and, as experiments show, practically independent of the rotative speed.

The reason for m being less than unity is that a considerable degradation of energy takes place in leakage, the oil heats in the clearances and its viscosity becomes less than in the main stream.

The actual delivery Q of a pump, i.e., the rate of discharge into the pipeline, is less than the theoretical delivery Q_t by the amount of leakage, and consequently,

$$\text{or} \qquad Q = Q_t - q = \frac{Wn}{60} - A \frac{p_{pump}}{\mu^m}, \tag{13.9}$$

$$Q = \eta_v Q_t,$$

where η_v = volumetric efficiency of pump.

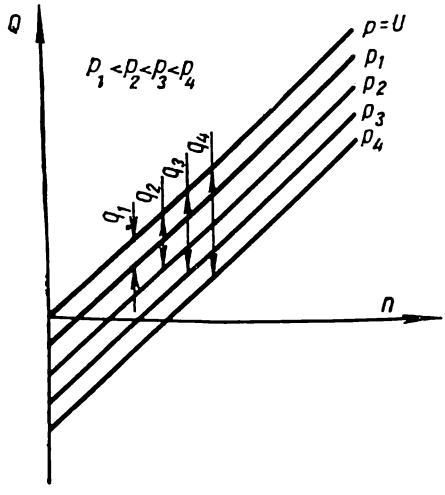

Fig. 162. Plot of pump delivery versus rpm

It follows from this that the actual characteristics of a rotary displacement pump, shown by solid lines in Fig. 161, are sloped straight lines intersecting the theoretical characteristics at $p_{pump} = 0$, i.e., on the axis of abscissas, where $q = 0$ and $Q = Q_t$.

The greater the viscosity of a hydraulic fluid the less the leakage and the steeper the characteristic curve. Deviations from the straight line that are sometimes observed are due to faults in pump operation, such as poor filling of the pump working spaces or cavitation.

Plotting of the actual characteristic of a displacement pump according to Eq. (13.9) suggests a method of calculating pump characteristics in going over from one set of operating conditions (n_1, μ_1) to another (n_2, μ_2):

Compute the new initial abscissas of the characteristic curves:

$$\frac{Q_{t1}}{Q_{t2}} = \frac{n_1}{n_2},$$

whence

$$Q_{t2} = Q_{t1}\frac{n_2}{n_1}. \tag{13.10}$$

Then express the ratio of leakage for equal pressures, i.e., for $p_{pump1} = p_{pump2}$,

$$\frac{q_1}{q_2} = \left(\frac{\mu_2}{\mu_1}\right)^m,$$

whence

$$q_2 = q_1\left(\frac{\mu_1}{\mu_2}\right)^m. \tag{13.11}$$

According to the obtained values of Q_{t2} and q_2, plot the new curve, as shown in Fig. 161, for the case when $n_2 > n_1$ and $\mu_2 < \mu_1$.

Test results of rotary pumps for a given $\mu = \text{const}$ are commonly represented in the form of Q as a function of the rotative speed n for several constant values of p_{pump} (Fig. 162). The result is several

more or less parallel straight lines (due to the independence of q on n), each corresponding to a constant p_{pump}. The higher the value of p_{pump} the greater the leakage and the lower the characteristic on the diagram.

As the characteristic of a displacement pump plotted for p as a function of Q is usually very steep, a decrease in delivery, say because of some increase in the resistance of the hydraulic system, may cause a substantial increase in pressure. Some safety device must be provided to protect the pump and the hydraulic system from a disastrous pressure increase if the flow drops.

Such a device may be an automatic relief or bypass valve (Fig. 163) which opens when pressure increases. The pump characteristic changes in this case as shown in Fig. 164. Section AB gives the pump performance when pressure is low and the valve is shut. Point B corresponds to the beginning of the opening of the valve, when the pressure developed by the pump equals the spring load per unit area of the valve. Pump delivery at section BC of the curve is

$$Q = Q_t - Q_{valve} - q,$$

where Q_{valve} = discharge through the valve.

Point C corresponds to the complete closure of the pipeline and the whole of the discharge passes back through the valve.

Much more efficient is so-called servomechanism control, illustrated schematically in Figs 156 and 157. When the pressure p_{pump} reaches a certain magnitude it pushes back piston *8* (Fig. 157) and compresses spring *9*. The swashplate angle γ decreases, the delivery drops and the pressure no longer increases. The corresponding characteristic curve is presented in Fig. 165. Between A and B the swashplate angle is maximum. At B it starts to decrease, and at C it is just large enough to enable the pump to compensate for leakage.

If the pressure in the servocylinder on the side of the spring (to the right of the piston in Figs 156 and 157) were constant and equal, say, to atmospheric pressure, the slope of the characteristic curve at section BC would be determined only by the stiffness of the spring. To obtain a very sloping curve the spring would have to be of small stiffness but considerable strength, i. e., large in size.

In order to reduce the size of the spring and at the same time to obtain a sloping curve at section BC the spring side of the servomotor cylinder is connected with the discharge port of the pump (see Fig. 157). The oil flows from the discharge port through passage *10* into the cylinder and out through valve *11* loaded by spring *12* and membrane *13*, which is subjected to the discharge pressure. When the swashplate angle is maximum (γ_{max}) valve *11* is closed and the pressure is the same on both sides of the piston and is equal to the discharge

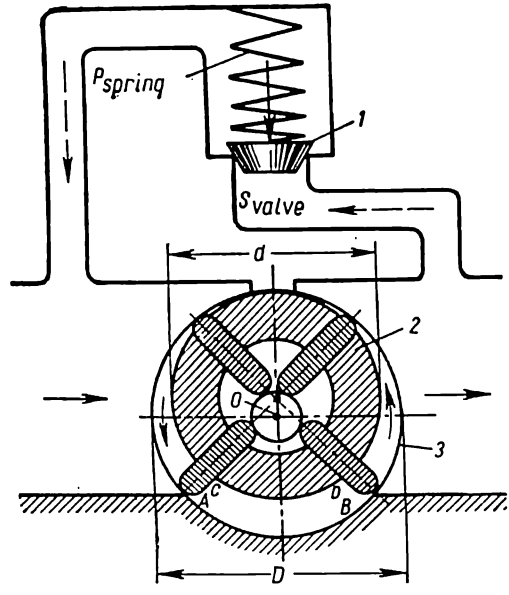

Fig. 163. Diagrammatic sketch of pump with bypass valve:
1 — bypass valve; *2* — rotor; *3* — housing

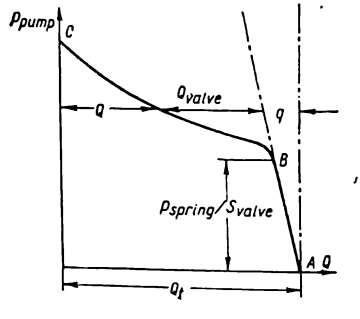

Fig. 164. Characteristic curve of pump with bypass valve

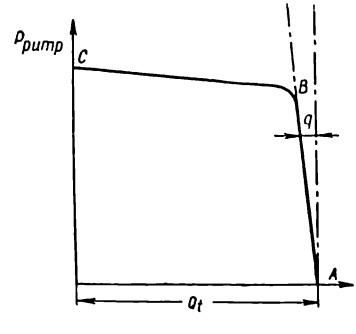

Fig. 165. Characteristic curve of variable-displacement pump

pressure. The swashplate is held inclined by the pressure of the spring and the liquid on the piston from right to left.

When the discharge pressure increases valve *11* opens, the oil starts flowing through the servomotor cylinder and the pressure there drops. The pressure of the oil, acting now from left to right, compresses the spring and reduces the swashplate angle.

Such control devices are used in fuel pumps for gas-turbine engines and aircraft hydraulic transmission pumps.

In conclusion, here are some data pertaining to the use of different types of rotary pumps in aeronautical engineering. Vane pumps have the least head delivery of all rotary pumps and are employed mainly as fuel pumps for piston aircraft engines and sometimes as oil pumps. Maximum pressure delivery of a vane pump is 10 to 20 atm.

Gear pumps can generate pressures of up to 100 atm, and pumps equipped with special devices for automatically reducing end clearances are capable of developing 150 to 200 atm. The disadvantage of the gear pump is that it is of necessity a constant-displacement pump. Therefore, when used in fuel systems or hydraulic transmissions, it must be provided with automatic relief or bypass valve.

Axial-piston pumps can be with variable displacement and they are capable of developing high pressures of up to 150-200 atm. They are widely used in fuel systems for gas-turbine engines (swashplate pumps) and in aircraft hydraulic transmissions (pumps with tilted cylinder barrel).

CHAPTER XIV

HYDRAULIC TRANSMISSIONS

A hydraulic transmission may be defined as a system of energy transmission by means of a fluid.

Any hydraulic transmission consists of two basic elements: a pump to convert mechanical work into hydraulic energy, and a hydraulic motor of reciprocating or rotary type to reconvert fluid energy into mechanical work. According to the motor kinematics, there are two main classifications of hydraulic transmissions: systems with intermittently operating (translational or reciprocating) motors, and systems with rotary motors. Both types are used in aviation engineering. Some examples of them will be described in this chapter.

63. TRANSLATIONAL HYDRAULIC ACTUATOR

The working element of a translational hydraulic transmission is essentially a cylinder with movable piston and rod. A typical hydraulic actuator used in aircraft design is shown schematically in Fig. 166. The solid lines denote the pipes along which oil flows during working operation, when the piston is moving up or down. The dashed lines denote the auxiliary piping.

Oil from a tank is pumped to high pressure and directed to a control valve which admits it to the desired side of the actuator cylinder (the lower end in Fig. 166). The oil pushes the piston up against the load P acting on the rod. Simultaneously, on the low-pressure side oil is emptied from the cylinder and returned through the respective ports of the spool valve to the tank.

Such hydraulic systems are widely used in aircraft for operating retractible undercarriages, flaps, ailerons, etc.

Such systems are powered by gear, radial-piston or swashplate pumps. Gear pumps are used with automatic relief valves which bypass the hydraulic fluid when peak pressure is reached.

Swashplate pumps are usually of the variable-displacement type which automatically adjust the delivery to maintain the required pressure in the hydraulic system.

An accumulator is commonly incorporated in hydraulic systems to cater for short-period peak demands above maximum pump capacity. This enables a relatively low-capacity pump to be used. Furthermore, in systems with automatic bypass an accumulator compen-

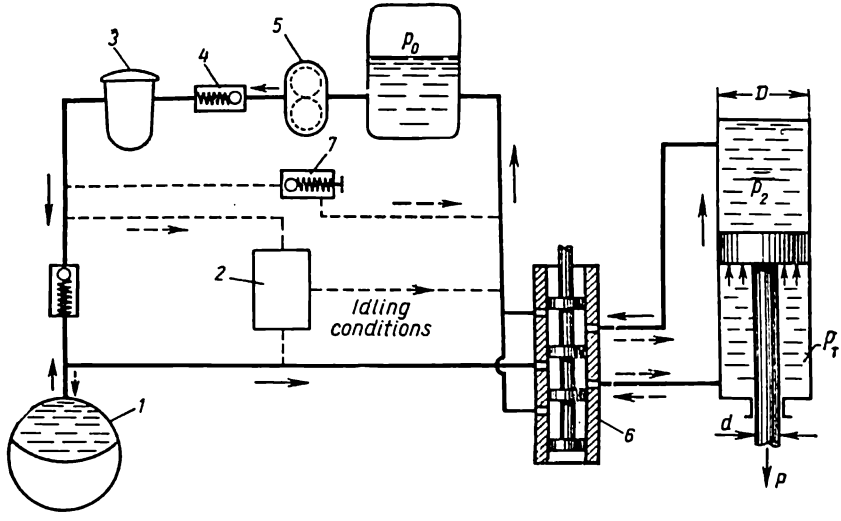

Fig. 166. Diagrammatic sketch of a translational hydraulic actuator:
1 — accumulator; *2* — automatic pump relief; *3* — filter; *4* — nonreturn valve; *5*—pump; *6* — control valve

sates for leakage from the high-pressure to the low-pressure side when the pump is idling.

Most Soviet aircraft systems use АМГ-10 hydraulic fluid consisting of heavy kerosene to which is added a special thickening fluid called vinipol to increase viscosity. The physical properties of АМГ-10 fluid are given in Table 1 (p. 24). At low temperatures the flow of АМГ-10 fluid through pipes is laminar. However, the relatively low viscosity of the fluid results in turbulence sometimes developing in a hydraulic system. Thus, in an undercarriage retracting system, if it is cold the regime in the low-pressure piping is laminar, while in the pressure line, where the fluid is warmer, the flow may be turbulent.

In calculating a hydraulic actuator it should be treated as a looping pipeline with pump delivery, the actuator cylinder representing a local disturbance causing a pressure drop Δp_{cyl} equal to the

pressure difference between both sides of the piston:

$$\Delta p_{cyl} = p_1 - p_2.$$

To a first approximation the delivery from the accumulator may be assumed zero, the piston displacement being due only to work done by the pump.* The pressure drop Δp_{cyl} can be expressed from the equilibrium equation for the cylinder. Referring to Fig. 166,

$$\frac{\pi}{4}(D^2 - d^2)\, p_1 = P + \frac{\pi D^2}{4} p_2,$$

whence

$$\Delta p_{cyl} = \frac{4P}{\pi (D^2 - d^2)} + \frac{d^2}{D^2 - d^2} p_2. \qquad (14.1)$$

The value of p_2 is approximately equal to the total pressure drop on the low-pressure side and, consequently, the second term in Eq. (14.1) is a function of the rate of discharge or of the velocity of the piston displacement.

Thus, the pressure required for a given system when the pump delivery is Q_{pump} must be found as the sum of the pressure drop Δp_{cyl} and the total pressure drop in the hydraulic system,

$$p_{req} = \Delta p_{cyl} + \Sigma p_{system}. \qquad (14.2)$$

In determining the hydraulic losses on the low-pressure side it should be taken into account that in the motion of a piston when the rod is on one side the rate of flow through the return piping Q_{ret} is not equal to the flow through the pressure line Q_{pump}, since the piston area on one side is greater than on the other. To compensate for this a coefficient a is introduced which is equal, when the piston moves up in Fig. 166, to

$$a = \frac{Q_{ret}}{Q_{pump}} = \frac{D^2}{D^2 - d^2}.$$

Let us consider the case of laminar flow in the return piping and turbulent flow in the pressure line. Then, using Eq. (14.1), taking into account the expression for a and grouping the terms according to their dependence on Q_{pump}, we obtain from Eq. (14.2)

$$p_{req} = \frac{4P}{\pi (D^2 - d^2)} + a^2 k_1 \gamma Q_{pump} + k_2 \gamma Q^2_{pump}. \qquad (14.3)$$

* Taking into account delivery from the accumulator presents no difficulties, all the more so that tests show that air expansion in the accumulator may be treated as an isothermal process.

The first term in the right-hand side of the equation represents the principal component in the expression for Δp_{cyl}, the second term represents the pressure loss in the return piping plus the second component in Eq. (14.1), and the third term is the pressure loss in the pressure line (from the tank to the cylinder). The meaning of the factors k_1 and k_2 is the same as in Sec. 43.

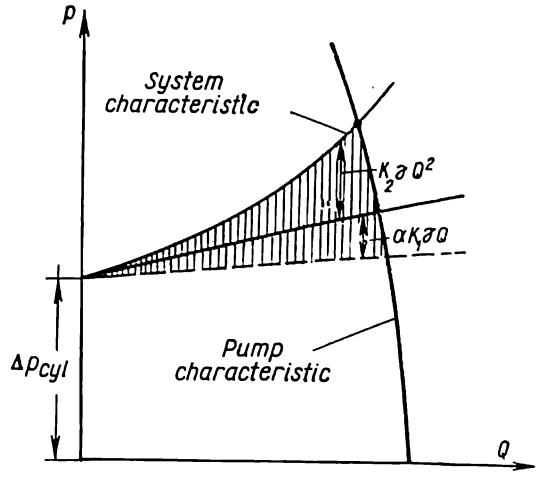

Fig. 167. Graphical determination of operating regime of a hydraulic transmission

This equation can be used to plot the characteristic curves of the system and the pump performance curve (Fig. 167). The intersection of the two curves gives the operating regime of the system, i. e., Q_{pump} and p_{pump}. If the load P along the rod does not change as the piston is moving, then the quotient of the cylinder displacement divided by the discharge yields the time required for the piston to travel from one extreme position to the other.

An aircraft undercarriage retracting system usually has three power cylinders joined in parallel. It must thus be treated as a compound looping pipeline and the methods of plotting the characteristic curves discussed in Sec. 46 applied in calculating it.

64. FOLLOW-UP SYSTEMS AND BOOSTERS

In a hydraulic actuator a piston simply travels from one extreme position to another against a load P acting along the piston rod.

In other cases the piston (rod) has to move according to a more complex law. Thus, in aircraft control systems the rod of the power cylinder must automatically "follow up" the motion of the control column, a specific position of the rod corresponding to every position of the control column. This is effected by means of a follow-up system incorporating a hydroamplifier, or booster. In such an arrangement the output force of the piston rod is much higher than the input load from the control column.

Power controls are employed in all modern high-speed airplanes and helicopters as the force required to actuate the flight controls is much greater than the pilot's strength.

A schematic diagram of a booster is presented in Fig. 168. When the pilot shifts the aircraft control column *1* say to the right, the control valve *2* moves to admit high-pressure oil to the left side of cylinder *4* through the upper passage *3* and permit low-pressure oil to flow out of the right side through the lower passage and into the return piping. Piston *5* moves to the right together with the valve housing *6* until the ports close. When the control column and valve move to the left pressure is supplied to the right side of the cylinder and the piston moves to the left.

Thus, the output linkage *7* attached to a control surface repeats the motion of valve *2* with much greater force than that applied by the pilot.

Let us investigate the principal characteristics of a booster as a power drive. We shall develop formulas for the force delivered by the output rod, the power developed by the system and its efficiency.

The pressure delivered to the booster is expended in overcoming the load P on the output rod and the hydraulic resistances:

$$p_o = \Delta p_{cyl} + \Sigma p, \tag{14.4}$$

where $p_o = p_{in} - p_{out}$ = pressure at booster intake minus pressure at outlet;

$\Delta p_{cyl} = p_1 - p_2 = \frac{P}{S}$ = pressure drop in the cylinder;

S = effective piston area (i. e., piston area less the cross-sectional area of the rod);

Σp = total pressure loss between intake and outlet.

Assuming the hydraulic losses to be mainly in the two partially closed valve ports and that they obey a quadratic law as a function

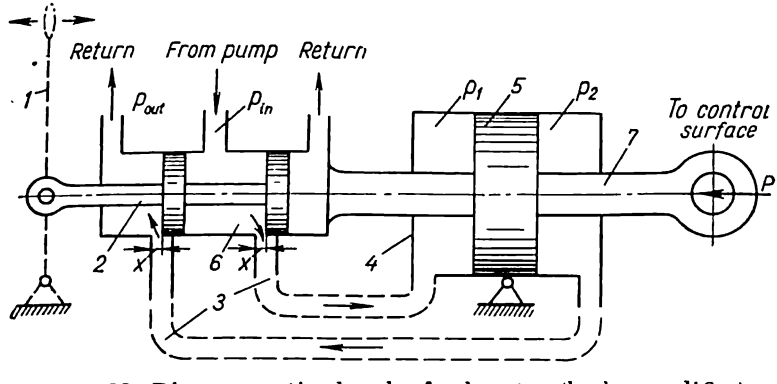

Fig. 168. Diagrammatic sketch of a booster (hydroamplifier):
1 — control column; *2* — control valve; *3* — passages; *4* — cylinder; *5* — piston; *6* —valve housing; *7* — output linkage

of the velocity (discharge), we may write

$$\Delta p = 2\zeta \frac{v^2}{2g} \gamma,$$

where ζ = loss coefficient of valve port;
v = velocity of flow through valve port.

As the valve ports are usually of rectangular cross-section of constant width b and variable length x, the continuity equation can be written in the form

$$Q = VS = vbx,$$

where V = piston velocity.

Expressing v in terms of Q and substituting into the formula for Σp, and then into (14.4), we obtain

$$p_0 = \Delta p_{cyl} + 2\zeta\gamma \frac{Q^2}{2g(bx)^2},$$

or

$$p_0 = \Delta p_{cyl} + k\frac{Q^2}{x^2}, \qquad (14.4')$$

where $k = \frac{\zeta\gamma}{gb^2}$.

The value of k may be assumed approximately constant and not dependent on the rate of discharge. If pressure is delivered by a variable-displacement constant-pressure pump (see Figs 157 and 165) and if hydraulic losses in the suction pipes can be neglected, then the pressure p_0 will be constant and equal to the pressure developed by the pump.

When no load is acting on the output rod ($P = 0$ and $\Delta p_{cyl} = 0$) and the valve ports are opened completely ($x = x_{max}$), the delivery (discharge) of the fluid into the booster actuator is $Q = Q_{max}$, and from Eq. (14.4′) we obtain

$$k = p_0 \frac{x^2_{max}}{Q^2_{max}}.$$

Substituting into Eq. (14.4) and solving for Δp_{cyl}, we have

$$\Delta p_{cyl} = p_0\left(1 - \frac{\overline{Q}^2}{\overline{x}^2}\right),$$

where $\overline{Q} = \frac{Q}{Q_{max}} = \frac{V}{V_{max}} = \overline{V}$ = relative rate of discharge, or

relative velocity of the output rod;

$\bar{x}=\frac{x}{x_{max}}$ = degree of opening of the valve ports.

From the foregoing, the load along the output rod is

$$P = \Delta p_{cyl} S = p_0 S \left(1 - \frac{\bar{Q}^2}{\bar{x}^2}\right), \tag{14.5}$$

and the relative load P is found by dividing P by $P_{max} = p_0 S$, i. e.,

$$P = \frac{P}{p_0 S} = 1 - \frac{\bar{Q}^2}{\bar{x}^2}. \tag{14.5'}$$

This equation makes it possible to plot a net of so-called static characteristics of the booster, that is, $\bar{P}$ as a function of $\bar{Q}$ for differ-

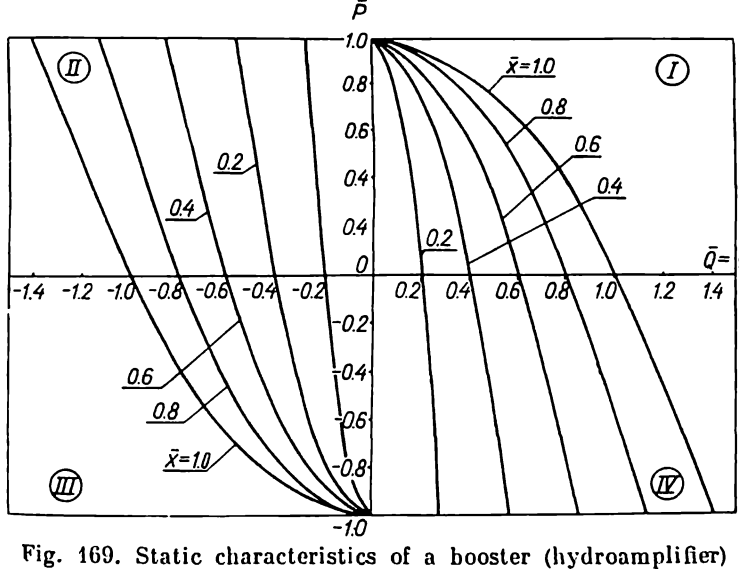

Fig. 169. Static characteristics of a booster (hydroamplifier)

ent values of $\bar{x}$ (Fig. 169). The diagram is plotted for positive and negative values of $\bar{Q}$ and $\bar{x}$, i. e., for the valve and shaft, and consequently the oil, moving in either direction.

It is seen from the diagram that the load on the output shaft approaches the maximum value $p_0 S$ only when the velocity of the shaft is small. The faster it moves the less the load it develops.

Where the curves intersect the axis of abscissas the load on the shaft changes its sign, i. e., it becomes a force pulling the shaft in

the direction of motion. The velocity increases and the cylinder operates as a pump. Thus, in quadrants I and III of the diagram the actuator operates as a hydraulic motor doing work against a load, in quadrants II and IV it operates as a pump delivering the oil in the same direction as the main pump.

Let us determine the efficiency η of the servomechanism as the ratio of the work done per second by the output rod to the fluid energy delivered to the actuator:

$$\eta = \frac{PV}{p_0 Q} = \frac{PV}{p_0 VS} = \frac{\Delta p_{cyl}}{p_0} = \overline{P}. \tag{14.6}$$

Consequently, the efficiency of the mechanism is numerically equal to the relative load on the rod and changes according to the same law as $\overline{P}$.

The effective power of the booster is

$$N = PV,$$

and the relative power is given by the ratio

$$\overline{N} = \frac{\overline{P}V}{p_0 S V_{max}} = \overline{P}\overline{V}.$$

Using Eq. (14.5′) and taking into account that $\overline{V} = \overline{Q}$, we obtain

$$\overline{N} = \left(1 - \frac{\overline{Q}_2^2}{\overline{x}^2}\right) Q. \tag{14.7}$$

Fig. 170 presents the curves of the relative power $\overline{N}$ as a function of $\overline{Q}$ for different values of $\overline{x}$ plotted according to Eq. (14.7).

Let us find the relative discharge $\overline{Q}$ at which the power is maximum. At $\overline{x} = 1$, instead of (14.7), we obtain

$$\overline{N}_{x=1} = (1 - \overline{Q}^2)\, Q.$$

Differentiating with respect to $\overline{Q}$ and equating the derivative to zero, we have

$$\frac{d\overline{N}}{d\overline{Q}} = 1 - 3\overline{Q}^2 = 0,$$

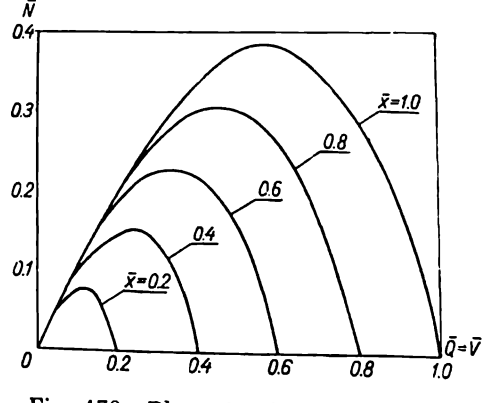

Fig. 170. Plot of relative power of a booster versus relative discharge

whence the optimum relative discharge

$$\overline{Q}_{opt} = \frac{1}{\sqrt{3}}$$

and the maximum relative power

$$\overline{N}_{max} = \left(1 - \frac{1}{3}\right)\frac{1}{\sqrt{3}} = \frac{2}{3\sqrt{3}}.$$

From Eqs (14.5′) and (14.6), the relative load on the rod and the efficiency are

$$\overline{P} = \eta = \frac{2}{3}.$$

The absolute value of the maximum power will be

$$N_{max} = \frac{2}{3\sqrt{3}} p_0 S V_{max} = \frac{2}{3\sqrt{3}} Q_{max} p_0,$$

where Q_{max} can be found from the expression for k developed before, viz.,

$$Q_{max} = x_{max}\sqrt{\frac{p_0}{k}}.$$

Substituting into the previous expression, we finally obtain

$$N_{max} = \frac{2}{3\sqrt{3}} = \frac{x_{max}}{\sqrt{k}} p_0^{3/2}.$$

Fig. 171 presents a schematic sketch of a hydrobooster with the control valve fitted inside the output rod. When valve *1* moves it admits through passages *7* high-pressure oil to one side of cylinder *3* and lets out low-pressure oil from the other side.

Other devices in aircraft servomechanisms may include:

(i) *A cylinder looping system*, which provides for the automatic connection of both sides of the cylinder if pressure in the system drops. This allows the pilot to operate the output rod by hand; the actuator does not work and acts merely as a kinematic link.

In Fig. 171 the cylinder is looped by means of a shuttle valve *5*. It is evident that when there is no pressure in the system the displacement of the piston by an external force causes the shuttles to open the ports through which oil can flow freely from one side of the cylinder to the other.

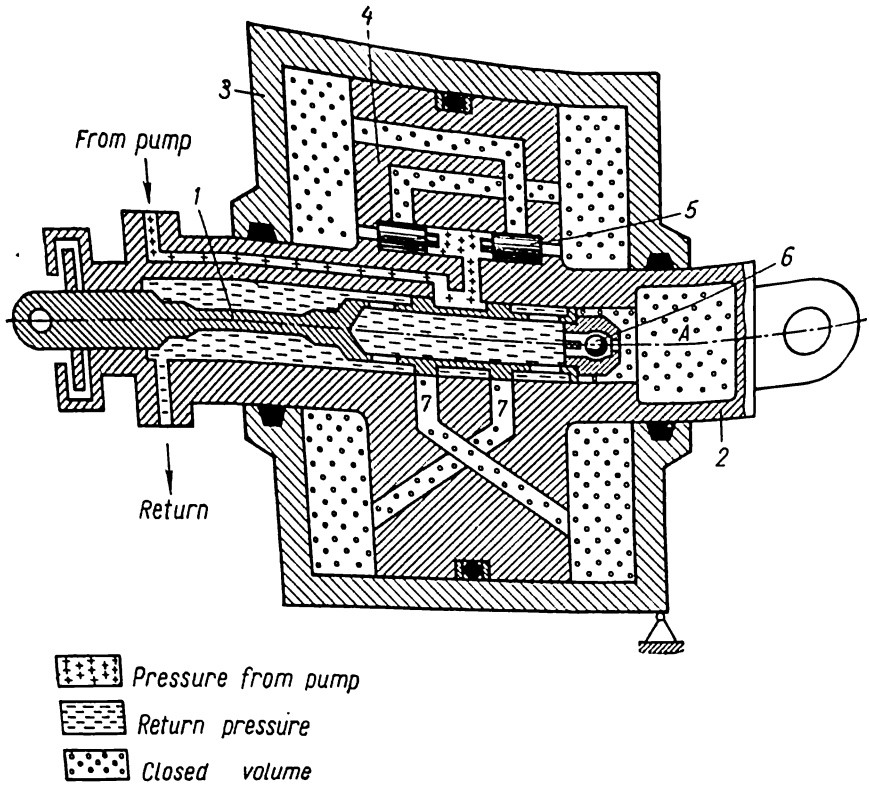

Fig. 171. Hydrobooster:

1 — control valve; *2* — output shaft; *3* — cylinder; *4* — piston; *5* — looping shuttles; *6* — damper valve; *7* — oil passages

(ii) *A control-valve damper*, which in Fig. 171 is a nonreturn ball valve *6*. The control valve with the ball operates as a pump removing the fluid from the damper *A*, where a vacuum is created. A constant one-way load is acting on the end of the control valve. As tests show, it prevents vibrations from developing in the booster.

Another power control mechanism is presented in Fig. 172. Here the control valve is placed outside the booster, with the valve housing rigidly attached to the output rod. The looping system is designed to operate in the following manner. When there is no pressure in the booster, looping valve *4* is pressed by a spring into its extreme left position (as shown in the drawing), connecting the left-hand and right-hand sides of the cylinder. If oil enters the booster under pressure, the looping valve moves to the right, closing port *5* and disconnecting the two sides of the cylinder.

The booster is built into an aircraft control system with or without feedback.

When feedback is provided a part of the load on the controls is transmitted to the pilot; without feedback the whole load is balanced by the hydraulic forces and nothing but friction in the control valve is felt at the control column.

Fig. 173 illustrates schematically a servomechanism with feedback. A system without feedback can be visualised if the feedback

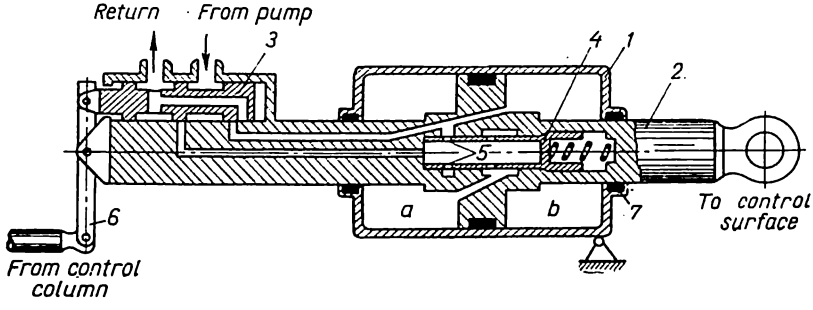

Fig. 172. Booster with external valve housing:
1 — cylinder; *2* — output shaft; *3* — control valve; *4* — looping valve; *5* — looping passages

linkage is assumed to be fixed rigidly and the axis of rotation of the rocker is shifted from A to B.

Example. *Given* (see Fig. 173):
cylinder bore $D = 50$ mm;
output rod diameter $d = 30$ mm;
efficiency $\eta = 0.9$;
load from controls $F = 960$ kg;

$$\text{arm ratio: } \frac{a}{b}=4,\ \frac{c}{e}=3,\ \frac{e}{f}=4,\ \frac{g}{h}=3/2.$$

To determine: (1) Pressure at booster input if pressure in return pipe $p_{ret}=3$ kg/cm².
(2) Load f_1 kg on control column with and without pressure in booster.
Solution. (i) Determine force P acting on output rod:

$$P=F\,\frac{g}{h}\,\frac{e-f}{e}=960\,\frac{3}{2}\left(1-\frac{1}{4}\right)=1{,}080\text{ kg.}$$

(ii) Determine pressure p_0 at input. As

$$P=\frac{\pi}{4}\,(D^2-d^2)\,(p_0-p_{ret})\,\eta,$$

then

$$p_0=\frac{4P}{\pi\eta\,(D^2-d^2)}+p_{ret}=\frac{4\times1{,}080}{3.14\times0.9\,(5^2-3^2)}+3=98.5\text{ kg/cm}^2.$$

(iii) Determine load on control column when there is pressure in the booster. Transmission ratio (so-called feedback factor):

$$i_1 = \frac{b}{a}\frac{e}{c}\frac{f}{e}\frac{g}{h} = \frac{1}{4}\times\frac{1}{3}\times\frac{1}{4}\times\frac{3}{2} = \frac{1}{32}.$$

Load on control column:

$$f_1 = i_1 F = \frac{1}{32}960 = 30 \text{ kg}.$$

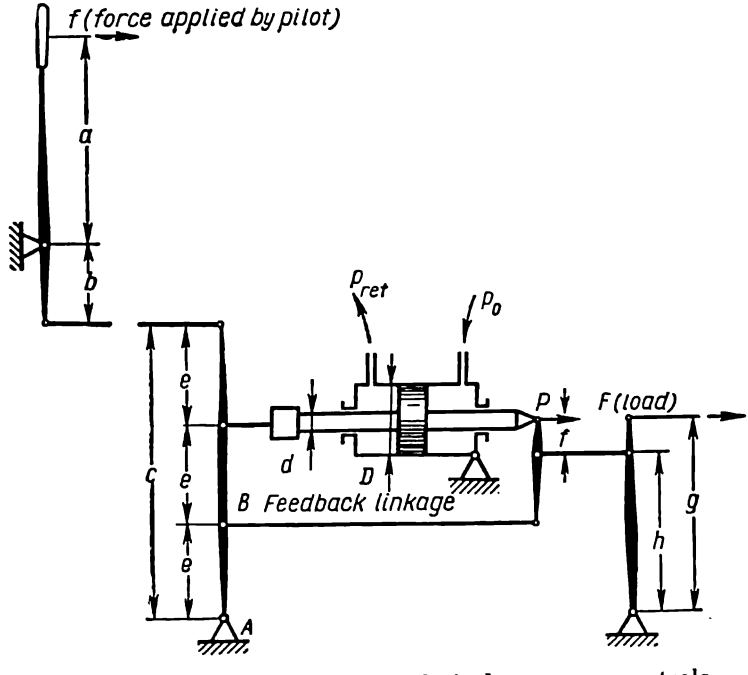

Fig. 173. Diagrammatic sketch of airplane power controls

(iv) Determine load on control column when there is no pressure in the booster. In this case the transmission ratio is

$$i_2 = \frac{b}{a}\frac{h}{c}\frac{g}{h} = \frac{b}{a}\frac{c-e-f}{c}\frac{g}{h} = \frac{7}{32}.$$

The load on the control column

$$f_2 = i_2 F = \frac{7}{32}960 = 210 \text{ kg},$$

which means that manual control of the aircraft is impossible and a power source must be provided for in case of failure of the hydraulic system.

65. ROTARY HYDRAULIC TRANSMISSIONS

According to the accepted classification of pumps into rotodynamic and positive-displacement machines, rotary hydraulic transmissions may also be classified into rotodynamic, or hydrokinetic, and positive-displacement or, to be more precise, rotary positive-displacement transmissions. We shall first discuss the latter group.

Rotary displacement hydraulic transmissions represent a combination of a pump and a rotary displacement hydraulic motor. The motor is essentially a pump working as an actuator. All rotary displacement pumps possess this quality of reversibility and can be used either as a pump or as a motor. This means that if hydraulic fluid is supplied to a rotary pump under sufficient pressure its rotor will revolve and do work.

The main advantage of rotary hydraulic transmissions, as compared with conventional mechanical systems, is their ability to allow for a smooth, stepless change in transmission ratio and torque conversion, which will be shown later on.

Fig. 174 presents a block diagram of a simple rotary displacement hydraulic transmission (hydraulic drive) incorporating a pump, hydromotor, oil tank and connecting pipelines. The tank is essential to compensate for external leakage and temperature changes of the fluid volume, and also to reduce heating in the working process. Furthermore, pressurisation of the tank creates conditions in the suction piping needed to prevent cavitation in the pump.

A hydraulic circuit could be made without a tank in the main loop, but this reduces cooling conditions. The tank would be joined to the system as in the case of a looping pipeline (see Fig. 124) and it would have to be pressurised by a booster pump.

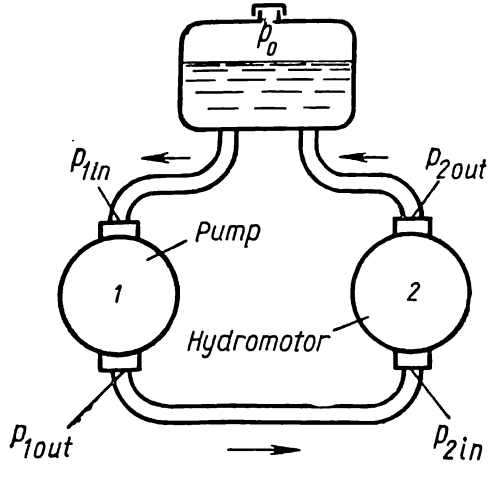

Fig. 174. Diagrammatic sketch of a rotary displacement hydraulic transmission

Let us investigate the basic relationships in a hydraulic system operating according to the scheme in Fig. 174, the subscript 1 referring to the pump and the subscript 2 to the hydromotor.

The useful delivery of the pump is equal to the actual discharge through the hydromotor, i. e.,

$$Q_1 = Q_2. \qquad (14.8)$$

Going over from actual to theoretical discharge and taking into account that the actual discharge through the hydromotor is greater than the theoretical, as leakage in the motor is in the direction of the main stream, we obtain instead of Eq. (14.8)

$$Q_{t1}\,\eta_{v1} = \frac{Q_{t2}}{\eta_{v2}}$$

where η_{v1} = volumetric efficiency of pump;
η_{v2} = volumetric efficiency of hydromotor, which is conventionally defined as the ratio of the theoretical discharge to the actual discharge.

Hence, the volumetric efficiency η_{vtr} of the hydraulic system is

$$\eta_{vtr} = \eta_{v1}\eta_{v2} = \frac{Q_{t2}}{Q_{t_1}}. \tag{14.9}$$

Assuming a variable-displacement pump and hydromotor we introduce a regulation factor ψ; for pumps and motors with eccentric rotors (see Sec. 60) $\psi = \frac{e}{e_{max}}$.

For rotary piston hydromachinery $\psi = \frac{\tan\gamma^*}{\tan\gamma_{max}}$. Evidently, in regulating hydromachinery the factor can vary from zero to unity.

Then, expressing the theoretical discharge in terms of the maximum working volumes W, the factor ψ, and the rotative speeds n, we obtain

$$\eta_{vtr} = \frac{\Psi_2 W_2 n_2}{\Psi_1 W_1 n_1} = \frac{\Psi_2 W_2}{\Psi_1 W_1}\frac{1}{i}, \tag{14.10}$$

where i = transmission ratio, equal to

$$i = \frac{n_1}{n_2} = \frac{\Psi_2 W_2}{\Psi_1 W_1}\frac{1}{\eta_{vtr}}. \tag{14.10'}$$

Owing to hydraulic losses in the piping, the pressure p_1 developed by the pump is greater than the pressure p_2 utilised by the hydromotor. The ratio of the latter to the former is called the hydraulic efficiency of the transmission

$$\eta_{htr} = \frac{p_2}{p_1}. \tag{14.11}$$

---

* If the pistons are at an angle ψ to the axis of rotation the factor ψ can be expressed in the same way with sufficient accuracy.

It should be borne in mind that here (see Fig. 174)

$$p_1 = p_{1out} - p_{1in};$$
$$p_2 = p_{2in} - p_{2out}.$$

Subtracting the second equation from the first, we obtain

$$p_1 - p_2 = (p_{1out} - p_{2in}) + (p_{2out} - p_{1in}) = \Sigma p_{pipe},$$

i. e., the difference between the pressure produced by the pump and the pressure utilised by the hydromotor is equal to the total loss of pressure in the pipeline (in the pressure, suction and return pipes).

Now write the energy equations for the pump and hydromotor in terms of the power N_1 needed to drive the pump shaft and the power N_2 developed by the hydromotor. Taking into account Eq. (12.4), for the pump we have

$$N_1 = T_1\omega_1 = \frac{p_1 Q_1}{\eta_{v1}\eta_{m1}}, \tag{14.12}$$

and for the hydromotor

$$N_2 = T_2\omega_2 = p_2 Q_2 \eta_{v2}\eta_{m2}, \tag{14.13}$$

where T = torque;

ω = angular velocity;

η_m = mechanical efficiency taking into account friction.

The hydraulic efficiency of rotary hydromachinery, whether pumps or motors, is commonly assumed to be unity, since the main losses are volumetric and mechanical, the hydraulic losses being included in the latter.

The overall efficiency of a hydraulic transmission is found by dividing Eq. (14.13) by Eq. (14.12):

$$\eta_{tr} = \frac{N_2}{N_1} = \frac{T_2\omega_2}{T_1\omega_1} = \frac{k}{i}, \tag{14.14}$$

where k = torque conversion factor.

On the other hand, taking into account Eqs (14.8) and (14.11), division gives

$$\eta_{tr} = \frac{p_2}{p_1}\eta_{v1}\eta_{v2}\eta_{m1}\eta_{m2} = \eta_{htr}\eta_{vtr}\eta_{mtr} = \eta_h\eta_1\eta_2, \tag{14.15}$$

i. e., the overall efficiency of a hydraulic transmission equals the product of its hydraulic, volumetric and mechanical efficiencies, or the product of the hydraulic efficiency (which takes into account

losses in the connecting pipelines) times the total pump efficiency and the total motor efficiency.

The overall efficiency of rotary hydraulic transmissions is usually 0.7-0.85.

Hydraulic transmissions may be regulated to change the transmission ratio i or the torque conversion factor k in one of the following ways:

(i) pump regulation (by changing eccentricity or swashplate or cylinder-barrel angle);

(ii) hydromotor regulation (by changing eccentricity or swashplate or cylinder-barrel angle);

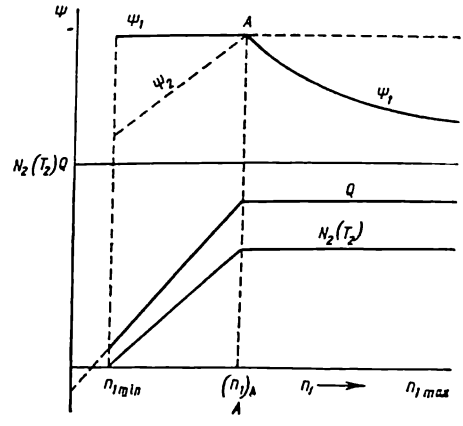

Fig. 175. Performance characteristics of an adjustable hydraulic transmission

(iii) bypassing part of the discharge from the pump through a valve.

The first method is most commonly employed, and hydraulic transmissions usually include a variable-displacement pump and a constant-displacement hydromotor. The second method may be used to supplement the first, in which cases both pump and motor are of the variable-displacement type. The third method of regulation is uneconomical and can be usefully employed only in hydraulic transmissions operating for short intervals.

The most important application of rotary positive-displacement systems in aircraft is for driving stable-frequency a-c generators from the aircraft engines. The generators must have a constant angular velocity which does not depend on changes in the rotative speed of the engine or the load in the electric system. Under such conditions the rotative speed of the hydromotor connected with the generator is $n_2 = \text{const}$, while the rotative speed of the pump n_1 changes within certain limits, depending on the type of engine. Consequently, the transmission ratio of the hydraulic system must change automatically and smoothly.

Fig. 175 presents the performance characteristics of such a hydraulic transmission, in which the coefficients ψ_1 and ψ_2, the discharge Q and the power N_2 (as well as the torque T_2) are functions of the rotative speed n_1 of the input shaft (of the pump) when the pressure and rpm n_2 are constant.

The vertical A-A corresponds to the case of maximum displacement of both hydromachines, i. e., $\psi_1 = \psi_2 = 1$. To the right of A-A is the pump control region in which ψ_1 decreases according to a

hyperbolic law [see Eq. (14.10′)] to the left of A-A is the motor control region in which ψ_2 increases according to a linear law.

The discharge is given by the formula

$$Q = \Psi_1 W_1 n_1 - q = \Psi_2 W_2 n_2 + q,$$

and, consequently, in the diagram for $p_1 = p_2 = p = \text{const}$ it is represented by a straight line with a bend at A-A. This means that in regulating a pump the discharge does not change while in regulating a hydromotor it decreases along a straight line.

The effective power N_2 of the hydromotor is determined by Eq. (14.13), with the assumptions made, and is represented graphically in approximately the same way as the discharge; the torque is represented in the same way as the power.

The minimum rotative speed n_{1min} of the input shaft and ψ_{2min} are determined by the self-braking of the hydromotor, i.e., by the equality $T_2 = 0$.

The maximum rotative speed n_{1max} and ψ_{1min} are determined by the limiting capacity of the pump according to rpm. For modern rotary piston pumps $n_{1max} \approx 4{,}500$ rpm.

Applying Eq. (14.10′) to the operating conditions of the transmission when $\psi_1 = \psi_2 = 1$ and $n_1 = (n_1)_A$, and then to the operating conditions for n_{1max} and dividing the one equation by the other, we obtain

$$\frac{n_{1max}}{(n_1)_A} = \frac{1}{(\Psi_1)_{min}}.$$

This rpm ratio is called the rpm regulation range for constant capacity.

Assuming, as is frequently done, that $n_2 = (n_1)_{max}$, from Eq. (14.10′)

$$\Psi_{1min} = \frac{W_2 n_2}{W_1 n_{1max} \eta_v} \frac{1}{} = \frac{W_2}{W_1} \frac{1}{\eta_v},$$

or

$$\frac{n_{1max}}{(n_1)_A} = \frac{W_1}{W_2} \eta_v.$$

This means that if we wish to provide a regulation range with constant power equal to, say, two, pump displacement must be approximately twice that of the hydromotor.

The rpm regulation range, as is clear from the foregoing, can be expanded by regulating the hydromotor, but in this case the power will change as well.

Besides such simple hydraulic transmissions, so-called differential transmissions are used, in particular to drive aircraft synchron-

ous generators. Such a transmission is a combination of a differential gear train and a hydraulic transmission. When operating in the rated regime the total power is transmitted mechanically through a planetary gear train and the hydraulic transmission idles. When the rotative speed of the input shaft deviates from the rated speed the hydraulic transmission is cut in to contribute additional power or take off excess power, as the case may be. Of course, there are other types of differential hydraulic transmissions based on different principles.

66. ROTODYNAMIC TRANSMISSIONS

Rotodynamic, or hydrokinetic, transmissions represent a combination of a centrifugal pump and a hydroturbine, with the pump impeller and turbine runner brought close together in the same case.

To these belong *fluid couplings* (fluid drives or hydraulic clutches) and *torque converters*. The basic difference between the two is that the torque output of a fluid coupling is equal to the torque input. If it is desired to multiply or reduce the torque, a torque converter is used.

A fluid coupling is shown schematically in Fig. 176*a*, where *1* is the input shaft, *2* is the output shaft, *3* is the pump impeller and *4* is the turbine runner. When the pump impeller, which is mounted on the driving shaft, starts turning, oil in the coupling is thrown outward and enters the turbine runner.

The flow actuates the turbine runner, imparting to it the energy received by the oil in the pump impeller. The oil recirculates in a closed path inside the coupling and power is transmitted from one shaft to the other though there is no rigid connection between them.

Neglecting friction of the outer surfaces of the rotors on the fluid, the torques of the input and output shafts are equal, i. e.,

$$T_1 = T_2, \tag{14.16}$$

and the efficiency of the coupling η_{fc} is consequently determined by the rpm ratio:

$$\eta_{fc} = \frac{n_1}{n_2} = \frac{1}{i}. \tag{14.17}$$

The difference between unity and coupling efficiency is called the slip

$$s = 1 - \eta_{fc}.$$

Fluid couplings are commonly designed to provide for only a few per cent slip (about 2-4 per cent) when operating in the rated steady regime, the transmission, ratio and coupling efficiency being almost unity. However, when the transmitted torque is greater than the rated torque (i. e., the load is excessive) the slip increases, the rotative speed of the turbine runner decreases and efficiency drops.

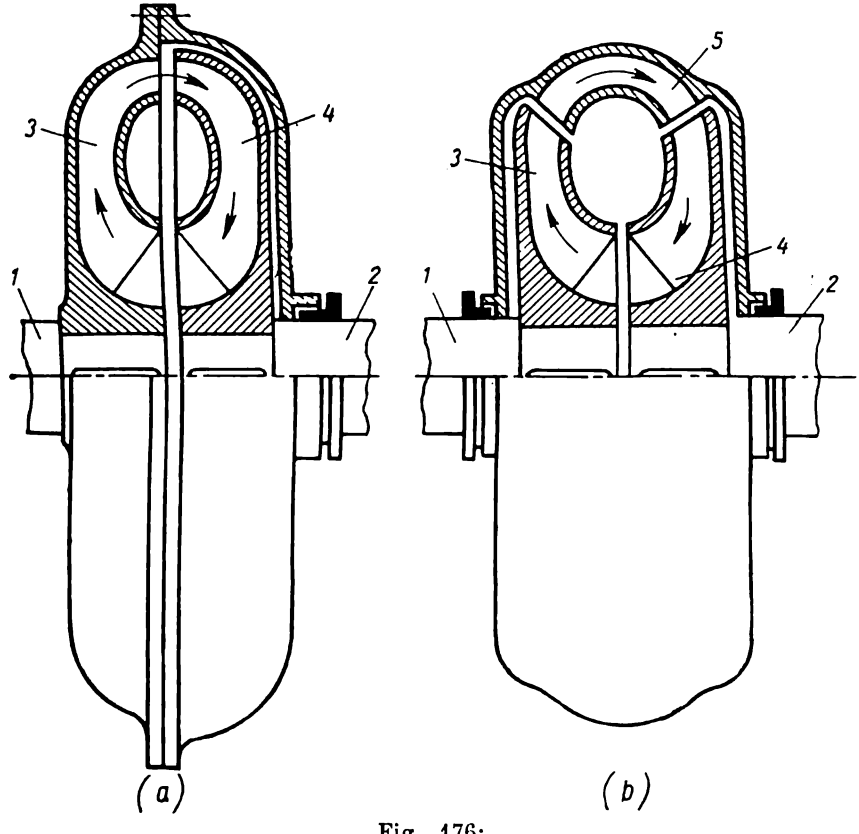

Fig. 176:
a — fluid coupling; *b* — torque converter

Torque converters are used when it is necessary to change the torque and develop a transmission ratio other than unity while retaining appreciable efficiency. An additional feature of the torque converter is the so-called reactor, which consists of a series of fixed guide vanes attached to the housing. In Fig. 176*b*, the reactor is numbered *5*, the other numbers corresponding to those of the fluid coupling in Fig. 176*a*.

For the torque converter we have, instead of Eq. (14.16),

$$T_1 + T_r = T_2$$

where T_r is the torque applied by the reactor.

As written down here, T_r is positive when output rotative speed is smaller, and torque greater, than the respective input speed and torque, and negative when the output speed is higher and torque is smaller. Thus, in the first case the reactor enhances the whirl produced by the impeller, which results in a higher torque T_2, in the second case it reduces the whirl.

The efficiency of a torque converter is given by the same expression as for a rotary positive-displacement transmission:*

$$\eta_{tc} = \frac{T_2 n_2}{T_1 n_1},$$

or, taking into account Eq. (14.17) and the torque conversion factor k,

$$\eta_{tc} = k\eta_{fc}.$$

In Fig. 177, the efficiency of a fluid coupling (η_{fc}) and a torque converter (η_{tc}) is plotted as a function of the speed ratio $\frac{n_2}{n_1}$ for $k > 1$.

The former, according to Eq. (14.17), is a straight line, the latter is a curve with a maximum at $\frac{n_2}{n_1}$ approximately equal to 0.5.

A comparison of the two curves shows that the torque converter is more economical than the fluid coupling at high transmission ratio i $\left(\text{low } \frac{n_2}{n_1}\right)$. Conversely, when i approaches unity the coupling is more economical. The main advantage of the torque converter over the fluid coupling at high values of i, however, lies in its ability to increase the torque, which is often very much desired.

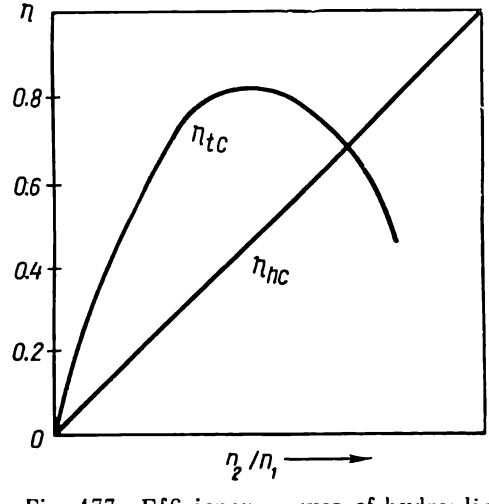

Fig. 177. Efficiency curves of hydraulic coupling and torque converter

* The rotary hydraulic transmissions described in Sec. 65 are essentially also torque converters, but of the rotary displacement type.

Rotodynamic transmissions are finding growing application in ground vehicles (automobiles, tractors, etc.) and ship installations whenever it is necessary to develop an increased torque on the output shaft to start a vehicle from rest. As the vehicle accelerates the transmission ratio decreases smoothly, and then the input shaft is either connected directly with the output shaft or the torque converter automatically begins to operate as a fluid coupling. This is achieved by a mechanism which causes the reactor to rotate together with the pump impeller or turbine runner.

In aircraft rotodynamic couplings are used to transmit torque from the starter engine to the rotor of the main gas-turbine engine.

DIFFERENTIAL EQUATIONS OF IDEAL FLUID FLOW AND THEIR INTEGRATION

1. DIFFERENTIAL EQUATIONS OF IDEAL FLUID FLOW

Let us show that the fundamental equations of hydrostatics and Bernoulli's equation for the cases discussed before can be developed by integrating the differential equations of ideal fluid flow. We shall develop these equations and then integrate them for the main special cases of equilibrium and motion.

In a steady stream of an ideal fluid take an arbitrary point M whose coordinates are x, y, z (Fig. 178). In some differential time interval dt a fluid particle will move from point M to point M'. The displacement is dl, and its projections on the coordinate axes are dx, dy, dz. The segment dl is thus a pathline element which, in the case of steady motion, coincides with the stream line.

With dl as the diagonal, construct a rectangular parallelepiped having sides dx, dy, dz parallel to the coordinate axes.

Let us develop the differential equation of the fluid volume, the mass of which is $\rho dxdydz$.

Let the components of the unit body force acting on the fluid at point M be X, Y and Z. Then the body forces acting on the

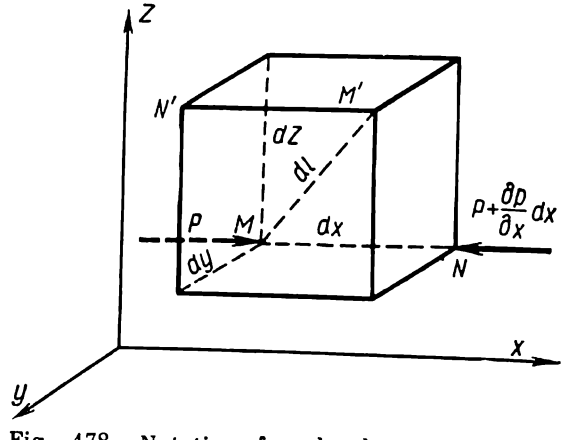

Fig. 178. Notation for developing differential equations of motion of an ideal fluid

parallelepiped in the direction of the coordinate axes are equal to these components times the mass of the fluid volume.

Denoting by v the velocity of the fluid at point M and by v_x, v_y, v_z its respective components, the corresponding components of the acceleration will be given in the form

$$\frac{dv_x}{dt}; \quad \frac{dv_y}{dt}; \quad \frac{dv_z}{dt}.$$

Let the pressure at M be p. It is a function of the coordinates x, y, z. However, in going over from point M to, say, N (see Fig. 178), only the x coordinate changes, by the infinitesimal dx, and the function p receives an increment equal to the partial differential

$$\frac{\partial p}{\partial x} dx.$$

Therefore, the pressure at N will be equal to

$$p + \frac{\partial p}{\partial x} dx.$$

The pressure at other corresponding points on the edges normal to the x axis, for instance at N' and M', we find, differs by the same value (to an accuracy of infinitesimals of higher orders), equal to

$$p - (p + \frac{\partial p}{\partial x} dx) = -\frac{\partial p}{\partial x} dx.$$

In view of this the difference between the pressure forces acting on the volume in the x direction is

$$-\frac{\partial p}{\partial x} dxdydz.$$

The equations of motion of the volume in terms of the projections on the coordinate axes are

$$\varrho dxdydz \frac{dv_x}{dt} = X \varrho dxdydz - \frac{\partial p}{\partial x} dxdydz;$$

$$\varrho dxdydz \frac{dv_y}{dt} = Y \varrho dxdydz - \frac{\partial p}{\partial y} dxdydz;$$

$$\varrho dxdydz \frac{dv_z}{dt} = Z \varrho dxdydz - \frac{\partial p}{\partial z} dxdydz.$$

Dividing these equations through by the elemental mass $\varrho dxdydz$ and going over to the limit, in which dx, dy and dz tend to zero and

the volume, therefore, tends to the initial point M, we obtain the flow equations referred to point M:

$$\left.\begin{aligned} \frac{dv_x}{dt} &= X - \frac{1}{\varrho}\frac{\partial p}{\partial x}; \\ \frac{dv_y}{dt} &= Y - \frac{1}{\varrho}\frac{\partial p}{\partial y}; \\ \frac{dv_z}{dt} &= Z - \frac{1}{\varrho}\frac{\partial p}{\partial z}. \end{aligned}\right\} \tag{A.1}$$

These equations were developed in 1755 by Leonhard Euler and bear his name. The terms represent the corresponding accelerations, the meaning of each equation being that the total acceleration of a particle along a coordinate axis is the sum of the acceleration due to body forces and the acceleration due to pressure forces.

Euler's equation is valid in this form for both incompressible and compressible fluids, as well as when gravity is the only acting body force and for relative motion of a fluid. In the latter case the quantities X, Y and Z must include the components of the acceleration in the transport or rotational motion.

For a motionless fluid,

$$\frac{dv_x}{dt} = \frac{dv_y}{dt} = \frac{dv_z}{dt} = 0,$$

and Euler's equations take the form

$$\left.\begin{aligned} X - \frac{1}{\varrho}\frac{\partial p}{\partial x} &= 0; \\ Y - \frac{1}{\varrho}\frac{\partial p}{\partial y} &= 0; \\ Z - \frac{1}{\varrho}\frac{\partial p}{\partial z} &= 0. \end{aligned}\right\} \tag{A.2}$$

These are the differential equations for fluid equilibrium.

2. FORCE FUNCTION. EQUIPOTENTIAL SURFACE

Let us use the differential equations obtained in the previous section to investigate some questions of fluid equilibrium.

Multiplication of each of Eqs (A.2) by dx, dy and dz, respectively, and their addition yields

$$X\,dx + Y\,dy + Z\,dz = \frac{1}{\varrho}\left(\frac{\partial p}{\partial x}\,dx + \frac{\partial p}{\partial y}\,dy + \frac{\partial p}{\partial z}\,dz\right). \tag{A.3}$$

The term in parentheses in the right-hand side of this equation is the total differential of the function $p\ (x,\ y,\ z)$, i. e.,

$$\frac{\partial p}{\partial x}\,dx + \frac{\partial p}{\partial y}\,dy + \frac{\partial p}{\partial z}\,dz = dp,$$

and Eq. (A.3) can be rewritten in the form

$$X\,dx + Y\,dy + Z\,dz = \frac{1}{\varrho}\,dp. \qquad (A.3')$$

We may conclude from this that the left-hand side of Eq. (A.3′) must be the total differential of some function $U\ (x,\ y,\ z)$. This function must possess the following property: the partial derivatives with respect to it along the x, y and z coordinates must be equal to X, Y and Z, respectively, i. e.,

$$\frac{\partial U}{\partial x} = X; \quad \frac{\partial U}{\partial y} = Y; \quad \frac{\partial U}{\partial z} = Z.$$

The function U is called a force function. It will be recalled from the course in theoretical mechanics that it equals the force potential taken with the sign reversed.

The conclusion is that fluid equilibrium is possible only under the action of body forces possessing potential energy. Introducing the function U into the basic Eq. (A.3′), we obtain

$$\frac{\partial U}{\partial x}\,dx + \frac{\partial U}{\partial y}\,dy + \frac{\partial U}{\partial z}\,dz = \frac{1}{\varrho}\,dp,$$

or

$$dU = \frac{1}{\varrho}\,dp. \qquad (A.4)$$

Integrating, we obtain in general form

$$p = \varrho U + C. \qquad (A.5)$$

The integration constant is found from the boundary conditions. If, at $U = U_0$, $p = p_0$, then,

$$p = p_0 + \varrho\,(U - U_0). \qquad (A.5')$$

A surface satisfying the condition

$$U\,(x, y, z) = 0$$

is called an equipotential surface. It follows from Eqs (A.4) and (A.5′) that for all points of such a surface the condition

$$dp = 0$$

holds, or

$$p(x,y,z) = \text{const.}$$

Hence, an equipotential surface is also a surface of equal pressure.

Furthermore, it can be concluded from the foregoing that the density of a nonhomogeneous liquid is a function of pressure. This means that equipotential surfaces in a nonhomogeneous liquid are also surfaces of equal density, i. e., a nonhomogeneous liquid in equilibrium is stratified by equipotential surfaces into layers of equal density. This property is used to separate the components of nonhomogeneous liquids in centrifuges.

Let us introduce a resultant unit body force j whose projections on the coordinate axes are X, Y, Z, i. e., we take the total acceleration caused by the action of all body forces at a given point. We also take into account that the quantities dx, dy and dz are the projections of an infinitesimal line dl representing the distance between two very close points M and M' (see Fig. 178).

On the basis of the foregoing we can write the following equalities

$$X = j\cos(\hat{j,x}); \quad Y = j\cos(\hat{j,y}); \quad Z = j\cos(\hat{j,z})$$

and

$$dx = dl\cos(\hat{dl,x}); \quad dy = dl\cos(\hat{dl,y}); \quad dz = dl\cos(\hat{dl,z}).$$

The formula for the cosine of an angle between two straight lines: in space yields

$$X\,dx + Y\,dy + Z\,dz = j\,dl\cos(\hat{j,dl}) = dU.$$

Substituting this expression for dU into Eq. (A.4) and solving for dp, we have

$$dp = \varrho j\,dl\cos(\hat{j,dl}). \tag{A.6}$$

It is seen from this equation that the greatest maximum pressure increment is in the direction of the resultant body force j, as in this case $\cos(\hat{j,dl}) = 1$.

For any line dl in an equipotential surface the increment $dp = 0$. But in the general case j and dl are not zero, and consequently, $\cos(\hat{j,dl}) = 0$, i. e., *the resultant body force is normal to an equipotential surface.*

Using this property of equipotential surfaces it is simple to determine the configuration of the free surface of a liquid when there are other body forces besides gravity acting on it.

3. INTEGRATION OF THE DIFFERENTIAL EQUATION OF FLUID EQUILIBRIUM

Let us consider the integration of the differential equation of fluid equilibrium in the form (A.3′) or (A.6) for three specific cases, which were discussed in Chapters II and III, namely, the principal case of equilibrium of a fluid under the action of gravity and the two cases of relative rest.

1. Let gravity be the only body force acting on a fluid. Directing the z axis vertically up, we have

$$X = 0; \quad Y = 0; \quad Z = -g.$$

Substituting into Eq. (A.3′), we obtain

$$-g\,dz = \frac{dp}{\varrho},$$

or

$$dp = -\varrho\, g\,dz = -\gamma\,dz,$$

and integrating

$$p = -\gamma z + C.$$

The integration constant can be found from the free-surface conditions where, at $z = z_0$, $p = p_0$ (see Fig. 6). Consequently,

$$C = p_0 + \gamma z_0,$$

whence

$$p = p_0 + (z_0 - z)\gamma,$$

or

$$p = p_0 + h\gamma.$$

We have thus arrived at Eq. (2.2), which was developed in another way in Sec. 6.

2. Let a liquid be contained in a vessel moving with uniform acceleration in a straight line, i. e., the case of relative rest of a liquid discussed in Sec. 11. Here Eq. (A.6) is more convenient, the direction of l being taken parallel to the resultant body force j (see Fig. 19). We have

$$\cos(\hat{j}, dl) = 0,$$

and consequently,

$$dp = \varrho j\,dl.$$

Integrating,

$$p = \varrho j l + C.$$

Since, at $l = 0$, $p = p_0$, then $C = p_0$ and we obtain Eq. (3.1):

$$p = p_0 + j\varrho l.$$

3. Let a liquid be contained in a vessel revolving uniformly about its vertical axis with an angular velocity ω, i. e., the case of relative rest examined in Sec. 12. Placing the origin of the coordinate system in the centre of the bottom and directing the x axis straight up, we have

$$X = \omega^2 r \cos(\hat{r,x}) = \omega^2 x;$$

$$Y = \omega^2 r \cos(\hat{r,y}) = \omega^2 y;$$

$$Z = -g.$$

Substituting these values into the equilibrium equation (A.3′), we obtain

$$\omega^2 x dx + \omega^2 y dy - g dz = \frac{dp}{\varrho},$$

or

$$dp = \frac{\gamma}{g}\omega^2 (x dx + y dy) - \gamma dz.$$

Taking into account that

$$x dx + y dy = d\left(\frac{r^2}{2}\right),$$

integrating, we obtain

$$p = \frac{\gamma}{2g}\omega^2 r^2 - \gamma z + C.$$

At $r = 0$ and $z = h$, $p = p_0$, consequently,

$$C = p_0 + h\gamma,$$

and finally

$$p = p_0 + \gamma(h - z) + \frac{\gamma}{2g}\omega^2 r^2. \qquad \text{(A.7)}$$

The equation of the free surface can be obtained by assuming $p = p_0$ in Eq. (A.7). Cancelling out and performing the necessary transformations, we obtain

$$z = \frac{\omega^2 r^2}{2g} + h,$$

which fully agrees with Eq. (3.2) obtained before.

If in the above discourse gravity is neglected ($Z = 0$) and the integration constant is determined from the condition that, at $r = r_0$, $p = p_0$, we obtain Eq. (3.3):

$$p = p_0 + \gamma \frac{\omega^2}{2g}(r^2 - r_0^2).$$

4. INTEGRATION OF THE DIFFERENTIAL EQUATIONS OF FLUID FLOW

Considering the case of steady flow, multiply each of the equations (A.1) by the respective projections of the elementary displacement, which are

$$dx = v_x dt; \quad dy = v_y dt; \quad dz = v_z dt.$$

Summing, we have

$$X dx + Y dy + Z dz - \frac{1}{\varrho}\left(\frac{\partial p}{\partial x} dx + \frac{\partial p}{\partial y} dy + \frac{\partial p}{\partial z} dz\right) = v_x dv_x + v_y dv_y + v_z dv_z.$$

Taking into account that

$$v_x dv_x = d\left(\frac{v_x^2}{2}\right);$$

$$v_y dv_y = d\left(\frac{v_y^2}{2}\right);$$

$$v_z dv_z = d\left(\frac{v_z^2}{2}\right);$$

$$v_x^2 + v_y^2 + v_z^2 = v^2;$$

the foregoing equation can be rewritten as follows:

$$X dx + Y dy + Z dz = \frac{1}{\varrho} dp + d\left(\frac{v^2}{2}\right), \tag{A.8}$$

or

$$dU = \frac{1}{\varrho} dp + d\left(\frac{v^2}{2}\right).$$

Let us integrate this equation for the principal case of ideal fluid flow, when gravity is the only body force acting on the fluid, and for the two cases of relative motion.

1. Directing the z axis vertically up, in the first case we have

$$X = 0; \quad Y = 0; \quad Z = -g.$$

Substituting these values into Eq. (A.8), we have

$$g dz + \frac{1}{\varrho} dp + d\left(\frac{v^2}{2}\right) = 0,$$

or

$$dz + \frac{1}{\gamma} dp + d\left(\frac{v^2}{2g}\right) = 0.$$

Since for an incompressible fluid $\gamma = \text{const}$, the foregoing equation can be written in the form

$$d\left(z + \frac{p}{\gamma} + \frac{v^2}{2g}\right) = 0.$$

This equation means that the increment of the sum of the three terms in the parentheses in a displacement along a streamline (or pathline) is zero. We conclude from this that the trinomial is a constant along the streamline and, consequently, along the whole of a differential stream tube, i. e.,

$$z + \frac{p}{\gamma} + \frac{v^2}{2g} = \text{const}.$$

This is Bernoulli's equation for a stream tube of an ideal fluid, which we developed in Sec. 15.

Written between two cross-sections of the stream tube, the equation takes the familiar form (4.12):

$$z_1 + \frac{p_1}{\gamma} + \frac{v_1^2}{2g} = z_2 + \frac{p_2}{\gamma} + \frac{v_2^2}{2g}.$$

2. Let a liquid be flowing along a channel which is in turn moving through space with a uniform acceleration a (Fig. 104). Acting on all the fluid particles will be a unit body force j', numerically equal to the acceleration but oppositely directed. Denoting the components of this force by j'_x, j'_y, j'_z,

$$X = j'_x; \quad Y = j'_y; \quad Z = j'_z - g,$$

and the increment of the force function is

$$dU = j'_x dx + j'_y dy + (j'_z - g) dz.$$

Equation (A.8) can be written in the form

$$j'_x dx + j'_y dy + (j'_z - g)\, dz = \frac{1}{\varrho} dp + d\left(\frac{v^2}{2}\right).$$

Integrating and carrying out the basic transformations, we have

$$z + \frac{p}{\gamma} + \frac{v^2}{2g} - (j'_x dx + j'_y dy + j'_z dz) = \text{const.}$$

If this equation is written between two cross-sections of a stream tube with the coordinates of their centres of gravity at x_1, y_1, z_1 and x_2, y_2, z_2, it takes the form

$$z_1 + \frac{p_1}{\gamma} + \frac{v_1^2}{2g} - \frac{1}{g}(j'_x x_1 + j'_y y_1 + j'_z z_1) = z_2 + \frac{p_2}{\gamma} + \frac{v_2^2}{2g} - \frac{1}{g}(j'_x x_2 + j'_y y_2 + j'_z z_2),$$

or

$$z_1 + \frac{p_1}{\gamma} + \frac{v_1^2}{2g} = z_2 + \frac{p_2}{\gamma} + \frac{v_2^2}{2g} + \Delta H_{in},$$

where ΔH_{in} is the inertia head:

$$\Delta H_{in} = \frac{j'_x}{g}(x_1 - x_2) + \frac{j'_y}{g}(y_1 - y_2) + \frac{j'_z}{g}(z_1 - z_2)$$

or

$$\Delta H_{in} = \frac{j'}{g} l_a = \frac{a}{g} l_a.$$

Here l_a is the length of the projection of the portion of the stream tube (or channel) under consideration on the direction of the acceleration a, i. e., the distance between the two points (x_1, y_1, z_1) and (x_2, y_2, z_2). The same results were obtained in Sec. 40.

3. Let a liquid be flowing through a channel which is revolving uniformly about a vertical axis with an angular velocity ω (Fig. 105). Then

$$X = \omega^2 x; \quad Y = \omega^2 y; \quad Z = -g,$$

and Eq. (A.8) takes the form

$$\omega^2 x dx + \omega^2 y dy - g dz = \frac{1}{\varrho} dp + d\left(\frac{v^2}{2}\right)$$

or

$$\omega^2 d\left(\frac{r^2}{2}\right) - g dz = \frac{1}{\varrho} dp + d\left(\frac{v^2}{2}\right).$$

After integration and the necessary transformations,

$$z + \frac{p}{\gamma} + \frac{v^2}{2g} - \frac{\omega^2 r^2}{2g} = const$$

or

$$z_1 + \frac{p_1}{\gamma} + \frac{v_1^2}{2g} = z_2 + \frac{p_2}{\gamma} + \frac{v_2^2}{2g} + \Delta H_{in},$$

where

$$\Delta H_{in} = \frac{\omega^2}{2g}(r_1^2 - r_2^2).$$

We have thus arrived at the equation (10.3) developed in Sec. 40. Thus, all the basic equilibrium and flow equations for an ideal fluid which we originally obtained by investigating the specific physical phenomena can be developed very nicely by integrating Euler's general differential equations.

INDEX

A

Abramovich, G. N.—115, 141
Abrupt contraction—111
Abrupt expansion—105
Absolute pressure—18
Absolute roughness size—97
Absolute viscosity—21
Accumulator—38
Acherkan, N. S.—230
Acoustic velocity—160
Actuator, hydraulic—236
Aerodynamics—11
Air ejector pump—66
Archimedes' law—37-38
Atmosphere—29
  standard—18
Atmospheric pressure—18
Available head—163
Axial-flow pump—204
Axial-piston pump—226

B

Barometric pressure—18
Basic hydrostatic equation—27
Basic pump equation—186, 188
Bell-mouthed orifice—134
Bend,
  circular—114
  pipe—113
  sharp—113
  smooth—114
Bernoulli, Daniel—13
Bernoulli's equation—52, 56, 257, 265
  for an ideal liquid—54
  for real flow—57, 59
Blasius equation—96
Body force—17, 261
Booster—239
  static characteristics of—342
Borda-Carnot theorem—106
Boundary of a fluid—25
Bourdon-tube gauge—33
Branching pipeline—170
Bulk modulus of elasticity—19
Buoyancy,
  centre of—38
  force—38
Bypass valve—233

C

Capacity, pump—182
Capillarity—20
Carburettor—65
Cavitation—77, 210
Cavitation parameter—213
Centre of buoyancy—38
Centre of pressure—34
Centrifugal pump—182
  cavitation in—210
  regulation—201
  similarity—198
  vane design—188
  volute casing—214
Characteristics,
  cavitation—210
  pipeline—163
  pump—94, 175, 188, 200
  rotary displacement pump—230
Circular bend—114
Circular pipe, velocity distribution in—82
Circulation—214
Clearance spaces, flow through—205
Closed impeller—218
Clutch, hydraulic—253
Coefficient,
  compressibility—19
  discharge—126
  friction—206
  loss—61
  pressure—75

vane-number—191
velocity—126
Compensation tank—176
Composite pipeline—171
Compound pipes,
in parallel—168
in series—167
Compressibility of a liquid—19
Continuity, equation of—52
Contraction,
abrupt—111
gradual—112
suppressed—129
Converter, torque—254
Coupling, fluid—253
Critical Reynolds number—70
Critical velocity of flow—70
Cross-section of stream—51

D

Darcy's formula—63
Degree of reaction of pump—189
Delivered head, geodetic—172
Delivery, pump—182, 222
Density—18
Depth, hydraulic mean—102
Diaphragm gauge—33
Differential equations,
of fluid equilibrium—259, 262
of ideal fluid flow—257
Differential manometer—31
differential transmission—252
Diffuser—107
optimum cone angle—110
rate of divergence—109
Diffuser mouthpiece—134
Discharge,
coefficient of—126
rate of,
between parallel walls—88-89
mass—51
through pipe—82
volume—51
weight—51
with varying head—137
Discharge line—172
Discharge pipe—172
Displacement pump—222
Drive, fluid—253
Dynamic similarity—72
Dynamic viscosity—21

E

Eddy losses—107
Effective specific weight—32
Efficiency,
hydraulic—193, 210
mechanical—196, 208
pump—183, 196, 205
volumetric—196, 205
Efflux, velocity of—126
Elasticity,
bulk modulus of—19
volume modulus of—19
Elbow—113
Elevation—28
Elevation head—54
Emptying of vessels—137
Energy,
kinetic—55, 87
potential—55
pressure—55
specific—54, 58
total, of a flowing liquid—55
velocity—55
Energy gradient—60
Energy losses—196
Entrance pipe length—84-85
Equal density, surface of—261
Equal pressure, surface of—28, 261
Equation,
basic hydrostatic—27
basic pump—186, 188
Bernoulli's—52, 54, 56, 57, 59, 257, 265
Blasius—96
of continuity—52
differential, of fluid equilibrium—259, 262
of ideal fluid flow—257
Euler's—186, 259
Hagen-Poiseuille—83
of head losses—62
hydrostatic—27
Konakov's—101
pump power—186
Equipotential surface—28, 261
Equivalent pipe length—120
Euler, Leonhard—14
Euler number—75
Euler's equation—186, 259
Evaporability—22
Expansion,
abrupt—105
gradual—107
thermal—19
Expansion loss—109
Expansion tank—176
Eye, pump—184

F

Factor,
friction—63
shock reduction—109
Features, local—61
Feedback—246
Flow,
Bernoulli's equation—57, 59
between moving walls—89
between parallel flat walls—87
critical velocity of—70
differential equations of—257
energy of—55, 87
ideal—49
in a moving channel—150
in a rotating channel—150
laminar—69, 80, 83, 84, 87, 118
pipe—69, 97, 101, 151
power of—58
rate of—51
secondary—115
steady—49
through clearance spaces—205
turbulent—69, 92, 97, 101
twin-eddy secondary—115
unsteady—49, 151
Flow nozzle—65
Fluid,
boundary—25
definition—11
energy—56
ideal—49
nonviscous—49
pressure—33, 36
work done by—56
Fluid coupling—253
Fluid drive—253
Fluid mechanics—11
Fluidity—20
Follow-up system—239
Force,
body—17, 261
buoyancy—38
friction—17, 20
pressure—17
shear—17, 20
surface—20
Force function—260
Form losses—61
Formula,
Darcy's—63
Joukowski's—159-60
Konakov's—95
Weisbach's—61
Free surface—261, 263
Free vortex—141
Friction,
coefficient—206
factor—63
force—17, 20
losses—61, 83, 207
Froude number—77
Function, force—260

G

Galileo Galilei—13
Gas—11
Gauge,
Bourdon-tube—33
diaphragm—33
Gauge pressure—18
Gear pump—224
Geodetic head—54, 172
Geometric similarity—72
G-load—44
Gradient,
energy—60
hydraulic—54, 60
velocity—21
Gradual contraction—112
Gradual expansion—107
Granular wall roughness, uniform—97
Gravity, specific—19
Gravity pipeline—164

H

Hagen-Poiseuille equation—83
Head,
available—163
elevation—54
geodetic—54
geodetic delivered—172
geodetic suction—172
inertia—149, 152
losses—60, 62, 83, 193
piezometric—28
potential—54
pressure—28, 54
pumping—174, 182
required—163
shutoff—195
static—54
total—54
varying—137
velocity—54
Homologous pumps—197
Horsepower,
hydraulic—196
internal—196
shaft—183

water—183
Hydraulic,
actuator—236
clutch—253
efficiency—193, 210
gradient—54, 60
horsepower—196
jack—39
losses—193, 196
mean depth—102
press—39
radius—102
resistances—61
transmissions—236, 248, 252
Hydraulics—11
Hydroamplifier—239
Hydrodynamics—11
Hydrodynamic similarity—72, 197
Hydrokinetic transmission—253
Hydromechanics—11
Hydrostatic equation—27
Hydrostatic pressure—17

I

Ideal fluid flow—49, 54, 257
Ideal pump—186
Ideal velocity of efflux—126
Impeller,
design—203
closed—218
propeller-type—218
pump—183
relative width of—203
semi-open—218
shrouded—218
unshrouded—218
Inertia head—149, 152
Injector,
bypass—146, 148
helical-nozzle—145
swirl—140
twin-nozzle—145
two-stage—146
Intake line—172
Intake pipe—172
Intensifier, pressure—39
Internal horsepower—196
Inverted U-tube—32

J

Jack, hydraulic—39
Jet,
complete contraction—125
submerged—131
Joukowski, Nikolai—15, 129, 155
Joukowski's formula—159, 160

K

Karman, Theodor von—16
Kinetic energy—55, 87
Kinematic similarity—73
Kinematic viscosity—21
Konakov's formula—95, 101

L

Laminar flow—69, 80
entrance conditions—84
friction losses—83
kinetic energy—87
head losses—83
local disturbances—118
mean velocity—83
momentum of—87
Laminar sublayer—96, 99
Law,
Archimedes'—37-38
Pascal's—28
Reynolds' of similarity—76
Leakage—196, 205
Leibenzon, L. S.—16
Levkoyeva, N. V.—122
Length,
entrance pipe—84-85
relative—62
Line,
intake—172
outlet—172
piezometric—54
pressure—172
suction—172
Liquid,
compressibility—19
definition—11
relative rest of—42, 262
specific energy—54
tensile strength—20
thermal expansion—19
viscosity—20
Local disturbances—118
Local features—61, 104
Local losses—61
Lomonosov, Mikhail—14
Looping pipeline—176
Loss coefficient—61
Losses,
eddy—107
energy—196
expansion—109

form—61
friction—61, 62, 83, 207
head—60, 62, 83, 193
hydraulic—193, 196
local—61
major—61
mechanical—196
minor—61, 104
shock—107, 193
turbulence—109
volumetric—196

M

Major losses—61
Manometer,
differential—31
U-tube—30
well-type—32
Mass rate of discharge—51
Mean depth, hydraulic—102
Mean specific energy—58
Mean velocity—58, 83
Measurement of pressure—28
Mechanical efficiency—196, 208
Mechanical losses—196
Mechanics, fluid—11
Meniscus effect—20
Meter,
orifice—65
venturi—64
Minor losses—61, 104
Mixed-flow pump—204
Modulus of elasticity—19
Momentum of laminar flow—87
Motion, relative—149
Moving channel, flow in—150

N

Newton, Isaac—13, 21
Newton number—74
Nikuradse, Johann—16, 97
Nonviscous fluid—49
Nozzle—113
Number,
critical Reynolds—70
Euler—75
Froude—77
Newton—74
Reynolds—71

O

Open pipeline—172
Operating point—175, 201
Optimum diffuser cone angle—110
Orifice,
bell-mouthed—134
sharp-edged—124
Orifice meter—65
Outlet line—172
Outlet pipe—172

P

Parallel walls, flow between—88
Pascal's law—28
Pavlovsky, N. N.—16
Petrov, N. P.—15, 21
Piezometer—28
Piezometric head—28
Piezometric line—54
Pipes,
bends in—113
circular—82
compound in parallel—118
compound in series—167
contraction in —111
entrance conditions—84-85
equivalent length—120
flow through—69, 82, 97, 101
intake—172
laminar flow through—83
noncircular—101
outlet—172
parallel—118
pressure—172
rough—97
rate of discharge through—82
smooth—96
suction—172
turbulent flow through—97, 101
unsteady flow through—151
velocity distribution in—82
Pipeline,
branching—170
characteristic of—163
composite—171
compound in parallel—168
compound in series—167
gravity—164
looping—176
open—172
plain—162
with pump—172, 176
Piston pump—224, 226
Pitot tube—67
Plain pipeline—162
Point,
operating—175, 201
stagnation—67

Poise—21
Positive-displacement pump—222
Potential energy—55
Potential head—54
Power controls—239
Power of a flow—58
Power of a pump—183, 186
Prandtl, Ludwig—16
Press, hydraulic—39
Pressure,
  absolute—18
  atmospheric—18
  barometric—18
  centre of—34
  coefficient of—34
  definition—17, 57
  dynamic—57
  gauge—18
  hydrostatic—17, 25
  measurement of—28
  on surfaces—33, 36
  saturation vapour—23
  static—57
  weight—57
Pressure coefficient—75
Pressure energy—55
Pressure force—17
Pressure head—28, 54
Pressure intensifier—39
Pressure intensity—57
Pressure line—172
Pressure wave—155
Profile,
  shear stress—81
  velocity—57, 81
Propeller pump—204
Propeller-type impeller—218
Pump,
  air ejector—66
  axial-flow—204
  axial-piston—226
  capacity of—182
  centrifugal—182
    cavitation in —210
    regulation of—201
    similarity of—198
    vane design of—188
    volute casing of—214
  characteristics of—94, 175, 188, 200, 230
  characteristic volume of—222
  degree of reaction of—189
  delivery of—182, 222
  displacement—222
  displacement of—222
  efficiency—183, 196, 205
    hydraulic—193
    mechanical—196
    volumetric—196
  energy losses—196
  equation of—186, 188
  friction losses—207
  gear—224
  head losses—193
  homologous—197
  hydraulic efficiency—193
  hydraulic losses—193, 196
  hydrodynamic similarity of—197
  ideal—186
  impeller of—183
  leakage—196
  losses in,
    energy—196
    friction—207
    head—193
    hydraulic—193, 196
    mechanical—196
    shock—193
    volumetric—196
  mechanical efficiency—196
  mechanical losses—196
  mixed-flow—204
  piston—224, 226
  positive-displacement—222
  power of—183
  power equation—186
  propeller—204
  radial-flow—204
  radial-piston—226
  reciprocating—222
  rotary—223
  rotary displacement—230
  rotary piston—226
  screw—224, 225
  shock losses—193
  shroud of—184
  standard—202
  swashplate—226
  theoretical delivery of—222
  vane—224, 225
  variable-displacement—228, 229, 234
  volumetric efficiency—196
  volumetric losses—196
Pump displacement—222
Pump eye—184
Pump impeller—183
Pumping element—222
Pump shroud—184
Pump volute—183, 214
Pumping head—174, 182

R

Radial-flow pump—204
Radial-piston pump—226
Radius, hydraulic—102
Rate of discharge,
between parallel walls—88, 89
mass—51
through pipe—82
volume—51
weight—51
Rate of divergence of a diffuser—109
Rate of flow—51
Reaction of a pump, degree of—189
Reciprocating pump—222
Reducer—112
Regulation range, hydraulic transmission—252
Relative leakage—205
Relative pipe length—62
Relative motion—149
Relative rest—42, 262
Relative impeller width—203
Relative roughness—97
Required head—163
Resistances, hydraulic—61
Reynolds, Osborne—15, 70
Reynolds' law of similarity—76
Reynolds number—70, 71
Rotary hydraulic transmission—248
Rotary pump—223
Rotary displacement pump—230
Rotary piston pump—226
Rotating channel, flow through—150
Rotodynamic transmission—253
Rough-law regime—99
Rough pipes—97
Roughness,
absolute—97
relative—97
uniform granular—97
Rudnev, S. S.—210

S

Saturation vapour pressure—23
Screw pump—224, 225
Secondary flow—115
Semi-open impeller—218
Shaft horsepower—183
Sharp bend—113
Sharp-edged orifice—124
Shear force—17, 20
Shear stress—18, 21, 80
Shear stress profile—81
Shock absorber—139
Shock losses—107, 193
Shock reduction factor—109
Shock wave—155
Shroud—184
Shrouded impeller—218
Shutoff head—195
Similarity,
dynamic—72
geometric—72
hydrodynamic—72
kinematic—73
of pumps—197, 198
Reynolds' law of—76
Siphon—166
Slip—253
Smooth bend—114
Smooth pipes—96
Specific energy—54, 58
Specific speed—202, 205
Specific weight—18, 32
Stagnation point—67
Standard atmosphere—18
Standard pump—202
Static head—54
Static pressure—57
Steady flow—49
Stoke—21
Stokes, George—15
Stream,
cross-section of—51
velocity distribution across—59
Streamline—50
Stream tube—50
Stress, shear—18, 21, 80
Sublayer, laminar—96, 97, 99
Submerged jet—131
Suction line—172
Suction pipe—172
Suppressed contraction—129
Surface,
equipotential—28, 261
free—261, 263
of equal density—261
of equal pressure—28, 261
Surface forces—17
Surface tension—20
Swashplate pump—226

T

Technically smooth pipes—96
Tensile strength of a liquid—20
Tension, surface—20
Theorem, Borda-Carnot—106
Theoretical hydromechanics—12
Theoretical pump delivery—222

Theoretical velocity of efflux—126
Thermal expansion of a liquid—19
Torque converter—254
Torricelli, Evangelista—13
Total head—54
Transition pipe length—84-85
Transmission,
differential—252
hydraulic—236, 252
hydrokinetic—253
regulation range—252
rotary hydraulic—248
rotodynamic—253
Tube—132
Turbulence losses—109
Turbulent flow—69, 92, 101
Twin-eddy secondary flow—115

U

Unshrouded impeller—218
Unsteady flow—49, 151
U-tube manometers—30-32

V

Vacuum—29
Valve, bypass—233
Vane design—188
Vane-number coefficient—191
Vane pump—224, 225
Vapour pressure, saturation—23
Variable-displacement pump—228, 229, 234
Varying head, discharge with—137
Velocity,
acoustic—160
coefficient of—126
critical—70
ideal—126
mean—58, 83
theoretical—126
Velocity distribution—59, 82
Velocity energy—55
Velocity gradient—21
Velocity head—54
Velocity parallelogram—185
Velocity profile—57, 81
Velocity triangle—187, 191
Vena contracta—125
Venturi meter—64
Vinci, Leonardo da—13
Viscosity—20
absolute—21
dynamic—21
kinematic—21
Volume modulus of elasticity—19
Volume rate of discharge—51
Volumetric efficiency—196, 205
Volumetric losses—196
Volute casing—183, 214
Vortex, free—141

W

Water hammer—155
Water horsepower—183
Weight pressure—57
Weight rate of discharge—51
Weisbach's formula—61
Well-type manometer—32
Work done by a fluid—56

TO THE READER

Peace Publishers would be glad to have your opinion of the translation and the design of the book.

Please send all suggestions to 2, Pervy Rizhsky Pereylok, Moscow, U.S.S.R.